

Dynamic combinatorial libraries
of complexes with
oligopyridine ligands

Inauguraldissertation

zur

Erlangung der Würde eines Doktors der Philosophie
vorgelegt der
Philosophisch-Naturwissenschaftlichen Fakultät
der Universität Basel

von

Barbara Brisig
aus St. Gallen-Tablat, St. Gallen

Basel, 2006

Genehmigt von der Philosophisch-Naturwissenschaftlichen Fakultät
auf Antrag von

Prof. Dr. E. C. Constable

Dr. E. Stulz

Basel, den 4. Juli 2006

Prof. Dr. H.-J. Wirz

Dekan

*Now faith is being sure of what we hope for
and certain of what we do not see.*

-The Bible, Hebrews 11.1-

Acknowledgements

I would like to thank the following people for their help and support during the years devoted to this work:

Prof. Ed Constable for giving me a second chance to do a Ph.D. research after a false start in another university, for allowing me to try out my ideas and for helping me whenever I was stuck; Prof. Catherine Housecroft for her help, support and encouragement at any time during the past years, but especially in the last months when I was feeling I would never get to the end of this thesis.

Dr. Eugen Stulz for accepting to be my co-examiner despite having to come all the way from Southampton just for me.

The scientific staff in the Department of Chemistry of the University of Basel for their work, without which I would never had all the analytical data of my compounds; I am sure you must have cursed my samples sometimes! Thank you to Bobby for showing me how to use the error propagation formula, to Markus Neuburger for solving the crystal structure, and to Beatrice for sorting out any kind of administrative matter. Many thanks especially to Markus for providing whatever I needed, was it for my own research or for the practical, in record times.

All the members of the Constable-Housecroft group, past and present, for helping me whenever I needed, and for the friendly atmosphere during the coffee-breaks.

Alexandra and Diana for their help in putting together the last semester of practical and for the good hours spent playing as the “Trio infernale”.

Deborah and Sébastien for their help of any kind and on any occasion, and for rendering the working days funnier. Thank you also to Rémi: without you and Sébastien in the practical with me, I would have broken down!

Acknowledgements

My parents for giving me the opportunity to come so far in my studies, and for their support in everything I embarked upon.

Christophe for having been my optimistic half, for having loved and accepted me as I am, and for forgiving my sometimes “strange” sides. Thank you also for proofreading the first version of this thesis and helping me to win every battle against the computer.

The University of Basel and the Swiss National Science Foundation for the financial support.

Table of Contents

Summary	vi
Abbreviations	viii
1. Introduction	1
1.1. Dynamic combinatorial libraries	1
1.2. Bipyridine and terpyridine	4
1.3. Ferrocene	12
2. Cobalt(II)-directed assembly of dynamic combinatorial libraries with 2,2'-bipyridine and 1,10-phenanthroline ligands	18
2.1. Complexes containing a single ligand	18
2.2. Libraries containing two ligands	22
2.3. Libraries containing three different ligands	32
2.4. Conclusions	38
3. Co ²⁺ /Co ³⁺ ligand exchange	39
3.1. Introduction	39
3.2. Synthesis of the complexes	39
3.3. [Co(bpy) ₃] ³⁺ and [Co(phen) ₃] ³⁺	41
3.4. [Co(bpy) ₃] ³⁺ and [Co(phen) ₃] ²⁺	42
3.5. [Co(bpy) ₃] ²⁺ and [Co(phen) ₃] ³⁺	45
3.6. Conclusions	47
4. Cobalt(II) directed assembly of dynamic combinatorial libraries with asymmetric 2,2'-bipyridine ligands	48
4.1. Introduction	48
4.2. Synthesis of the ligands	48
4.3. Synthesis of the complexes	53
4.4. Templating of the Co(II) / 5-formyl-2,2'-bipyridine library	62
Synthesis of one template	64
Templating with tris(2-aminoethyl)amine (tren)	66
Templating with 1,1,1-tris(aminomethyl)ethane (tris)	75
Templating with cis-1,3,5-triaminocyclohexane (tach)	78

Table of Contents

4.5. Conclusions	80
5. Cobalt(II)-directed assembly of dynamic combinatorial libraries with asymmetric 2,2':6',2''-terpyridine ligands	83
5.1. Introduction	83
5.2. Synthesis of the ligands	83
5.3. Synthesis of the complexes	86
Synthesis of 5-carboxy-2,2':6',2''-terpyridine	90
Synthesis of the [Co(terpy-COOH) ₂][PF ₆] ₂ complex	91
5.4. Interaction of [Co(terpy-COOH) ₂][PF ₆] ₂ with bis-amine templates	93
5.5. Ligand exchange at one metal centre	97
Synthesis and characterisation of [Co(terpy) ₂][PF ₆] ₂ , [Fe(terpy) ₂][PF ₆] ₂ and [Fe(terpy-CH ₃) ₂][PF ₆] ₂	97
Library containing two ligands and one metal centre	100
5.6. Ligand exchange at two metal centres	110
5.7. Conclusions	115
6. Self-assembly of polynuclear macrocycles containing 2,2':6',2''-terpyridine- and sandwich-complexes	117
6.1. Introduction	117
6.2. Synthesis of the ligand	119
6.3. Synthesis of the complexes	122
6.4. Attempts at the formation of the macrocycles	124
6.5. Synthesis of new ferrocene complexes	127
6.6. Synthesis of the polynuclear macrocycles	139
6.7. Exchange between macrocycles	150
6.8. Conclusions and outlook	155
7. Experimental	157
7.1. General experimental	157
Materials	157
Instrumentation	158
7.2. Organic syntheses	159
1-(2-Pyridylacetyl)pyridinium iodide (M = 326.15) (PPI, 12)	159

Table of Contents

5-Methyl-2,2'-bipyridine (M = 170.23) (9)	159
5-[2-(N,N-Dimethylamino)vinyl]-2,2'-bipyridine (M = 225.32) (13)	160
5-Formyl-2,2'-bipyridine (M = 184.21) (10)	161
1,1,1-Tris(p-toluenesulfonyloxymethyl)ethane (M = 582.77) (20)	162
1,1,1-Tris(phthalimidomethyl)ethane (M = 507.53) (21)	163
1,1,1-Tris(aminomethyl)ethane hydrochloride (M = 226.61) (23)	164
1,1,1-Tris(azidomethyl)ethane (M = 195.23) (22)	165
1,1,1-Tris(aminomethyl)ethane (M = 117.23) (17)	165
2-Acetyl-5-methylpyridine (M = 135.18) (29)	166
2-(3'-(N,N-Dimethylamino)-1'-oxoprop-2'-en-1'-yl)pyridine (M = 176.24) (31)	167
5-Methyl-2,2':6',2''-terpyridine (M = 247.32) (34)	168
5-[2-(N,N-Dimethylamino)vinyl]-2,2':6',2''-terpyridine (M = 302.41) (35)	169
5-Formyl-2,2':6',2''-terpyridine (M = 261.30) (36)	170
5,5'-Diformyl-2,2':6',2''-terpyridine (M = 261.30)	171
5-Carboxy-2,2':6',2''-terpyridine (M = 277.30) (39)	172
5-(4-Phenylbutyl)-2,2':6',2''-terpyridine (M = 365.51) (47)	173
3-Cyclohexa-1,4-dienylpropan-1-ol (M = 138.23) (Birch reduction) (49)	175
Toluene-4-sulfonic acid 3-cyclohexa-1,4-dienyl-propyl ester (M = 292.43) (51)	176
5-(4-Cyclohexa-1,4-dienyl-butyl)-2,2':6',2''-terpyridine (M = 367.53) (53)	177
2-(3-Bromopropanoxy)tetrahydropyran (M = 233.13) (58)	178
2-(4-Chlorobutoxy)tetrahydropyran (M = 192.71) (59)	179
2-[3-(1,3-Cyclopentadienyl)propoxy]tetrahydro-2 <i>H</i> -pyran (M = 208.33) (61)	180
2-[4-(1,3-Cyclopentadienyl)butoxy]tetrahydro-2 <i>H</i> -pyran (M = 222.36) (62)	181
1,1'-Bis[3(2-pyranoxy)propyl]ferrocene (M = 470.49) (63)	182
1,1'-Bis[4-(2-pyranoxy)butyl]ferrocene (M = 498.55) (64)	183
1,1'-Bis(3-hydroxypropyl)ferrocene (M = 302.23) (65)	184
1,1'-Bis(4-hydroxybutyl)ferrocene (M = 330.29) (66)	185

Table of Contents

Pyridinium p-toluenesulfonate (PPTS) (M = 251.33)	186
1,1'-Bis(3-(methylsulfonyloxy)propyl)ferrocene (M = 458.43) (67)	186
1,1'-Bis(4-(methylsulfonyloxy)butyl)ferrocene (M = 486.49) (68)	187
1,1'-Bis(3-bromopropyl)ferrocene (M = 428.01) (70)	188
1,1'-Bis(4-bromobutyl)ferrocene (M = 456.07) (71)	189
1,1'-Bis(4-(2,2':6',2''-terpyridin-5-yl)butyl)ferrocene (M = 760.83) (69)	190
1,1'-Bis(5-(2,2':6',2''-terpyridin-5-yl)pentyl)ferrocene (M = 788.89) (72)	191
2-Amino-5-iodopyridine (M = 220.02) (79)	192
1-(5-Iodopyridin-2-yl)-2,5-dimethyl-1 <i>H</i> -pyrrole (M = 298.14) (80)	193
1-(5-Methoxypyridin-2-yl)-2,5-dimethyl-1 <i>H</i> -pyrrole (M = 202.28) (81)	194
2-Amino-5-methoxypyridine (M = 124.16) (82)	195
2-Bromo-5-methoxypyridine (M = 188.03) (83)	196
2-Acetyl-5-methoxypyridine (M = 151.18) (84)	197
Attempt at 5-methoxy-2,2':6',2''-terpyridine (M = 263.32) (85)	197
1,5-Bis(2'-pyridyl)pentane-1,3,5-trione (M = 268.29) (88)	199
4'-Hydroxy-2,2':6',2''-terpyridine (M = 249.29) (89)	199
1,1'-Bis(4-bromobutanoyl)ferrocene (M = 484.03) (75)	200
1,1'-Bis(4-bromobutyl)ferrocene (M = 456.07) (71)	201
1,1'-Bis(4-(2,2':6',2''-terpyridin-4'-yl)butanoyl)ferrocene (M = 820.79)	202
1,1'-Bis(4-(2,2':6',2''-terpyridin-4'-yl)butoxy)ferrocene (M = 792.83) (90)	203
1,1'-Bis(6-bromohexanoyl)ferrocene (M = 540.15) (76)	204
1,1'-Bis(bromoacetyl)ferrocene (M = 427.91) (74)	205
1,1'-Bis(6-bromohexyl)ferrocene (M = 512.19) (77)	206
1,1'-Bis(2-bromoethyl)ferrocene (M = 399.95)	207
1,1'-Bis(6-(2,2':6',2''-terpyridin-4'-yl)hexoxy)ferrocene (M = 848.95) (91)	209
7.3. Inorganic syntheses	210
General method for synthesising [CoL ₃][PF ₆] ₂ complexes	210
[Co(bpy) ₃][PF ₆] ₂ (M = 817.44) (4)	210
[Co(Me ₂ bpy) ₃][PF ₆] ₂ (M = 901.62) (5)	211
[Co(phen) ₃][PF ₆] ₂ (M = 889.50) (6)	211
[Co(bpy-CH ₃) ₃][PF ₆] ₂ (M = 859.11) (15)	212

Table of Contents

[Co(bpy-CHO) ₃][PF ₆] ₂ (M = 901.50) (14)	212
General method for synthesising [CoL ₃][PF ₆] ₃ complexes	213
[Co(bpy) ₃][PF ₆] ₃ (M = 962.41) (7)	213
[Co(Me ₂ bpy) ₃][PF ₆] ₃ (M = 1046.59)	213
[Co(phen) ₃][PF ₆] ₃ (M = 1034.47) (8)	214
General method for synthesising [CoL ₂][PF ₆] ₂ complexes	214
[Co(terpy) ₂][PF ₆] ₂ (M = 815.43) (44)	215
[Co(terpy-CHO) ₂][PF ₆] ₂ (M = 871.47) (38)	215
[Co(terpy-COOH) ₂][PF ₆] ₂ (M = 903.47) (40)	216
[Co(terpy-CH ₃) ₂][PF ₆] ₂ (M = 843.51) (37)	216
[Co(terpy-C4-Ph) ₂][PF ₆] ₂ (M = 1079.89)	217
[Co(terpy-C4-chd) ₂][PF ₆] ₂ (M = 1083.93) (55)	218
General method for synthesising [FeL ₂][PF ₆] ₂ complexes	218
[Fe(terpy) ₂][PF ₆] ₂ (M = 812.37) (45)	219
[Fe(terpy-CH ₃) ₂][PF ₆] ₂ (M = 840.43) (46)	219
[Fe(terpy-C4-Ph) ₂][PF ₆] ₂ (M = 1076.81)	220
[Fe(terpy-(C4-Ph) ₂) ₂][PF ₆] ₂ (M = 1341.21)	221
[Fe(terpy-CHO) ₂][PF ₆] ₂ (M = 868.39)	221
[Fe(terpy-C4-chd) ₂][PF ₆] ₂ (M = 1080.85) (54)	222
[Ru(terpy-C4-Ph) ₂][PF ₆] ₂ (M = 1122.03)	223
8. Appendix	225
8.1. Crystal structure data for 1,1'-bis(4-bromobutanoyl)ferrocene (75)	225
Crystal data	225
Data collection	225
Refinement	226

Summary

Chapter 1 gives a background of some achievements reached in the fields of dynamic combinatorial libraries, 2,2'-bipyridine and 2,2':6',2''-terpyridine chemistry, and ferrocenes compounds in the years preceding the present work.

Chapter 2 describes the study by ¹H-NMR spectroscopy of the composition of different mixtures of cobalt(II) complexes with 2,2'-bipyridine and 1,10-phenanthroline ligands.

Chapter 3 discusses the ¹H-NMR analysis of different mixtures of complexes with different cobalt oxidation states and 2,2'-bipyridine and 1,10-phenanthroline ligands.

Chapter 4 describes a new synthesis for the previously reported bpy-CH₃ and bpy-CHO. The ¹H-NMR spectra of their cobalt(II) complexes are discussed. It was established that the complexes in solution spontaneously formed a DCL of the *fac* and *mer* stereoisomers. Templating experiments are discussed that have the goal to change the composition of the library.

Chapter 5 describes the synthesis of new 5-substituted 2,2':6',2''-terpyridines and the ¹H-NMR characterisation of their cobalt(II) and iron(II) complexes. Attempts to bind the complexes with different templates are discussed. Ligand exchange at one metal centre and between two different metals is also studied.

Chapter 6 describes the synthesis of new 2,2':6',2''-terpyridines functionalised with a ring capable of forming sandwich complexes. The ¹H-NMR characterisation of their cobalt(II) and iron(II) complexes is discussed. The possibility of forming macrocycles containing two metal centres with two different complexing sites was studied. In these systems the ligand exchange could be controlled by independent actions influencing only one complex.

Chapter 7 reports the detailed synthetic procedures for the products encountered and their characterisation data.

Abbreviations

°C	degree Celsius
Alox	aluminium oxide
β	complex stability constant
b. p.	boiling point
BnEt ₃ NBr	benzyltriethylammonium bromide
bpy	2,2'-bipyridine
bpy-CH ₃	5-methyl-2,2'-bipyridine
bpy-CHO	5-formyl-2,2'-bipyridine
br	broad (IR)
BuLi	butyl lithium
calc.	calculated
Co(OAc) ₂	cobalt acetate
COSY	correlated spectroscopy
Cp	cyclopentadienyl
d	doublet (NMR)
DCL	dynamic combinatorial library
δ	chemical shift (NMR)
DMA	<i>N,N</i> -dimethylacetamide
DMF	<i>N,N</i> -dimethylformamide
DMSO	dimethylsulfoxide
E ⁰	standard reduction potential
ED	1,2-diaminoethane
EI-MS	electron impact mass spectrometry
Elem. an.	elemental analysis
ϵ_{\max}	extinction coefficient at λ_{\max} (UV/Vis)
ESI-MS	electrospray ionisation mass spectrometry
Et ₂ O	diethyl ether
EtOAc	ethyl acetate
EtOH	ethanol
EXCSY	chemical exchange difference spectroscopy
FAB-MS	fast atom bombardment mass spectrometry
<i>fac</i>	facial
Fe(Cp-C4-Br) ₂	1,1'-bis(4-bromobutyl)ferrocene
Fe(Cp-C4-O-terpy) ₂	1,1'-bis(4-(2,2':6',2''-terpyridin-4'-yl)butoxy)ferrocene

Abbreviations

Fe(Cp-C4-terpy) ₂	1,1'-bis(4-(2,2':6',2''-terpyridin-5-yl)butyl)ferrocene
Fe(Cp-C5-terpy) ₂	1,1'-bis(5-(2,2':6',2''-terpyridin-5-yl)pentyl)ferrocene
Fe(Cp-C6-Br) ₂	1,1'-bis(6-bromohexyl)ferrocene
Fe(Cp-C6-O-terpy) ₂	1,1'-bis(6-(2,2':6',2''-terpyridin-4'-yl)hexoxy)ferrocene
HD	1,6-diaminohexane
HOAc	acetic acid
ⁱ Pr	isopropyl
IR	infra-red spectroscopy
<i>J</i>	coupling constant (NMR)
K	degree Kelvin
<i>K</i>	equilibrium constant
λ _{max}	wavelength at which maximum absorption occurs (UV/Vis)
LDA	lithium diisopropylamide
m	medium (IR)
M	parent ion (MS)
m. p.	melting point
m/z	mass to charge ratio
Me	methyl
Me ₂ bpy	4,4'-dimethyl-2,2'-bipyridine
MeOH	methanol
<i>mer</i>	meridional
MsCl	methanesulfonylchloride
NEt ₃	triethylamine
NH ₄ OAc	ammonium acetate
NMR	nuclear magnetic resonance
NOESY	nuclear Overhauser effect spectroscopy
OAc ⁻	acetate
OTHP	tetrahydro-2 <i>H</i> -pyranyl ether
phen	1,10-phenanthroline
PhthNK	potassium phthalimide
PPI	1-(2-pyridylacetyl)pyridinium iodide
ppm	parts per million (NMR)
PPTS	pyridinium <i>p</i> -toluenesulfonate
Py	pyridine
R _f	retention factor
s	strong (IR)
s	singlet (NMR)

Abbreviations

t	time
t	triplet (NMR)
tach	<i>cis</i> -1,3,5-triaminocyclohexane
^t Bu	tert-butyl
TD	1,4-diaminobutane
terpy	2,2':6',2''-terpyridine
terpy-(C4-Ph) ₂	5,5''-bis(4-phenylbutyl)-2,2':6',2''-terpyridine
terpy-C4-chd	5-(4-cyclohexa-1,4-dienyl-butyl)-2,2':6',2''-terpyridine
terpy-C4-Ph	5-(4-phenylbutyl)-2,2':6',2''-terpyridine
terpy-CH ₃	5-methyl-2,2':6',2''-terpyridine
terpy-CHO	5-formyl-2,2':6',2''-terpyridine
terpy-COOH	5-carboxy-2,2':6',2''-terpyridine
THF	tetrahydrofuran
TLC	thin layer chromatography
TosCl	<i>p</i> -toluenesulfonyl chloride
TosOH	<i>p</i> -toluenesulfonic acid
tren	tris(2-aminoethyl)amine
tris	1,1,1-tris(aminomethyl)ethane
UV/Vis	ultra-violet/visible
w	weak (IR)

1. Introduction

1.1. Dynamic combinatorial libraries

In the search for a new substance with a given activity, combinatorial chemistry has emerged as an important tool. Instead of designing the new active substance, trying to synthesise it and then testing whether its functionality is really what it should be, in the combinatorial approach, a collection (a combinatorial library) of molecules is constituted from a set of units connected by successive or repetitive use of specific chemical reactions. The challenge then moves towards the identification of the active molecules from amongst large numbers of inactive species.

Dynamic combinatorial chemistry (DCC) is a new, different approach, based on the reversible self-assembly of the components of a combinatorial library and on molecular recognition events of a given target. The first article introducing this concept was published in 1996 [1]; for other references see [2, 3, 4, 5, 6].

A dynamic combinatorial library (DCL) contains assemblies of building blocks connected through reversible reactions or interactions in thermodynamic equilibrium. When a molecular template (a biopolymer, or a small molecule) is added to the DCL, some of the library members bind to it selectively and are therefore removed from the pool of interconverting compounds. The equilibrium is then shifted, amplifying the strong binders and minimising the concentration of the poor binders in the library (Figure 1.1).

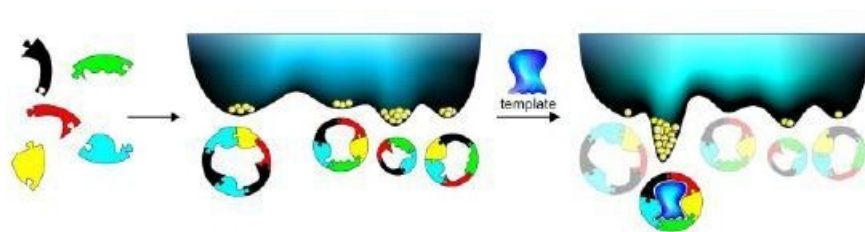


Figure 1.1: A small DCL and its free energy landscape, showing the effect of adding a template that strongly and selectively binds to one of the equilibrating species [7].

It was recently demonstrated that the target concentration has a strong influence on the outcome of a selection experiment. In special cases, the competition between receptors within a DCL is not necessarily won by the best receptor, and weak binders can beat strong binders [8, 9]. However, it seems that reducing the amount of template to close to stoichiometric concentrations ensures amplification of the best receptor without any serious loss of templating efficiency [9].

The generation of DCLs can be applied to both the discovery of a substrate for a given receptor or the construction of a receptor for a given substrate. The “lock and key” approach means that a DCL of substrates consists of a set of building blocks that can reversibly assemble to generate a potentially large collection of keys, with the hope that one of them will fit in the lock/receptor with a high degree of complementarity. A similar comparison can be applied to DCLs of receptors for a given substrate [10] (Figure 1.2).

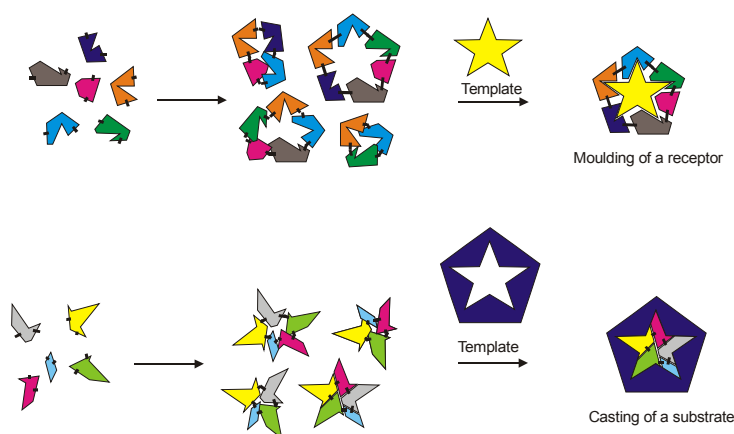


Figure 1.2: Schematic representation of casting and moulding processes from a DCL.

DCC presents three basic requirements:

- every single member of the library must be sufficiently soluble;
- the linkages between the building blocks must be reversible;
- it must be possible to turn off (and eventually on again) the exchange reactions at will.

The problem of the solubility of the library members is perhaps the most important constraint: the rate of redissolving of a precipitated material is often so slow that that

material can be considered as being trapped in the solid form. This results in the shift of the equilibrium towards this kinetic trap.

The reversible reaction can be the formation of covalent or non-covalent bonds, or a reversible intramolecular process. As examples for the use of reversible covalent bond formation, we can list transesterification [1], exchange over the C-N double bond [11, 12, 13, 14, 15, 16, 17, 18, 19, 20], disulfide exchange [7, 21, 22, 23, 24, 25], thioester exchange [23], olefin metathesis [26], and Diels-Alder reaction [27]. For the formation of non-covalent bonds the most examples come from metal-ion coordination [28, 29, 30, 31, 32, 33, 34]. Among the reversible intramolecular processes, we can cite *cis-trans* isomerisation of double bonds [35].

The recognition process between a template and the library members is first of all directed by the sterical compatibility of the two partners. Subsequently, different kinds of interaction can bind the template and the selected members of the library: electrostatic interactions [7, 8, 14], hydrogen bonding [29, 35], or formation of coordination complexes [17, 36].

In some cases, the building blocks themselves choose to form the best compound from among the different possible members of the DCL, and there is no need to add any target to the mixture to obtain a single compound. These libraries are called self-sorting [32, 37].

The composition of the DCL can be analysed by different techniques. Most of the reported examples use high-performance liquid chromatography (HPLC), sometimes combined with mass spectroscopy [1, 7, 10-18, 20-26, 28, 35]. Some systems have a specific feature that allows the analysis of the mixture by NMR spectroscopy, mainly of the ^1H nucleus, but also of other nuclei [8, 17, 29, 30, 32, 33, 36]. Among the unusual techniques of analysis for a DCL, an example is X-ray crystallography, used to detect small-molecule ligands generated *in situ* and bound to a target protein [38]. Another example of a technique specifically adapted to libraries screened against a protein is an enzyme linked assay [19]. Finally, when the DCL is constructed by metal-dye complexes, and the library members have each a different colour, the analysis method can be UV/Vis spectroscopy [34].

When combining two different levels of exchange that can be used as independent equilibrium processes controlled by different types of external intervention, the result is a double-level, orthogonal DCL. An example based on transition metal complexes has been described [39]. The first level consists of the coordination of terpyridine-based ligands to the transition metal template, and is controlled by the oxidation state of the metal centre. The second level is formed by the imine formation with the aldehyde substituents on the terpyridine moieties and is controlled by pH and temperature (Figure 1.3).

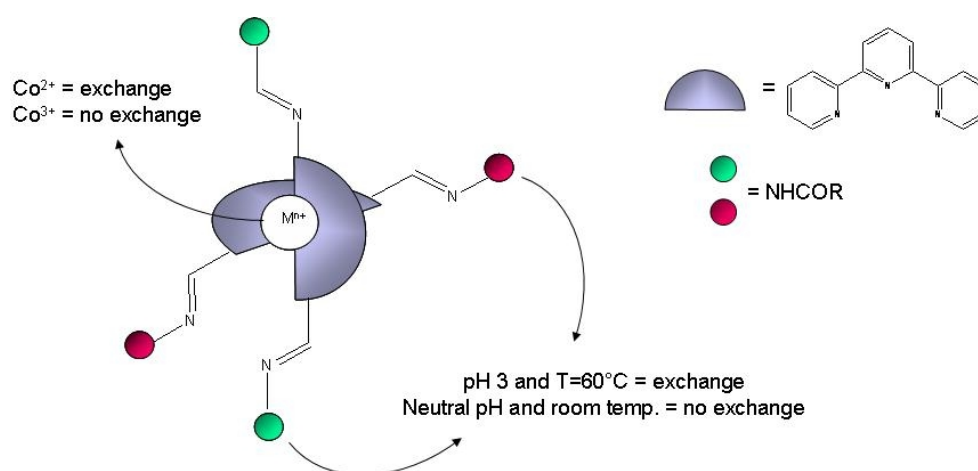


Figure 1.3: Schematic representation of the two levels of exchange in the orthogonal DCL described in [39].

In this work, a similar approach has been adopted in the construction of a DCL of tris-bipyridine metal complexes. With other systems then, attempts were made to combine more than two levels of exchange within a single DCL.

1.2. Bipyridine and terpyridine

Bipyridines and terpyridines are compounds where two and respectively three pyridine rings are connected together. In the present work, only 2,2'-bipyridines (bpy) and 2,2':6'-2''-terpyridines (terpy) were used, where the bonds between the pyridine rings are in the α positions of the nitrogen (Figure 1.4).

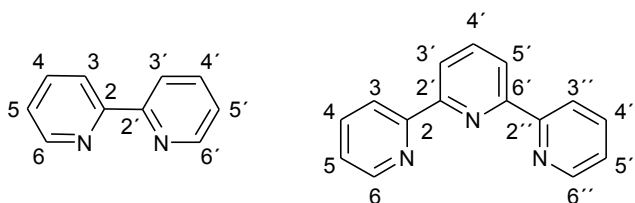


Figure 1.4: Numbering scheme of *bpy* and *terpy*.

Bipyridines can be prepared in several ways [40, 41], but in our work we used only the Kröhnke condensation, where a pyridine-carrying pyridinium salt was reacted with an α,β -unsaturated ketone in the presence of ammonium acetate and acetic acid (Figure 1.5).

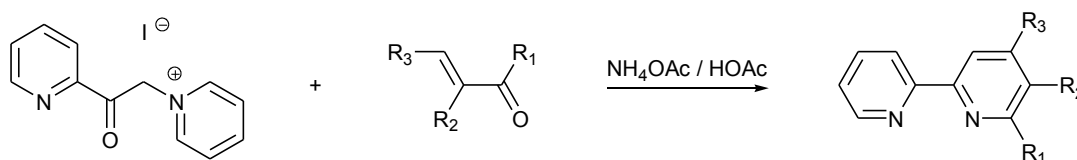


Figure 1.5: Synthetic method used for the preparation of *bpy* derivatives [40].

When one of the R substituents is a pyridyl moiety, a terpyridine can be obtained [40, 42]. The synthesis of *terpy* has however been improved, namely by Jameson [42, 43], with the use of acetylpyridine and an enaminone (Figure 1.6). This is the method that was used in this work for the preparation of asymmetrically substituted *terpys*.

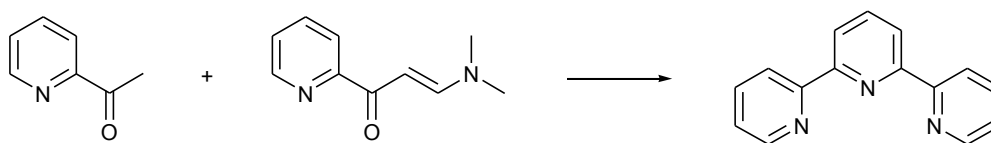


Figure 1.6: Synthetic method used for the preparation of *terpy* [43].

Both the Kröhnke and the Jameson strategies are ring assembly methodologies, where one of the pyridine rings are formed in the course of the synthesis. An alternative methodology is the cross-coupling procedure. For example, in the Stille cross

coupling, a dihalopyridine and a trimethylstannylpyridine (or vice versa) are coupled together by treatment with a palladium catalyst in toluene [42] (Figure 1.7).

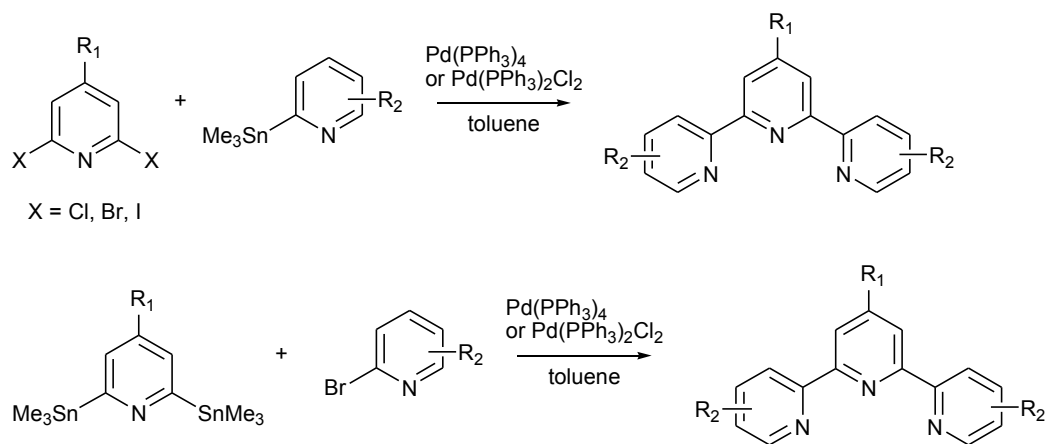


Figure 1.7: Stille cross-coupling applied to the preparation of terpy [42].

Most of the functionalised 2,2':6',2''-terpyridines reported so far (for summaries see [42, 44, 45]) bear a substituent on the 4'-position. For the functionalisation in this position, two intermediates have mainly been used: 4'-chloro-2,2':6',2''-terpyridine [46, 47] and 4'-hydroxy-2,2':6',2''-terpyridine [48] (Figures 1.8 and 1.9). A synthetic pathway for 4'-hydroxy derivatives bearing an additional functionality at the 4,4'-, 5,5''- or 6,6''-positions was proposed by Fallahpour and Constable [49].

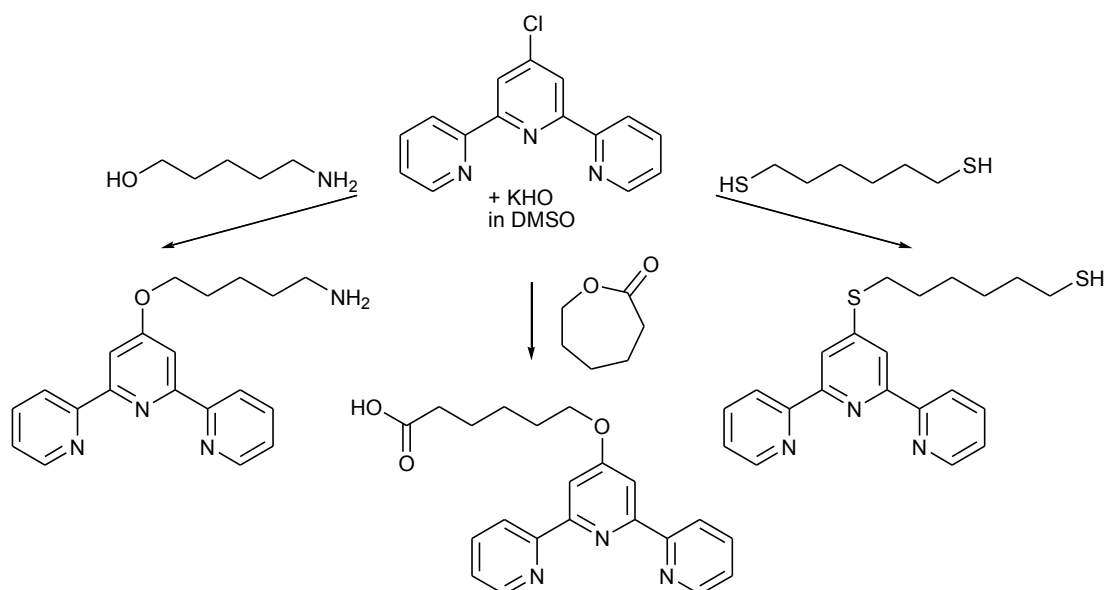


Figure 1.8: 4'-Functionalisation of terpy starting from 4'-chloro-2,2':6,2''-terpyridine [46].

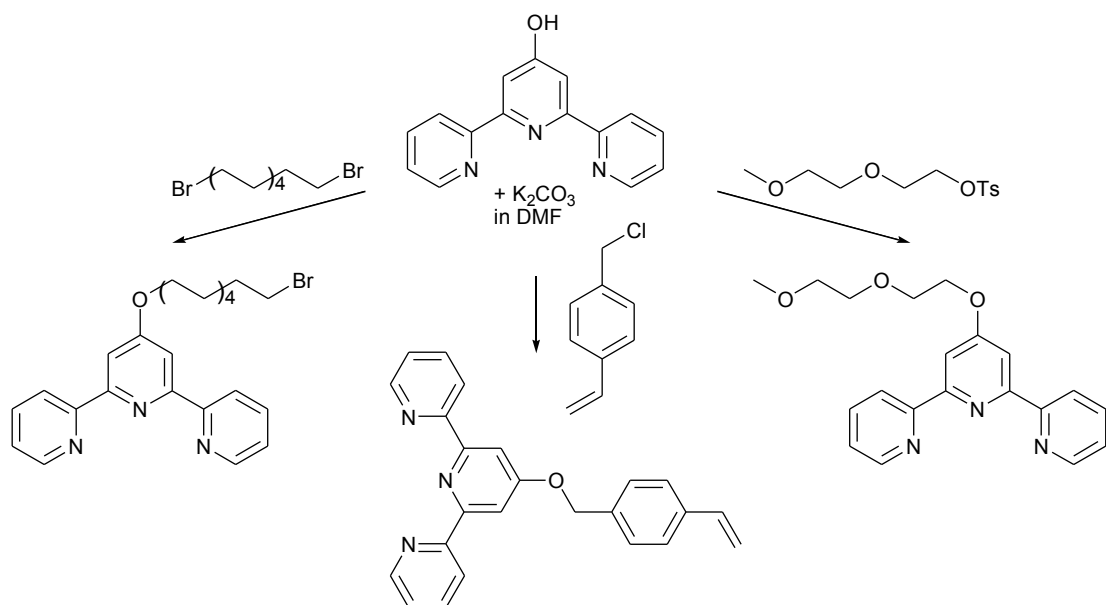


Figure 1.9: 4'-Functionalisation of terpy starting from 4'-hydroxy-2,2':6,2''-terpyridine [48].

An interesting feature of 4'-hydroxy-2,2':6,2''-terpyridine is its tautomerism with the keto form (Figure 1.10). Studies of the equilibrium between keto and enol tautomers show that solvent, hydrogen bonding (both inter- and intramolecular) and structural

substituents all play a role in affecting the population distribution of the two forms [50].

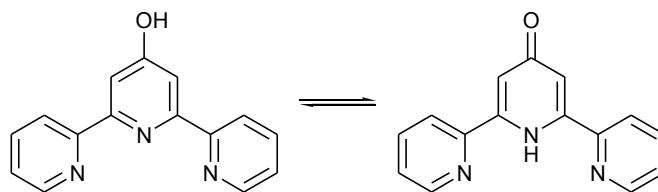


Figure 1.10: Tautomers of 4'-hydroxy-2,2':6',2''-terpyridine: enol (left) and keto form (right).

When the functional group is an alkyl chain, this is introduced by deprotonation of methyl-2,2':6',2''-terpyridine and subsequent reaction with the corresponding alkyl halide [42, 51].

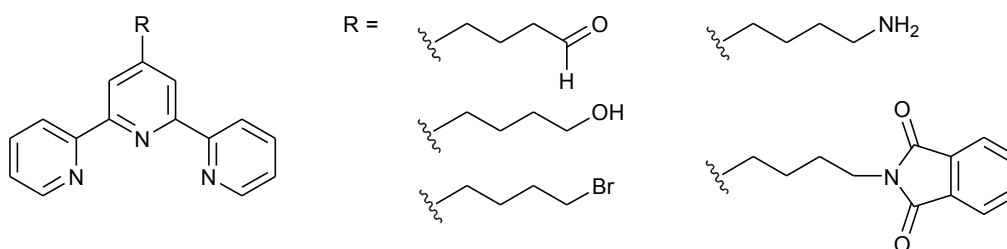


Figure 1.11: Examples of 4'-alkyl-2,2':6',2''-terpyridine [42].

The $^1\text{H-NMR}$ spectra of terpy and the bis-terpy complexes of cobalt(III) and iron(II) were first studied by comparison with each other and with the published spectra of the related bpy ligand [52]. Recently, Constable demonstrated how a combination of NMR techniques and electron exchange process can be used for the full assignment of Co(II) oligopyridine complexes [53].

Bipyridines and terpyridines have been used as chelating ligands in the preparation of supramolecular entities that possess the potential to form new materials with interesting features [44, 54]. For example, ruthenium complexes have very interesting photochemical properties that make them suitable for applications in solar energy conversion [55]. In the next figures are presented some of the fascinating dendritic and polymeric structures obtained with bpy and terpy and reviewed in [44].

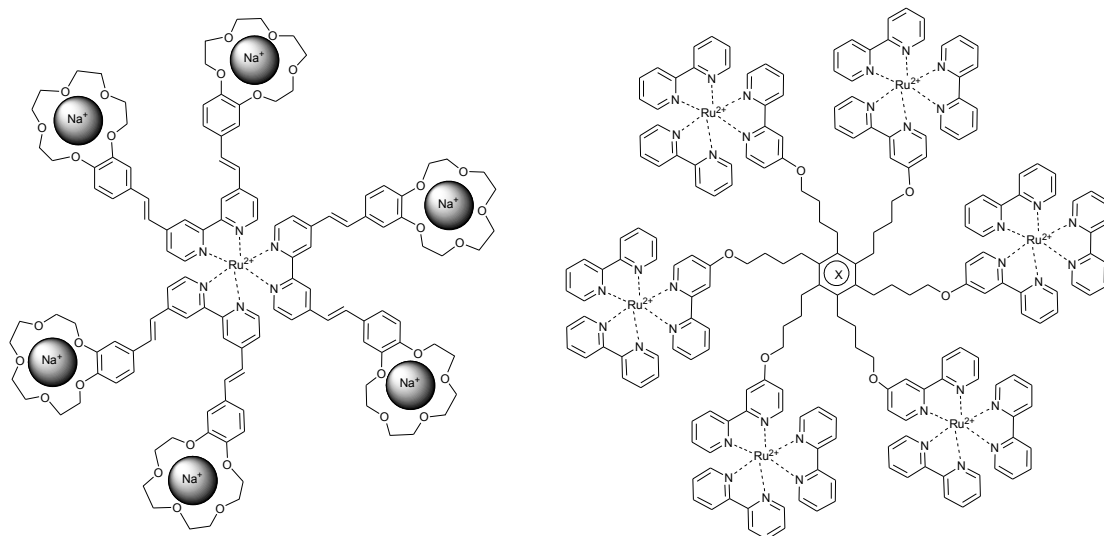


Figure 1.12: Examples of dendrimers with bipyridine-metal complexes within the core (left) or at the surface (right, $X = \text{Fe}(\eta\text{-C}_5\text{H}_5)^+$) [44].

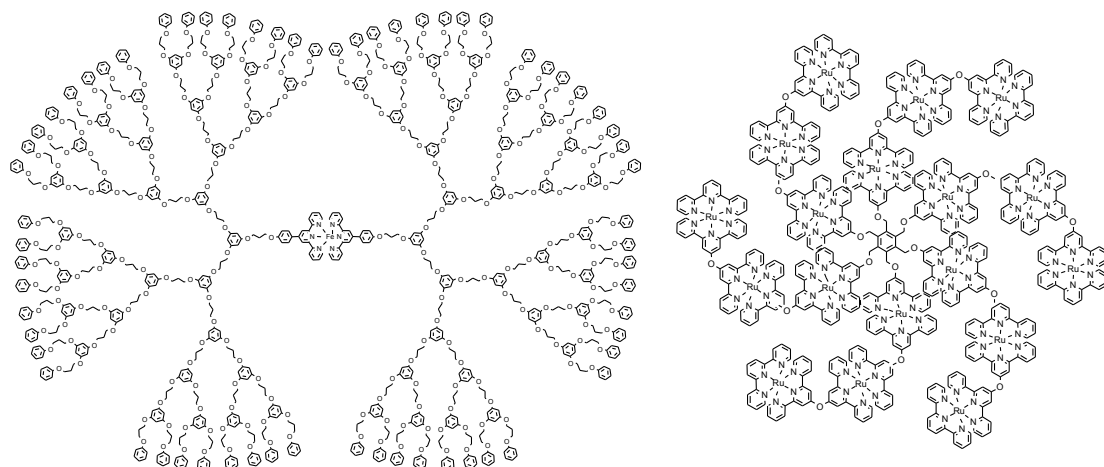


Figure 1.13: Examples of dendrimers with terpyridine-metal complexes within the core (left) or at the surface (right) [44].

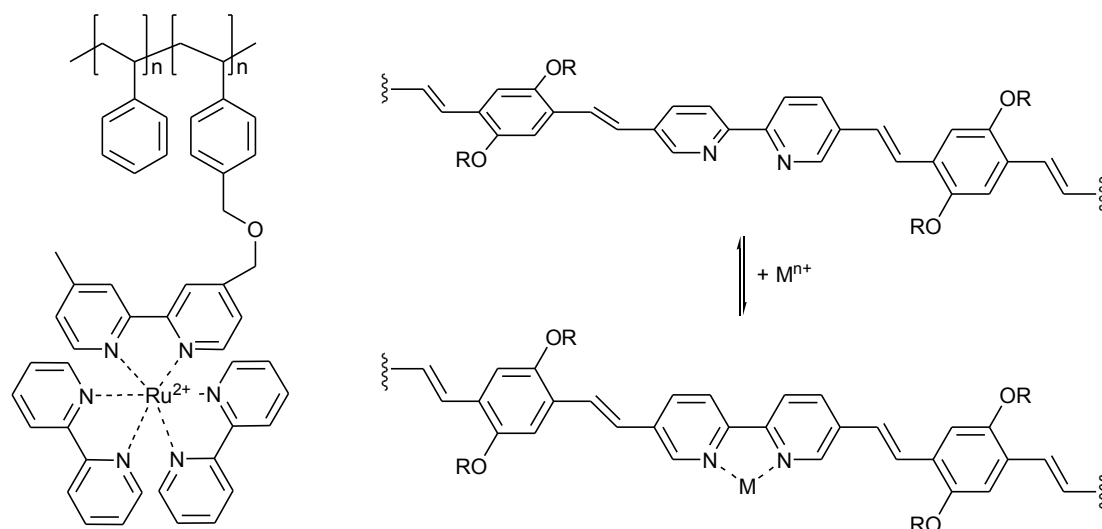


Figure 1.14: Examples of polymers with the bpy unit in the side chain (left) and in the polymer backbone (right). In the example on the right, the metal-free polymer has a twisted conformation that is forced into a planar one upon metal complexation. This enables a full π -conjugation that brings different physical properties from the partially conjugated form [44].

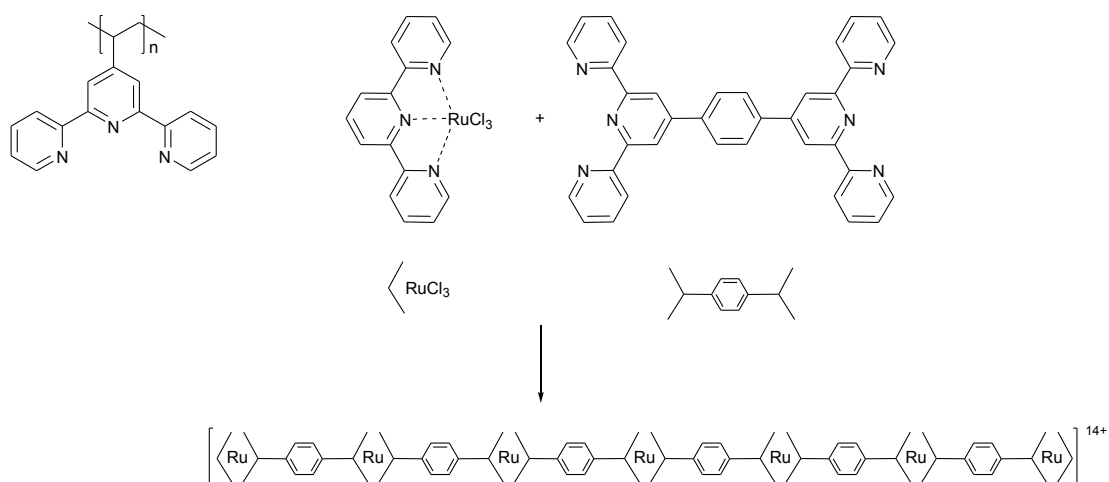


Figure 1.15: Examples of polymers with the terpy unit in the side chain (left) and in the polymer backbone (right) [44].

Kaes, Katz and Hosseini reviewed a range of compounds containing at least two bpy units [54]. Among them are the tripodal ligands shown in Figure 1.16. Some of their complexes have been synthesised to investigate their electrochemical and luminescence properties. Furthermore, **1.16f** is reported to gel in toluene by

establishing a network of hydrogen bonds, while **1.16h** and **1.16i**, containing both soft sites (bpy units) and hard sites (salicylamide units), have been investigated as redox molecular switches. In our work, a complex with a similar tripodal ligand was formed upon templating of a dynamic combinatorial library of tris-bpy Co(II) complexes.

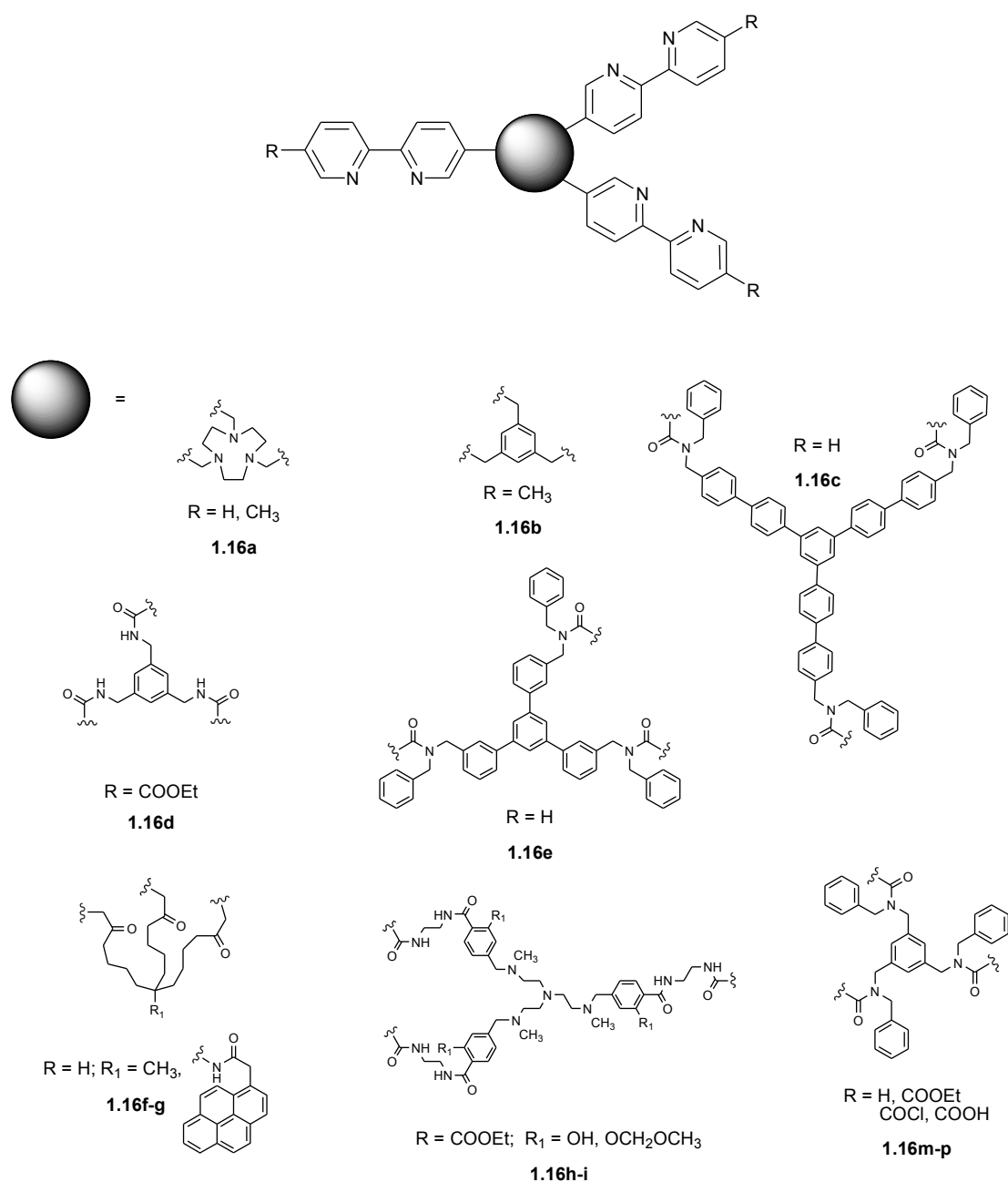


Figure 1.16: Examples of tripodal ligands with 2,2'-bipyridine molecules connected in positions 5 and 5' [54].

Examples of applications of bipyridine ligands include the formation of helical complexes that contain chiral spacer cavities [56] (Figure 1.17). Terpyridine ligands are being studied for their use in metal extraction and actinides-lanthanides separation [57], or for the use of their complexes as light-harvesting components [55].

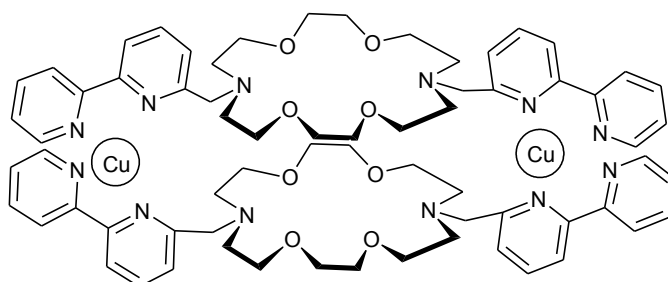


Figure 1.17: Example of [2+2] helical complex with a chiral cavity [56].

1.3. Ferrocene

The first publications reporting the synthesis of ferrocene appeared in 1951-1952. A compound with molecular formula $C_{10}H_{10}Fe$ was unexpectedly obtained by Kealy and Pauson during an attempt at the synthesis of fulvalene [58]. Later, Miller, Tebboth and Tremaine reported the synthesis of the same compound by the reaction of freshly reduced iron and cyclopentadiene vapour at 300 °C [59].

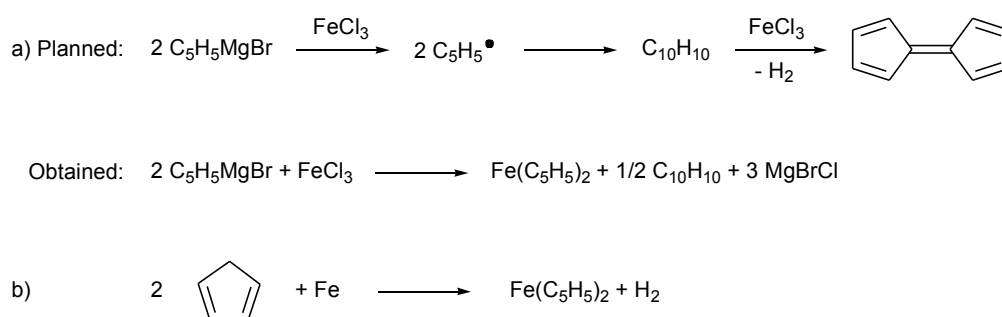


Figure 1.18: First syntheses of $Fe(C_5H_5)_2$: as an unexpected product in the attempt of making fulvalene (a) [58], and in a vapour synthesis (b) [59].

The structure of the new dicyclopentadienyl iron was not immediately clear: it was first believed that the iron was covalently bound to the methylene carbon of each ring,

but this form would be in resonance with a structure where the cyclopentadienyl rings would become aromatic by acquisition of a negative charge.

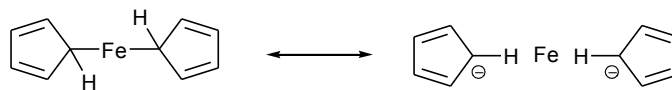


Figure 1.19: First structures proposed for dicyclopentadienyl iron [58].

Further studies led to the suggestion of a double-cone structure with iron in its centre. The iron would be coordinated in an octahedral geometry by three electron pairs for each aromatic anionic ring [60, 61, 62]. The true aromatic character of this new compound was then identified in 1952, and the name “ferrocene” by analogy with “benzene” was proposed by Woodward, Rosenblum and Whiting [63].

Ferrocenyl compounds have acquired importance principally for their electronic properties, their characteristic being the reversible one-electron oxidation. Ferrocene derivatives were incorporated into DNA oligonucleotides and used as signalling probes for the electronic detection of nucleic acids [64]. But attention was also paid to the study of non-racemic ferrocenes, as they have found application as ligands for asymmetric catalysts. Among the ligands with a potential to be useful in this field, we can cite the compounds where the two cyclopentadienyl rings are bridged by a P-C-P chain [65] (Figure 1.20).

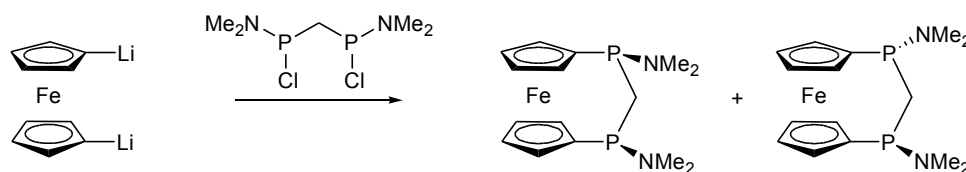


Figure 1.20: Synthetic method of bridging dilithioferrocene. The different positions of the substituents at the phosphorus atom give rise to the *cis*- and *trans*- isomers [65].

Others have focused their efforts on the introduction of additional metals in the proximity of the redox-active ferrocene unit, expecting new interesting features on the basis of the possible interaction of the two metal centres. Osmaferrocenophanes and

ferrocene bis-rhenium complexes were synthesised and their electrochemistry investigated by Lindner and co-workers (Figure 1.21). It was reported that all substituents have a consistent effect on the oxidation of the ferrocene, and this effect was attributed to a Coulomb through-space interaction decreasing with increasing spacer length [66].

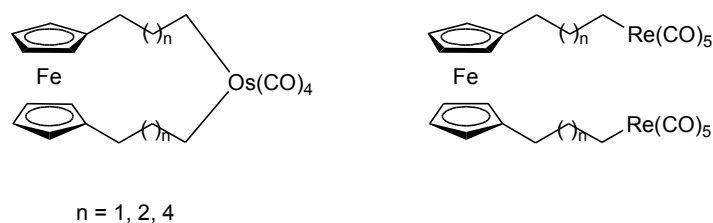


Figure 1.21: Osmaferrocenophanes (left) and bis-rhenium ferrocenes (right) studied by Lindner [66].

Ferrocenes-based ligands have been found to be useful for incorporating redox functions into supramolecular complexes. For this purpose, pyrazine- and pyrimidine-functionalised ferrocenes were designed to pursue the possibility of synergy or competition between chelating and bridging properties (Figure 1.22) [67].

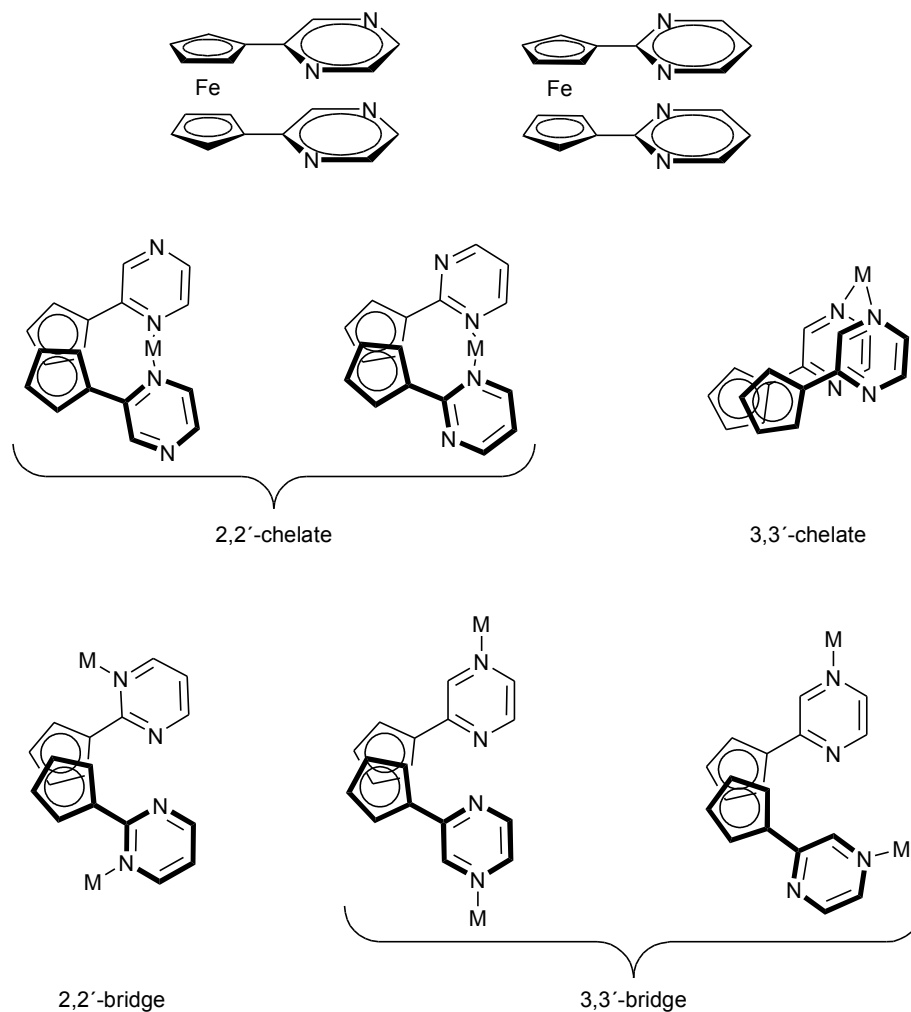


Figure 1.22: Structures of 1,1'-di(pyrazinyl)ferrocene (top left) and 1,1'-di(2-pyrimidinyl)ferrocene (top right), and their possible modes of coordination of a second metal (each couple of ligands has an iron(II) in the middle to form a ferrocene) [67].

Examples of functionalisation of ferrocene with other nitrogen carrying rings include ferrocenyl bipyridines and terpyridines (Figure 1.23) [68, 69, 70, 71]. These were prepared because of their attractiveness as ligands for photochemical and electrochemical studies, and as building blocks for novel metallocsupramolecular architectures.

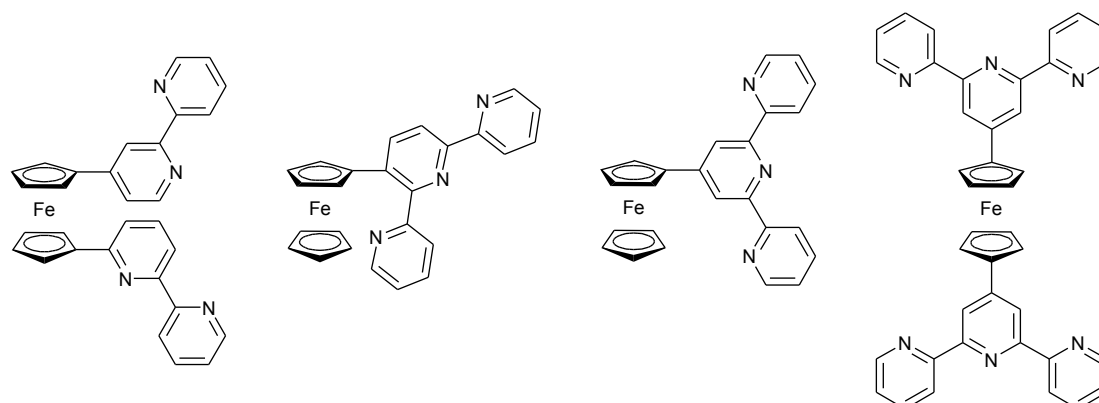


Figure 1.23: Examples of ferrocenyl bipyridines and terpyridines with the oligopyridine ligand directly bound to the cyclopentadienyl ring [68, 69, 70, 71].

In these last examples, the bipyridine and terpyridine groups are bound directly to the cyclopentadienyl ring of the ferrocene. Similar compounds were also reported where the ferrocene nucleus and the terpyridyl unit were linked through a spacer. The spacer can be a π -system like an acetylene, benzene or vinyl group [72, 73, 74], but also an alkyl chain [72]. In the present work, the synthesis of new ferrocenyl terpyridines with alkyl spacers will be presented, and their complexation behaviour investigated.

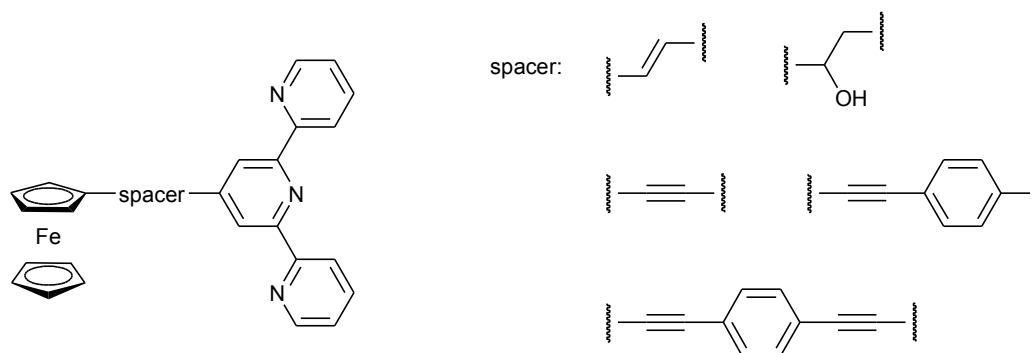


Figure 1.24: Examples of ferrocenyl-functionalised terpyridines with the oligopyridine ligand bound to the cyclopentadienyl ring through different spacers [72, 74].

Along with the typical substitution reactions of classical aromatic systems, it was reported that alkylferrocenes undergo disproportionation to ferrocene and 1,1'-dialkylferrocene in the presence of a catalyst. The mechanism was shown to involve ring exchange as opposed to the usual carbon-carbon cleavage found in

benzene chemistry (Figure 1.25) [75]. This property was used in our work to insert a level of exchange in the construction of dynamic combinatorial libraries of ferrocenyl functionalised terpyridines.

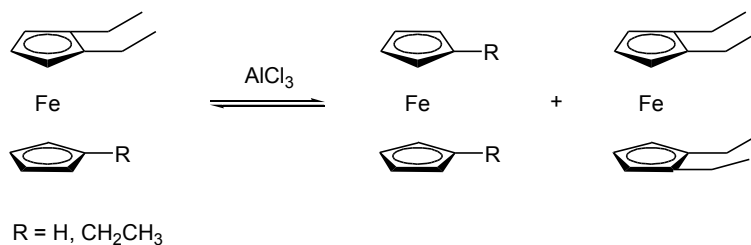


Figure 1.25: Disproportionation of alkylferrocenes, confirming the mechanism proceeding via ring-metal scission [75].

2. Cobalt(II)-directed assembly of dynamic combinatorial libraries with 2,2'-bipyridine and 1,10-phenanthroline ligands

2.1. Complexes containing a single ligand

The first step towards the creation of a new dynamic combinatorial library is to check whether the chosen system is suitable for this purpose. In our case we had to see if the metal-ligand bond formation was a reversible process in a useful time scale, if it was eventually possible to switch the exchange process on and off, and if the products were easy to characterise and isolate.

We decided to concentrate on cobalt(II) complexes because they were already known to undergo ligand exchange reactions reasonably fast while remaining thermodynamically stable. For example, the rate constant for the exchange of water molecules from the first coordination sphere of Co^{2+} is about 10^6 sec^{-1} [76].

The electronic configuration of the octahedral d^7 cobalt(II) ion can be $t_{2g}^5 e_g^2$ or $t_{2g}^6 e_g^1$, high spin or low spin, depending on the ligand, but in both cases the cation possesses at least one unpaired electron that makes it paramagnetic. The $^1\text{H-NMR}$ spectra of complexes with a paramagnetic centre show a large chemical shift range (-20 to 250 ppm) because of the perturbation of the local magnetic field by the field arising from the unpaired electron, and this can simplify a good deal the study of these spectra, especially with mixtures of different complexes [77]. Three cobalt(II) complexes were chosen and prepared with commercially available ligands that were similar in structure but with characteristic NMR peaks, so that individual complexes could be recognised in a library. The ligands chosen were 2,2'-bipyridine (bpy, **1**), 4,4'-dimethyl-2,2'-bipyridine (Me_2bpy , **2**) and 1,10-phenanthroline (phen, **3**).

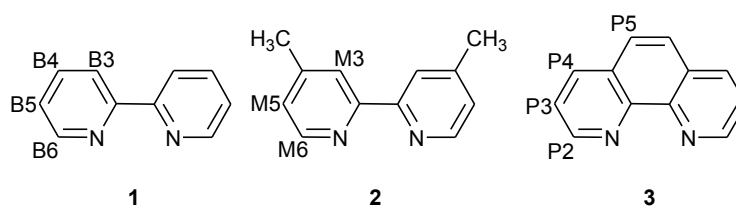


Figure 2.1: Ligands used for the Co/bpy library showing the numbering scheme used for the protons.

When preparing the complexes by mixing one equivalent of Co(II) with three equivalents of the ligand, we automatically formed a statistical 1:1 mixture of the enantiomers Δ and Λ , but as the NMR spectra were measured in the absence of any other chiral centre (solvent, counterion, functional group on the ligand), only a single series of peaks corresponding to the enantiomeric pair could be seen [78].

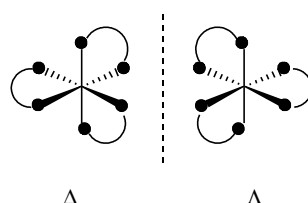


Figure 2.2: Enantiomers of $[MA_3]$ three-bladed propellor complexes.

The NMR peaks of CD₃CN solutions of the [PF₆]⁻ salts of the homoleptic complexes [Co(bpy)₃]²⁺, [Co(Me₂bpy)₃]²⁺ and [Co(phen)₃]²⁺ were assigned by comparison with each other and with the help of their ¹H-¹H gradient COSY spectra. In each case peaks were observed in the range δ 0 to about 100 ppm, typical of a low-spin solution species [30].

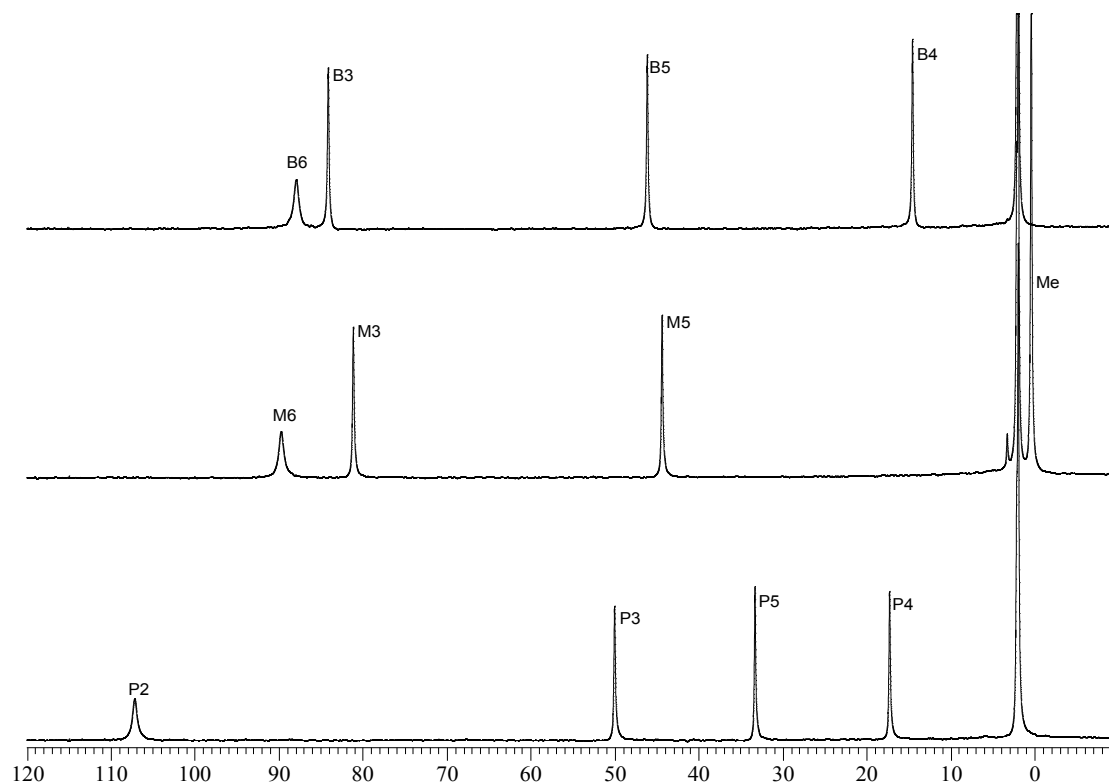


Figure 2.3: 250 MHz $^1\text{H-NMR}$ spectra (in CD_3CN) of the homoleptic complexes $[\text{Co}(\text{bpy})_3][\text{PF}_6]_2$ (4, top), $[\text{Co}(\text{Me}_2\text{bpy})_3][\text{PF}_6]_2$ (5, middle) and $[\text{Co}(\text{phen})_3][\text{PF}_6]_2$ (6, bottom).

In the $^1\text{H-}^1\text{H}$ COSY spectrum of $[\text{Co}(\text{bpy})_3][\text{PF}_6]_2$ there were two cross peaks arising from the signal at δ 14.58 ppm. Since it was known from previous studies [53], that the most shifted, broad peak can be assigned to the proton B6, M6 or P2 respectively (Figure 2.1), and the coupling of B5-B6 is not visible because of the line width of the B6 signal (about 80 Hz), the peak at δ 14.58 ppm had to belong to proton B4, the only proton making two observable couplings, with B3 and B5. With this COSY spectrum we could not distinguish between B3 and B5, but after comparing the spectra of $[\text{Co}(\text{bpy})_3][\text{PF}_6]_2$ and $[\text{Co}(\text{phen})_3][\text{PF}_6]_2$, where the equivalent of B3 is missing, it could be assumed that the signal at δ 84.48 ppm belonged to B3, and the one at δ 46.25 ppm to B5.

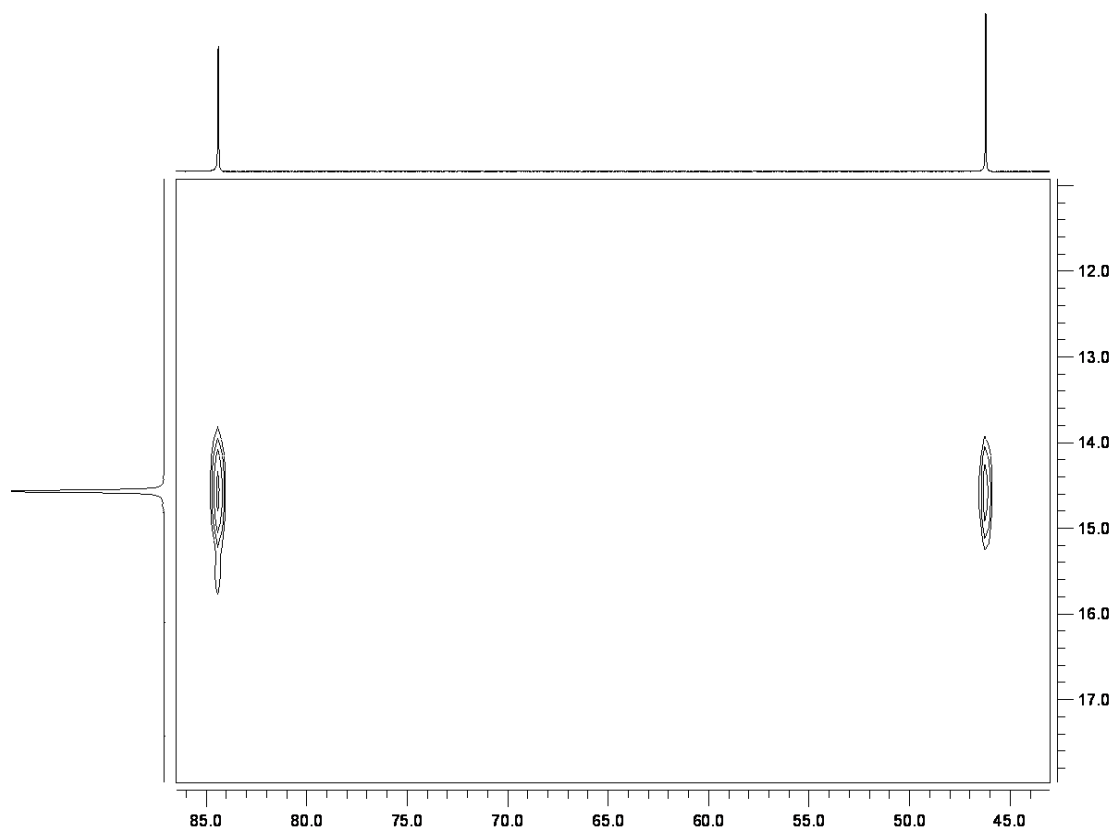


Figure 2.4: Part of the 500 MHz ^1H - ^1H COSY spectrum (in CD_3CN) of $[\text{Co}(\text{bpy})_3][\text{PF}_6]_2$ (**4**) showing the coupling of B4 with B3 (left) and B5 (right).

A similar comparison was made when assigning the spectrum of $[\text{Co}(\text{Me}_2\text{bpy})_3][\text{PF}_6]_2$. Here there were no cross peaks in the COSY spectrum, so this technique did not help in assigning the signals to M3 or M5. By comparing the resonances with $[\text{Co}(\text{bpy})_3][\text{PF}_6]_2$ and $[\text{Co}(\text{phen})_3][\text{PF}_6]_2$ the assumption could be made again that the peak at δ 81.52 ppm belonged to proton M3 and the peak at δ 44.50 ppm to M5. In the COSY spectrum of $[\text{Co}(\text{phen})_3][\text{PF}_6]_2$, a cross peak was expected from the coupling between protons P3 and P4, but not for the P3-P2 coupling, for the same reason as was explained above. To be consistent with the assumptions made before about the chemical shifts, the signal at δ 50.18 ppm was assigned to P3, δ 33.43 ppm to P5 and δ 17.33 ppm to P4.

A list of the assigned NMR peaks can be found in the chapter for experimental part.

2.2. Libraries containing two ligands

When mixing any two complexes of type $[MA_3]$ and $[MB_3]$, in which A and B are exchangeable ligands, a solution containing four different species could be expected: the two original homoleptic complexes and their exchange products $[MA_2B]$ and $[MAB_2]$. Such a mixture will be called a binary library, because it results from the mixing of two complexes. The statistical relative concentration of the products would be 1 for each of the homoleptic complexes and 3 for each of the mixing products, indeed there is only one possibility of arranging three ligands of the same kind around the metal, but there are three possible arrangements for three ligands of two different kinds (Figure 2.5).

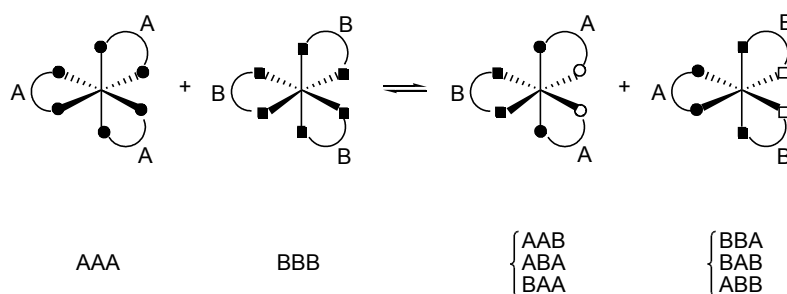


Figure 2.5: Products and distribution of the species in a binary mixture of model systems $[MA_3]$, $[MB_3]$.

In practice, a 1:1 mixture of two homoleptic complexes led to the expected library of four components. Each NMR peak for a given proton on a ligand was splitted into four signals because the formation of the mixing products resulted in four different environments for every proton.

In the heteroleptic complex $[MA_2B]$, ligand B gives one set of NMR peaks because the protons on both its pyridine rings are chemically and magnetically equivalent.

This is depicted in Figure 2.5: both filled squares are *trans* to an open circle. In ligand A, on the other hand, the two rings are no longer equivalent as one ring is *trans* to ligand A (two filled circles *trans* to each other) while the second one is *trans* to ligand B (two open circles *trans* to a filled square). So each pair of protons that are chemically equivalent in the free ligand and the $[MA_3]$ complex will give two peaks

of the same integral in $[\text{MA}_2\text{B}]$. The same explanation is valid for ligand B in $[\text{MAB}_2]$.

Let us take as an example H5 of Me_2bpy (M5) in the $\text{Co}/\text{Me}_2\text{bpy}/\text{phen}$ library. One peak arose from the six equivalent protons in the $[\text{Co}(\text{Me}_2\text{bpy})_3]^{2+}$ complex. Another signal came from the protons in the $[\text{Co}(\text{Me}_2\text{bpy})(\text{phen})_2]^{2+}$ complex: as explained previously, both M5 protons are equivalent within this cation. For the $[\text{Co}(\text{Me}_2\text{bpy})_2(\text{phen})]^{2+}$ complex, two peaks for M5 were observed because, of the four protons, two are on the pyridine ring *trans* to a Me_2bpy whereas the other two are on the ring *trans* to a phen. All peaks are observed in sets of four, allowing facile correlation with the parent homoleptic compounds.

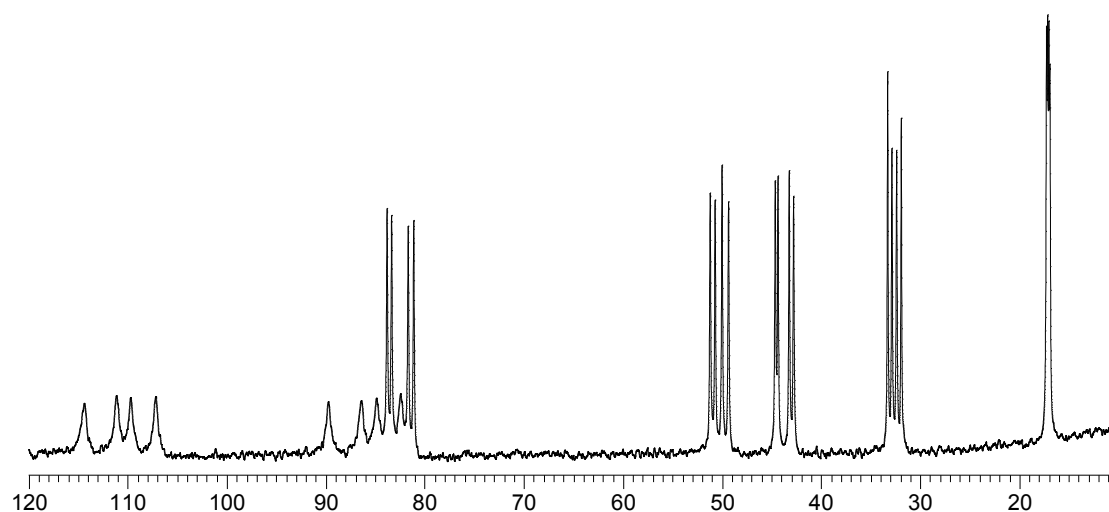


Figure 2.6: 250 MHz ^1H -NMR spectrum of the 1:1 mixture of $[\text{Co}(\text{Me}_2\text{bpy})_3][\text{PF}_6]_2$ and $[\text{Co}(\text{phen})_3][\text{PF}_6]_2$ (CD_3CN) in the region δ 120-10 ppm. Note the eight broader peaks which can be assigned to the M6 and P2 protons.

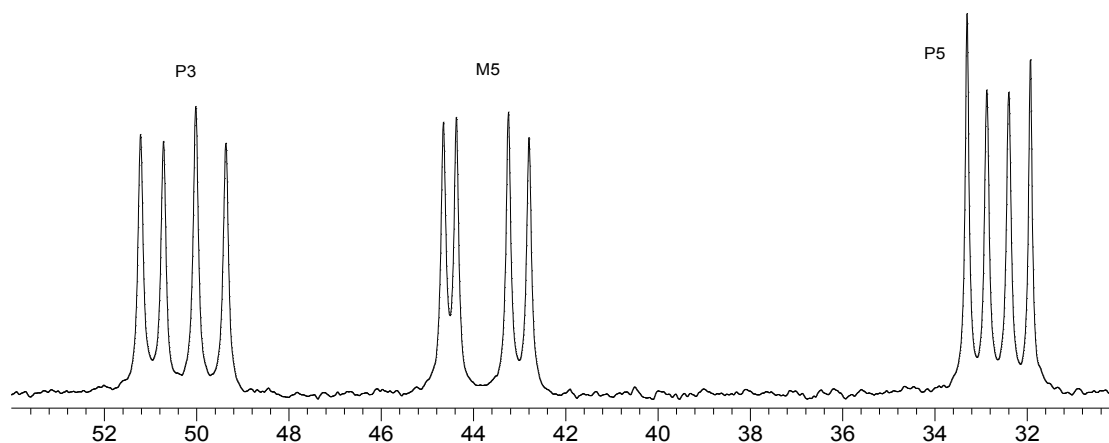


Figure 2.7: Expansion for the peaks of protons P3 and P5 of phen and M5 of Me₂bpy in the 1:1 mixture of [Co(phen)₃][PF₆]₂ and [Co(Me₂bpy)₃][PF₆]₂.

The formation of three binary libraries was investigated using combinations from the three complexes [Co(bpy)₃][PF₆]₂, [Co(Me₂bpy)₃][PF₆]₂, and [Co(phen)₃][PF₆]₂. In each case, equal amounts of 5 mM solutions in CD₃CN were mixed in an NMR tube to give solutions with a total cobalt concentration of 5 mM. The NMR spectra were measured within 5 minutes of mixing and all showed splitting into four signals for every chemically unique proton in each ligand. Later measurements of the same samples confirmed that equilibration was virtually immediate and that it was complete by the time of the first measurement.

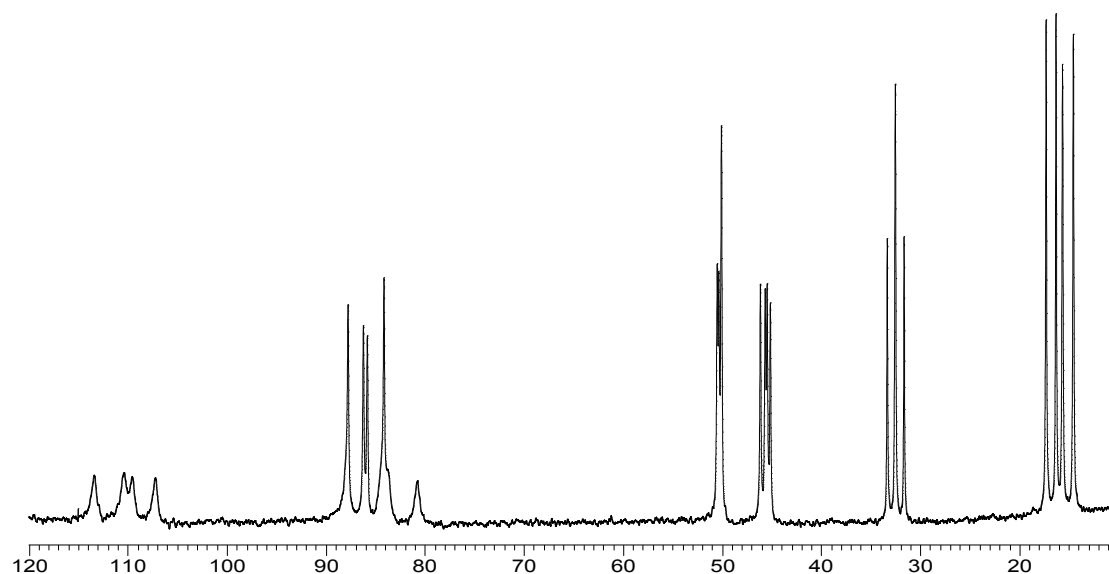


Figure 2.8: 250 MHz ^1H -NMR spectrum of the 1:1 mixture of $[\text{Co}(\text{bpy})_3][\text{PF}_6]_2$ and $[\text{Co}(\text{phen})_3][\text{PF}_6]_2$ (CD_3CN) in the region δ 120-10 ppm.

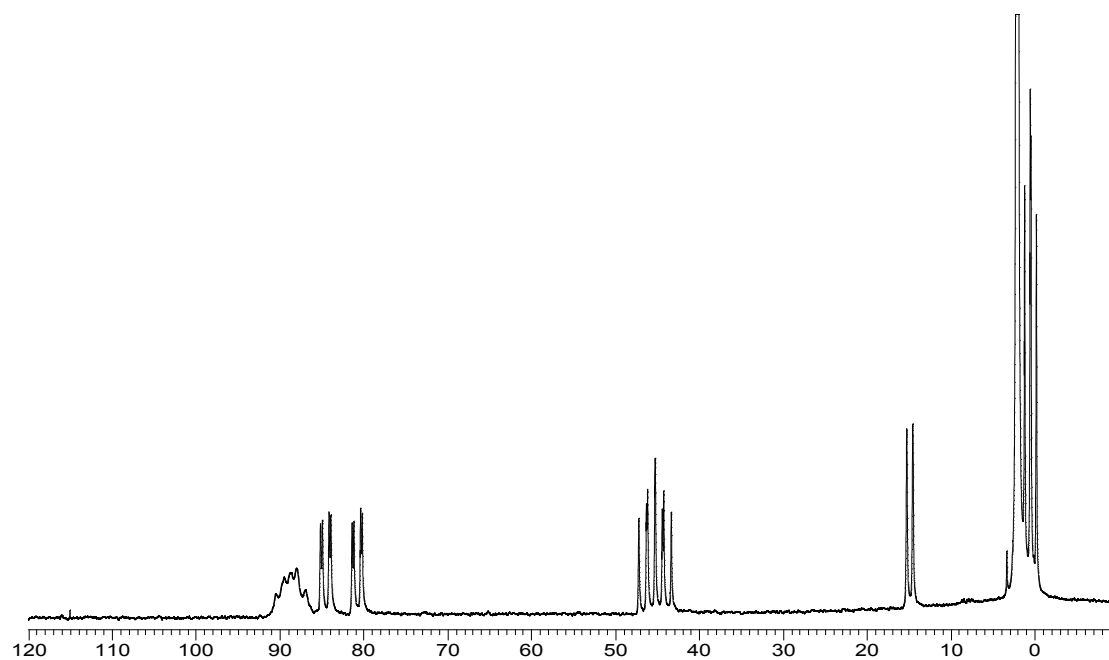


Figure 2.9: 250 MHz ^1H -NMR spectrum of the 1:1 mixture of $[\text{Co}(\text{Me}_2\text{bpy})_3][\text{PF}_6]_2$ and $[\text{Co}(\text{bpy})_3][\text{PF}_6]_2$ (CD_3CN).

In the NMR spectra, it was noticed that within each group of 4 signals for a proton in a given position, the intensities of the four signals were equal. This allowed us to calculate the relative concentration of each species in the library.

The relative concentration of one species in a mixture of $[MA_3]$, $[MAB_2]$, $[MA_2B]$ and $[MB_3]$ is obtained by dividing the integral of the peak by the number of ligands carrying the proton and by the number of equivalent protons on the ligand. Let us take again the example of M5 in the Co/Me₂bpy/phen library, where the peaks were in a 1:1:1:1 ratio:

	$[Co(Me_2bpy)_3]^{2+}$	$[Co(Me_2bpy)(phen)_2]^{2+}$	$[Co(Me_2bpy)_2(phen)]^{2+}$	$[Co(phen)_3]^{2+}$
Number of Me ₂ bpy ligands	3	1	2	0
Nr of equivalent protons on the ligand	2	2	1 and 1	0
Relative integral measured	1	1	1 and 1	0
Relative concentration	$1/(3 \times 2) = 0.167$	$1/(1 \times 2) = 0.5$	$1/(2 \times 1) = 0.5$ and $1/(2 \times 1) = 0.5$	0
Normalised concentration	1	3	3 and 3	0

Table 2.1: Calculations for the relative concentration of the products in the binary library.

When we did a similar calculation for a peak assigned to a proton in a phen ligand, we obtained the same relative concentration of 3 for each of the heteroleptic complexes and 1 for the homoleptic $[Co(phen)_3][PF_6]_2$. This confirmed that the experimental mixture reflects the predicted statistical relative concentration of its components, and this behaviour was observed in all the three possible binary combinations.

Normally, the experimental distribution of the complexes in a mixture should also be influenced by the relative stability of the species, so that it should be slightly different than what is predicted by the statistics. However, here the differences in the stabilities of the complexes were minimal (in 0.1 M KCl: $\log \beta_3 = 20.10$ for $[Co(phen)_3]^{2+}$ [79], $\log \beta_3 = 15.82$ for $[Co(bpy)_3]^{2+}$ and $\log \beta_3 = 17.55$ for $[Co(Me_2bpy)_3]^{2+}$ [80]), and the concentrations were calculated by starting from the integrals of the ¹H-NMR peaks, which were estimated to be accurate to within 5-10%, so that the differences in concentration due to the different β_3 remain unnoticed.

In the spectra obtained, each group of four peaks could be assigned to a position in the ligand but not to a precise complex, apart from the homoleptic one. For the full assignment, libraries were prepared by mixing the starting complexes in a 2:1 ratio. This caused a change in the relative integrals of the peaks and allowed us to assign each peak to a given complex.

A way to calculate the statistical composition for a 2:1 mixture of $[MA_3]$ and $[MB_3]$ is shown in Figure 2.10. Knowing the rapidity of the ligand exchange, mixing $[MA_3]$ and $[MB_3]$ in a 2:1 ratio can be considered to be the same as mixing M, A and B in a $3:6:3 = 1:2:1$ ratio. Assuming that the metal binds the ligands sequentially and without selectivity, the probability that the metal binds a ligand A as its first ligand is twice the probability of binding a ligand B, so we end up with the complexes $[MA]$ and $[MB]$ in a 2:1 ratio. Now a second ligand is added, and again the probability of adding A is twice the probability of adding B, so the probability of having each species with two ligands is obtained by multiplying the relative concentration of the previous complex with the factor 2 or 1, i.e. ($[MA_2] = 2 \times 2 = 4$), ($[MAB] = 2 \times 1 + 1 \times 2 = 4$) and ($[MB_2] = 1 \times 1 = 1$). A similar calculation is applied for the binding of the third ligand and we find that a statistical 2:1 mixture of $[MA_3]$ and $[MB_3]$ will contain the products $[MA_3]$, $[MA_2B]$, $[MAB_2]$ and $[MB_3]$ in the ratio 8:12:6:1.

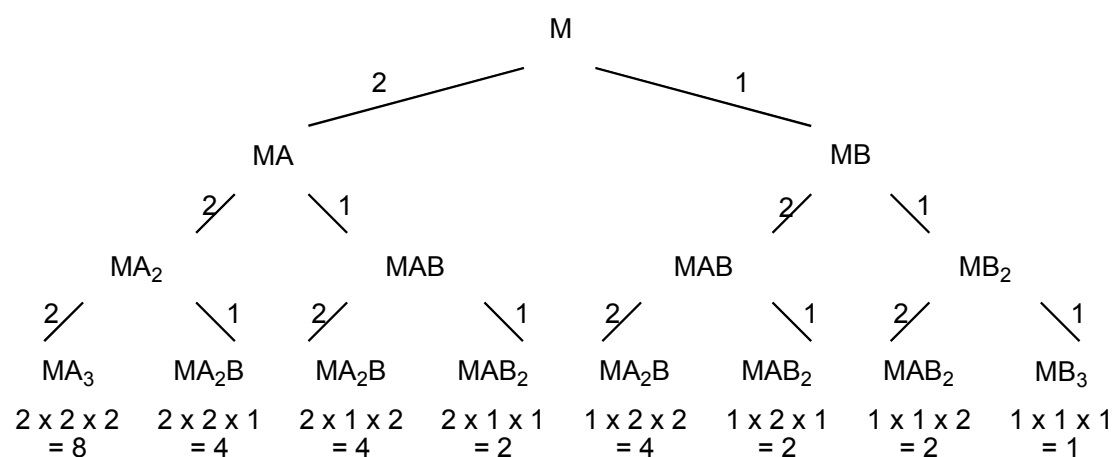


Figure 2.10: Statistical distribution of the products in the library with $M : A : B = 1 : 2 : 1$.

For any given proton in ligand A the same four NMR signals as in the 1:1 mixture were expected because the species present did not change, but their integrals, if the

distribution followed the statistics again, would be given by (statistical weight x number of ligands A x number of equivalent protons) i.e. ($[\text{MA}_3]$ $8 \times 3 \times 2 = 48$) : ($[\text{MA}_2\text{B}]$ $12 \times 2 \times 1 = 24$ twice) : ($[\text{MAB}_2]$ $6 \times 1 \times 2 = 12$). Every proton from A and B that was giving a cluster of four signals in 1:1:1:1 ratio in the 1:1 mixture would give the same four peaks in a 4:2:2:1 ratio in the 2:1 mixture.

As a good example, let us take the libraries formed by mixing $[\text{Co}(\text{bpy})_3][\text{PF}_6]_2$ and $[\text{Co}(\text{Me}_2\text{bpy})_3][\text{PF}_6]_2$ in 1:2 and 2:1 ratios. A similar analysis was made for all the other binary combinations.

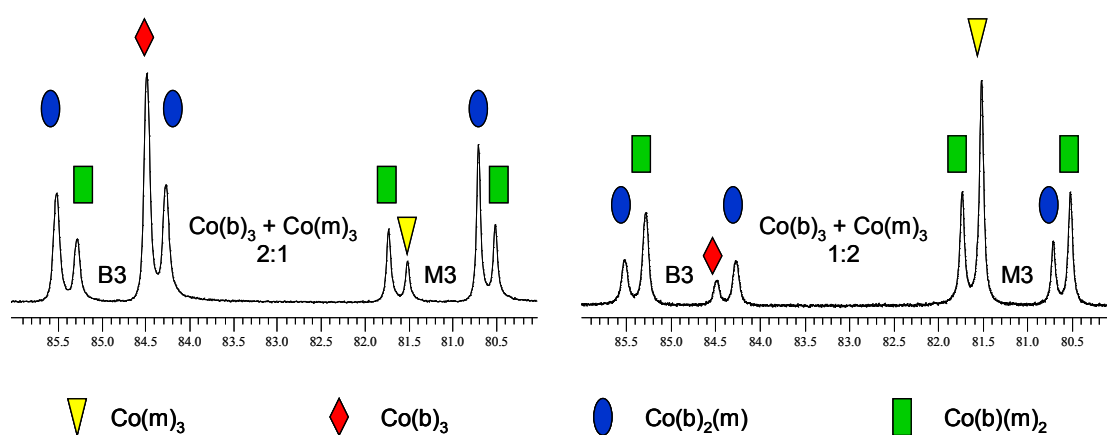


Figure 2.11: 250 MHz $^1\text{H-NMR}$ resonances (in CD_3CN) of the H3 protons of bpy (B3) and Me_2bpy (M3) in the 2:1 and 1:2 libraries. $b = \text{bpy}$, $m = \text{Me}_2\text{bpy}$.

In the example shown in Figure 2.11, the peaks belonging to the homoleptic species could be easily assigned because their shifts were known from the spectra of the pure homoleptic compounds. Of the remaining peaks we could also say that those which had the same integral within the cluster of four signals must have arisen from the same compound: one molecule of $[\text{Co}(\text{bpy})_2(\text{Me}_2\text{bpy})]^{2+}$, marked with the oval in Figure 2.11, has two non-equivalent partners of B3's, and one molecule of $[\text{Co}(\text{bpy})(\text{Me}_2\text{bpy})_2]^{2+}$, marked with the rectangle, gives rise to two peaks for M3. The fourth peak of the cluster belonged to the second mixing product. As each of the three signals for the mixing products were given by two protons, the integrals of the peaks were expected to be the same for B3 and M3, and it can be seen from the figure that the experiment was consistent with the statistical expectation.

In the same way as was done with the library prepared with equimolar amounts of pure complexes, the relative concentration of each component in the 1:2 mixtures could again be calculated.

In the 1:1 mixture, the fact that all the peaks had the same integral suggested that there was the same amount of both homoleptic complexes left and the same amount of the formed mixing products, so it was sufficient to look only at one series of four peaks to calculate the composition of the library, while the others were used just as a confirmation. In the 1:2 mixture, the peaks had different integrals, so two series of four peaks, one for each ligand, had to be considered to calculate the concentration of all four components of the library.

In the example given in Table 2.2, the mixture $[\text{Co}(\text{Me}_2\text{bpy})_3]^{2+} : [\text{Co}(\text{bpy})_3]^{2+}$ equal to 1:2 is considered. The four peaks for M3 allowed us to calculate the relative concentrations of $[\text{Co}(\text{Me}_2\text{bpy})_3]^{2+}$, $[\text{Co}(\text{bpy})(\text{Me}_2\text{bpy})_2]^{2+}$ and $[\text{Co}(\text{bpy})_2(\text{Me}_2\text{bpy})]^{2+}$, whereas to find the concentration of $[\text{Co}(\text{bpy})_3]^{2+}$, a series of peaks belonging to the bpy ligand had to be considered, and here the peaks for B3 were chosen. The values obtained with the peaks of B3 for the mixing products should be the same as those obtained with M3, and the results given in the table confirmed the calculations.

M3	$[\text{Co}(\text{m})_3]^{2+}$	$[\text{Co}(\text{b})_2(\text{m})]^{2+}$	$[\text{Co}(\text{b})(\text{m})_2]^{2+}$	B3	$[\text{Co}(\text{b})_3]^{2+}$	$[\text{Co}(\text{b})_2(\text{m})]^{2+}$	$[\text{Co}(\text{b})(\text{m})_2]^{2+}$
Nr of ligands	3	1	2	Nr of ligands	3	2	1
Nr of equivalent protons	2	2	1 and 1	Nr of equivalent protons	2	1 and 1	2
Rel. int. measured	0.2	1.0	0.5 and 0.5	Rel. int. measured	2.1	1.0 and 1.2	0.5
Rel. conc.	0.03	0.50	0.25	Rel. conc	0.35	0.55	0.25

Table 2.2: Calculation of the composition of the 1:2 mixture of $[\text{Co}(\text{Me}_2\text{bpy})_3][\text{PF}_6]_2$ and $[\text{Co}(\text{bpy})_3][\text{PF}_6]_2$; $b = \text{bpy}$, $m = \text{Me}_2\text{bpy}$.

Putting everything together, the results could be normalised to the concentration of one of the four compounds. Here, the compound in the smallest amount was chosen each time, then the average considering several peaks, and the equilibrium constant K

for the library was then calculated. In the following section, [] is used to mean concentration and the use of square brackets to designate a “complex” is ignored. The equilibrium constant for the reaction



is given by the equation:

$$K = \frac{[MAB_2][MA_2B]}{[MA_3][MB_3]} \quad \text{Eq. 2.2}$$

In the 1:1 mixture, where the relative concentrations are $[MA_3] : [MA_2B] : [MAB_2] : [MB_3] = 1:3:3:1$, the equilibrium constant K is

$$K = \frac{3 \cdot 3}{1 \cdot 1} = 9 \quad \text{Eq. 2.3}$$

and

$$\log K = 0.95 \quad \text{Eq. 2.4}$$

This value depends only on the reaction conditions (temperature and pressure) and not on the starting concentrations. Therefore, it should be the same, even when the starting concentrations are different from 1:1, because the reaction conditions were kept constant (room temperature and atmospheric pressure).

In Table 2.3 are listed all the normalised concentrations for the four compounds in the binary libraries studied. It was noticed that the expected theoretical distribution of $[MA_3] : [MA_2B] : [MAB_2] : [MB_3] = 8:12:6:1$ in the 2:1 mixtures was relatively well reflected in the experiments. Also the equilibrium constant K was approximately the same for all the libraries considered. Differences from the theoretical value were due either to experimental errors, or errors in the calculation of the integrals in the NMR spectra.

Chapter 2

A	B	ratio	[Co(A) ₃] ²⁺	[Co(A) ₂ (B)] ²⁺	[Co(A)(B) ₂] ²⁺	[Co(B) ₂] ²⁺	K	log K
bpy	Me ₂ bpy	2:1	11.0	18.0	7.5	1.0	12.0 ± 2.4	1.08
bpy	Me ₂ bpy	1:2	1.0	7.1	15.0	9.5	11.0 ± 2.2	1.04
Me ₂ bpy	phen	2:1	9.0	12.0	6.0	1.0	8.0 ± 1.6	0.90
Me ₂ bpy	phen	1:2	1.0	5.8	12.0	8.8	7.9 ± 1.6	0.90
bpy	phen	2:1	7.7	12.0	6.0	1.0	9.4 ± 1.9	0.97
bpy	phen	1:2	1.0	6.3	13.0	9.2	8.9 ± 1.8	0.95

Table 2.3: Relative concentrations of each species in different mixtures, and equilibrium constants for the mixtures. The concentrations were calculated from the ¹H-NMR integrals with an estimated error of 10% and rounded to two significant digits. The error in K was calculated with the error propagation formula.

A final confirmation of the assignments and the formation of a dynamic combinatorial library of complexes came from the ¹H-NMR spectra of 1:3 and 3:1 mixtures of two homoleptic complexes. In this case, the expected composition of the 3:1 mixture of [MA₃] and [MB₃] is a 27:27:9:1 mixture of [MA₃], [MA₂B], [MAB₂] and [MB₃]. These values were calculated in a similar way as explained in Figure 2.9 for the 2:1 mixture.

The position of the ¹H-NMR peaks would be the same as for the 1:1 mixture again, so each non equivalent proton on the free ligand would give rise to a cluster of four signals in the library of complexes. The relative integrals of the signals within a cluster is again given by (statistical weight x number of ligands A (or B) x number of equivalent protons), so it could be predicted that each proton of each ligand would give rise to four peaks in a 9:3:3:1 ratio. This is illustrated in Figure 2.12 for the methyl protons of Me₂bpy and H3 protons of bpy in a 3:1 mixture of [Co(Me₂bpy)₃][PF₆]₂ and [Co(bpy)₃][PF₆]₂. Within experimental error, the expected 9:3:3:1 ratio of peaks was obtained.

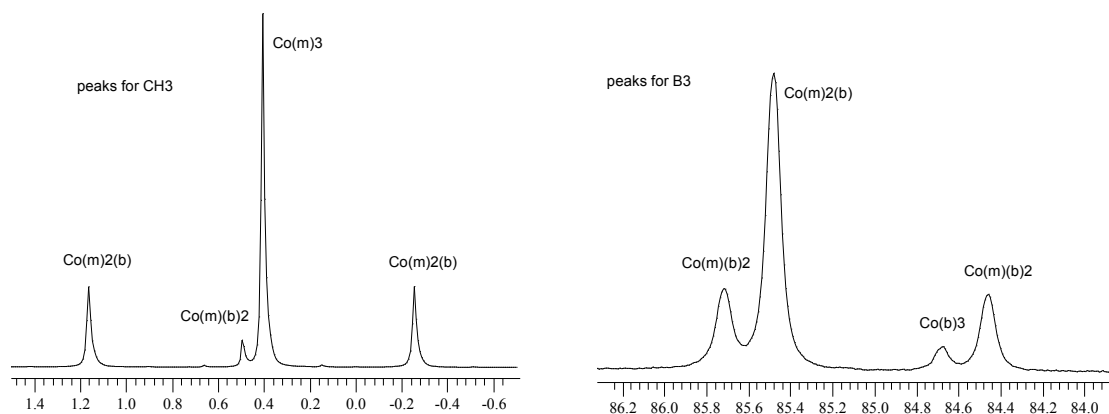


Figure 2.12: 250 MHz ^1H -NMR resonances of the methyl protons of Me_2bpy (left) and H_3 protons of bpy (B3, right) in a 3:1 mixture of $[\text{Co}(\text{Me}_2\text{bpy})_3][\text{PF}_6]_2$ and $[\text{Co}(\text{bpy})_3][\text{PF}_6]_2$ in CD_3CN .

2.3. Libraries containing three different ligands

The same three complexes, $[\text{Co}(\text{bpy})_3][\text{PF}_6]_2$ (**4**), $[\text{Co}(\text{Me}_2\text{bpy})_3][\text{PF}_6]_2$ (**5**) and $[\text{Co}(\text{phen})_3][\text{PF}_6]_2$ (**6**), that were used to form the binary libraries were mixed together to give rise to a ternary library; ternary because it is created with three starting complexes.

The resulting spectrum looked more complicated and some peaks overlapped because the number of compounds in equilibrium in the library had increased to ten (Figures 2.13 and 2.14). In addition to the homoleptic complexes, the mixing products of each possible combination of two ligands and the compound formed by the complexation of all three ligands around one cobalt were found. The statistical relative concentration was 1 for the homoleptic complexes, 3 for the binary mixed products and 6 for the ternary mixed product.

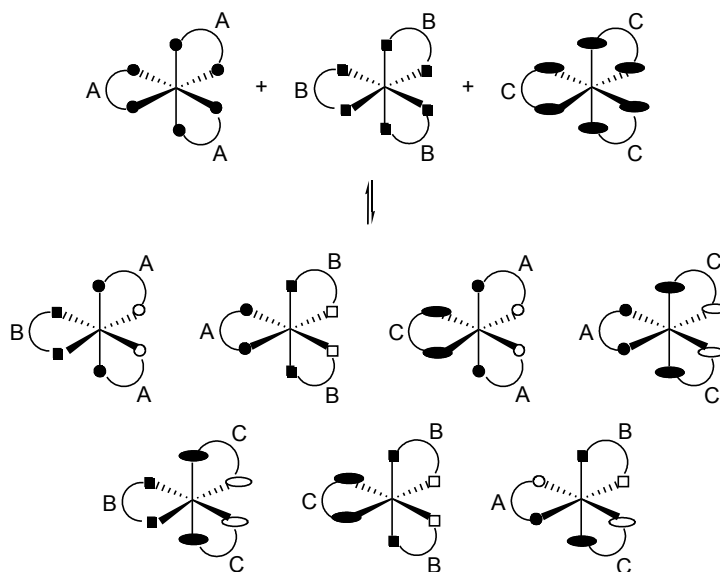


Figure 2.13: Products of the ternary library of model systems $[MA_3]$, $[MB_3]$ and $[MC_3]$.

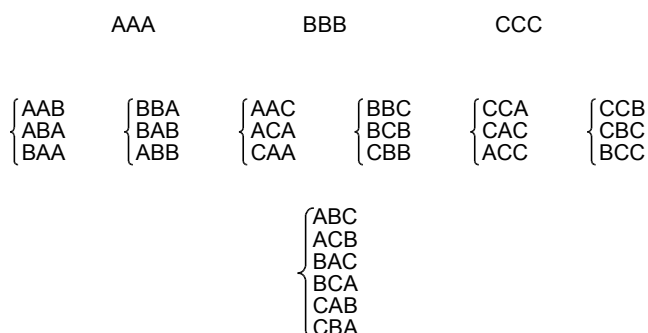


Figure 2.14: Statistical distribution of the species in the ternary library.

A 1:1:1 mixture of the three homoleptic complexes led, as in the binary case, to a library with the expected number of components, here ten. Each proton could be in nine different environments, and so each proton of a given ligand gave rise to nine signals. These different environments were, for example for a proton of ligand A: one for $[MA_3]$, two each for $[MA_2B]$, $[MA_2C]$, and $[MABC]$, and one each for $[MAB_2]$ and $[MAC_2]$.

It could be observed from the NMR spectrum that all the peaks showed the same integral. At first sight it looked as if a few peaks were twice the integral of the others,

but by observing more closely and counting the number of signals, it was noticed that those “anomalous” peaks were the result of the overlapping of two signals. If the expected relative integrals of the NMR peaks for a statistical mixture of $[\text{MA}_3]$, $[\text{MAB}_2]$, $[\text{MAC}_2]$, $[\text{MA}_2\text{B}]$, $[\text{MA}_2\text{C}]$ and $[\text{MABC}]$ are calculated with (statistical weight \times number of ligands A \times number of equivalent protons), a ratio of $(1 \times 3 \times 2 = 6) : (3 \times 1 \times 2 = 6) : (3 \times 1 \times 2 = 6) : (3 \times 2 \times 1 = 6)$ and $(3 \times 2 \times 1 = 6) : (3 \times 2 \times 1 = 6) : (6 \times 1 \times 1 = 6)$ and $(6 \times 1 \times 1 = 6)$ is obtained, i.e. 1:1:1:1:1:1:1:1:1. Every proton of ligand A would give nine peaks of equal intensity, and by similar analysis also every proton of B and C. So, from this calculation and the signals observed on the NMR spectrum, it could be concluded once again that the library reached its statistical composition.

Here again, the signals could not be fully assigned just from the spectrum of the 1:1:1 mixture of complexes, but help came when comparing this spectrum with those previously obtained with the binary mixtures. The only new signals that had not been observed in the binary mixtures were the ones arising from the ternary complex $[\text{Co}(\text{bpy})(\text{Me}_2\text{bpy})(\text{phen})]^{2+}$. By overlapping the spectrum of the ternary mixture with the three of the binary mixtures that had already be assigned, the peaks overlapped and the assignment became purely a game of patience. The peaks that did not find their identical partners in any of the binary libraries had to belong to the ternary complex. Furthermore, ^1H - ^1H COSY spectroscopy was used to confirm the assignments made. In any binary complex $[\text{MA}_2\text{B}]$ and $[\text{MA}_2\text{C}]$, and in the ternary complex $[\text{MABC}]$, each proton on the ligand A gave rise to two signals and the two sub-spectra were identified on the COSY spectrum. Nevertheless, it was not possible to assign these to pyridine rings *trans* to A, B or C through NOESY spectroscopy, because the ligand exchange reaction was too fast for the NMR time scale and exchange cross-peaks would also be obtained, as explained in more details in Chapter 4. The full assignment of the ternary library, following from a COSY spectrum, is presented in the Tables 2.4 and 2.5.

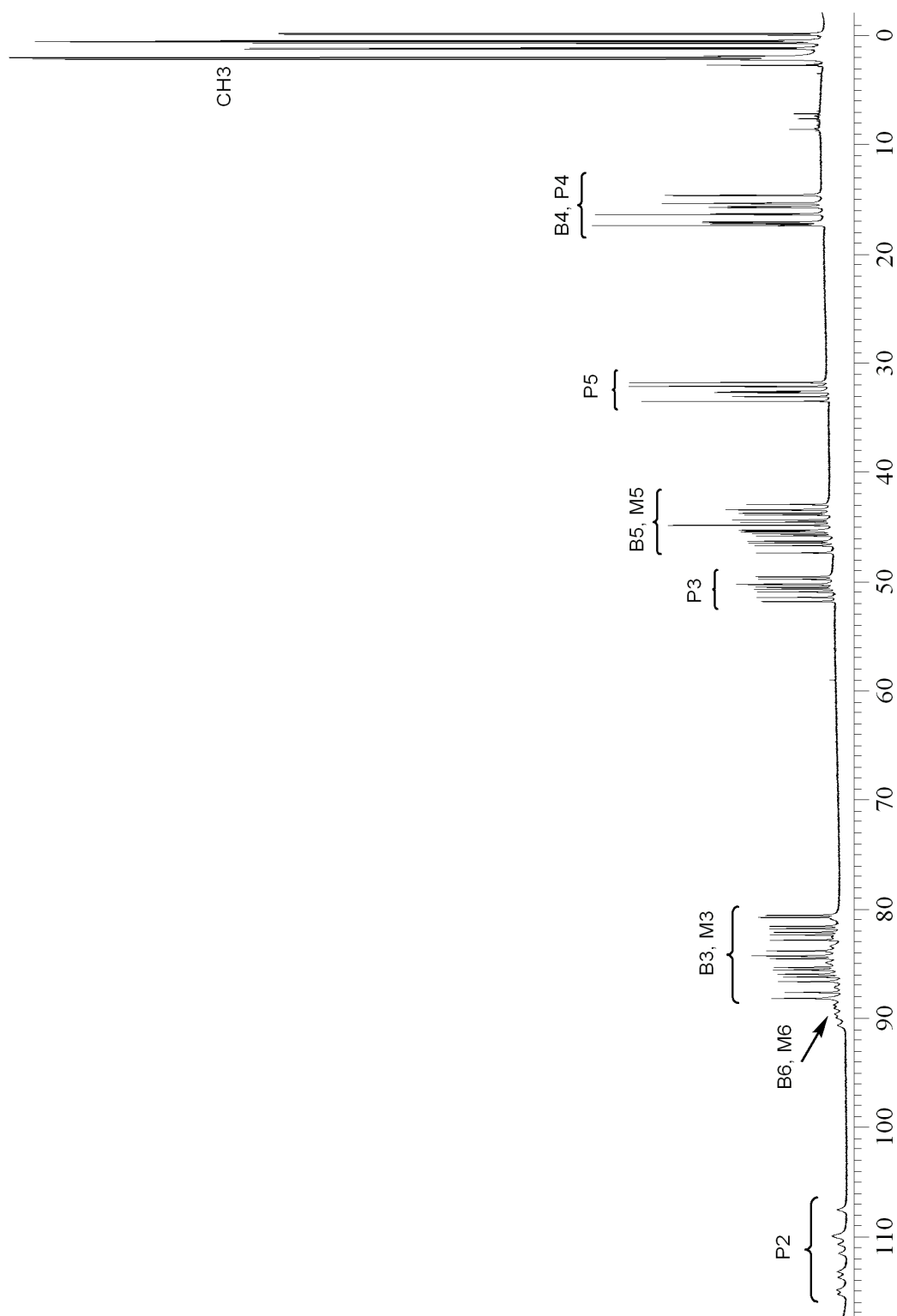


Figure 2.15: 500 MHz $^1\text{H-NMR}$ spectrum of a 1:1:1 mixture of $[\text{Co}(\text{bpy})_3][\text{PF}_6]_2$, $[\text{Co}(\text{Me}_2\text{bpy})_3][\text{PF}_6]_2$ and $[\text{Co}(\text{phen})_3][\text{PF}_6]_2$ in CD_3CN .

		bpy				phen				Me ₂ bpy				
		H ₆	H ₅	H ₄	H ₃	H ₂	H ₃	H ₄	H ₅	H ₆	H ₅	H ₆	H ₃	CH ₃
bpy	bpy	87.96	46.25	14.58	84.48	-	-	-	-	-	-	-	-	-
Me ₂ bpy	Me ₂ bpy	-	-	-	-	-	-	-	-	89.74	44.50	81.52	0.40	
phen	phen	-	-	-	-	107.20	50.18	17.33	33.43	-	-	-	-	
bpy	bpy	84.50 [†]	45.57	14.58	86.58	113.7	50.64	16.33	31.73	-	-	-	-	
phen	phen	83.88 [†]	45.76	15.69	86.16	-	-	-	-	-	-	-	-	
phen	bpy	80.91	45.24	15.66	88.13	110.7 [†]	50.46	17.33	32.64 [†]	-	-	-	-	
bpy	Me ₂ bpy	90.68	46.41	15.26	85.28	110.0 [†]	50.23	16.33	32.58 [†]	-	-	-	-	
Me ₂ bpy	Me ₂ bpy	*	47.32	15.32	85.51	-	-	-	-	*	43.39 [†]	81.73 [†]	1.16 [†]	
Me ₂ bpy	bpy	*	45.31	14.53	84.26	-	-	-	-	*	45.38 [†]	80.51 [†]	-0.25 [†]	
Me ₂ bpy	phen	-	-	-	-	111.5 [†]	51.40	17.10	33.01 [†]	82.48	43.35	84.22	0.49	
phen	Me ₂ bpy	-	-	-	-	110.0 [†]	49.51	17.22	32.52 [†]	-	-	-	-	
phen	Me ₂ bpy	-	-	-	-	114.8	50.89	17.00	32.06	86.43	44.79 [†]	83.78	1.06 [†]	
	Me ₂ bpy	-	-	-	-	-	-	-	-	84.91	42.89 [†]	82.06	-0.12 [†]	

Table 2.4: 500 MHz ¹H-NMR peaks (δ / ppm) of the homoleptic [CoA₃]²⁺ and binary complexes [CoAB₂]²⁺ in the 1:1:1 mixture of [Co(bpy)₃][PF₆]₂, [Co(Me₂bpy)₃][PF₆]₂ and [Co(phen)₃][PF₆]₂ in CD₃CN.

* δ 89.49, 88.81, 88.61, 87.97 ppm, ambiguous.

[†] Assignment to individual sub-spectrum ambiguous.

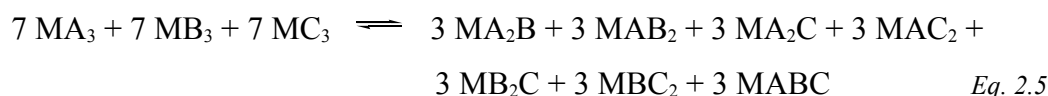
Chapter 2

	H ₆ (H ₂)	H ₅ (H ₃)	H ₄	H ₃ (H ₅)	CH ₃
bpy	87.96	46.66	15.32	87.58	-
		44.79	15.59	85.91	-
Me ₂ bpy	89.74	43.84 [†]	-	82.79 [†]	0.38 [†]
		43.68 [†]	-	82.30 [†]	0.64 [†]
phen	115.2 [†]	51.77	17.07	32.00 [†]	-
	113.1 [†]	49.74	16.25	31.69 [†]	-

Table 2.5: 500 MHz ¹H-NMR peaks (δ / ppm) of the ternary complex [CoABC]²⁺ in the 1:1:1 mixture of [Co(bpy)₃][PF₆]₂, [Co(Me₂bpy)₃][PF₆]₂ and [Co(phen)₃][PF₆]₂ in CD₃CN.

[†] Assignment to individual sub-spectrum ambiguous.

The equilibrium constant for the reaction



is given by

$$K = \frac{[\text{MA}_2\text{B}]^3 [\text{MAB}_2]^3 [\text{MA}_2\text{C}]^3 [\text{MAC}_2]^3 [\text{MB}_2\text{C}]^3 [\text{MBC}_2]^3 [\text{MABC}]^3}{[\text{MA}_3]^7 [\text{MB}_3]^7 [\text{MC}_3]^7} \quad \text{Eq. 2.6}$$

For the statistical mixture with the distribution 1:1:1:3:3:3:3:3:6, *K* takes the value

$$K = \frac{3^3 \cdot 3^3 \cdot 3^3 \cdot 3^3 \cdot 3^3 \cdot 3^3 \cdot 6^3}{1^7 \cdot 1^7 \cdot 1^7} = 8.37 \cdot 10^{10} \quad \text{Eq. 2.7}$$

And

$$\log K = 10.92 \quad \text{Eq. 2.8}$$

In the calculation of the equilibrium constant we needed to be careful about the stoichiometric coefficients of the chemical equation we used, which were not all equal to 1 as in the binary mixtures. Furthermore, for a comparison of several equilibrium constants, it was important to always use the same coefficients: if they are multiplied or divided by any value, the equilibrium constant will change by a power of that value.

A non-equimolar mixture of the three complexes was prepared ([Co(bpy)₃]²⁺ : [Co(Me₂bpy)₃]²⁺ : [Co(phen)₃]²⁺ = 2:1:1) and the composition at equilibrium was

studied by $^1\text{H-NMR}$ spectroscopy. The equilibrium constant was compared with the K of the equimolar mixture and it revealed itself consistent with the previous value.

bpy : Me ₂ bpy : phen	[Co(b) ₃] ²⁺	[Co(m) ₃] ²⁺	[Co(p) ₃] ²⁺	[Co(b) ₂ (m)] ²⁺	[Co(b)(m) ₂] ²⁺
1 : 1 : 1	1	1	1	3	3
2 : 1 : 1	1.00	0.10	0.10	1.46	0.86
bpy : Me ₂ bpy : phen	[Co(b) ₂ (p)] ²⁺	[Co(b)(p) ₂] ²⁺	[Co(m) ₂ (p)] ²⁺	[Co(m)(p) ₂] ²⁺	[Co(b)(m)(p)] ²⁺
1 : 1 : 1	3	3	3	3	6
2 : 1 : 1	1.39	0.75	0.30	0.15	1.30
bpy : Me ₂ bpy : phen	K		log K		
1 : 1 : 1	8.37·10 ¹⁰		10.92		
2 : 1 : 1	4.49·10 ¹⁰		10.65		

Table 2.6: Relative concentration of each compound and equilibrium constants in the two ternary libraries; $b = \text{bpy}$, $m = \text{Me}_2\text{bpy}$, $p = \text{phen}$.

2.4. Conclusions

In this chapter it was demonstrated that the Co(II)/2,2'-bipyridine ligand system exchanges its ligands virtually instantaneously and that a mixture of different complexes forms a library of compounds in the predicted statistical distribution. These are the two base requisites for the formation of a dynamic combinatorial library. In addition to this, it was shown that the composition of the libraries could be analysed relatively easily by $^1\text{H-NMR}$ spectroscopy. These characteristics establish the Co(II)/2,2'-bipyridine ligands system as an ideal candidate for the formation of new dynamic combinatorial libraries.

3. Co²⁺/Co³⁺ ligand exchange

3.1. Introduction

It was demonstrated in the previous chapter that Co(II) complexes with diimine ligands are kinetically labile and exchange their 2,2'-bipyridine and 1,10-phenanthroline ligands very rapidly to easily form a dynamic combinatorial library of [CoL₃]²⁺ complexes. It is known that if the complex is oxidised to the Co(III) state, ligand exchange reactions are much slower: rate constants are in the range of 10⁻³ M⁻¹s⁻¹, compared to 10-10³ M⁻¹s⁻¹ for complexes with Co(II) centres [39]. In fact it should be possible to freeze the rapid exchange of the components of a Co(II)-complex library by oxidising the metal ion, and it was reported that after oxidation of the metal, no meaningful ligand exchange occurred for several days [39]. But what happens with a mixture of Co(II) and Co(III) species? Can a second level of exchange be added to the already known library?

The metal centre of the complexes used for the experiments described in Chapter 2 was oxidised, and different mixtures of two complexes with different ligands and different cobalt oxidation states were prepared and analysed by ¹H-NMR spectroscopy to see whether any exchange reaction was occurring.

3.2. Synthesis of the complexes

For these experiments, the ligands 2,2'-bipyridine (bpy) and 1,10-phenanthroline (phen) were chosen because their ¹H-NMR signals were easy to distinguish.

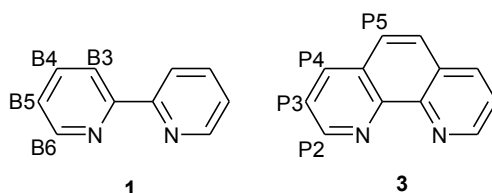


Figure 3.1: Ligands used for the Co(II)/Co(III) mixtures showing the numbering scheme used for the protons.

The Co(III) complexes were obtained by treating the Co(II) complexes suspended in water with aqueous bromine, and then precipitated as the $[\text{PF}_6]^-$ salts. The completion of the reaction was recognised when the colour of the suspension became darker, and the $^1\text{H-NMR}$ spectrum confirmed the absence of any Co(II) species. The Co(III) centre has a low spin d^6 electronic configuration and is diamagnetic, therefore the $^1\text{H-NMR}$ spectra of its complexes do not show the large chemical shift range observed with the paramagnetic Co(II), but instead exhibit signals ranging from δ 0 to 10 ppm.

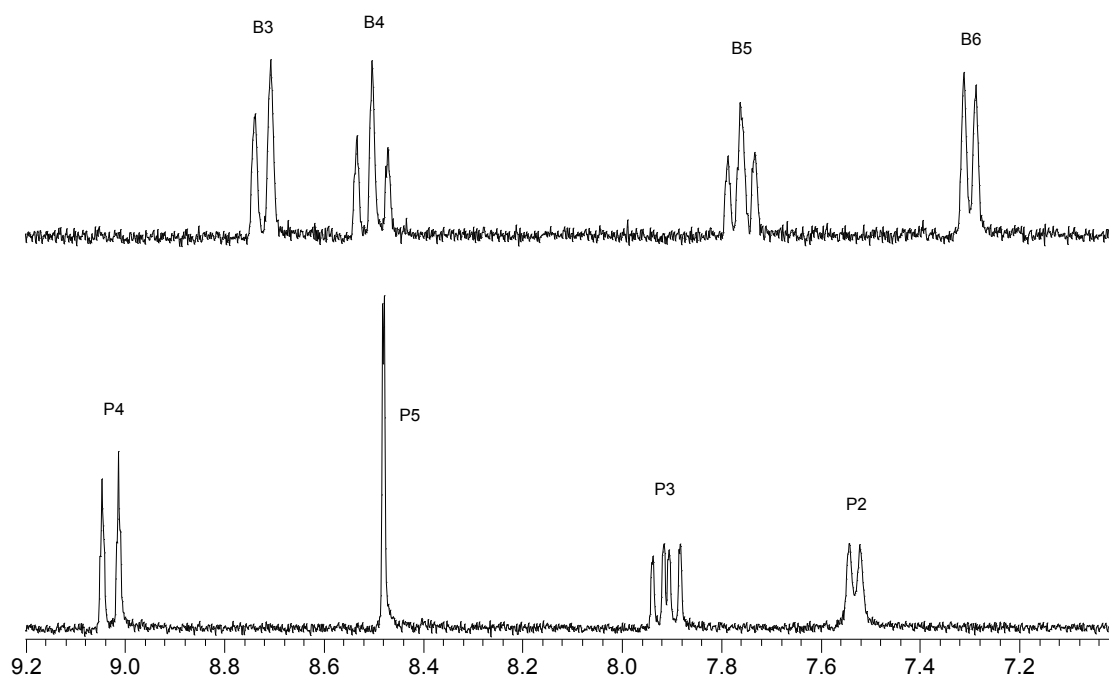


Figure 3.2: 250 MHz $^1\text{H-NMR}$ spectra of $[\text{Co}(\text{bpy})_3][\text{PF}_6]_3$ (7, top) and $[\text{Co}(\text{phen})_3][\text{PF}_6]_3$ (8, bottom) in CD_3CN .

The least shifted peak in the spectrum of $[\text{Co}(\text{phen})_3][\text{PF}_6]_3$ was assigned to proton P2 on the basis of its coupling constant: a value of $J \approx 4.8$ Hz (here $J = 5.25$ Hz) is typical for the coupling between the proton closest to the nitrogen and its neighbour [52]. Consequently, the second doublet at δ 9.03 ppm with $J = 8.25$ Hz was attributed to P4. Of the remaining protons, the one that was coupling to two protons was P3, and it was assigned to the doublet of doublets at δ 7.91 ppm, while P5 was assigned to the signal at δ 8.48 ppm. This was a thin doublet, and the coupling constant was so small that it was not visible on the signal of its coupling partner, P4 or eventually P3.

The spectrum for $[\text{Co}(\text{bpy})_3][\text{PF}_6]_3$ was interpreted with the help of that of $[\text{Co}(\text{phen})_3][\text{PF}_6]_3$, especially for the assignment of the two triplets: proton B5 was attributed to the signal at δ 7.76 ppm because its analogue on phen (P3) had a shift around that value, consequently the second triplet of the spectrum was assigned to the second proton on bpy able to give two couplings, B4. The least shifted doublet, with its coupling constant of $J = 6.00$ Hz, was assigned to B6 for the same reasons explained above, and the most shifted signal with $J = 7.75$ Hz to the remaining B3. This is also in good agreement with the coupling constant of about 8.0 Hz known for the coupling between protons H3 and H4 of $[\text{Co}(\text{terpy})_2]^{3+}$ (terpy = 2,2':6',2''-terpyridine) and $[\text{Fe}(\text{bpy})_3]^{2+}$ [52].

3.3. $[\text{Co}(\text{bpy})_3]^{3+}$ and $[\text{Co}(\text{phen})_3]^{3+}$

$[\text{Co}(\text{bpy})_3][\text{PF}_6]_3$ and $[\text{Co}(\text{phen})_3][\text{PF}_6]_3$ in CD_3CN were mixed in an NMR tube in a 1:2 ratio. ^1H -NMR spectra were measured immediately after mixing and then at different later times, while the mixture was kept at room temperature. All the spectra showed the sum of the peaks of the single complexes and no new signals appeared. This experiment indicates that Co(III) complexes do not undergo any ligand exchange for at least 1 week at room temperature.

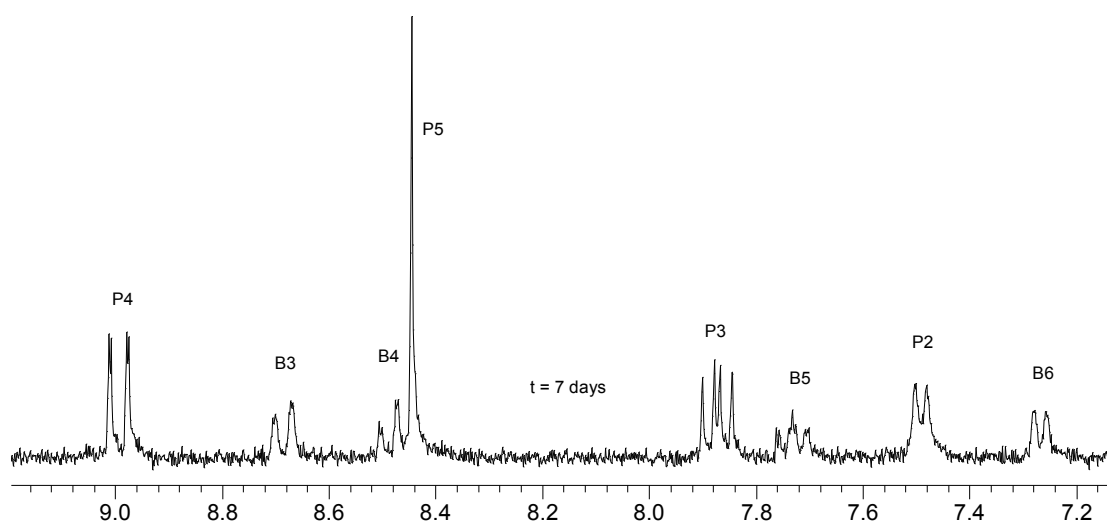


Figure 3.3: Expansion of a 250 MHz ^1H -NMR spectrum of a mixture of $[\text{Co}(\text{bpy})_3][\text{PF}_6]_3$ and $[\text{Co}(\text{phen})_3][\text{PF}_6]_3$ one week after mixing.

3.4. $[\text{Co}(\text{bpy})_3]^{3+}$ and $[\text{Co}(\text{phen})_3]^{2+}$

Equal amounts of 5 mM solutions in CD_3CN of $[\text{Co}(\text{bpy})_3][\text{PF}_6]_3$ and $[\text{Co}(\text{phen})_3][\text{PF}_6]_2$ were mixed in an NMR tube. ^1H -NMR spectra were recorded immediately after mixing and then after 1, 2, and 7 days at room temperature.

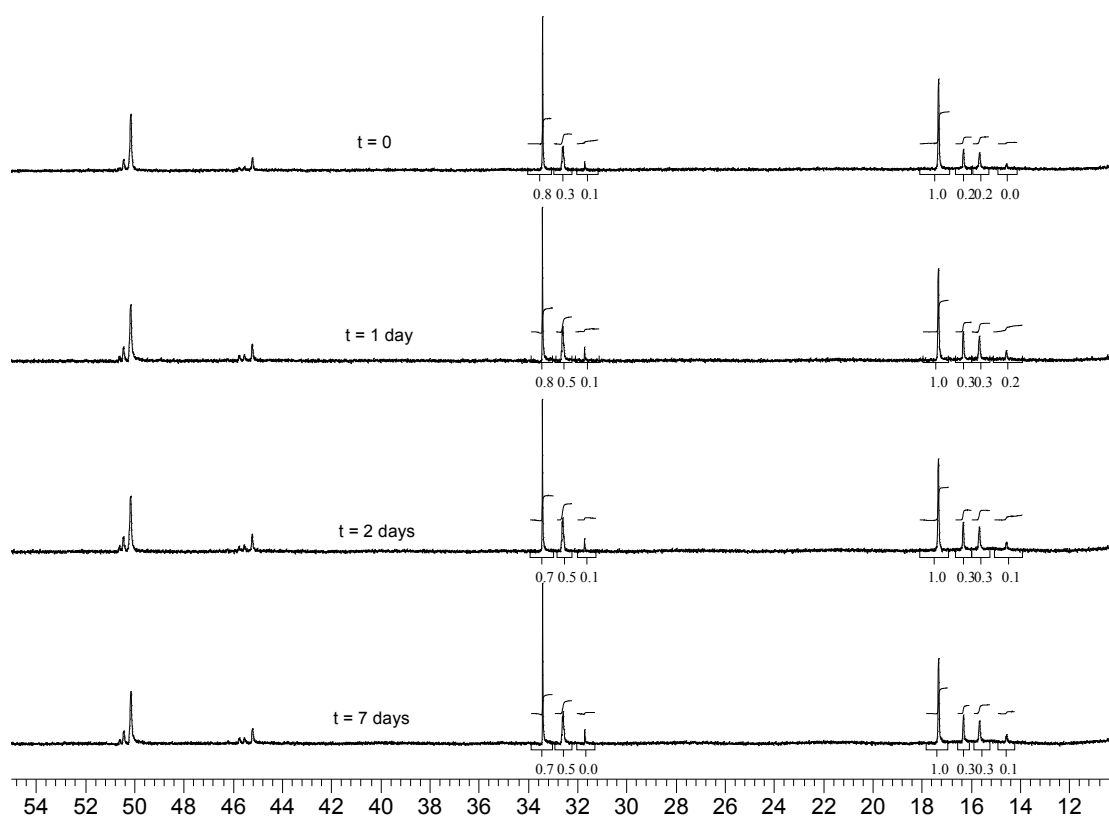


Figure 3.4: Expansions of 250 MHz ^1H -NMR spectra (CD_3CN) of a 1:1 mixture of $[\text{Co}(\text{bpy})_3]^{3+}$ and $[\text{Co}(\text{phen})_2]^{2+}$ at different times showing the integrals of some peaks.

In Figure 3.4 are shown the ^1H -NMR spectra of the mixtures in the range where the Co(II) species resonate. Right after the mixing, at time $t = 0$, the peaks for $[\text{Co}(\text{phen})_3]^{2+}$ were clearly predominant, but some other small signals were already visible. After one day the composition of the mixture had changed, and the species present were recognisable by comparison with the spectra encountered in the previous chapter with the mixtures of $[\text{Co}(\text{bpy})_3]^{2+}$ and $[\text{Co}(\text{phen})_3]^{2+}$: the four signals around δ 16 ppm corresponded to the cluster of four peaks for P4 and B4, which happened to overlap, in $[\text{Co}(\text{phen})_3]^{2+}$, $[\text{Co}(\text{phen})_2(\text{bpy})]^{2+}$ and $[\text{Co}(\text{phen})(\text{bpy})_2]^{2+}$, while the three signals around δ 32 ppm were the result of the overlapping of the peaks for P5 in the

same complexes. The very small peaks around δ 46 ppm belonged to B5 in the different Co(II) complexes. Other signals for the bpy ligand were visible around δ 86 ppm (not shown in the figure), but their intensity was also very weak, suggesting that $[\text{Co}(\text{phen})_2]^{2+}$ and $[\text{Co}(\text{phen})_2(\text{bpy})]^{2+}$ were present in the mixture in significant larger concentration than $[\text{Co}(\text{phen})(\text{bpy})_2]^{2+}$ and $[\text{Co}(\text{bpy})_3]^{2+}$.

The composition of the mixture (based on the NMR spectra) did not change after one day, equilibrium having then been reached.

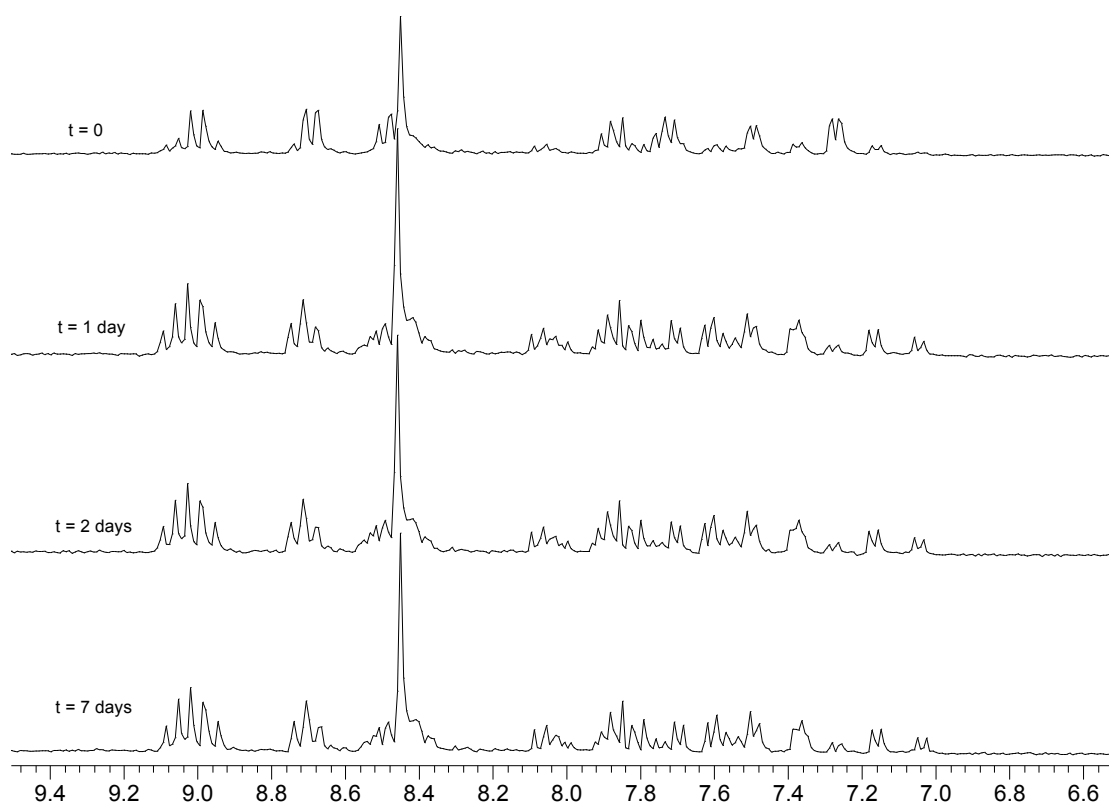


Figure 3.5: Expansions of 250 MHz ^1H -NMR spectra (CD_3CN) of a 1:1 mixture of $[\text{Co}(\text{bpy})_3]^{3+}$ and $[\text{Co}(\text{phen})_2]^{2+}$ at different times.

Figure 3.5 shows the same NMR spectra as Figure 3.4, but in the range for the Co(III) species. At $t = 0$, peaks for the homoleptic $[\text{Co}(\text{phen})_3]^{3+}$ were recognisable along with the peaks for the starting material $[\text{Co}(\text{bpy})_3]^{3+}$. The relative amounts of the two compounds were approximately the same. Some other peaks were observed, but not with any significant intensity. After one day a number of other signals were observed. These were not studied in detail but intuitively they could be assigned to the two

heteroleptic Co(III) complexes. The relative intensities of the peaks did not change after $t = 1$ day, which confirmed the observation made with the signals of the Co(II) species that equilibration of the system was reached within one day.

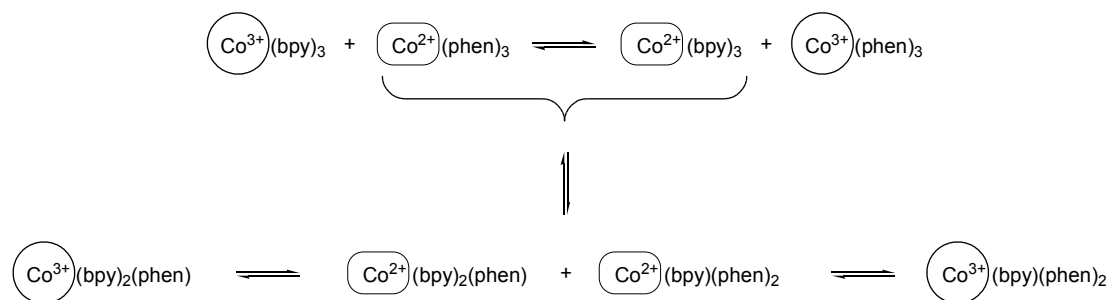


Figure 3.6: Reaction scheme of the exchange in the mixture of $[\text{Co}(\text{bpy})_3][\text{PF}_6]_3$ and $[\text{Co}(\text{phen})_3][\text{PF}_6]_2$.

From the experiment described in the section 3.3, we know that Co(III) complexes are inert and do not exchange their ligands; a mechanism involving a redox equilibrium was proposed for the formation of the mixing products observed in the NMR spectra. This is illustrated in Figure 3.6: in the first step there was a redox exchange between $[\text{Co}(\text{bpy})_3]^{3+}$ and $[\text{Co}(\text{phen})_3]^{2+}$, yielding the same homoleptic complexes but in the other oxidation state. At this point, two Co(II) species were present in the mixture, that could easily exchange their ligands as in the experiments presented in Chapter 2. This ligand exchange gave as products the heteroleptic complexes $[\text{Co}(\text{bpy})_2(\text{phen})]^{2+}$ and $[\text{Co}(\text{bpy})(\text{phen})_2]^{2+}$. In the last step, both newly formed heteroleptic complexes underwent a redox reaction with a Co(III) species, to form $[\text{Co}(\text{bpy})_2(\text{phen})]^{3+}$ and $[\text{Co}(\text{bpy})(\text{phen})_2]^{3+}$.

In this way, a mixture of eight compounds was obtained, forming two subsets of ^1H -NMR peaks: one set for the four Co(II) complexes already encountered in the previous chapter, visible in the range δ 110 to 10 ppm, and one set for their corresponding Co(III) species, visible in the range δ 10 to 0 ppm.

The analysis of the relative concentrations of the Co(III) species was not possible with just this spectrum, the peaks are so close to each other that not even a ^1H - ^1H -COSY spectrum would be of much help, its study being already very complicated for the Co(II) species. For this reason, and also because this library involves not only one but

four equilibria linked between each other, no further investigation was made on this system.

3.5. $[\text{Co}(\text{bpy})_3]^{2+}$ and $[\text{Co}(\text{phen})_3]^{3+}$

A 1:1 mixture of $[\text{Co}(\text{bpy})_3][\text{PF}_6]_2$ and $[\text{Co}(\text{phen})_3][\text{PF}_6]_3$ in CD_3CN was prepared in an NMR tube and was analysed by ^1H -NMR spectroscopy immediately after mixing and at several later times. The mixture was kept at room temperature.

The first ^1H -NMR spectrum was surprising because only very low intensity signals were visible above δ 10 ppm, in the region where usually Co(II) complexes appear. After one day there was virtually no Co(II) species left in the mixture. It looked as though all the cobalt(II) centres had oxidised, but nothing had been reduced.

The first attempt at an explanation was to say that the Co(II) species had reacted with oxygen from the air. The experiment was repeated with a degassed solution and under a nitrogen atmosphere, but the result was the same.

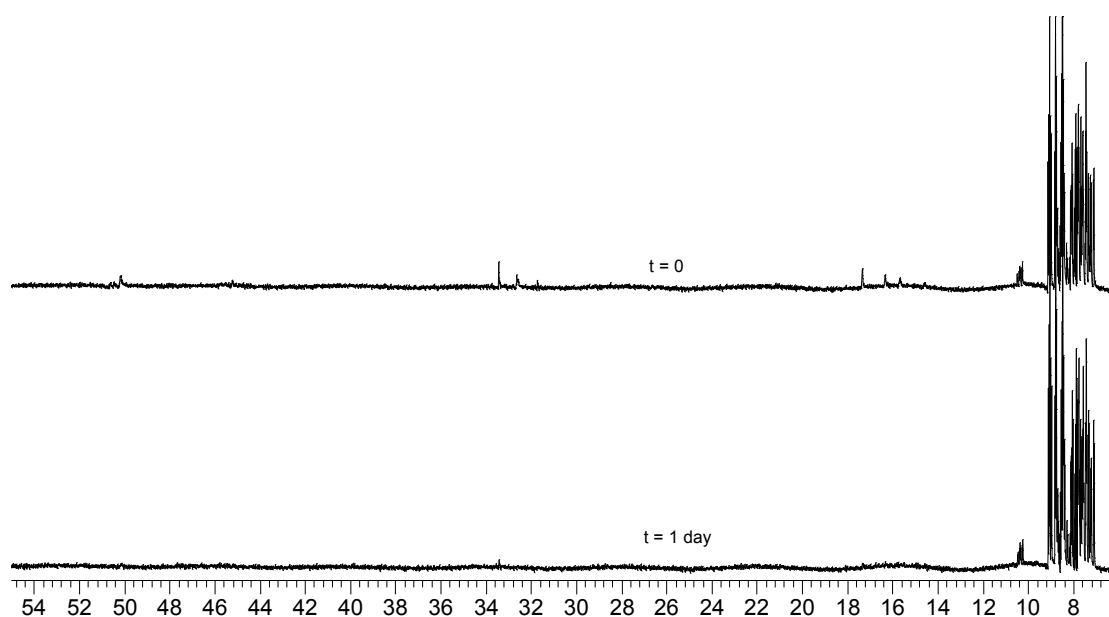


Figure 3.7: 250 MHz ^1H -NMR spectra (CD_3CN) of a 1:1 mixture of $[\text{Co}(\text{bpy})_3]^{2+}$ and $[\text{Co}(\text{phen})_2]^{3+}$ at the times $t = 0$ and $t = 1$ day, in the region δ 55-6 ppm.

There was no potential oxidising agent in the mixture, the only species being the CD_3CN solvent and the $[\text{PF}_6]^-$ counterion. The second possible reason could have

been a rapid redox exchange causing a large broadening of the peaks [81], but this possibility was excluded after another experiment. A 1:1 mixture of $[\text{Co}(\text{bpy})_3][\text{PF}_6]_2$ and $[\text{Co}(\text{bpy})_3][\text{PF}_6]_3$ was prepared and its $^1\text{H-NMR}$ spectrum was measured right after mixing. If the cause of the “disappearance” of the peaks had been the line broadening due to the redox exchange, the same fast exchange should have happened with this system as well and some line broadening should have been observed. However, the NMR spectrum was simply the sum of the individual spectra of the two species, with the same sharp peaks for $[\text{Co}(\text{bpy})_3]^{2+}$ as were observed for the pure compound.

The $^1\text{H-NMR}$ spectra showing the Co(III) species of the mixture of $[\text{Co}(\text{bpy})_3][\text{PF}_6]_2$ and $[\text{Co}(\text{phen})_3][\text{PF}_6]_3$ are reported in Figure 3.8.

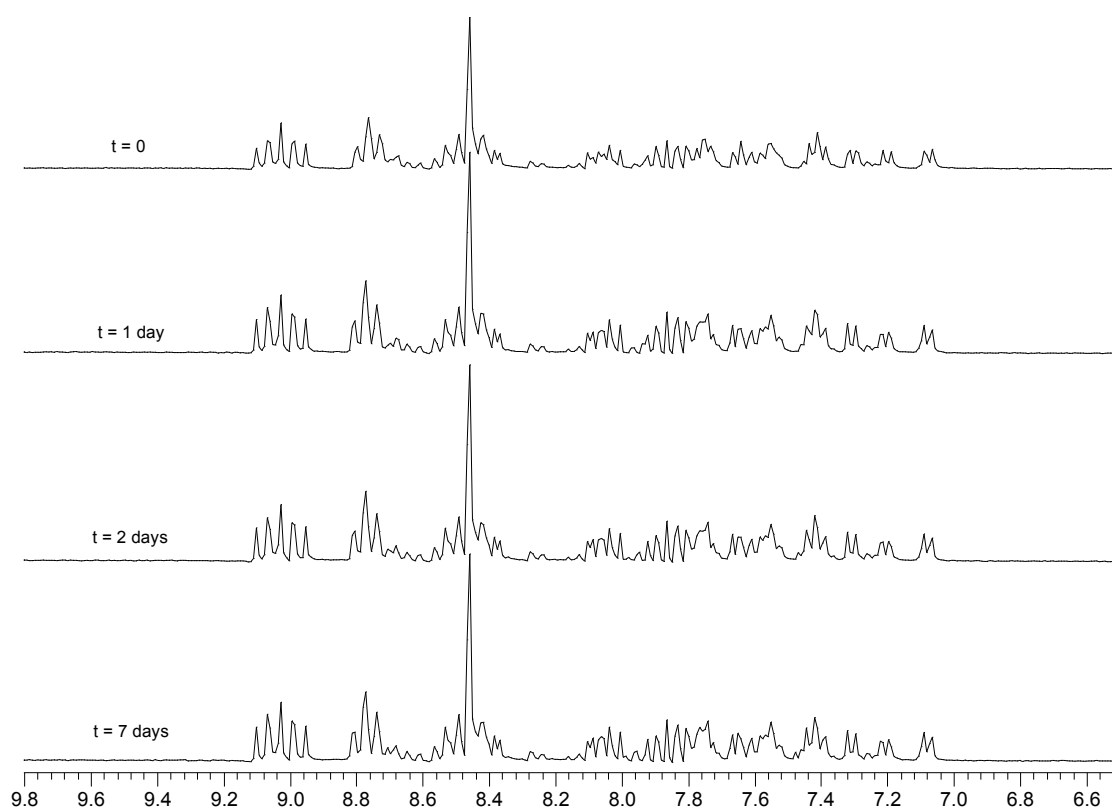


Figure 3.8: Expansions of 250 MHz $^1\text{H-NMR}$ spectra (CD_3CN) of a 1:1 mixture of $[\text{Co}(\text{bpy})_3]^{2+}$ and $[\text{Co}(\text{phen})_2]^{3+}$ at different times.

As can be seen from the spectra, the species present in the mixture did not seem to change with time: the signals of the last spectrum were already visible at $t = 0$. The

relative intensity of the peaks changed very slightly during the first day after mixing, but then stayed constant. This confirmed the observation made with the full spectra, where at $t = 0$ some Co(II) species were still visible, that later disappeared. With this system again, it could be concluded that the equilibrium was reached within one day of mixing.

As was explained above, a complete analysis of the composition of the library was not possible by NMR spectroscopy, so no further investigation was made on the composition or the equilibrium constant. However, a comparison with the same NMR region of the spectra obtained in the previous experiments told us that the Co(III) species present here were more than just the homoleptic $[\text{Co}(\text{bpy})_3]^{3+}$ and $[\text{Co}(\text{phen})_3]^{3+}$, in fact there probably was a good amount of the mixing products $[\text{Co}(\text{bpy})_2(\text{phen})]^{3+}$ and $[\text{Co}(\text{bpy})(\text{phen})_2]^{3+}$ as well. Keeping in mind that ligand exchange would take place only around the Co(II) centres, but seeing the absence of ^1H -NMR signals for these Co(II) complexes starting from one day after mixing, it could be suggested that the same mechanism of exchange as for the $[\text{Co}(\text{bpy})_3]^{3+}$ - $[\text{Co}(\text{phen})_3]^{2+}$ mixture took place in the very first seconds after mixing. In this way a mixture containing at least $[\text{Co}(\text{bpy})_3]^{3+}$, $[\text{Co}(\text{bpy})_2(\text{phen})]^{3+}$, $[\text{Co}(\text{bpy})(\text{phen})_2]^{3+}$ and $[\text{Co}(\text{phen})_3]^{3+}$ was obtained. It then appears that a process (details are unknown) made the NMR peaks of the Co(II) complexes disappear.

3.6. Conclusions

In this chapter it was confirmed that ligand exchange processes do not take place between Co(III) complexes. Nevertheless, when mixing Co(II) and Co(III) species, a whole range of mixing products could be obtained. It was suggested that they were formed via the coupling of redox self-exchange reactions between Co(III) and Co(II) and the ligand exchange reactions around the Co(II) centres. The detailed analysis of the composition of these mixtures was not possible just by NMR spectroscopy and was therefore not carried out, however, the experiments described here establish a possible second level of exchange in the dynamic combinatorial libraries formed by cobalt and 2,2'-bipyridine ligands.

4. Cobalt(II) directed assembly of dynamic combinatorial libraries with asymmetric 2,2'-bipyridine ligands

4.1. Introduction

A dynamic combinatorial library (DCL) is useful only if the information contained in it can be read-out, or if the distribution of the library members can be altered by an external constraint. So far, it has been shown that cobalt(II) complexes of 2,2'-bipyridine are good building blocks for the formation of new DCLs, that the reversible process enabling the establishment of the dynamic equilibrium within the library members can be switched off if the Co(II) centres are oxidised to Co(III), and that the composition of the library of Co(II) complexes can be relatively easily analysed by ¹H-NMR spectroscopy. We saw in the previous chapter that if both Co(II) and Co(III) species are present, a combined redox/ligand exchange takes place, therefore, ideally, the switching off of the exchange reaction by oxidation of the Co(II) centre should be instantaneous in order to give a right “picture” of the DCL. In this chapter, it will be discussed how two asymmetrically substituted 2,2'-bipyridines and their Co(II) complexes were synthesised. These complexes in solution spontaneously formed a DCL of *fac* and *mer* isomers. The composition at equilibrium of the libraries was studied by ¹H-NMR spectroscopy, then attempts were made to change this composition by adding different template molecules that should bind preferentially to one component.

4.2. Synthesis of the ligands

The asymmetrically substituted 5-methyl-2,2'-bipyridine (bpy-CH₃, **9**) was prepared. This was then used to synthesise 5-formyl-2,2'-bipyridine (bpy-CHO, **10**). The structures of these ligands are shown in Figure 4.1. Both compounds were already

known [41], but the synthetic pathway was modified slightly from what had been published.

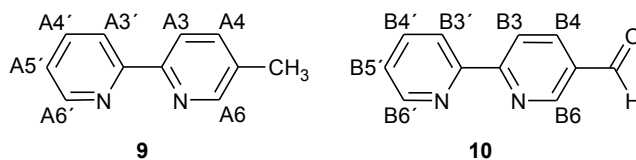


Figure 4.1: Ligands used for the *fac-mer* libraries, showing the numbering scheme used for the protons.

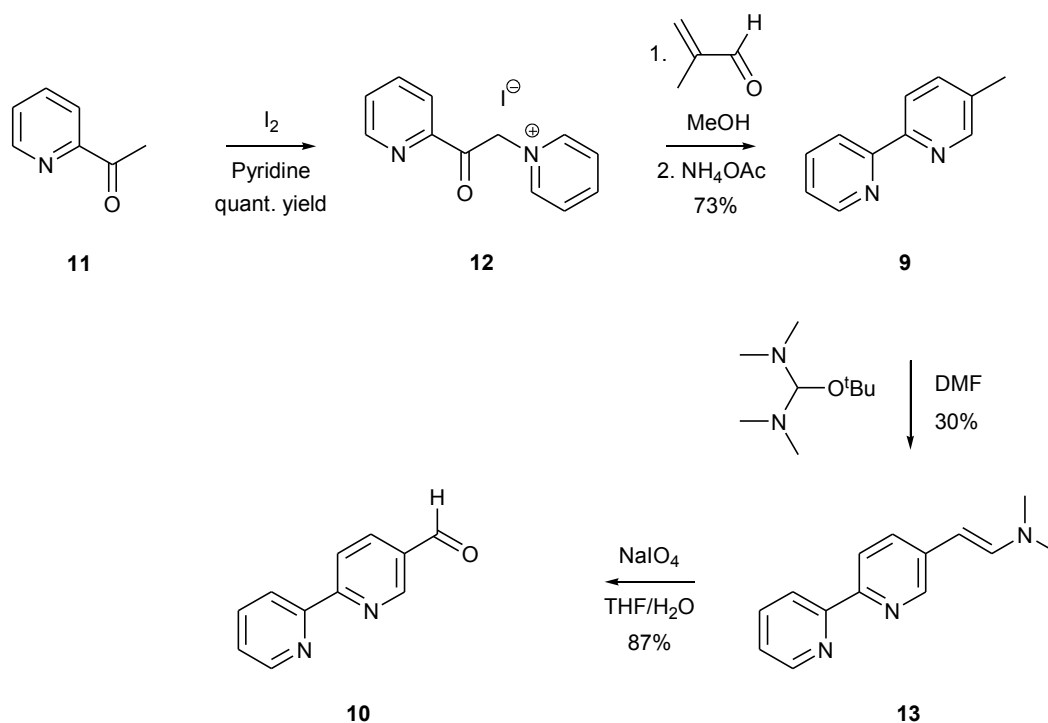


Figure 4.2: Synthesis of the two asymmetric ligands: 5-methyl-2,2'-bipyridine (**9**) and 5-formyl-2,2'-bipyridine (**10**).

Firstly, 1-(2-oxo-2-(2-pyridyl)ethyl)pyridinium iodide (PPI, **12**) was prepared following a well established procedure [41, 82] by reacting the commercially available 2-acetylpyridine (**11**) with iodine in pyridine (Figure 4.2). The yellow needles so obtained were used for the next step to carry out a Kröhnke reaction [40] with methacrolein and ammonium acetate to yield the asymmetric bpy-CH₃ (**9**). This reaction consists in a Michael-addition of the deprotonated pyridinium salt to the α,β -

unsaturated carbonyl compound to form a 1,5-diketone. This is not isolated, but reacts *in situ* with excess ammonium acetate to form a new ring with the substituent in the desired place. Finally, a proton and the pyridine ring are cleaved to allow the aromatisation of the newly formed ring into a pyridine (Figure 4.3).

The Kröhnke reaction was carried out under the same conditions reported by Schmolke and co-workers [41]: 6 hours at 80 °C in *N,N*-dimethylformamide. The result was more than satisfactory, with a good yield of 66%, but it was difficult to completely get rid of the solvent, therefore another solvent was tried. Methanol was chosen as it had already been used in our group for the synthesis of 4-methyl-2,2'-bipyridine [55]. With the new solvent, the reaction was complete after only 3.5 hours at 65 °C, and the yield reached 73%.

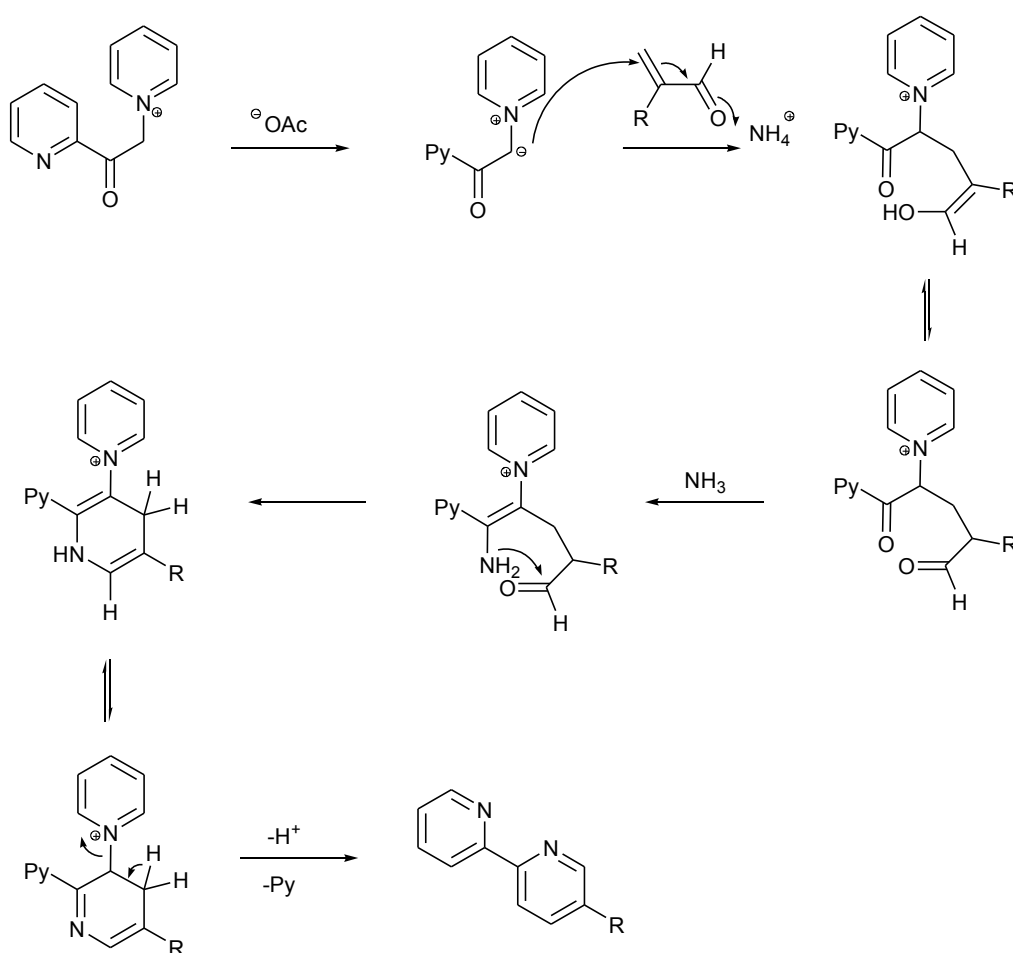


Figure 4.3: Mechanism of the Kröhnke reaction for the formation of substituted 2,2'-bipyridines.

The $^1\text{H-NMR}$ spectrum (Figure 4.4) of bpy-CH_3 clearly showed a signal for every aromatic proton, because of the loss of symmetry due to the substituent. The spectrum was fully assigned by comparison with the chemical shifts of the known bpy , and with the help of the coupling constants between neighbouring protons. The signal for A6 showed a very thin splitting in four peaks, arising from the long range coupling with both A4 and A3. This coupling is visible in the signal assigned to A4, next to the coupling with A3 and another splitting, probably due to some coupling with the methyl group. The signal assigned to A3 appeared as a relatively broad doublet, but it probably contained two thin doublets for the coupling with A6, which were not resolved.

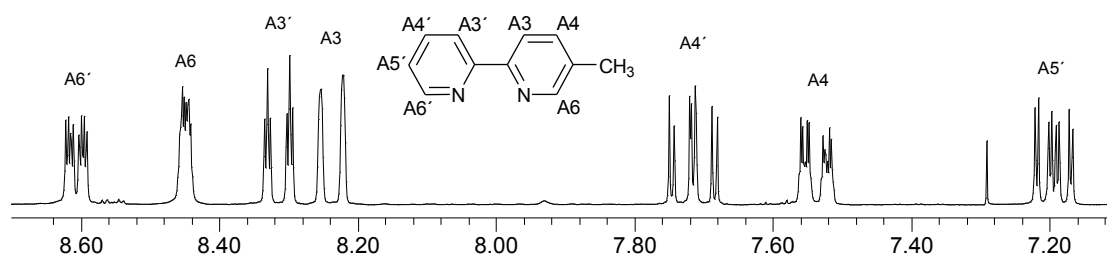


Figure 4.4: 250 MHz $^1\text{H-NMR}$ (in CDCl_3) of bpy-CH_3 (**9**) in the aromatic region. The peak for the methyl group arose at δ 2.29 ppm.

From bpy-CH_3 the synthesis was continued towards the formation of bpy-CHO (**10**). Schmolch proposes a synthetic route where **9** is converted into 5-bromomethyl-2,2'-bipyridine by a photochemical reaction with *N*-bromosuccinimide in CCl_4 , then the bromo compound is treated first with 1,3,5,7-tetraaza-adamantane in CCl_4 and then with boiling acetic acid to give the aldehyde [41]. Our attempts at the photochemical reaction failed, and another route was tried that was already known to be successful with the methyl group on position 4 of the bpy [55] and that did not require the use of the toxic solvent CCl_4 . Bpy-CH_3 was converted into the enamine **13** using *t*-butoxybis(dimethylamino)methane (Bredereck's reagent), a procedure first proposed by Bredereck for the transformation of substituted toluenes and heterocycles [83], and that had since then established itself as a key step in the formation of aromatic aldehydes from activated methyl groups. The mechanism of this reaction is shown in Figure 4.5. The Bredereck's reagent dissociates to give the basic *tert*-

butoxide able to deprotonate the methyl group of **9**. This methyl group is not strongly acidic ($pK_a \sim 30$), which renders its deprotonation the key step of the mechanism. The resulting carbanion then adds to the second species from the dissociation of the Bredereck's reagent: the amidinium cation. The intermediate product so obtained undergoes a β -elimination of dimethylamine to afford the enamine **13**.

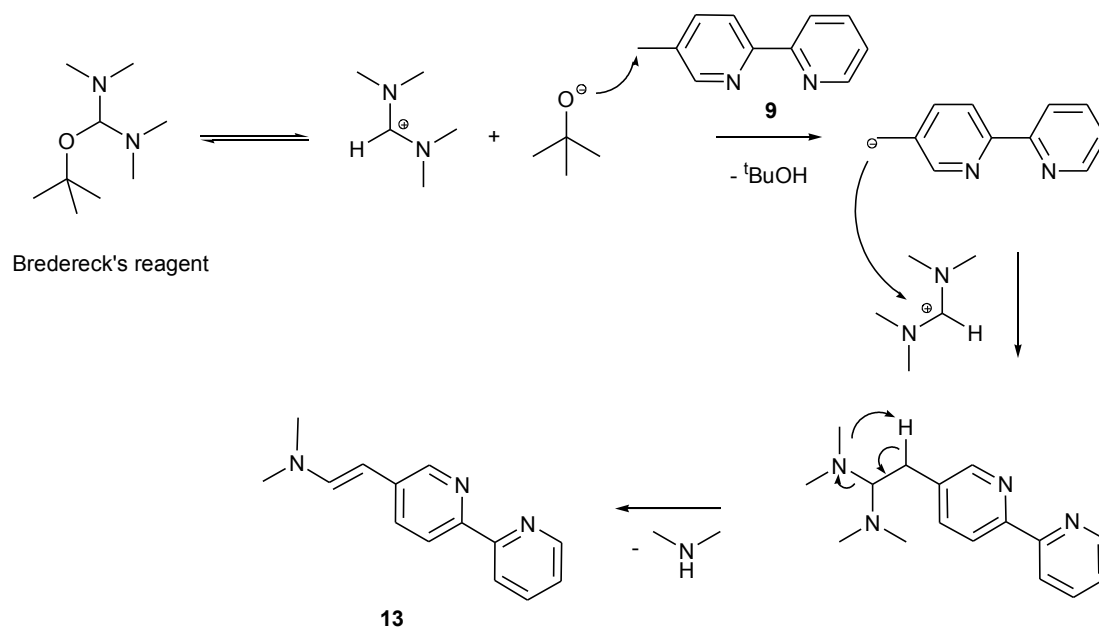


Figure 4.5: Mechanism of the Bredereck's reaction for the formation of the enamine **13**.

A mild method for the uncatalysed oxidative cleavage of enamines using sodium periodate was first reported by Coe for the preparation of aromatic carboxaldehydes [84]. This was a good alternative to methods using highly toxic reagents that were difficult to dispose of, such as ozone, singlet oxygen, sodium dichromate or $\text{RuO}_4/\text{NaIO}_4$. Le Bozec showed that this method could be successfully applied to 2,2'-bipyridines [85]. Our final aldehyde **10** was generated from the enamine **13** in nearly quantitative yield.

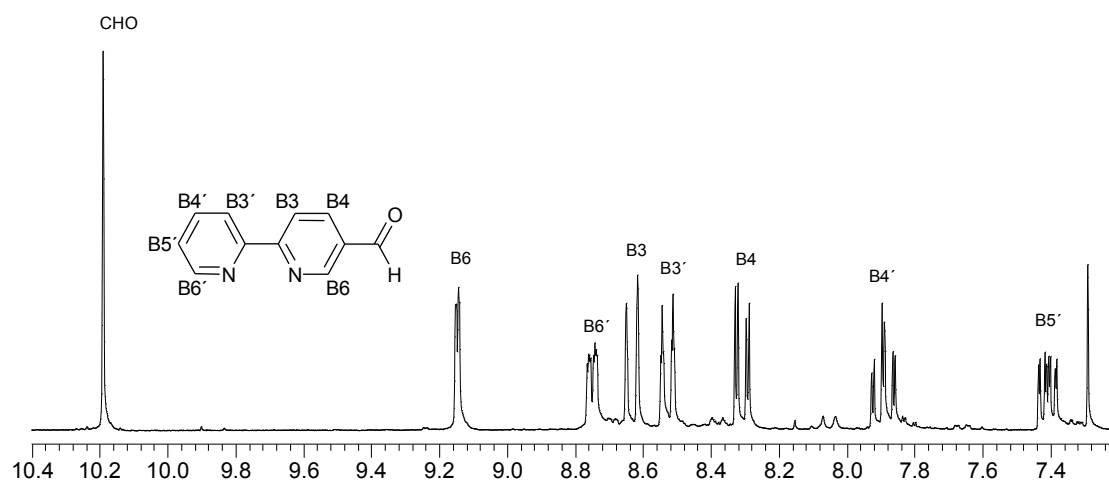


Figure 4.6: 250 MHz $^1\text{H-NMR}$ (in CDCl_3) of *bpy-CHO* (**10**) in the region δ 10.4-7.2 ppm.

The $^1\text{H-NMR}$ spectrum of *bpy-CHO* (Figure 4.6) was assigned by comparison with the spectrum of *bpy-CH₃*. The signals for the protons of the unsubstituted pyridine ring hardly changed from one compound to the other and were easy to recognise. The peaks for the protons of the substituted ring were all shifted downfield because of the inductive effect of the electronegative aldehyde group. The most shifted singlet was finally unambiguously assigned to the aldehyde proton.

4.3. Synthesis of the complexes

When mixing 3 equivalents of *bpy-CH₃* or *bpy-CHO* with one equivalent of cobalt(II), two isomers, *fac* and *mer*, were spontaneously formed. The *mer* and *fac* labels arise from the relative position of the substituting groups: in the *mer* isomer the R groups are on a plane cutting the octahedral complex, while in the *fac* isomer the R groups lay on a plane that forms one face of the octahedron (Figure 4.7). Since the ligands exchanged rapidly at the metal centre, we could consider this mixture as a dynamic combinatorial library of two members (without considering the enantiomers of each diastereomer, undistinguishable under the conditions used here).

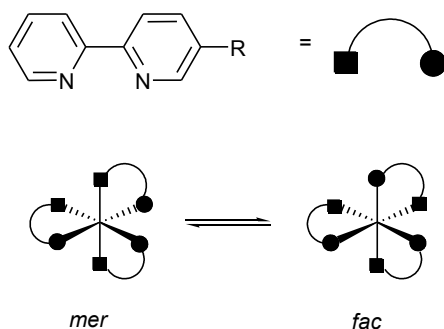


Figure 4.7: Isomers of the complex formed with three equivalents of an asymmetric 2,2'-bipyridine and one equivalent of cobalt(II).

The statistical weighting of each of the two isomers was derived as follows. Let us start with the *mer* isomer, which is illustrated in Figure 4.8. When considering the complex as an octahedron with the metal in its centre and a pyridine ring on each vertex, there are three possible square planes crossing the octahedron: one horizontal, and two vertical. For each of these planes, the three circles representing the substituted pyridine rings are on three of the four angles of the plane, which gives four possible arrangements of the three circles around one plane. Finally, for a specific arrangement of the three substituted rings, there are four possible, non superimposable arrangements of the ligands. By multiplying everything together, a statistical weighting of $(3 \text{ planes}) \times (4 \text{ possible } mer \text{ arrangements on a plane}) \times (4 \text{ possible arrangements of the ligands}) = 48$ is obtained.

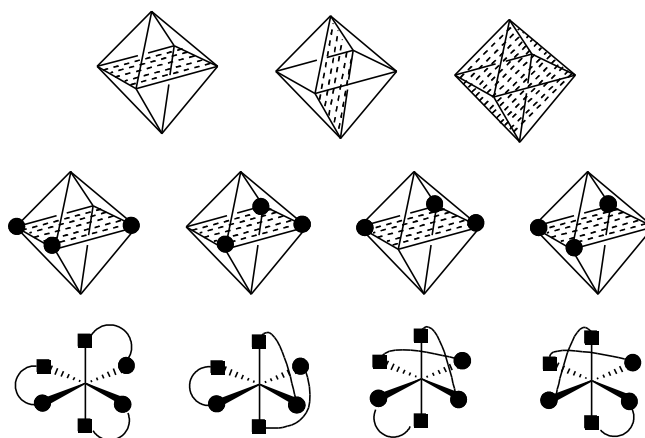


Figure 4.8: Examples for the arrangement of the ligands in the *mer* isomer.

For the *fac* isomer (Figure 4.9), in the octahedral representation, the three circles for the substituted pyridine rings are on each angle of a triangular face of the octahedron. For each of the eight faces of the octahedron there is only one possibility to place three circles, but there are each time two non superimposable possibilities to connect a substituted pyridine ring (circle) with an unsubstituted one (square). In total, the statistical weight of the *fac* isomer is (8 planes) x (1 possible *fac* arrangement on a plane) x (2 possible arrangements of the ligands) = 16. The statistical *mer* : *fac* ratio is then $48:16 = 3:1$.

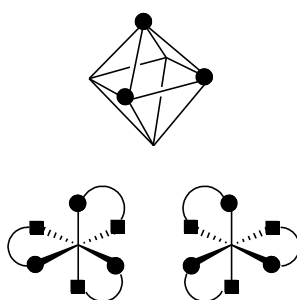


Figure 4.9: Examples for the arrangement of the ligands in the *fac* isomer.

The two diastereomers differ also in their $^1\text{H-NMR}$ spectra. In the *fac* isomer, each substituted pyridine ring is *trans* to an unsubstituted ring (Figure 4.10), so that all three ligands are chemically and magnetically equivalent and each chemically unique proton will give one signal. In the *mer* isomer the situation is more complicated.

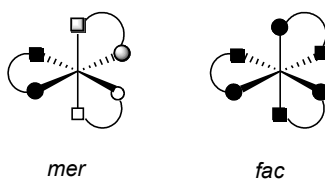


Figure 4.10: Schematic representation of the *mer* and *fac* isomers. The circles represent the substituted rings of the ligands, the squares represent the unsubstituted rings.

In Figure 4.10 we can see that in the *mer* isomer, the white circle is *trans* to a square while the black and grey circles are *trans* to each other. This makes two different environments for each chemically unique proton. Furthermore, when looking even

more closely, we notice that the grey circle is bound to the grey square, which is *trans* to another square (white), whereas the black circle is bound to the black square that is *trans* to a circle (white). This difference is enough to influence the magnetic environment of each pyridine ring, so that, in the end, each chemically unique proton of each ligand is in a magnetically unique environment.

The relative integrals of the $^1\text{H-NMR}$ peaks in a statistical mixture of *fac* and *mer* isomers were predicted to be (statistical weight x number of equivalent protons) i.e. (*fac* 1 x 3) : (*mer* 3 x 1 + 3 x 1 + 3 x 1). Every unique proton in the parent ligand was expected to give four signals of equal intensity.

A sample of the solid $[\text{Co}(\text{bpy-CHO})_3][\text{PF}_6]_2$ complex (**14**) was dissolved in CD_3CN and the $^1\text{H-NMR}$ spectrum was measured (Figure 4.11). It was immediately evident that all signals were present in sets of four of equal intensity, thus confirming that, during the synthesis of the complex, a mixture of the *fac* and *mer* isomers was formed, and these isomers interchanged rapidly in solution until the establishment of a statistical mixture.

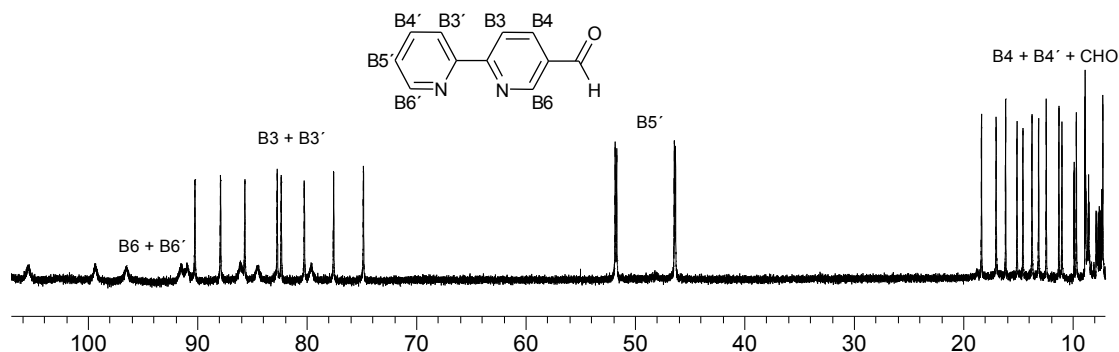


Figure 4.11: 500 MHz $^1\text{H-NMR}$ spectrum (in CD_3CN) of $[\text{Co}(\text{bpy-CHO})_3][\text{PF}_6]_2$ (**14**) in the region δ 107-7 ppm.

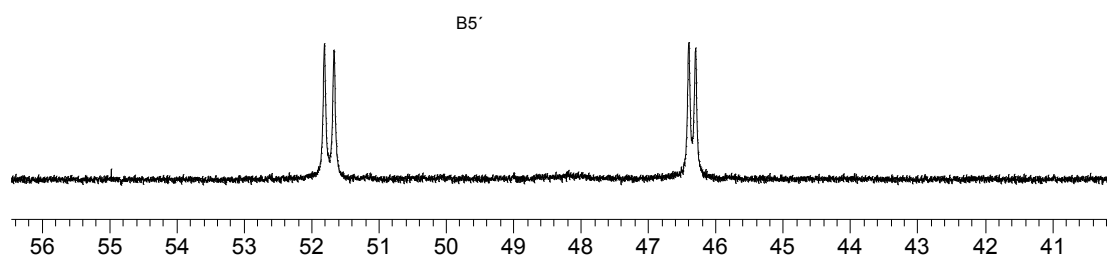


Figure 4.12: Expansion of the peaks for $\text{B5}'$ of $[\text{Co}(\text{bpy-CHO})_3][\text{PF}_6]_2$ (**14**) in CD_3CN , showing the four peaks arising from the two stereoisomers.

A first rough assignment of the peaks was made by comparison with the spectra of the already known $[\text{Co}(\text{bpy})_3][\text{PF}_6]_2$ (**4**, see Chapter 2), but for a precise distinction between the two pyridine rings of the ligand, a ^1H - ^1H COSY spectrum was needed. However, the eight broad signals at δ 105, 99, 96, 91.5, 91, 86, 84 and 80 ppm did not show any COSY peaks, therefore they were unambiguously assigned to B6 and B6', although their detailed assignment is not possible.

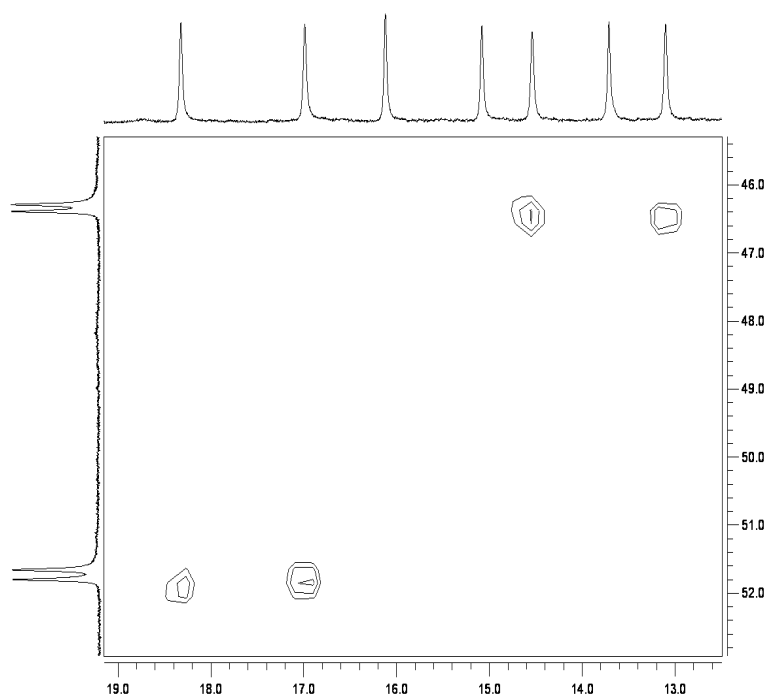


Figure 4.13: Part of the 500 MHz ^1H - ^1H COSY spectrum (CD_3CN) of $[\text{Co}(\text{bpy-CHO})_3][\text{PF}_6]_2$ (**14**) showing the couplings of the B5' protons with the B4' protons.

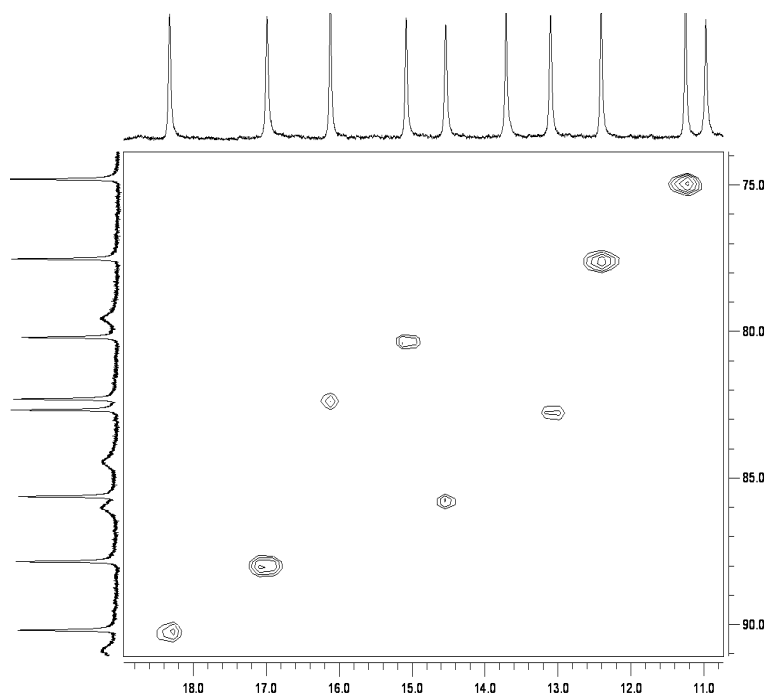


Figure 4.14: Part of the 500 MHz ^1H - ^1H COSY spectrum (in CD_3CN) of $[\text{Co}(\text{bpy-CHO})_3][\text{PF}_6]_2$ (**14**) showing the couplings of the B3' protons with the B4' protons.

For the next peak assignment, we start from the assumption that the four peaks around δ 50 ppm arise from protons B5'. This is the only proton present on only one of the two pyridine rings of the ligand, and therefore it gives rise to only one set of four peaks. The cross peaks arising from these four signals must then lead to the identification of the B4' peaks among the twelve signals between δ 7 and 19 ppm (Figure 4.13). Knowing the resonances for B4', it was possible to correlate them to the B3' peaks from among the eight sharp signals in the range δ 90 to 75 ppm (Figure 4.14). These happened to be the most downfield four (δ 90 to 82 ppm) while the remaining four peaks of this set were then assigned to B3. With the attribution of the B3 signals, it was now possible to go back to the set in the range δ 19-7 ppm and identify the four peaks for B4. The remaining four signals of this set of twelve were finally assigned to the aldehyde protons (Figure 4.15).

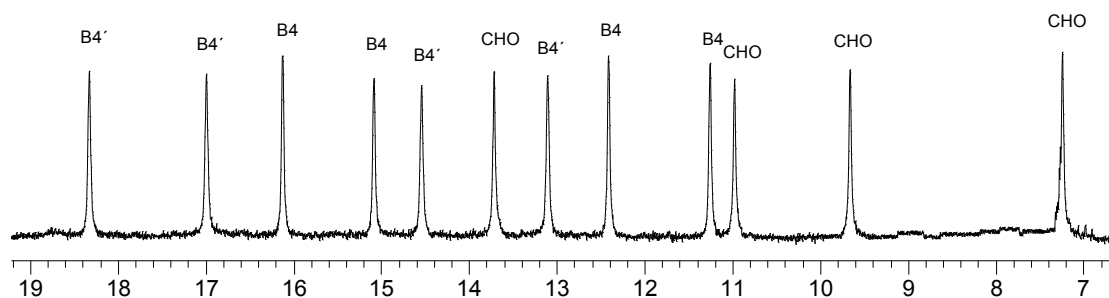


Figure 4.15: Expansion for the peaks of protons B4, B4' and CHO in a solution of $[\text{Co}(\text{bpy-CHO})_3][\text{PF}_6]_2$ (**14**) in CD_3CN .

By using the COSY spectrum, it was possible to identify the four spin systems corresponding to the four magnetic environments experienced by the protons. However, it was only possible to correlate protons B3 and B4 on one side of the ligand, and the other group of protons, B3'-B4'-B5', on the other side. These two groups of protons could not be correlated with one another, nor with the aldehyde protons or the B6 and B6'. They could not either be unambiguously attributed to particular rings in particular complexes.

	A	B	C	D
B3	82.32	80.21	77.53	74.81
B4	16.12	15.08	12.41	11.25
B3'	90.20	87.86	85.66	82.69
B4'	18.32	16.99	14.54	13.10
B5'	51.80	51.66	46.29	46.39
B6, B6'	105, 99, 96, 91.5, 91, 86, 84, 80			
CHO	13.71, 10.97, 9.66, 7.24			

Table 4.1: 500 MHz $^1\text{H-NMR}$ peaks (δ / ppm) of $[\text{Co}(\text{bpy-CHO})_3][\text{PF}_6]_2$ (**14**, in CD_3CN), grouped in the four identifiable spin systems A to D.

The statistical distribution of isomers, confirmed by the equal integral of all the peaks, was strong evidence for the dynamic equilibrium between the two complexes. This was further established through the use of NOESY spectroscopy.

In a NOESY experiment, cross peaks may arise from chemical exchange, because if two sites are exchanging, even though they may not be close to each other, then they can “see” each other and their neighbours. These cross peaks are called EXCSY peaks [86]. They are usually very intense and always have the same phase as the diagonal peaks (positive), while for NOESY peaks the phase can change depending on the molecule, and in our case it was expected to be negative.

The NOESY spectrum of $[\text{Co}(\text{bpy-CHO})_3][\text{PF}_6]_2$ (Figures 4.16 and 4.17) exhibited positive EXCSY cross peaks, corresponding to chemical exchange, but no detectable NOESY peak. Figure 4.17 shows the region of the B3 and B3' protons and demonstrates that every B3 proton showed an exchange peak with every other B3 environment (top right), and the same for all B3' protons (bottom left). This means that ligand exchange was occurring both between the *mer* and *fac* isomers and between the three sites of the *mer* isomer. This exchange process was slow enough for the “normal” NMR time scale, so as to show sharp spectra of the different species but fast enough for the NOESY time scale, yielding the exchange peaks [86].

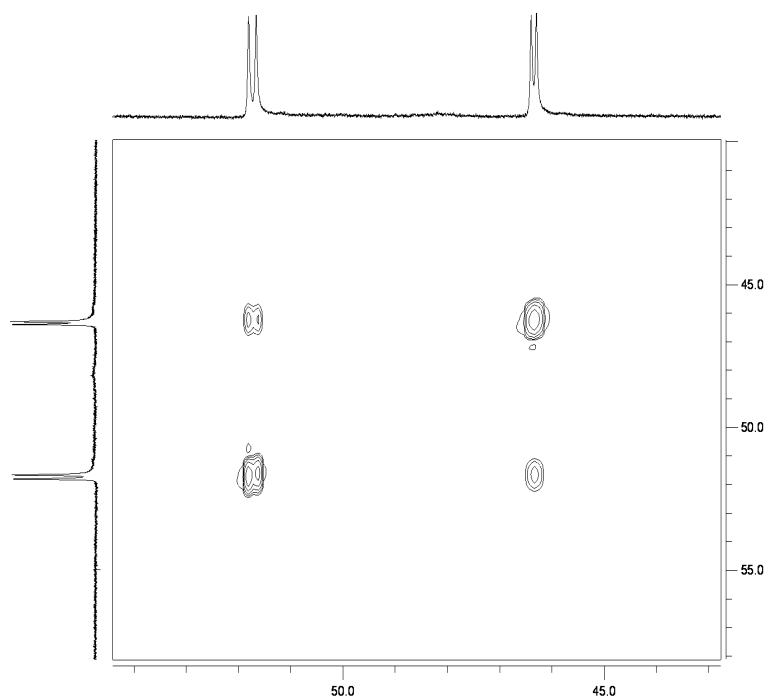


Figure 4.16: Part of the 500 MHz ^1H - ^1H NOESY spectrum (in CD_3CN) of $[\text{Co}(\text{bpy-CHO})_3][\text{PF}_6]_2$ (**14**) showing the exchange of all four $B5'$ environments.

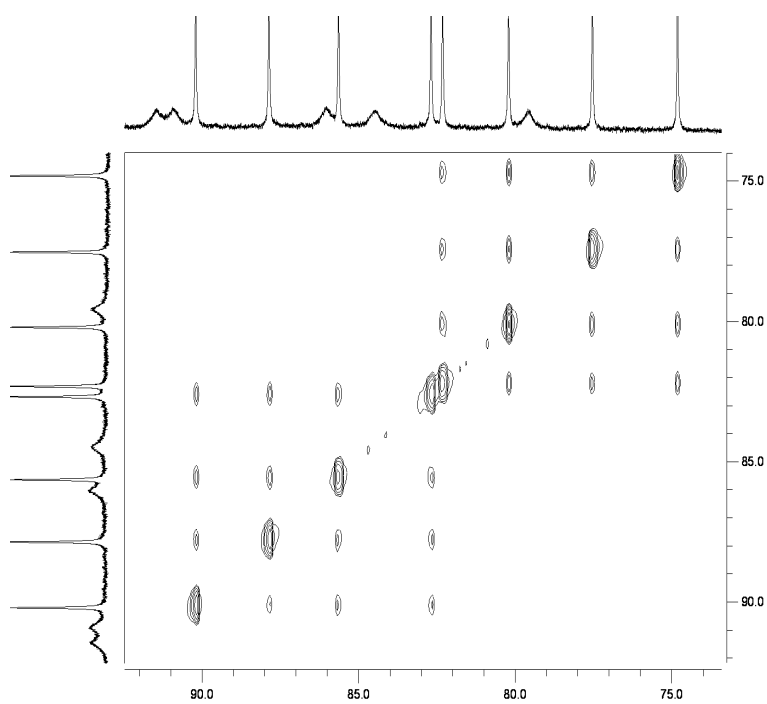


Figure 4.17: Part of the 500 MHz ^1H - ^1H NOESY spectrum (in CD_3CN) of $[\text{Co}(\text{bpy-CHO})_3][\text{PF}_6]_2$ (**14**) showing the exchange of all four $B3$ and $B3'$ environments.

The $^1\text{H-NMR}$ spectrum of the second complex, $[\text{Co}(\text{bpy-CH}_3)_3][\text{PF}_6]_2$ (**15**), was unfortunately not so rich in information as that of the previous complex. Assuming that again the mixture of *fac* and *mer* isomers had reached a statistical distribution, so that every peak would exhibit the same integral, the sets of four peaks for each chemically unique proton could somehow be guessed. However, within each set of four, two or more peaks were overlapping, and the cross peaks in the $^1\text{H-}^1\text{H}$ COSY spectrum were very broad, therefore it was not possible to make a full assignment of the signals. No further investigations were made with this compound.

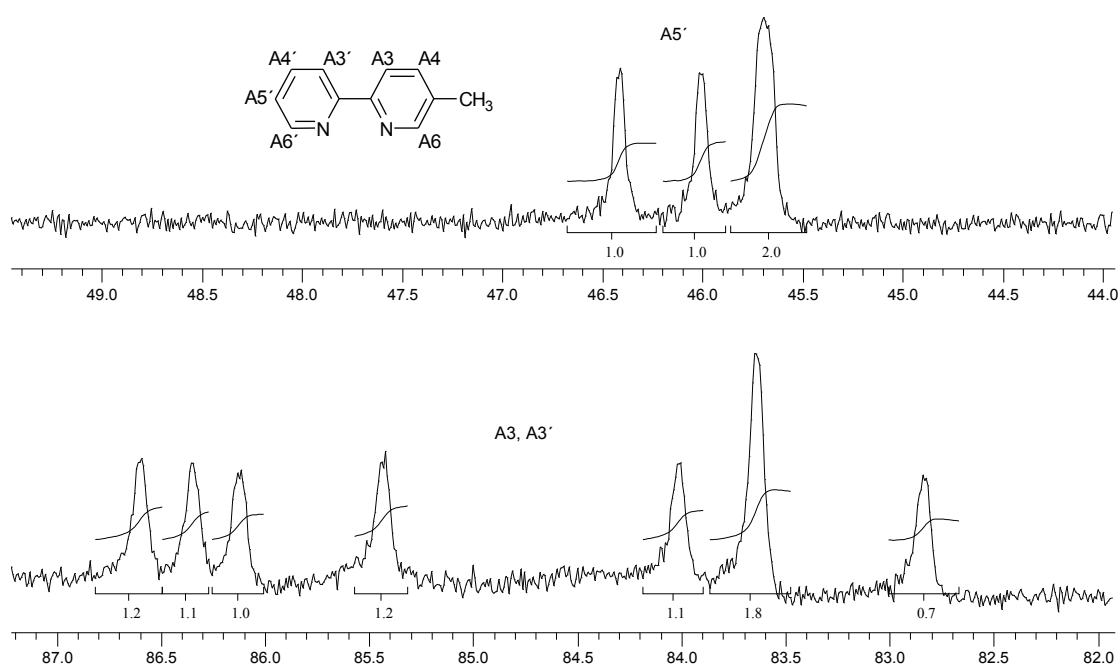


Figure 4.18: Expansions of the 250 MHz $^1\text{H-NMR}$ spectrum (in CD_3CN) of $[\text{Co}(\text{bpy-CH}_3)_3][\text{PF}_6]_2$ (**15**) showing the peaks arising from proton $\text{A5}'$ (top) and A3 and $\text{A3}'$ (bottom).

4.4. Templating of the Co(II) / 5-formyl-2,2'-bipyridine library

Having established the formation of a dynamic combinatorial library with two members, the *fac* and *mer* isomers of the complex $[\text{Co}(\text{bpy-CHO})_3][\text{PF}_6]_2$ (**14**), and having had evidence that the composition of this library at room temperature reflected the statistics, attempts were made to change this composition with the influence of different template molecules. Taking advantage of the three aldehyde groups on every

library member, templates were chosen that could react reversibly with these functional groups. For this reason three tris-amines were tried. These were expected to react with the three aldehyde functionalities on a complex to form a tris-imine capped complex. The three templates chosen were tris(2-aminoethyl)amine (tren, **16**), 1,1,1-tris(aminomethyl)ethane (tris, **17**) and *cis*-1,3,5-triaminocyclohexane (tach, **18**) (Figure 4.19).

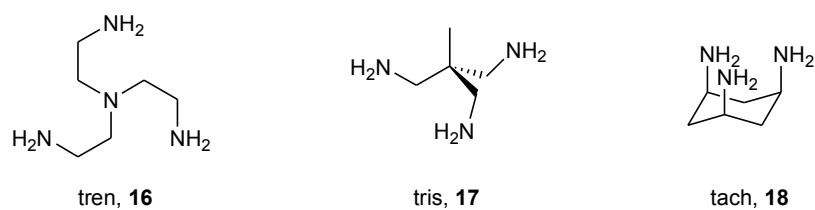


Figure 4.19: Template molecules used to try and influence the composition of the DCL.

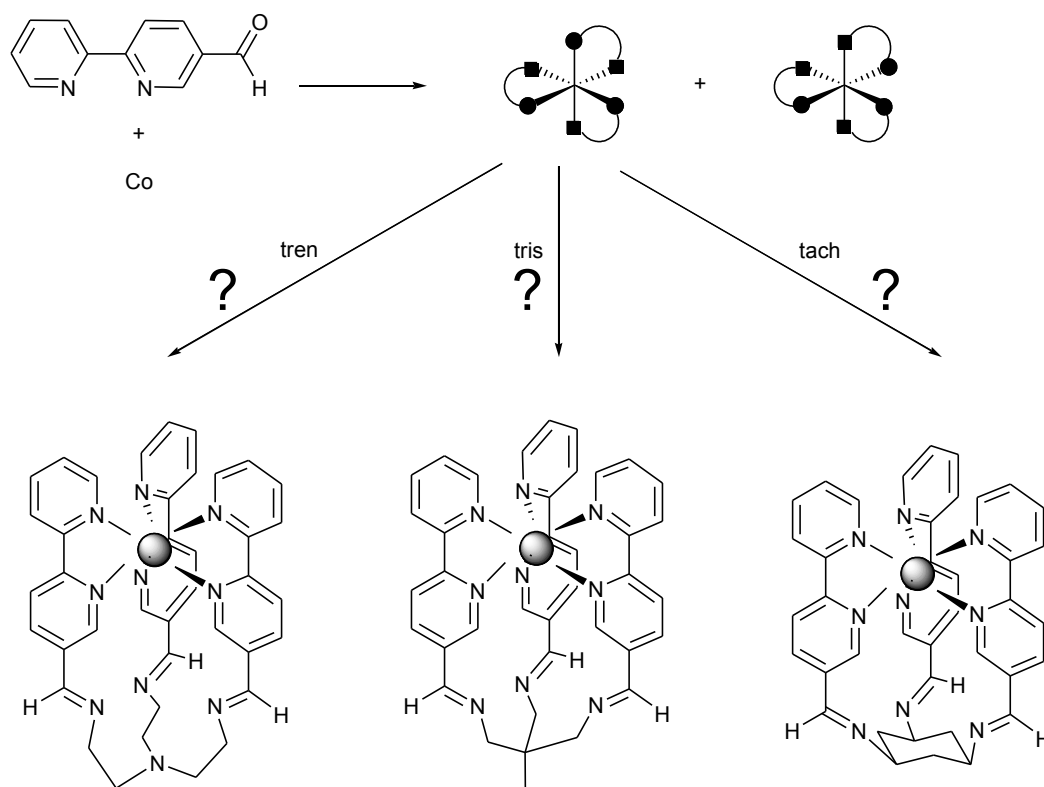


Figure 4.20: Possible products of the fac-mer DCL after templating with the different triamines.

Modelling experiments indicated that only the *fac* isomer, the minor component, would react with the triamine templates. If the reaction is quantitative, all *fac* components will be removed from the *fac-mer* equilibrium, leading to the conversion of some *mer* into *fac* to re-establish the equilibrium. When the amount of template reaches one equivalent for every cobalt, always for a quantitative reaction, all the members of the library will be converted into the *fac* isomer that will bind to the template, and the dynamic library will be driven to form a single compound.

Concerning the templates, while tren and tris have alkyl chains that are free to move and find the best conformation for the favourable interaction with the complex, tach, with its cyclohexane ring, is more rigid and has only two possible relative orientations of the NH₂ groups. The template can undergo ring flipping and the amino groups change between all axial and all equatorial positions. For the free molecule, the conformation where all substituents are equatorial is more favourable because of steric reasons. However, for the desired binding with the complex to be possible, the amino groups must be in the axial conformation.

Synthesis of one template

Tris(2-aminoethyl)amine (**16**) was purchased from Aldrich and was used without further purification.

cis-1,3,5-Triaminocyclohexane (**18**) was provided by Prof. L. Cronin (University of Glasgow).

For 1,1,1-tris(aminomethyl)ethane (**17**, tris), several attempts were made at its synthesis, following different, already published procedures (Figure 4.21). All had a common starting material, 1,1,1-tris(hydroxymethyl)ethane (**19**), and started with the activation of the hydroxy groups with *p*-toluenesulfonyl chloride. This step was reproduced in good yields without any problem.

Stetter and Böckmann [87] chose to use the Gabriel synthesis for the preparation of primary amines, a procedure that consists in the insertion of the nitrogen atom by substitution of a leaving group with the phthalimide anion, followed by the cleavage of phthalic acid yielding the desired primary amine. They converted the

tris(toluenesulfonate) compound **20** into the tris(phthalimido) derivative **21** by heterogeneous reaction with potassium phthalimide in xylene, but our attempt to repeat this reaction failed, giving only a brown sticky product that was not the desired **21**.

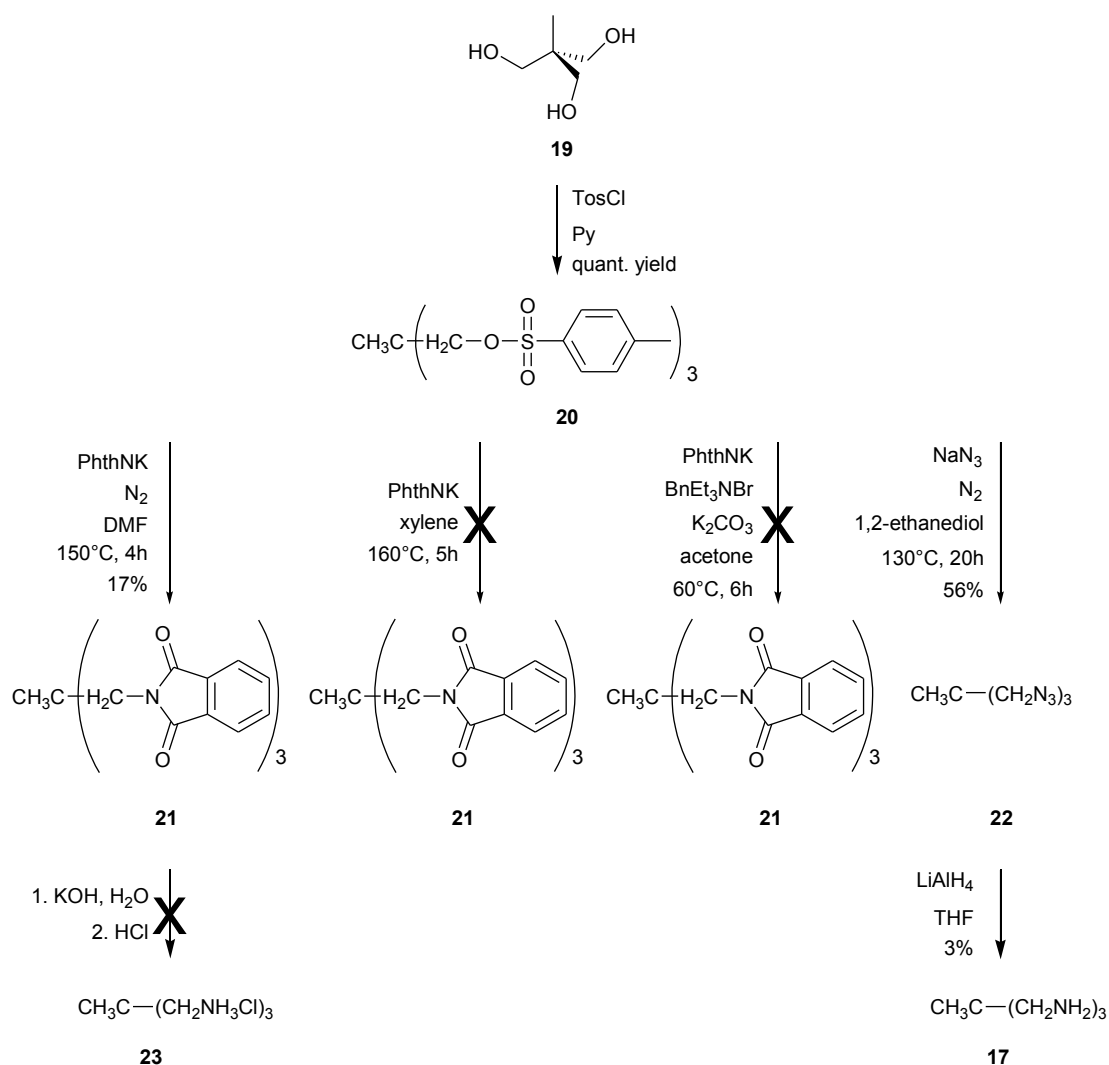


Figure 4.21: Synthetic strategies for the preparation of tris.

Geue and Searle [88] proposed an alternative procedure for the conversion of **20** into **21**, carrying out the reaction in *N,N*-dimethylformamide under a nitrogen atmosphere. This reaction went smoothly and gave a white precipitate. However, the yield was unfortunately low, partly because the product was rather difficult to collect.

A likely problem influencing the yield was the different solubility of the two reactants: potassium phthalimide is insoluble in organic solvents, while **20** is insoluble in water. To overcome this problem, a third procedure for the same step was adapted from a synthesis published by Schunack and co-workers, where they carried out the Gabriel synthesis under phase-transfer conditions [89, 90]. Potassium phthalimide was mixed in acetone with benzyltriethylammonium bromide, so that the two cations were exchanged allowing the phthalimide to go in solution as a benzyltriethylammonium salt while potassium bromide precipitated. Then, an acetone solution of **20** was added and the reaction could take place homogeneously in solution. Unfortunately, in our case, this synthesis yielded only unreacted starting material.

We therefore returned to the only procedure that gave the desired **21**, although in low yield. An attempt was made to carry out the next step and make 1,1,1-tris(aminomethyl)ethane hydrochloride (**23**) by reaction of the starting material with potassium hydroxide and subsequent acidic workup, as reported by Stetter and Böckmann [87]. However, the resulting product, although unidentified, was not the desired **23**.

At this point, the Gabriel synthesis was abandoned and another published route was tried. This involved going via the azide, followed by reduction to the amine [91]. The step from the tris-tosylate **20** to the tris-azide **22**, a simple substitution, looked promising and gave the desired product in a relatively good yield. The last step, the reduction of **22** with lithium aluminium hydride in tetrahydrofuran, however, gave only a very poor yield of product.

Finally, the tris-amine **17** was purchased from Fluka and used without further purification.

Templating with tris(2-aminoethyl)amine (tren)

A solution of tris(2-aminoethyl)amine (tren) in CD₃CN was added stepwise to a solution of [Co(bpy-CHO)₃][PF₆]₂ in CD₃CN in an NMR tube. The 250 MHz ¹H-NMR spectrum was measured after each sequential addition.

The $^1\text{H-NMR}$ spectra of the mixtures with the complex to template ratios 1:0.5, 1:1 and 1:1.6 are shown in Figure 4.22. The same figure also shows the spectrum of the solution of the complex before any template was added.

It was observed that after the addition of half an equivalent of tren new signals started to appear. The chemical shift of the most downfield peaks (δ about 170 ppm) was typical of a high-spin Co(II) solution species [30]. It was therefore assumed that whatever new species had formed, the spin state of the central cobalt(II) had changed from low-spin to high-spin.

The mixture with 0.5 equivalents of tren was not investigated in depth. However, it could be deduced from the number of peaks that more than one species was present, and no one species was significantly favoured. In the range δ 170 to 120 ppm, eight new signals with approximately the same intensity were visible, which suggested a situation where *fac* and *mer* isomers of the same (eventually new) complex were present in a 1:3 ratio, as in the starting mixture. It looked as though the two isomers present in the starting library had partially reacted with the template, regardless of any stereoselectivity.

A number of new peaks also appeared in the region δ 10 to 0 ppm, and this will be discussed later.

After the addition of a total of one equivalent of tren, the $^1\text{H-NMR}$ spectrum showed what we were hoping for: all signals of the starting members of the library had disappeared and a single new species formed. This showed a pattern of NMR signals typical of a Co(II) (high spin) complex. The template reacted favourably with the *fac* isomer of $[\text{Co}(\text{bpy-CHO})_3]^{2+}$ and formed a tris-imine capping ligand, thus driving the dynamic library to form a single complex.

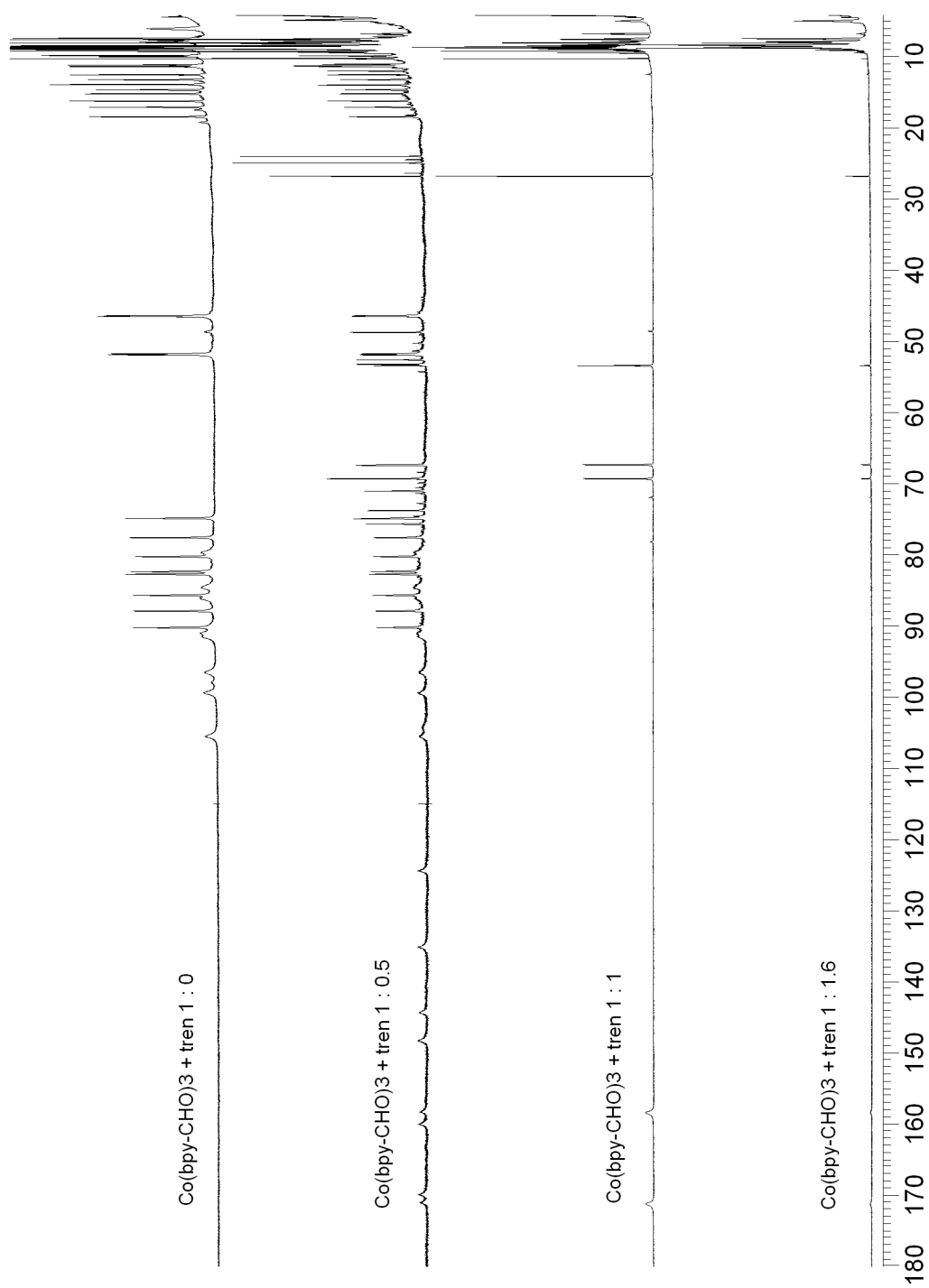


Figure 4.22: 250 MHz $^1\text{H-NMR}$ spectra (in CD_3CN) of $[\text{Co}(\text{bpy-CHO})_3][\text{PF}_6]_2$ before the addition of any template and after addition of different equivalents of tren .

An assignment of the paramagnetically shifted peaks of the new capped complex $[\text{Co}(\text{bpy})_3\text{tren}][\text{PF}_6]_2$ was possible with the help of its ^1H - ^1H COSY spectrum and the result is reported in Figure 4.23. The chemical shifts for protons H6 and H6' remained ambiguous because the peaks were too broad to show any COSY cross peaks, while the signals for the two CH_2 groups could not be identified from among the remaining peaks in the region δ 10 to 0 ppm.

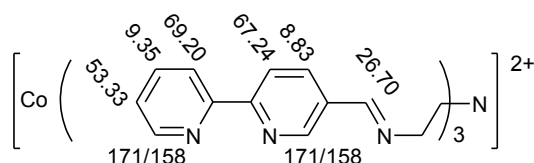


Figure 4.23: 250 MHz ^1H -NMR peaks (δ / ppm) of the capped complex resulting from the 1:1 mixture of $[\text{Co}(\text{bpy-CHO})_3][\text{PF}_6]_2$ and tren.

When the equivalents of tren were increased to 1.6, the signals for the Co(II) complex almost disappeared, in favour of the signals in the standard ^1H -NMR region (i.e. no paramagnetic shifting). The first explanations we thought of were that either the complex was decomposing and what appeared in that NMR region were only decomposition products, or the capped complex had been oxidised to its Co(III) analogue.

Expansions in the δ 11 to 5.5 ppm region of the spectra of the different mixtures of $[\text{Co}(\text{bpy-CHO})_3][\text{PF}_6]_2$ and tren are shown in Figure 4.24.

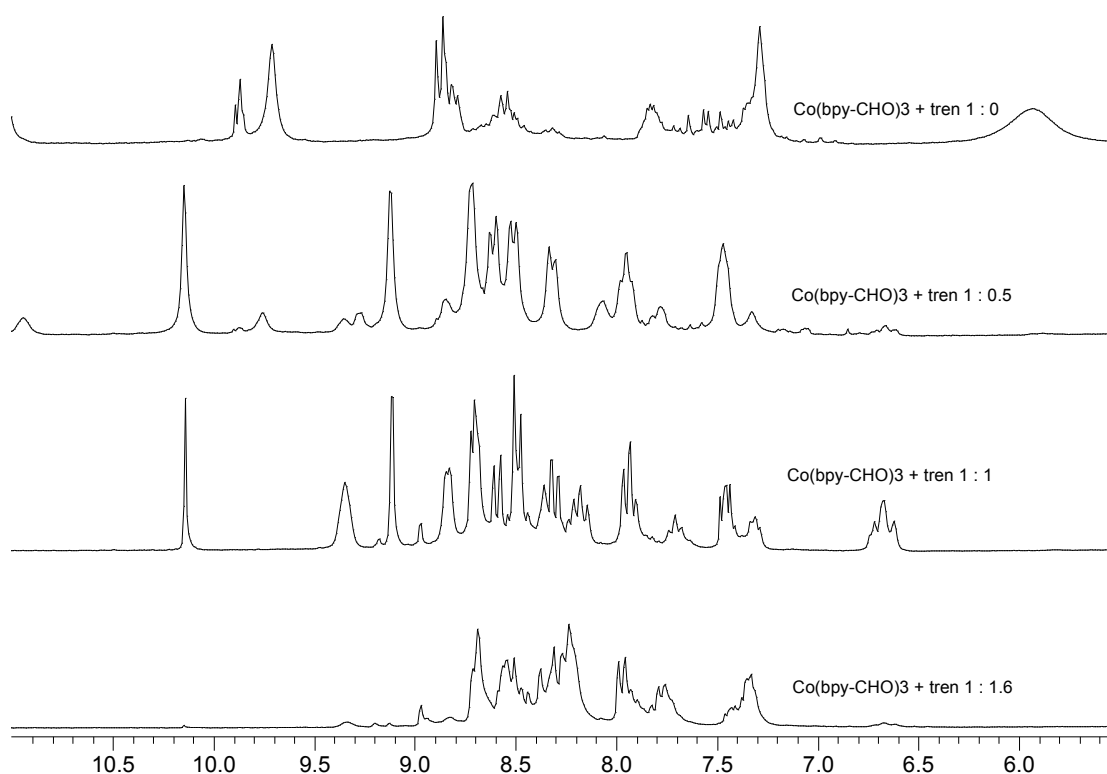


Figure 4.24: Expansions of 250 MHz ^1H -NMR spectra (in CD_3CN) of $[\text{Co}(\text{bpy-CHO})_3][\text{PF}_6]_2$ before the addition of any template and after addition of different equivalents of tren.

Immediately it could be observed that the pattern in the Co : tren 1:0.5 and 1:1 mixtures were too clean and well defined to be just from some impurity (as was probably the case for the spectrum before any addition of tren) or from decomposed species. The last spectrum, however, looked less well defined and was difficult to interpret. In this case, the decomposition theory became credible again. But what was happening in the previous mixtures?

After the assignments for $[\text{Co}(\text{bpy})_3]^{3+}$ from Chapter 3, it was known that, if the signals were arising from a Co(III) complex, we would expect two doublets for H6 and H6' around δ 7.2 ppm and two other doublets for H3 and H3' around δ 8.7 ppm. Here, however, no doublet was to be seen around δ 7 ppm, while two doublets and two broad signals were recognisable between δ 9.2 and 8.4 ppm. These four signals turned then out to be clearly defined doublets in the 500 MHz spectrum measured for the COSY. Such chemical shifts were more typical for a free ligand than for a Co(III)

complex, therefore the question now became: did the capping ligand dissociate from the Co(II) ion or did the tren displace the unreacted aldehyde bpy-CHO?

A comparison of the $^1\text{H-NMR}$ spectra of the mixtures with the spectrum of the free bpy-CHO gave an initial indication of what may have happened. However, apart from the fact that the chemical shifts of the bipyridine proton signals were not expected to change much from bpy-CHO to the capping $(\text{bpy})_3\text{tren}$, the spectra had been measured in different solvents, thus making interpretation of small chemical shift changes ambiguous.

An experiment was carried out to see if it was possible to understand what kind of ligand was being set free. A CDCl_3 solution of bpy-CHO was mixed with a CDCl_3 solution of tren, so as to obtain a bipyridine to tren ratio of 3:1 and hopefully form the free capping ligand $(\text{bpy})_3\text{tren}$.

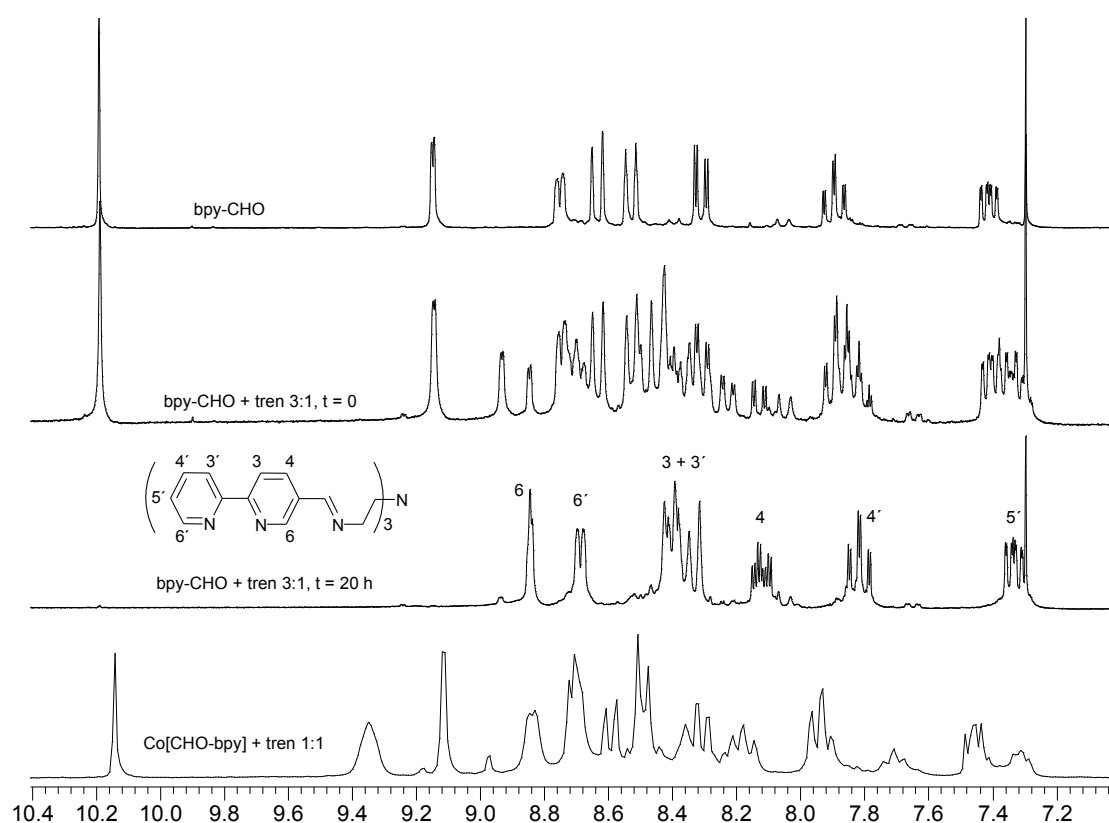


Figure 4.25: Comparison of the 250 MHz $^1\text{H-NMR}$ spectra of the free bpy-CHO ligand (in CDCl_3 , top), the 3:1 mixture of free ligand and tren at different times (in CDCl_3 , two spectra in the middle), and the 1:1 mixture of $[\text{Co}(\text{bpy-CHO})_3][\text{PF}_6]_2$ and tren (in CD_3CN , bottom).

Figure 4.25 shows the $^1\text{H-NMR}$ spectra of the 3:1 mixture of bpy-CHO and tren at different times after mixing, along with the spectra of bpy-CHO and of the 1:1 mixture of $[\text{Co}(\text{bpy-CHO})_3][\text{PF}_6]_2$ and tren. At time $t = 0$, i.e. right after mixing, the set of signals for bpy-CHO was still recognisable among all the peaks in the spectrum. The other compounds present in the mixture were probably the mono-, bis- and tris-imine formed by the reaction of the aldehyde with different amounts of the tris-amine. After 20 hours, the spectrum looked much cleaner and it could be assumed that the mixture now contained only the tris-imine $(\text{bpy})_3\text{tren}$. The signals were assigned by comparison with the known spectrum of bpy-CHO. The complete disappearance of the peak at δ 10.2 ppm was noteworthy. This was the peak that was visible in the mixture of complex and tren, and that then became the major indicator of the presence of free bpy-CHO in that mixture.

In the spectrum of the 1:1 mixture of $[\text{Co}(\text{bpy-CHO})_3][\text{PF}_6]_2$ and tren, it was possible to observe the presence of mainly free bpy-CHO and some free $(\text{bpy})_3\text{tren}$. The signals were much broader and not perfectly superimposable with the ones of the single free ligands, but these differences were due to the lower resolution of the spectrum, the presence in the sample of the paramagnetic Co(II) and the use of a different solvent.

In theory, complexes related to $[\text{Co}(\text{bpy})_3]^{2+}$, with stability constants $\log \beta_3$ around 16 [92], were expected to be stable with respect to displacement by tren ($\log K_1 = 13.08$) [93], but it did not seem to be the case here. It must be said, however, that complexes of bpy-CHO were possibly less stable than those of unsubstituted bpy because of the electron-withdrawing aldehyde group. Furthermore, the different dimensions of the data ($\text{L}^3 \cdot \text{mol}^{-3}$ for β_3 and $\text{L} \cdot \text{mol}^{-1}$ for K_1) rendered the comparison, even of their log values, not fully reliable. This issue was investigated by titrating tren into a solution of $[\text{Co}(\text{bpy})_3][\text{PF}_6]_2$ in CD_3CN . The $^1\text{H-NMR}$ spectra of the complex solution before and after the addition of different equivalents of tren are shown in Figures 4.26 and 4.27.

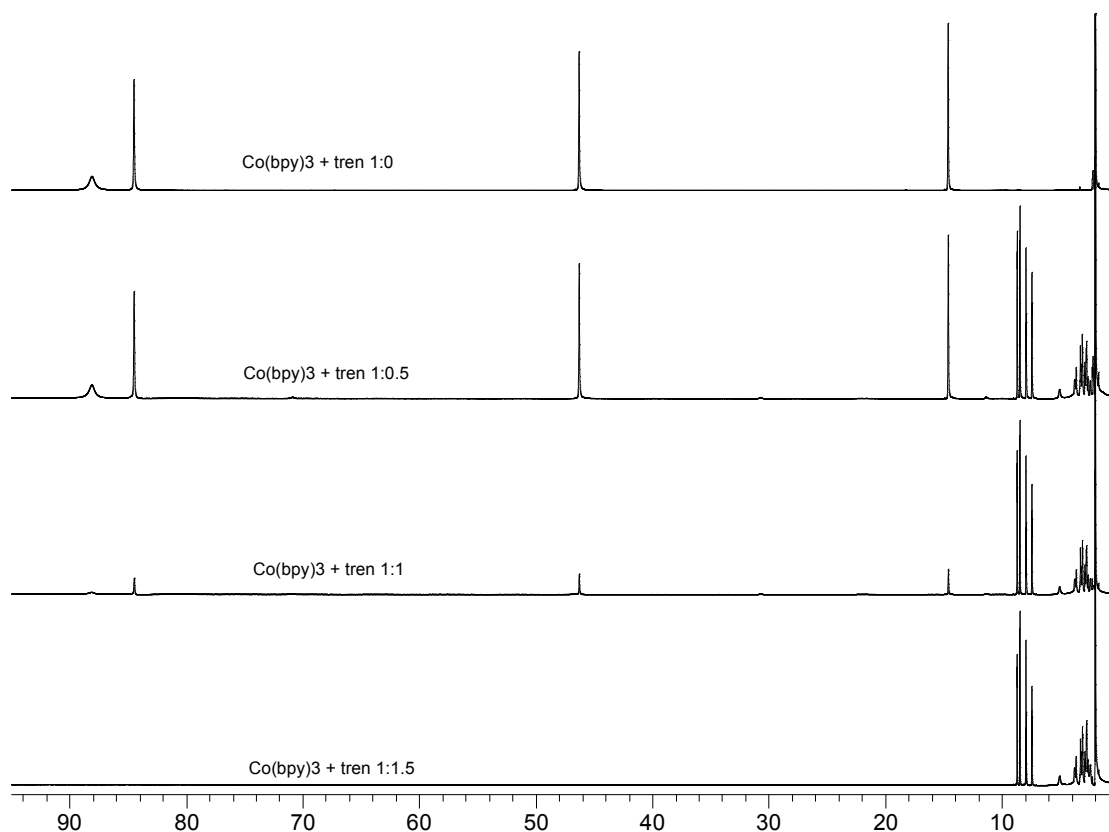


Figure 4.26: 250 MHz $^1\text{H-NMR}$ spectra (in CD_3CN) of $[\text{Co}(\text{bpy})_3][\text{PF}_6]_2$ before and after the addition of different equivalents of tren.

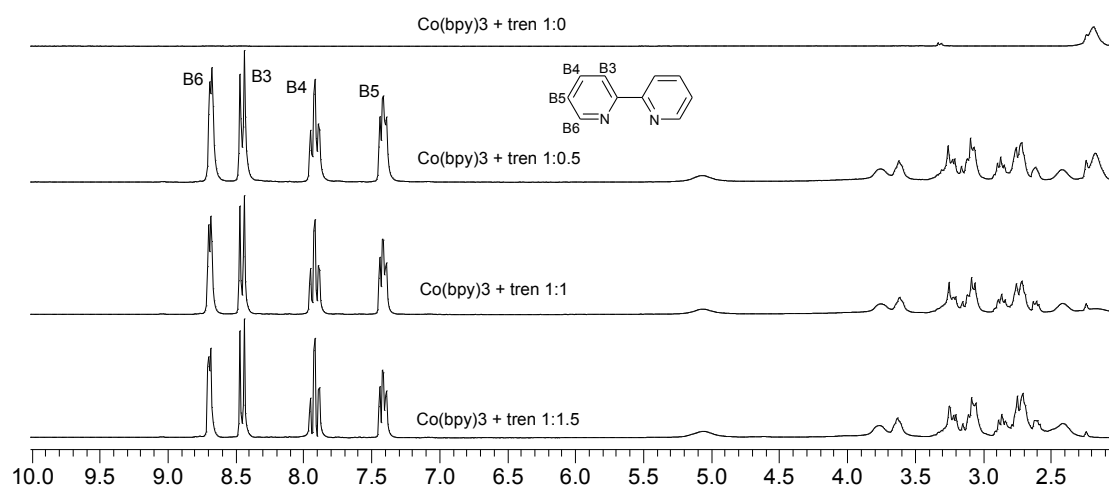


Figure 4.27: Expansions of the 250 MHz $^1\text{H-NMR}$ spectra (in CD_3CN) of $[\text{Co}(\text{bpy})_3][\text{PF}_6]_2$ before and after the addition of different equivalents of tren.

After the addition of 0.5 equivalents of tren for every cobalt, some bpy ligands had already been displaced. This could be stated on the basis of the signals between δ 9 and 7 ppm, which overlapped perfectly with the ones of pure 2,2'-bipyridine. The intensity of the paramagnetically shifted bpy signals decreased when the concentration of tren was increased to 1 equivalent, and eventually disappeared with 1.5 equivalents. In Figure 4.27 it could be seen that next to the signals for the free bpy, the group of broad peaks between δ 4 and 2 ppm was really difficult to interpret. These peaks possibly included the signals for the tren bound to Co(II) as well as for free tren, whose signals in CD₃CN would be two triplets at δ 2.6 and 2.4 ppm and a broad singlet at δ 1.2 ppm.

Attempts were made to rationalise the exchange in terms of equilibrium constants, but these were unsuccessful as the values of $\log K$ obtained for the 1:0.5 and the 1:1 case were significantly different. Besides, when one looked more carefully at the NMR spectra, it became apparent that there were other small paramagnetically shifted peaks along with signals assigned to [Co(bpy)₃]²⁺. These probably arose from mono- and bis-bpy complexes, indicating that more species were involved in the equilibrium. Going back to Figures 4.22 and 4.24, we could come to a few conclusions. When tren was added to the solution of [Co(bpy-CHO)₃][PF₆]₂, most of it reacted with the aldehyde groups of the ligands, while part of it displaced some bpy-CHO ligands from the complexes.

After the addition of 0.5 equivalents of tren, no particular Co(II) species were favoured, although the free bpy-CHO was already clearly recognisable in the NMR spectrum.

After the addition of 1 equivalent of tren, all the *mer* isomers of the initial complex were converted into *fac* isomers and reacted with the tris-amine to form a new complex with a tris-imine capping ligand. Free bpy-CHO was still present in the mixture (not quantified), and traces of free (bpy)₃tren were visible from the NMR spectrum. A confirmation for the formation of the capped complex was provided by ESI-MS, where the spectrum showed three intense peaks arising from this species (Table 4.2).

By continuous addition of tren up to 1.6 equivalents, both the capped complex $[\text{Co}(\text{bpy})_3\text{tren}]^{2+}$ and the free bpy-CHO disappeared from the $^1\text{H-NMR}$ spectrum. It was assumed that, on the one hand, the excess of tren displaced the capping ligand from the cobalt to form a $[\text{Co}(\text{tren})_x]^{n+}$ complex and, on the other hand, it reacted with the free bpy-CHO to form more free $(\text{bpy})_3\text{tren}$. These conclusions are speculative, as the $^1\text{H-NMR}$ of this last mixture in the region δ 10 to 0 ppm was very different from the one of the free $(\text{bpy})_3\text{tren}$, apart from being virtually impossible to interpret, and the attempts to form any complex with Co(II) and tren were unsuccessful. However, ESI-MS provided some support for the speculation by showing the masses of the fragments $[(\text{bpy})_3\text{tren} + \text{H}]^+$ and $[(\text{bpy})_3\text{tren} + \text{Na}]^+$ as major peaks (Table 4.2).

Co : tren	m/z	Fragment
1 : 1	352.2	$[\text{Co}(\text{bpy})_3\text{tren}]^{2+}$
	722.4	$[\text{Co}(\text{bpy})_3\text{tren}]^{2+}[\text{OH}]^-$
	848.1	$[\text{Co}(\text{bpy})_3\text{tren}]^{2+}[\text{PF}_6]^-$
1 : 1.6	645.6	$[(\text{bpy})_3\text{tren} + \text{H}]^+$
	667.6	$[(\text{bpy})_3\text{tren} + \text{Na}]^+$

Table 4.2: ESI-MS peaks of the 1:1 and 1:1.6 mixtures of $[\text{Co}(\text{bpy-CHO})_3][\text{PF}_6]_2$ and tren in CD_3CN and CH_3CN .

Templating with 1,1,1-tris(aminomethyl)ethane (tris)

A solution of $[\text{Co}(\text{bpy-CHO})_3][\text{PF}_6]_2$ in CD_3CN in an NMR tube was mixed with different volumes of a solution of 1,1,1-tris(aminomethyl)ethane (tris) in CDCl_3 . The $^1\text{H-NMR}$ spectra of the mixtures with the complex to template ratios 1:0, 1:0.4 and 1:1 are shown in Figures 4.28 and 4.29.

Unlike the case where the template was tren, no new paramagnetically shifted peak could be observed after the addition of 0.4 equivalents of tris. Similarly to the previous templating experiment, though, new peaks arose in the range δ 11 to 0 ppm. A closer look at these upfield peaks suggested that bpy-CHO was being displaced from the Co(II) complex again.

At the stage with 1 equivalent of tris, all the peaks for the Co(II) complexes had disappeared, while in the region δ 11 to 6 ppm the signals that were instinctively attributed to free bpy-CHO were clean and sharp.

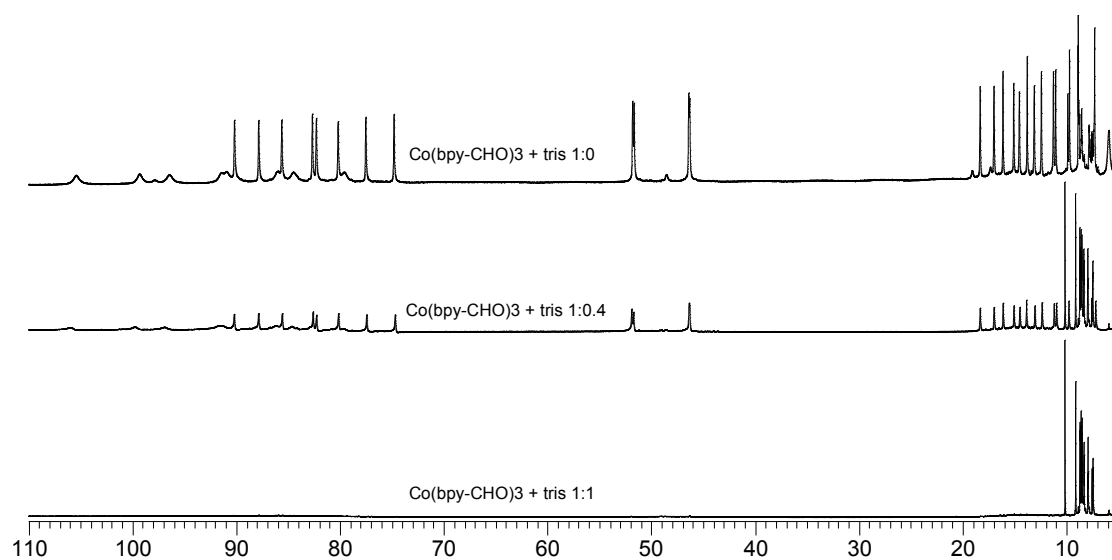


Figure 4.28: 250 MHz $^1\text{H-NMR}$ spectra (in CD_3CN) of $[\text{Co}(\text{bpy-CHO})_3][\text{PF}_6]_2$ before the addition of any template and after addition of different equivalents of tris.

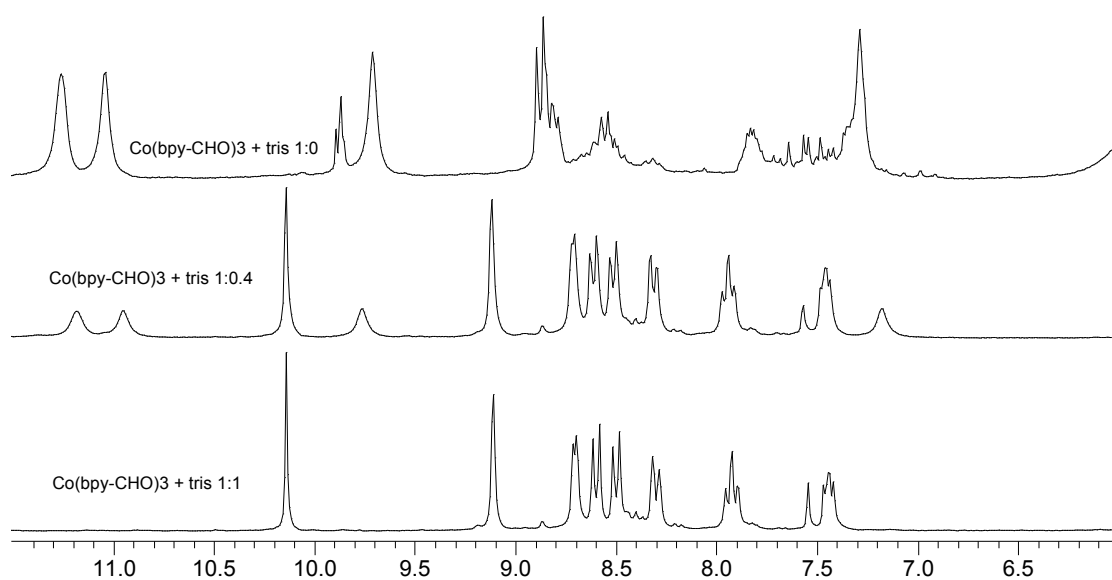


Figure 4.29: Expansions of 250 MHz $^1\text{H-NMR}$ spectra (in CD_3CN) of $[\text{Co}(\text{bpy-CHO})_3][\text{PF}_6]_2$ before the addition of any template and after addition of different equivalents of tris.

In order to provide evidence for the effective displacement of bpy-CHO rather than the decomplexation of a capping ligand (bpy)₃tris, an attempt was made to form the free capping ligand. For this purpose, to a solution of bpy-CHO in CDCl₃ was added a solution of tris in CDCl₃ for a final bpy-CHO : tris ratio of 3:1. ¹H-NMR spectra were measured within 5 minutes of mixing (t = 0) and at intervals thereafter. Figure 4.30 shows the ¹H-NMR spectra of pure bpy-CHO, of the 3:1 mixture of bpy-CHO and tris at t = 0 and after 20 h from mixing, and of the 1:1 mixture of [Co(bpy-CHO)₃][PF₆]₂ and tris.

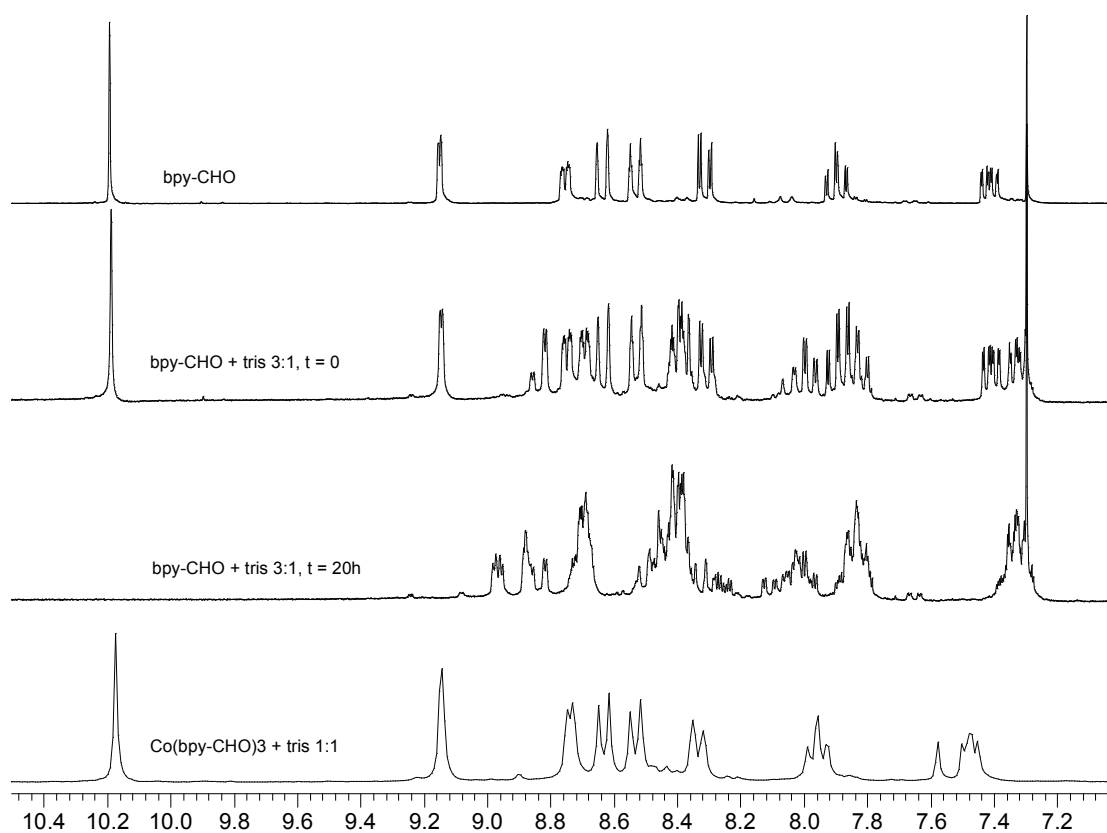


Figure 4.30: Comparison of the 250 MHz ¹H-NMR spectra of the free bpy-CHO ligand (in CDCl₃, top), the 3:1 mixture of free ligand and tris at different times (in CDCl₃, two spectra in the middle), and the 1:1 mixture of [Co(bpy-CHO)₃][PF₆]₂ and tris (in CD₃CN, bottom).

At t = 0, there were clearly new signals arising, and the spectrum was clean enough to assume that there were only two aromatic compounds present. It could be reasonably thought that (bpy)₃tris had formed and was present along with the aldehyde. The signals of the unreacted tris were in the upfield region not shown on the figure.

At time $t = 20$ h, the signals for bpy-CHO had gone, but what was left was not the series of sharp peaks that were assumed to come from $(\text{bpy})_3\text{tris}$, but rather a poorly defined pattern that probably arose from a mixture of condensation products. It must not be forgotten that the water being set free during the imine condensation was not removed from the mixture and was still able to induce the back-reaction to the half-aminal. An attempt was made to remove the water from the mixture by adding a granule of molecular sieve into the NMR solution, but this did not seem to have any effect on the final product.

A comparison of the last spectrum in the figure with the ones of pure bpy-CHO and of the bpy-CHO/tris mixture confirmed that the $^1\text{H-NMR}$ signals seen with the mixture of complex and tris belonged to free bpy-CHO rather than any product of the reaction between aldehyde and template.

Again, the attempts to prepare any complex with Co(II) and tris failed.

Templating with *cis*-1,3,5-triaminocyclohexane (tach)

cis-1,3,5-Triaminocyclohexane (tach) was finally tried as a potential template able to interact with the library of *fac*- and *mer*- $[\text{Co}(\text{bpy-CHO})_3][\text{PF}_6]_2$.

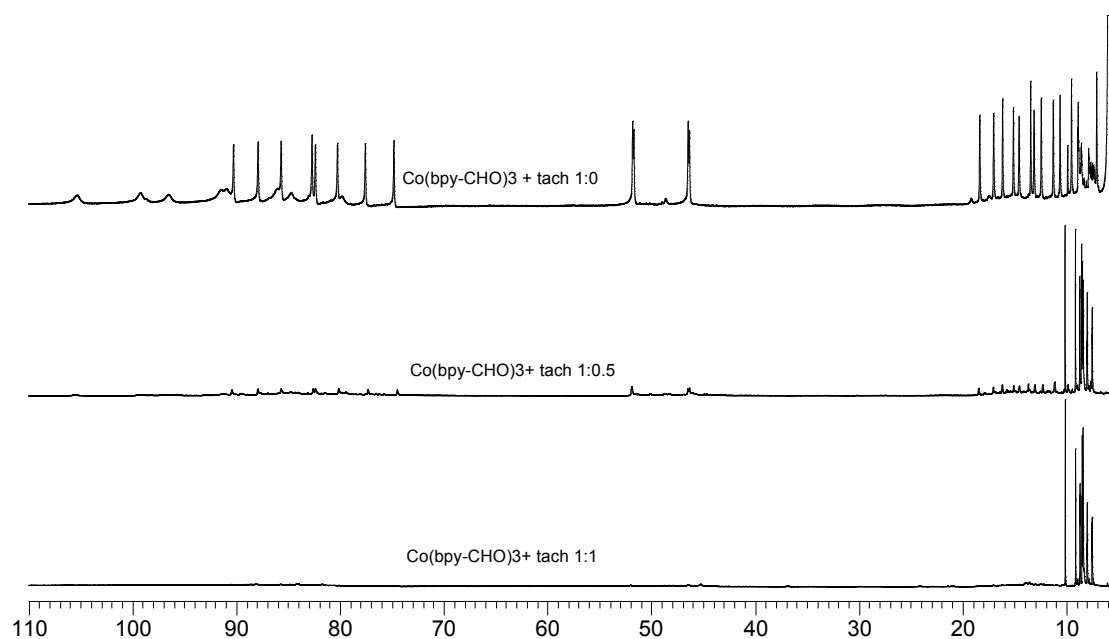


Figure 4.31: 250 MHz $^1\text{H-NMR}$ spectra (in $\text{CD}_3\text{CN}/\text{D}_2\text{O}$) of $[\text{Co}(\text{bpy-CHO})_3][\text{PF}_6]_2$ before the addition of any template and after addition of different equivalents of tach.

The initial complex was dissolved as usual in CD₃CN in the NMR tube, while the template stock solution was prepared in D₂O. Tach was added to the NMR sample in portions corresponding to 0.5 equivalents with respect to [Co(bpy-CHO)₃]²⁺, and ¹H-NMR spectra were measured after each addition. These are shown in Figure 4.31.

With this template it was noticed that after the addition of only 0.5 equivalents of tach, the peaks for the initial [Co(bpy-CHO)₃]²⁺ complexes disappeared almost completely. If it were again a situation of displacement of the bipyridine ligands by the template (as will be proven later), it would mean that one tach molecule was able to set six bpy-CHO molecules free and bind two cobalt ions.

Addition of another half equivalent of template (to reach a total of one equivalent of tach) caused the final complete disappearance of the paramagnetically shifted peaks, with the intense signals being confined to the standard region of resonance of the free bipyridines.

An expansion of the δ 10.5 to 7 ppm region for the 1:1 mixture of [Co(bpy-CHO)₃][PF₆]₂ and tach is shown in Figure 4.32, along with the spectra of pure bpy-CHO, and of a 3:1 mixture of bpy-CHO and tach at different times after mixing. A comparison of the first and the last spectra of this figure proves that the aromatic compound obtained after addition of one equivalent of tach into the library of *fac*- and *mer*-[Co(bpy-CHO)₃][PF₆]₂ is the free bpy-CHO ligand. As with tris, rather than binding to one member of the library, the template breaks the bonds within the building blocks (metal and ligands) of the library members.

Bpy-CHO and the template were again mixed in a 3:1 ratio in the attempt to make the free capping ligand (bpy)₃tach. In Figure 4.32, it was visible that at $t = 0$ (i.e. within 5 minutes of mixing) most of the aldehyde had already been converted. The characteristic peak for the CHO proton at δ 10.2 ppm decreased further after 20 hours, and the remaining signals were assumed to belong to a product of imine condensation with tach. However, these signals were too broad to allow us to assign them with certainty to the desired (bpy)₃tach product.

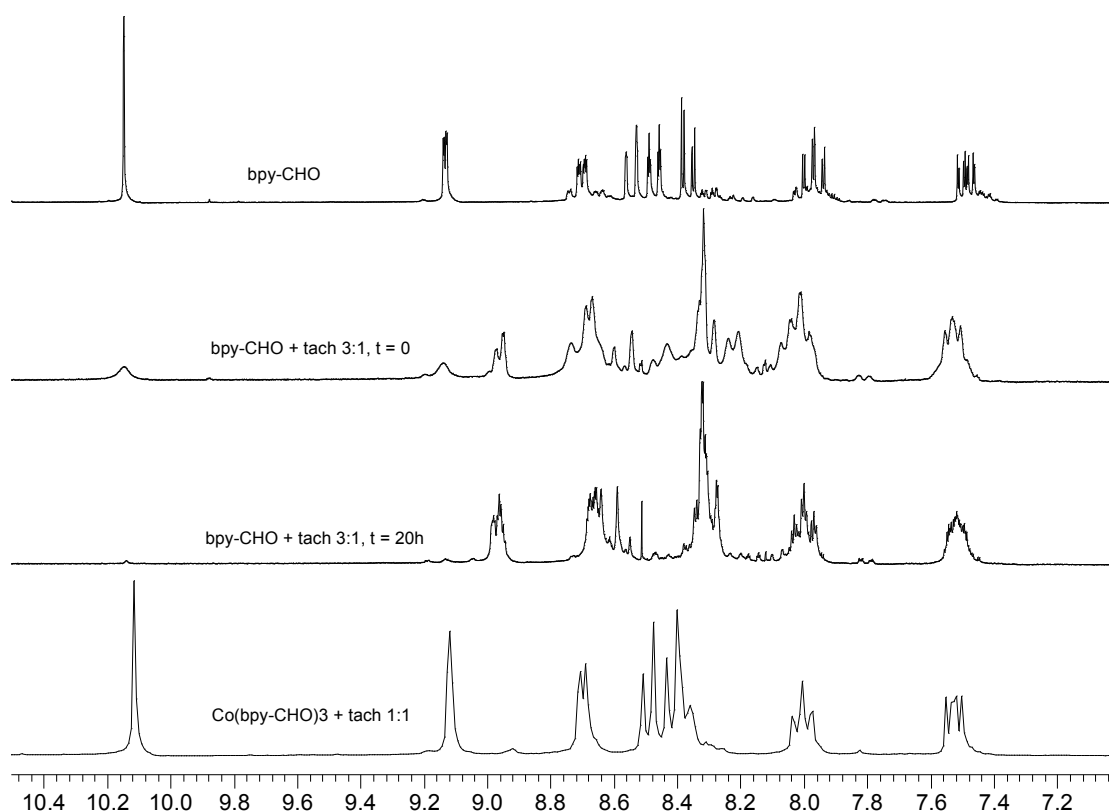


Figure 4.32: Comparison of the 250 MHz $^1\text{H-NMR}$ spectra of the free *bpy-CHO* ligand (in CD_3OD , top), the 3:1 mixture of free ligand and *tach* at different times (in $\text{CD}_3\text{OD}/\text{D}_2\text{O}$, two spectra in the middle), and the 1:1 mixture of $[\text{Co}(\text{bpy-CHO})_3][\text{PF}_6]_2$ and *tach* (in $\text{CD}_3\text{CN}/\text{D}_2\text{O}$, bottom).

The attempt to form a complex with $\text{Co}(\text{II})$ and *tach* was unsuccessful, a result that was consistent with the attempts using the templates *tris* and *tren*.

4.5. Conclusions

In this chapter, a new synthetic route was described for the synthesis of the previously reported 5-formyl-2,2'-bipyridine (*bpy-CHO*).

The cobalt(II) complexes of the asymmetric functionalised 5-methyl-2,2'-bipyridine and 5-formyl-2,2'-bipyridine were prepared and the $^1\text{H-NMR}$ spectra of their $[\text{PF}_6]^-$ salts in CD_3CN were studied. It was shown that the complexes were present in solution as mixtures of the *fac* and *mer* stereoisomers in the statistical distribution of 1:3. For the particular case of $[\text{Co}(\text{bpy-CHO})_3][\text{PF}_6]_2$, a full assignment of the NMR

peaks could be made with the help of the ^1H - ^1H COSY spectrum. The fast ligand exchange at the cobalt(II) centre resulted in a dynamic equilibrium between the two isomers, and this was confirmed by the presence of EXCSY peaks in the ^1H - ^1H NOESY spectrum of the complex.

Three tris-amine templates (tris(2-aminoethyl)amine (tren), 1,1,1-tris(aminomethyl)ethane (tris) and *cis*-1,3,5-triaminocyclohexane (tach)) were separately added to a sample of the *fac/mer* library of $[\text{Co}(\text{bpy-CHO})_3]^{2+}$. It was observed that the template was interacting with the library by adding four more equilibria to the one already established between the *fac* and *mer* isomers of the complex (Figure 4.33).

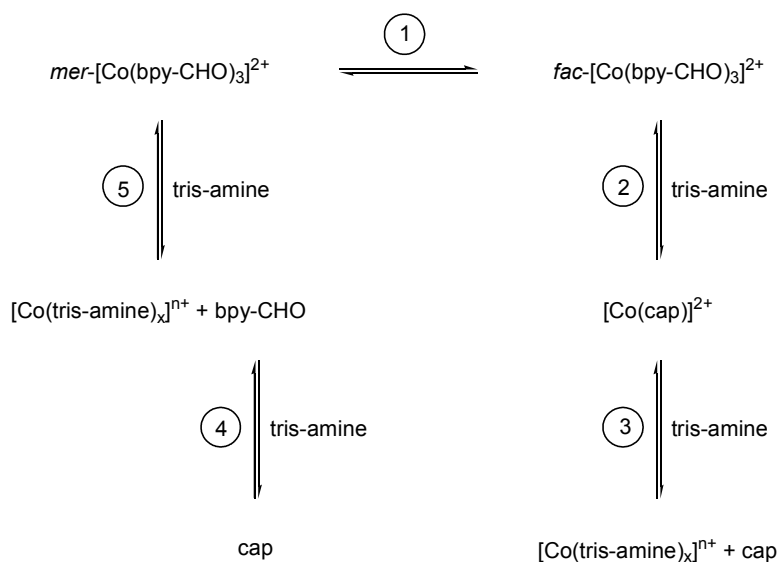


Figure 4.33: Schematic representation of the five equilibria involved in the mixture of $[\text{Co}(\text{bpy-CHO})_3][\text{PF}_6]_2$ and one of the tris-amine templates described in this chapter.

The tris-amine reacted with the aldehyde groups of the *fac* isomer to form a tris-imine capped complex, $[\text{Co}(\text{cap})]^{2+}$ (equilibrium 2 in the figure). By so doing, *fac*- $[\text{Co}(\text{bpy-CHO})_3]^{2+}$ was removed from the mixture, and equilibrium 1 was driven to form more of it at the expense of the *mer* isomer. If further tris-amine was added to the mixture containing $[\text{Co}(\text{cap})]^{2+}$, then it would substitute the capping ligand at the cobalt(II) centre (equilibrium 3).

In addition, the tris-amine ligand was able to displace bpy-CHO from the *mer* isomer, causing equilibrium 1 to move towards the left. A further addition of tris-amine gave the conversion of free bpy-CHO into the capping ligand.

With tren as the template, the first option prevailed: with one equivalent of tren for every cobalt, only $[\text{Co}(\text{bpy})_3\text{tren}]^{2+}$ was present. Some free bpy-CHO was also present in this mixture; we could explain this with the assumption that every *fac* isomer was converted into the capped complex, while the *mer* isomer underwent a displacement of the bipyridine ligands, apparently difficult to reverse. To have a quantitative conversion of the bipyridine complex into the capped complex, it would be necessary that equilibrium 1 (Figure 4.33) moved faster than equilibrium 5.

With tris and tach as templates, the only product identified in the mixtures was free bpy-CHO. This meant that the displacement of bpy-CHO was more favourable than the formation of a capped complex.

These experiments established the capacity of the library to choose the best template to react with.

5. Cobalt(II)-directed assembly of dynamic combinatorial libraries with asymmetric 2,2':6',2''-terpyridine ligands

5.1. Introduction

In the previous chapters it was demonstrated that 2,2'-bipyridine ligands and cobalt(II) ions are good building blocks for the formation of dynamic combinatorial libraries (DCLs). After asymmetric functionalisation of the ligands, it was possible to use a template molecule that was binding preferentially to one component of the DCL. This interaction caused the DCL to form more of this component at the expense of the other. In this way, the initial mixture of different components was transformed into a solution of a single species.

We tried to obtain a similar result with complexes of 2,2':6',2''-terpyridine (terpy) ligands. Three asymmetrically substituted terpys and their Co(II) or Fe(II) complexes were synthesised and attempts were made to bind the complexes with different templates.

At the same time, the ligand exchange at one metal centre and between two different metals was studied.

5.2. Synthesis of the ligands

The synthesis of 5-methyl-2,2':6',2''-terpyridine (terpy-CH₃, **34**) consisted of three separate steps. Two precursors, 2-acetyl-5-methylpyridine (**29**) and 2-(3'-(*N,N*-dimethylamino)-1'-oxoprop-2'-en-1'-yl)pyridine (**31**), were prepared separately and then reacted together in the presence of NH₄OAc to form terpy-CH₃.

From terpy-CH₃, the aldehyde 5-formyl-2,2':6',2''-terpyridine (terpy-CHO, **36**) was prepared in two further steps (Figure 5.4).

A first attempt at the synthesis of **29** was carried out by adapting the procedure proposed by Fort and co-workers for the preparation of (5-methylpyridin-2-yl)(phenyl)methanone (this is similar to **29** but with a phenyl ring instead of the methyl group α to the carbonyl) [94]. According to this publication, the base denoted BuLi-LiDMAE is prepared *in situ* from butyl lithium and 2-dimethylaminoethanol (**24**). When 3-methylpyridine (**25**) is added to the mixture, it is deprotonated at the methyl group but the intermediate product undergoes fast lithium migration to the 6-position. This position can now be attacked by an electrophile and the product aromatise spontaneously to the final **26** (Figure 5.1). This synthesis was tried with *N,N*-dimethylacetamide as the electrophile, but none of the three collected products, although unidentified, was the desired 2-acetyl-5-methylpyridine.

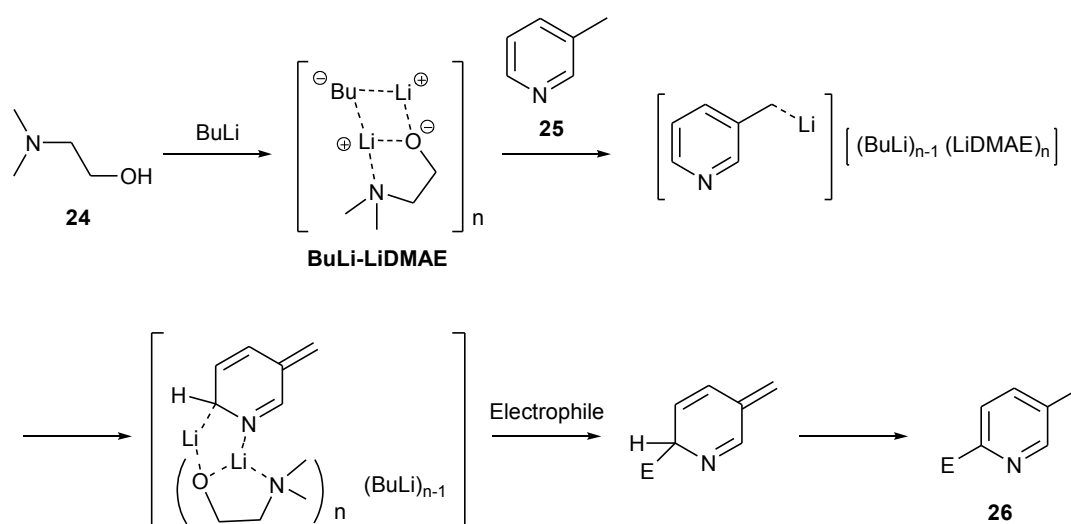


Figure 5.1: Mechanism proposed for the functionalisation of 3-methylpyridine [94].

The second approach to the synthesis of 2-acetyl-5-methylpyridine used a starting material where the pyridine ring had already two substituents at the desired positions (Figure 5.2). The procedure was an adaptation of the synthesis of 2-acetyl-4-methylpyridine, carried out in our group [95]. Commercially available 2-bromo-5-methylpyridine (**27**) was treated with butyl lithium to obtain the umpolung of carbon 2 in the intermediate **28** (not isolated). This then underwent a nucleophilic addition to *N,N*-dimethylacetamide to give the desired **29** in 89% yield (Figure 5.2).

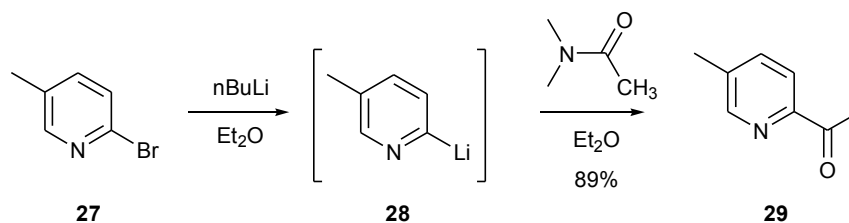


Figure 5.2: Synthesis of the first precursor of terpy-CH₃: **29**.

The second of the two precursors of terpy-CH₃, enaminone **31**, was prepared from the commercially available 2-acetylpyridine (**11**) and *N,N*-dimethylformamide dimethylacetal (**30**). A procedure for the preparation of **31** from the same starting materials had already been published by Jameson and Guise [96]. They reacted the two compounds in toluene while gradually removing the methanol formed during the condensation. We adopted a simplified procedure on the model of the synthesis of a similar compound already carried out in our group, with an additional methyl substituent on the pyridine ring [95]. The two starting materials were mixed and heated overnight under a nitrogen atmosphere without any solvent. After cooling to room temperature, a solid which formed was recrystallised to give the desired product in 76% yield (Figure 5.3).

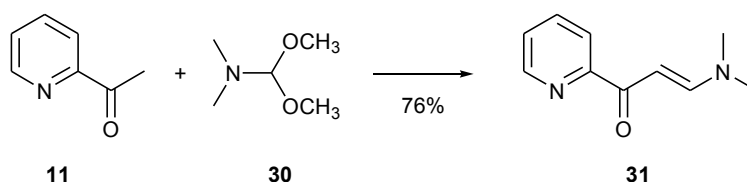


Figure 5.3: Synthesis of **31**, the second precursor of terpy-CH₃.

Terpy-CH₃ was prepared following the procedure published by Hasenknopf and Lehn [97] (Figure 5.4). The mechanism reflected the Kröhnke reaction already described for the preparation of bpy-CH₃ in the previous chapter (Figure 4.3). The potassium enolate of **29** reacted with enaminone **31** in a Michael-addition. The resulting 1,5-diketone **33** was not isolated, but it was treated *in situ* with excess ammonium acetate to allow the formation of the new pyridine ring with loss of dimethylamine.

The steps from terpy-CH₃ to **35** and finally terpy-CHO (**36**) were adapted from the Bredereck's reaction already described in Chapter 4 for the synthesis of 5-formyl-2,2'-bipyridine (**10**) (Figure 4.5).

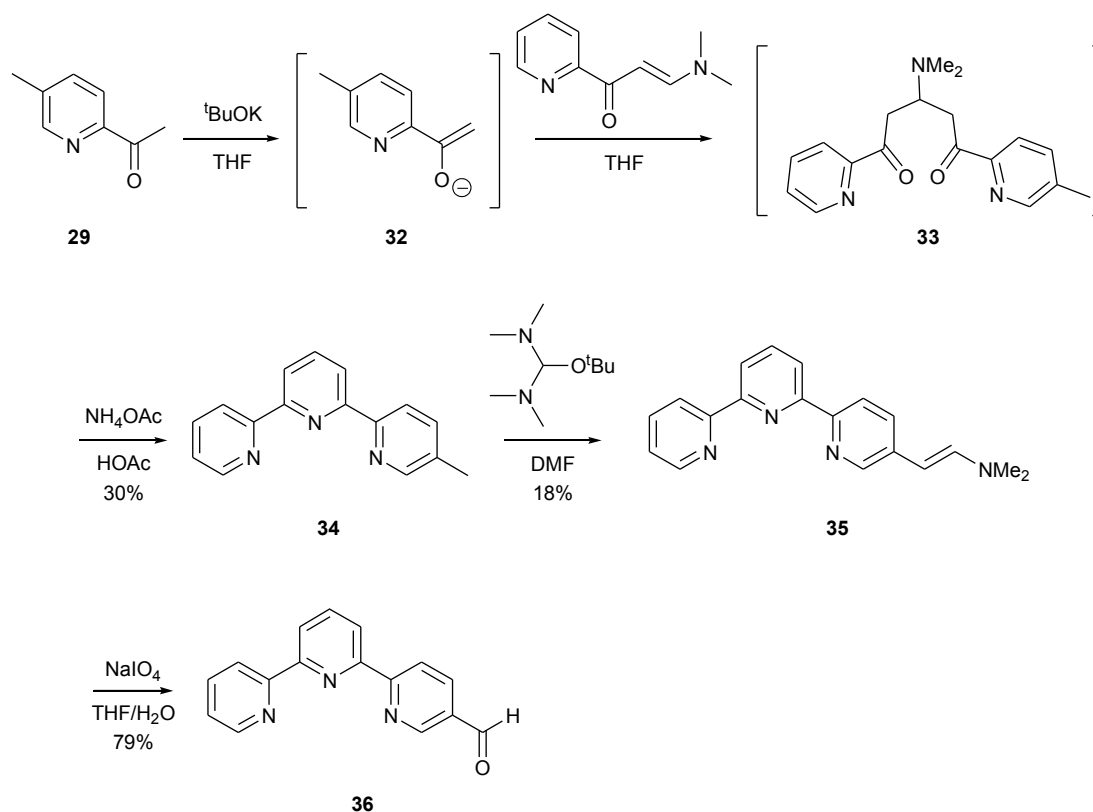


Figure 5.4: Synthesis of terpy-CH₃ (**34**) and, from it, terpy-CHO (**36**).

5.3. Synthesis of the complexes

The cobalt(II) complexes of terpy-CH₃ and terpy-CHO were prepared by mixing one equivalent of Co(OAc)₂ with two equivalents of the ligand in methanol. They were then precipitated as the [PF₆]⁻ salts. If the ligand was an unsubstituted 2,2':6',2''-terpyridine (terpy), the resulting octahedral complex would be achiral. The same is valid when the ligand is a terpy derivative where the substituents are attached symmetrically about the mirror plane running through the nitrogen and carbon 4 of the central pyridine ring (Figure 5.5).



Figure 5.5: Structures showing the achirality of the $[ML_2]$ complexes when L is an unsubstituted or a symmetrically substituted terpy. The black circles represent the substituents on the ligand.

However, if the ligands are asymmetrically substituted, as in our case, their complexes are chiral (Figure 5.6). When preparing the complexes, a 1:1 mixture of the enantiomers Δ and Λ formed spontaneously, but as the NMR spectra were measured in absence of any other chiral centre, only a single series of peaks corresponding to the enantiomeric pair was expected (as was the case with the $[MA_3]$ complexes treated in Chapter 2) [78].

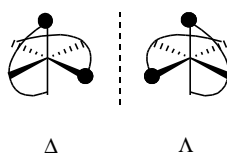


Figure 5.6: Enantiomers of the $[ML_2]$ complexes when L is an asymmetrically substituted terpy.

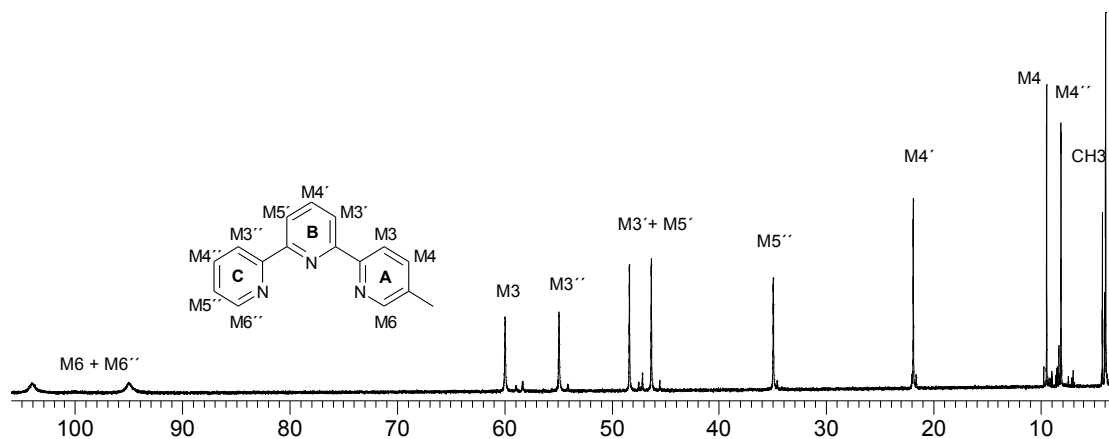


Figure 5.7: 500 MHz $^1\text{H-NMR}$ spectrum (in CD_3CN) of $[\text{Co}(\text{terpy-CH}_3)_2][\text{PF}_6]_2$ (**37**) in the region δ 106-3 ppm.

The $^1\text{H-NMR}$ spectrum of a CD_3CN solution of $[\text{Co}(\text{terpy-CH}_3)_2][\text{PF}_6]_2$ showed the expected single set of signals (Figure 5.7). These were assigned with the help of the

^1H - ^1H COSY spectrum. The two broad, most shifted peaks at δ 104 and 95 ppm were intuitively assigned to the two protons closest to the nitrogen, M6 and M6'', as was the case with 2,2'-bipyridine or 1,10-phenanthroline Co(II) complexes. An unambiguous distinction between the two was not possible because of the absence of any COSY cross peak. The singlet at δ 3.92 ppm was assigned to the methyl group because of its low frequency chemical shift, but also on the basis of its integral.

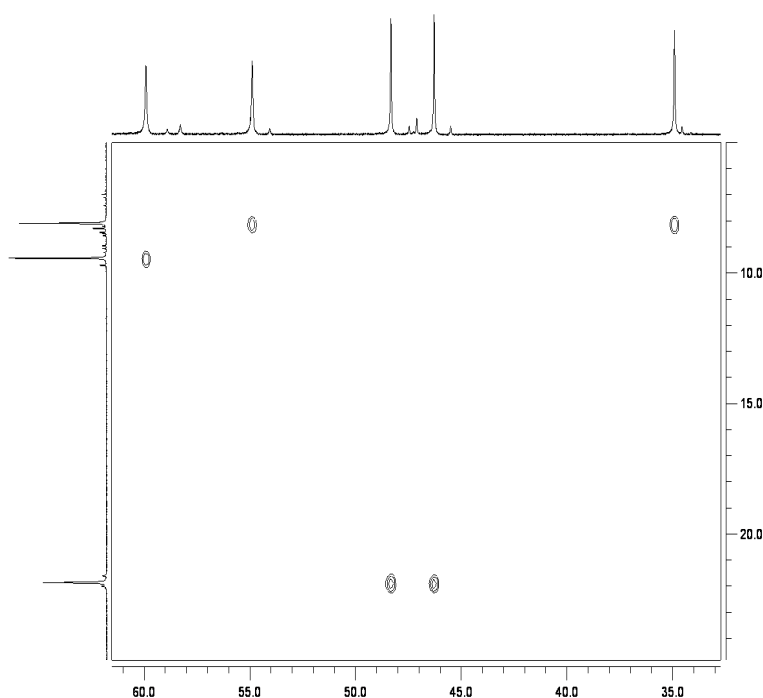


Figure 5.8: Part of the 500 MHz ^1H - ^1H COSY spectrum (in CD_3CN) of $[\text{Co}(\text{terpy-CH}_3)_2][\text{PF}_6]_2$ (37).

The COSY spectrum was helpful in identifying the three spin systems corresponding to the three rings of the ligand. The peaks at δ 9.42 and 59.90 ppm showed a single coupling between each other. The only protons able to couple with only one partner are M4 and M3. From previous studies on $[\text{Co}(\text{terpy})_2][\text{PF}_6]_2$, it was known that protons H4 and H3 on ring A resonates at δ 8.9 and 57.2 ppm respectively [53], therefore the peak at δ 9.42 ppm was assigned to M4 and the signal at δ 59.90 ppm to M3. The signal at δ 8.08 ppm gave rise to two cross peaks, with the signals at δ 54.87 and 34.90 ppm, indicating one three-proton spin system, belonging either to ring B or C. The three remaining signals formed a second three-proton spin system. Referring

again to the resonances known for the cobalt(II) complex of the unsubstituted terpy, it was possible to assign the spin system with the signals at δ 54.87-8.08-34.90 ppm to M3''-M4''-M5'' and the spin system with the signals at δ 48.31-21.85-46.26 ppm to M3'-M4'-M5'. However, in this spectrum, the assignment of M3' and M5' remained ambiguous.

The $^1\text{H-NMR}$ spectrum of $[\text{Co}(\text{terpy-CHO})_2][\text{PF}_6]_2$ (**38**) in CD_3CN was a surprise, because it showed many more signals than were expected. Besides, they all seemed to arise from a Co(II) species as they were paramagnetically shifted (Figure 5.9). It looked as though different isomers had formed, but this was not possible with this ligand, and the enantiomers should not be distinguishable under these measurement conditions.

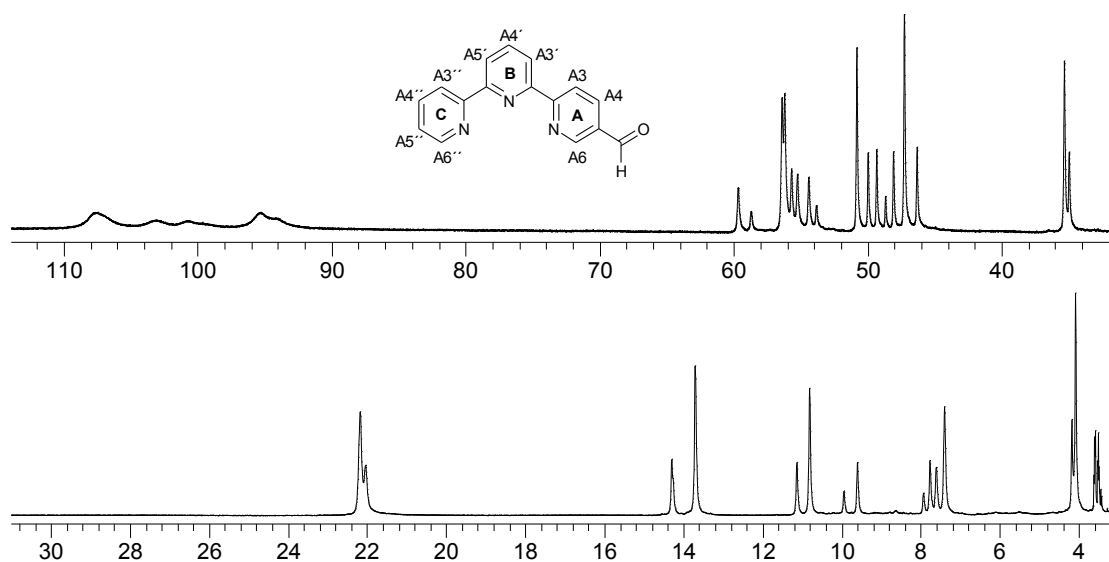


Figure 5.9: 250 MHz $^1\text{H-NMR}$ spectrum (in CD_3CN) of $[\text{Co}(\text{terpy-CHO})_2][\text{PF}_6]_2$ (**38**) in the region δ 114-3 ppm.

A possibility for such a spectrum could be that part of the aldehyde groups had been oxidised to acids (the Cannizzaro reaction, for example, is a disproportionation of aldehydes into the corresponding alcohols and acids, although it is normally carried out under strongly basic conditions [98]), and therefore the solution contained at least a mixture of complexes formed by the reaction of cobalt(II) with terpy-CHO and 5-carboxy-2,2':6',2''-terpyridine (terpy-COOH). An attempt to identify and separate the

eventual different compounds by column chromatography was carried out, but it remained unsuccessful. The IR spectrum of the solution was not of any help either. Only one absorption band was visible in the region for the C-O stretching, and it could have arisen from the overlapping of two bands. The addition of a deuterated base to the NMR sample to try and deprotonate the possible acid groups did not result in any change in the ^1H -NMR pattern. Neither did the addition of a deuterated acid to try and deuterate the possible carboxylate groups.

Two potential template molecules, 1,2-diaminoethane (ED) and 1,6-diaminohexane (HD), were added to two separate NMR samples. The hope was that the diamine would react with the aldehyde groups of a complex and form a capping diimine ligand. However, adding HD did not affect the NMR spectrum, while adding ED caused a broadening of the peaks, giving a spectrum impossible to interpret.

The only analysis providing some support for this oxidation theory was ESI-MS, where the masses for the homoleptic bis(terpy-CHO) and bis(terpy-COOH) complexes, as well as for the heteroleptic complex, were identified (Table 5.1).

m/z	Fragment
291.1	$[\text{Co}(\text{terpy-CHO})_2]^{2+}$
298.1	$[\text{Co}(\text{terpy-CHO})(\text{terpy-COOH})]^{2+}$
305.1	$[\text{Co}(\text{terpy-COOH})_2]^{2+}$
725.9	$[\text{Co}(\text{terpy-CHO})_2]^{2+}[\text{PF}_6]^-$
739.8	$[\text{Co}(\text{terpy-CHO})(\text{terpy-COOH})]^{2+}[\text{PF}_6]^-$

Table 5.1: ESI-MS peaks of the solution of $[\text{Co}(\text{terpy-CHO})_2][\text{PF}_6]_2$ (**38**) in CD_3CN and CH_3CN .

Synthesis of 5-carboxy-2,2':6',2''-terpyridine

Because of the unsuccessful results obtained with the terpy-CHO ligand, this was abandoned, and we tried to make and use another ligand. 5-Carboxy-2,2':6',2''-terpyridine (terpy-COOH) was chosen for two main reasons. Firstly, there was still the hope to identify the signals for $[\text{Co}(\text{terpy-COOH})_2]^{2+}$ in the NMR spectrum of the $[\text{Co}(\text{terpy-CHO})_2][\text{PF}_6]_2$ solution encountered before. Secondly, the acid functionality could still be used for templating with diamines through amide formation.

To obtain the carboxylic acid, terpy-CH₃ (**34**) was used as the starting material. The first oxidation was carried out with potassium permanganate in water, according to a procedure published in 1949 for the oxidation of 2-methylpyridine [99]. After workup, a white compound was collected, which was identified as the hydrochloride salt of the desired terpy-COOH. However, the yield was unsatisfactory and could not be reproduced. Therefore, another oxidation method was tried. This was an adaptation of a synthesis published by Borel and Deuel and involved the use of chromium trioxide [100]. The product obtained could not be identified. This fact, and the toxicity of the reagents and by-products, lead us to abandon this synthesis.

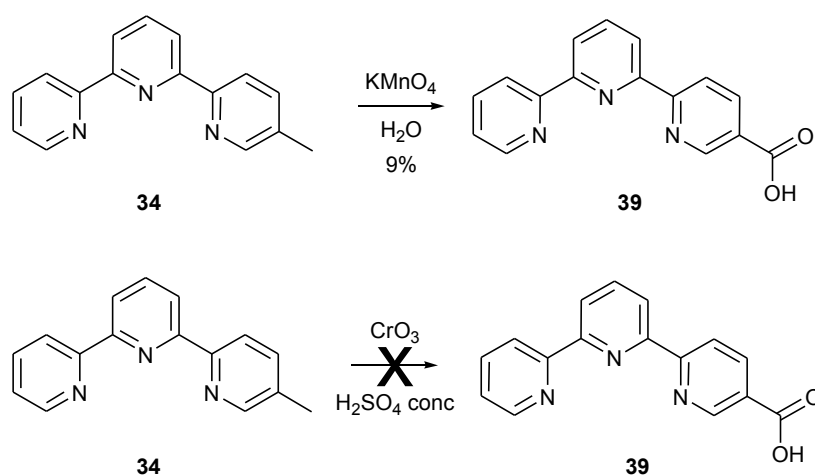


Figure 5.10: Synthesis of 5-carboxy-2,2':6',2''-terpyridine (**39**).

Synthesis of the [Co(terpy-COOH)₂][PF₆]₂ complex

The [Co(terpy-COOH)₂][PF₆]₂ complex (**40**) was prepared by mixing one equivalent of cobalt(II) acetate with two equivalents of ligand, followed by the precipitation of the [PF₆]⁻ salt. The ¹H-NMR spectrum of a CD₃CN solution of the complex showed the expected ten peaks for the aromatic protons (Figure 5.11). Apart from the signals for protons B6/B6'' and B3'/B5', which remain ambiguous for the reasons already explained, the peaks were fully assigned with the help of the ¹H-¹H COSY spectrum (Figure 5.12) and by comparison with the spectrum of [Co(terpy-CH₃)₂][PF₆]₂ (**37**).

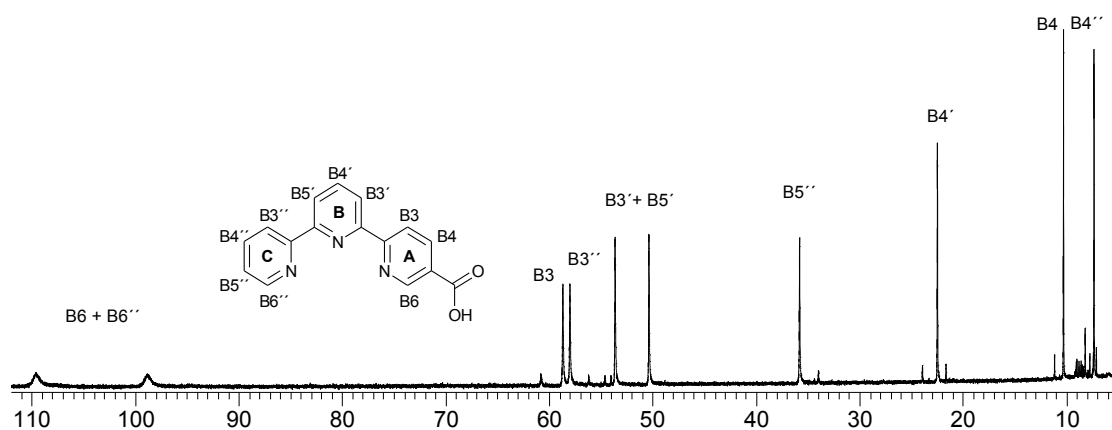


Figure 5.11: 500 MHz ^1H -NMR spectrum (in CD_3CN) of $[\text{Co}(\text{terpy-COOH})_2][\text{PF}_6]_2$ (**40**) in the region δ 112-5 ppm.

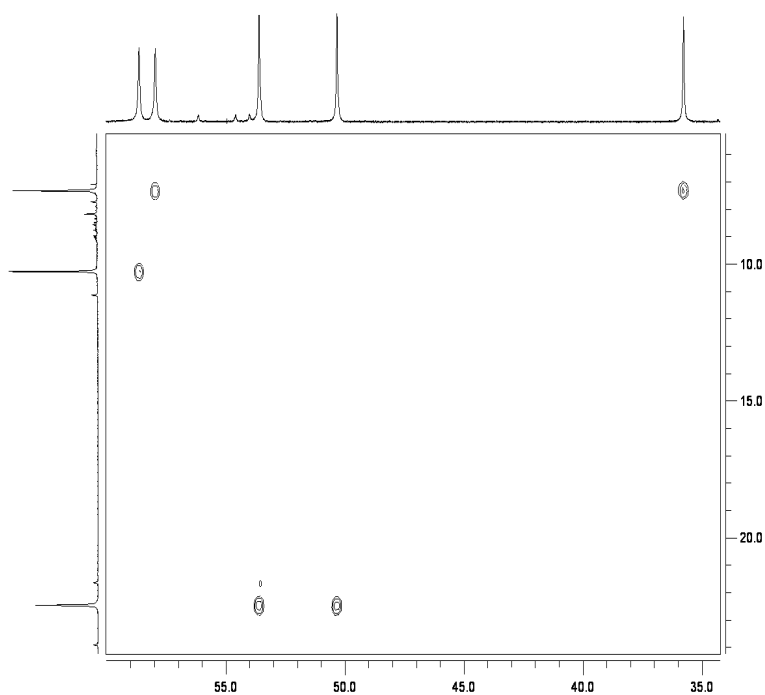


Figure 5.12: Part of the 500 MHz ^1H - ^1H COSY spectrum (in CD_3CN) of $[\text{Co}(\text{terpy-COOH})_2][\text{PF}_6]_2$ (**40**).

Superimposing the NMR spectrum of $[\text{Co}(\text{terpy-COOH})_2][\text{PF}_6]_2$ on the one of $[\text{Co}(\text{terpy-CHO})_2][\text{PF}_6]_2$ (**38**) indicated that there were differences between the two spectra. The protons $\text{B5}''$, $\text{B4}'$ and $\text{B4}''$ resonate at chemical shifts very close to three of the signals in the $[\text{Co}(\text{terpy-CHO})_2]^{2+}$ spectrum, but the other peaks are

significantly distant from one another. This is maybe due to deprotonation of the complex in one solution or the other, but this issue was not investigated further.

5.4. Interaction of $[\text{Co}(\text{terpy-COOH})_2][\text{PF}_6]_2$ with bis-amine templates

In the previous chapter, the templating experiments were carried out in an attempt to change the composition of a mixture. Here the starting point was different because we were starting with a single compound in the solution rather than a mixture.

Nevertheless, we decided to investigate how the carboxylic acid groups on the complexes would interact with bis-amine compounds. For this purpose, three bis-amines were chosen. These are shown in Figure 5.13: 1,2-diaminoethane (ED, **41**), 1,4-diaminobutane (TD, **42**) and 1,6-diaminohexane (HD, **43**).

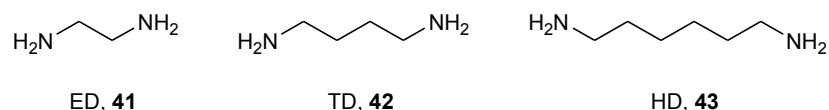


Figure 5.13: Template molecules used to try and bind to $[\text{Co}(\text{terpy-COOH})_2][\text{PF}_6]_2$.

The nature of the interaction could be of three kinds. One diamine molecule and two acid groups on a complex could react covalently and form a bis-amide hexadentate ligand. Otherwise, they could form a non-covalent six-membered ring with two hydrogen bonds. The third possibility is a proton transfer to form a salt.

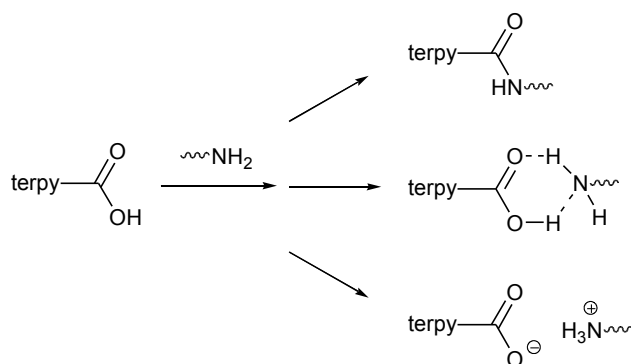


Figure 5.14: Possible interactions between the carboxylic acid and amine functionalities: formation of an amide (top), of hydrogen bonds (middle), or of a salt (bottom).

Three samples of $[\text{Co}(\text{terpy-COOH})_2][\text{PF}_6]_2$ were dissolved in CD_3CN in three NMR tubes. A stock solution for each template was prepared, ED and TD were dissolved in CD_3CN , while HD was dissolved in D_2O . One equivalent of each template was added to each sample of complex and the $^1\text{H-NMR}$ spectra of the mixtures were measured within 5 minutes of mixing.

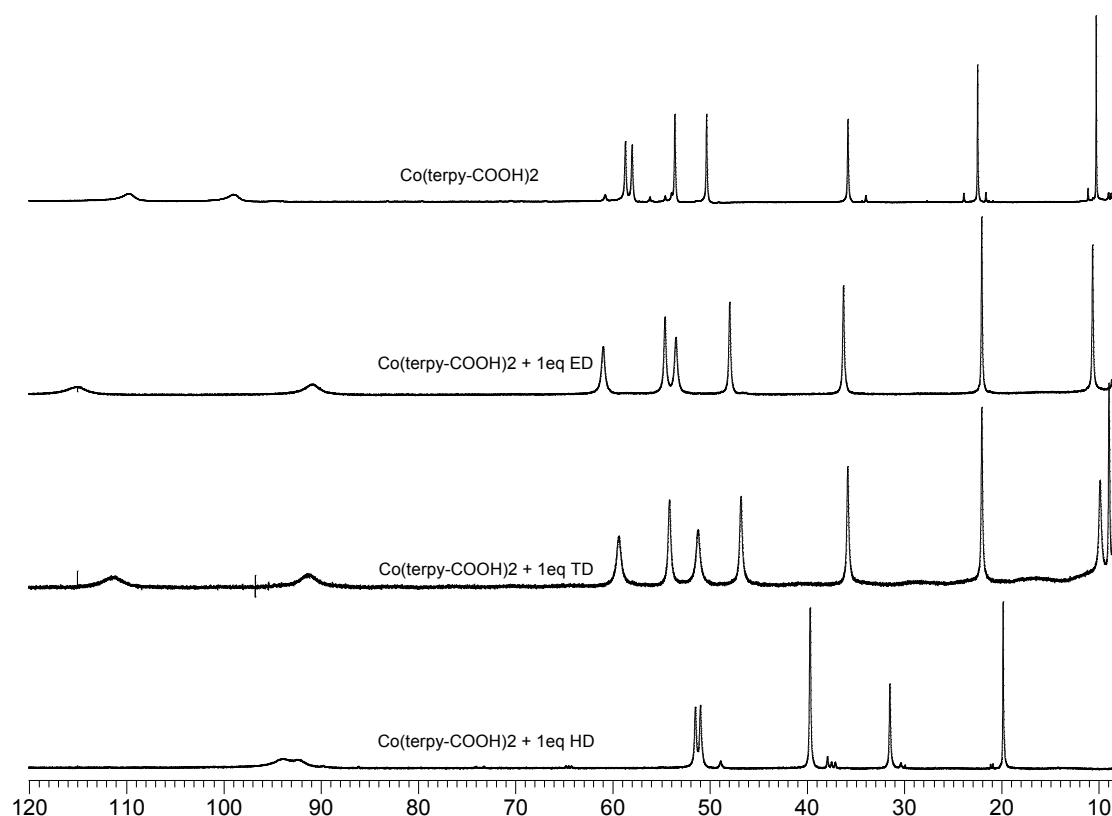


Figure 5.15: 250 MHz $^1\text{H-NMR}$ spectra of $[\text{Co}(\text{terpy-COOH})_2][\text{PF}_6]_2$ before the addition of any template, and after addition of one equivalent of ED, TD and HD. The first three spectra from the top were taken in CD_3CN , the spectrum at the bottom was taken in $\text{CD}_3\text{CN}/\text{D}_2\text{O}$.

Figure 5.15 shows the $^1\text{H-NMR}$ spectra of the mixtures of complex and the different diamines. The same figure also shows the spectrum of the complex before the addition of any template. There was a clear shifting of some signals upon addition of ED and TD, especially for the four sharp peaks between δ 60 and 50 ppm. When HD was added, the changes were even more dramatic, but it must be emphasised that the HD stock solution was prepared in D_2O instead of CD_3CN , and this could have an effect on the chemical shifts. In fact, adding deuterated water to the mixture of

complex and TD caused the signals to move towards a pattern very similar to the one observed with $[\text{Co}(\text{terpy-COOH})_2]^{2+}$ and aqueous HD (Figure 5.16).

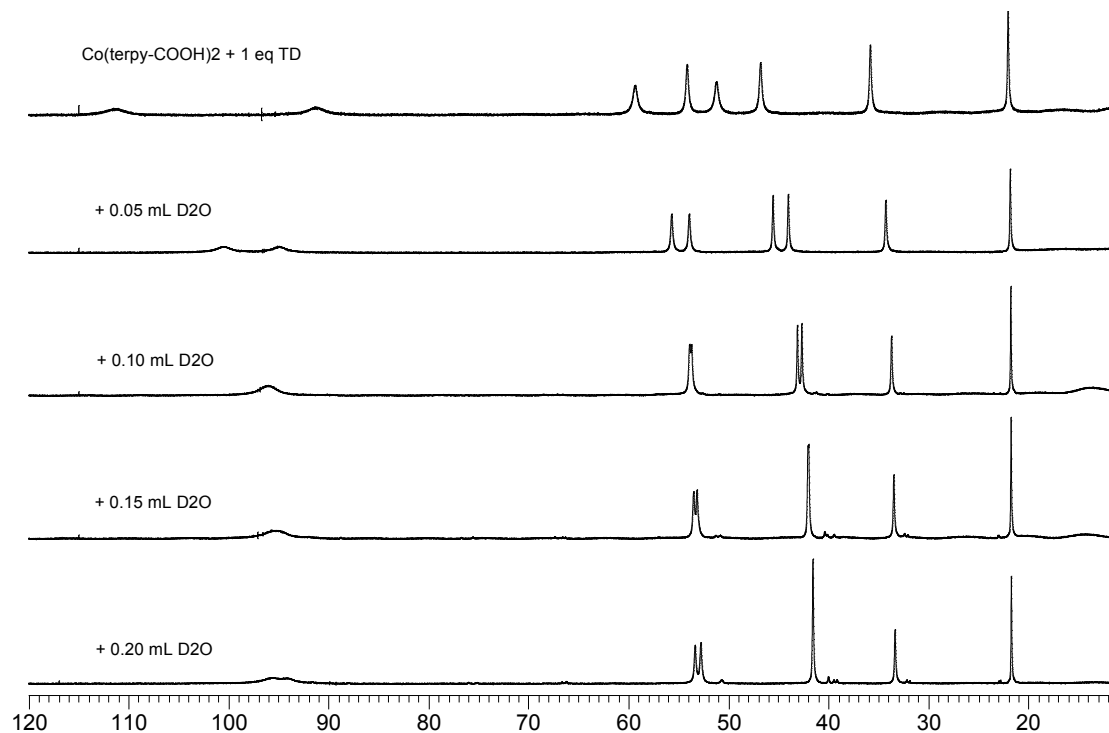


Figure 5.16: 250 MHz ^1H -NMR spectra of the 1:1 mixture of $[\text{Co}(\text{terpy-COOH})_2][\text{PF}_6]_2$ and TD before the addition of any water and after addition of different volumes of D_2O .

These observations provided some information about the nature of the interactions causing the changes of the chemical shifts. Figure 5.17 shows that addition of deuterated water to any of the complex-diamine mixtures lead to approximately the same NMR spectrum, no matter which template was present. Moreover, the resulting spectra are also similar to the one obtained with a solution of $[\text{Co}(\text{terpy})_2][\text{PF}_6]_2$ (**44**) in CD_3CN and D_2O . In the light of these observations it could be reasonably assumed that the first three spectra of Figure 5.17 belong to the same species, i.e. $[\text{Co}(\text{terpy-COOH})_2]^{2+}$ surrounded by D_2O molecules. This assumption is supported by the ESI-MS spectra of the mixtures of $[\text{Co}(\text{terpy-COOH})_2][\text{PF}_6]_2$ and ED or HD respectively, both diluted with H_2O . In these spectra there were only peaks for the fragments $[\text{Co}(\text{terpy-COOH})(\text{terpy-COO}^-)]^+$ and $[\text{Co}(\text{terpy-COOH})_2]^{2+}[\text{PF}_6]^-$.

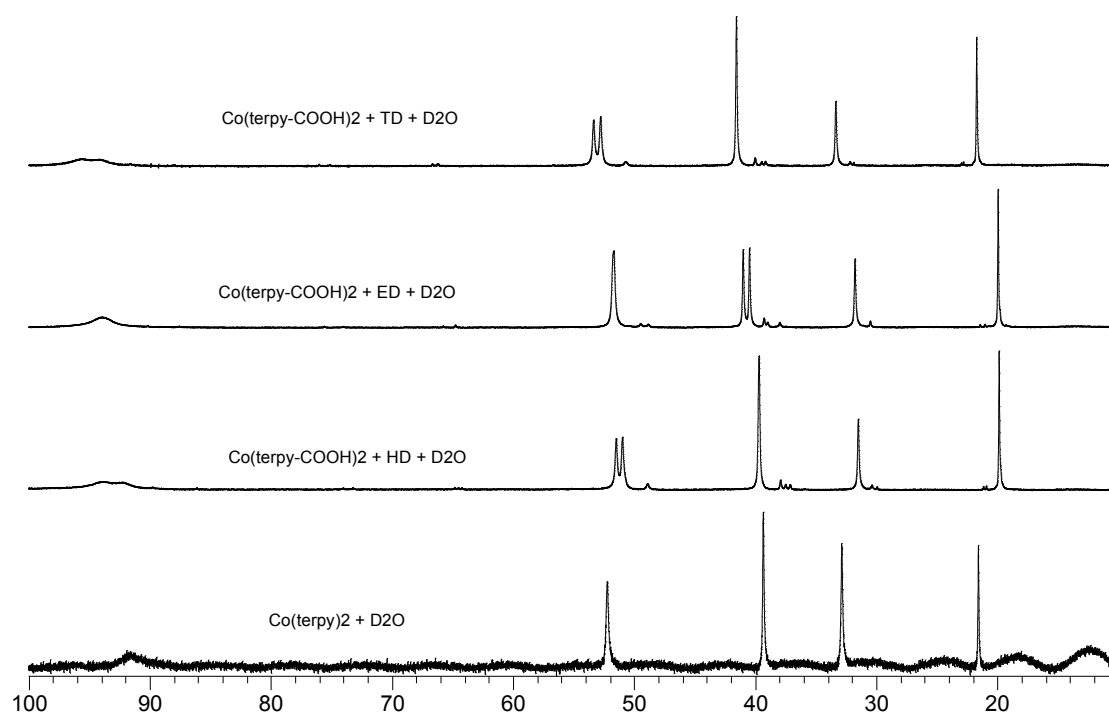


Figure 5.17: 250 MHz ¹H-NMR spectra of the complex and diamine mixtures in CD₃CN after addition of deuterated water, and comparison with the spectrum of [Co(terpy)₂][PF₆]₂ (**44**) in CD₃CN and D₂O.

Taking all the results together, we can conclude that, when ED and TD were added to the CD₃CN solution of complex, they interacted with the complex through hydrogen bonding. If water was added to the mixtures, it broke the interaction between complex and template and formed new H-bonds itself. HD was soluble only in water, and when its stock solution was added to the complex, the template probably did not have any possibility to interact with it, as the competition with water was too strong.

5.5. Ligand exchange at one metal centre

The ligand exchange reaction between cobalt(II) complexes of different 2,2'-bipyridines was discussed in the previous chapters. The exchange of 2,2':6',2''-terpyridine ligands at cobalt(II) when mixing two complexes has also already been established [30]. In this section, the exchange reaction between a complex and a free ligand will be studied. Furthermore, complexes of Fe(II) will be introduced and the possibility of ligand exchange at this metal centre will be investigated.

Synthesis and characterisation of $[\text{Co}(\text{terpy})_2][\text{PF}_6]_2$, $[\text{Fe}(\text{terpy})_2][\text{PF}_6]_2$ and $[\text{Fe}(\text{terpy-CH}_3)_2][\text{PF}_6]_2$

The complex $[\text{Co}(\text{terpy})_2][\text{PF}_6]_2$ (**44**) was prepared by mixing one equivalent of $\text{Co}(\text{OAc})_2$ with two equivalents of the commercially available terpy, followed by precipitation of the $[\text{PF}_6]^-$ salt. The ligand was symmetrical, and so no isomers resulted from this synthesis. The $^1\text{H-NMR}$ spectrum of this compound has already been fully assigned and discussed by Chow and co-workers [53]; here we show our spectrum only to allow a comparison with the spectra of the mixtures that will follow in the next section.

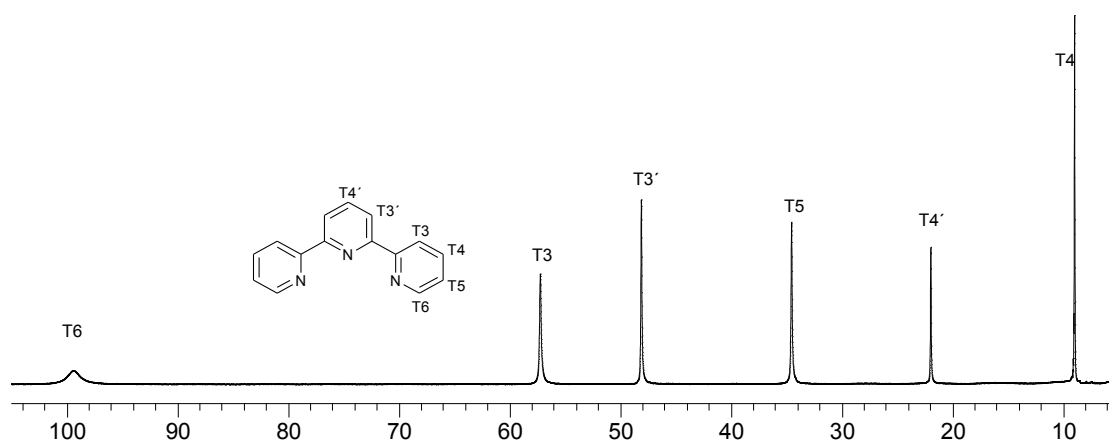


Figure 5.18: 250 MHz $^1\text{H-NMR}$ (in CD_3CN) of $[\text{Co}(\text{terpy})_2][\text{PF}_6]_2$ (**44**) in the region δ 105-5 ppm.

The complexes $[\text{Fe}(\text{terpy})_2][\text{PF}_6]_2$ (**45**) and $[\text{Fe}(\text{terpy-CH}_3)_2][\text{PF}_6]_2$ (**46**) were synthesised in a similar manner to that used for $[\text{Co}(\text{terpy})_2][\text{PF}_6]_2$. The electronic configuration of the d^6 Fe(II) ion (if we assume an octahedral coordination sphere)

can be $t_{2g}^4 e_g^2$ for high spin complexes or $t_{2g}^6 e_g^0$ for low spin complexes. If the metal centre is high spin, it is paramagnetic, and the $^1\text{H-NMR}$ spectrum of the complex might be similar to the one encountered with Co(II) complexes, with a large chemical shift range. If, instead, the metal centre is low spin, it will be diamagnetic. The $^1\text{H-NMR}$ spectrum of a low spin Fe(II) complex will not show any unusual shifting, and the peaks will show the regular couplings between neighbouring protons. The range of the chemical shifts obtained for the $[\text{Fe(terpy)}_2]^{2+}$ and $[\text{Fe(terpy-CH}_3)_2]^{2+}$ complexes indicated immediately the low spin state of the metal centre. For the full assignment of the spectra, the coupling constants and the $^1\text{H-}^1\text{H}$ COSY spectra of the complexes were used.

In the case of $[\text{Fe(terpy)}_2]^{2+}$, for example, T3 and T3' were distinguished by comparing their coupling constants with the one of the triplet at δ 8.67 ppm. This signal had previously been unambiguously assigned T4' on the basis of its integral, T4' being the only unique proton in the ligand.

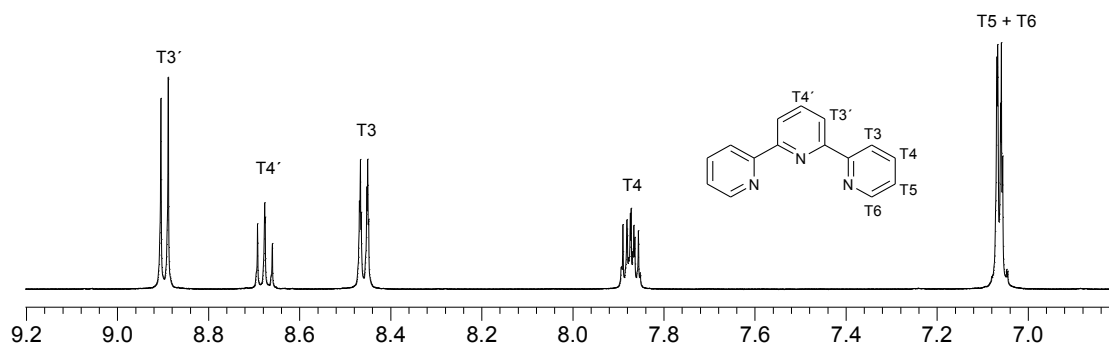


Figure 5.19: 500 MHz $^1\text{H-NMR}$ spectrum (in CD_3CN) of $[\text{Fe(terpy)}_2][\text{PF}_6]_2$ (**45**) in the region δ 9.2–6.8 ppm.

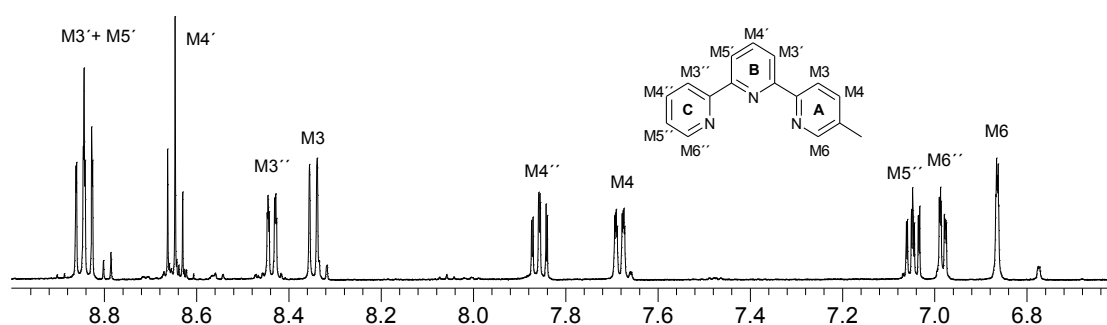


Figure 5.20: 500 MHz ^1H -NMR spectrum (in CD_3CN) of $[\text{Fe}(\text{terpy-CH}_3)_2][\text{PF}_6]_2$ (**46**) in the region δ 9.0-6.6 ppm. The signal for CH_3 is at δ 2.17 ppm.

The use of the ^1H - ^1H COSY spectrum was particularly helpful in the case of $[\text{Fe}(\text{terpy-CH}_3)_2]^{2+}$ as it allowed to identify the three spin systems corresponding to the three pyridine rings. The spin systems could be unambiguously assigned because each had a different number of protons, and here all the couplings were visible. This is thanks to the fact that, in a diamagnetic complex, there is no perturbation such as line broadening for the protons closest to the metal centre, and these can show a cross peak, as did here $\text{M6}''$. Concerning $\text{M3}'$ and $\text{M5}'$, their assignment remained ambiguous with this analysis.

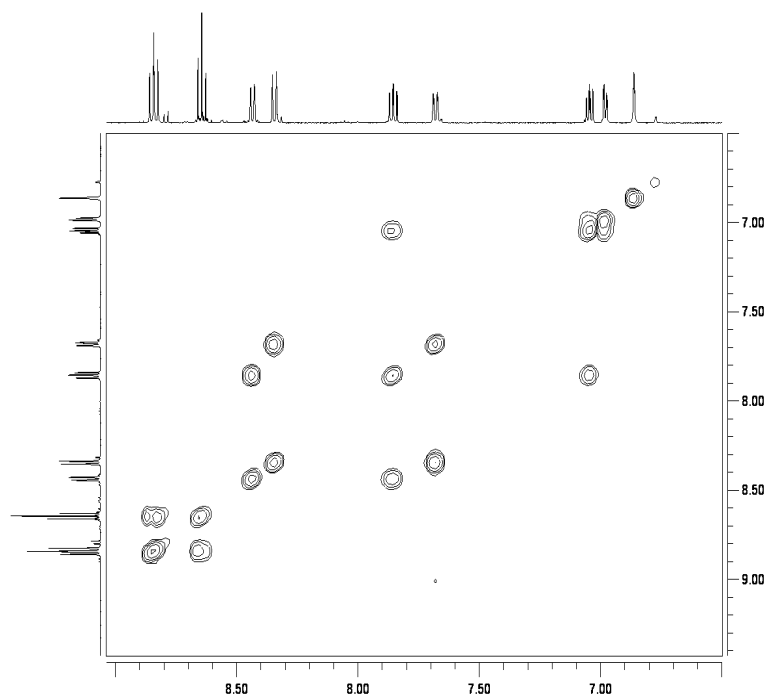


Figure 5.21: Part of the 500 MHz ^1H - ^1H COSY spectrum (in CD_3CN) of $[\text{Fe}(\text{terpy-CH}_3)_2][\text{PF}_6]_2$ (**46**).

Library containing two ligands and one metal centre

The two cobalt(II) complexes introduced in this chapter, $[\text{Co}(\text{terpy})_2][\text{PF}_6]_2$ (**44**) and $[\text{Co}(\text{terpy-CH}_3)_2][\text{PF}_6]_2$ (**37**), were mixed in CD_3CN in a 1:1 ratio in an NMR tube. The ^1H -NMR spectrum of the mixture was studied to investigate the ligand exchange, the composition of the library and, hence, determine the equilibrium constant. The only mixing product formed by ligand exchange between $[\text{Co}(\text{terpy})_2]^{2+}$ and $[\text{Co}(\text{terpy-CH}_3)_2]^{2+}$ is the heteroleptic $[\text{Co}(\text{terpy})(\text{terpy-CH}_3)]^{2+}$. The relative weighting of these three compounds in a statistical mixture would be 1 for each homoleptic complex and 2 for the heteroleptic mixing product. We saw already that the complex of the unsubstituted ligand, terpy, gave rise to six ^1H -NMR peaks, with the relative integral 1:1:1:1:1:0.5. The complex with the asymmetrical terpy- CH_3 gave rise to 10 signals of the same integral for the aromatic rings, and one signal for the methyl group, with relative integral 3. The ^1H -NMR spectrum of the heteroleptic complex will then show a total of 17 peaks. The signals arising from the aromatic protons of terpy- CH_3 will all correspond to one proton, while the signals arising from terpy, with

the exception of T4', will be twice as intense. If the mixture reached the statistical composition, we should see, for a given proton of terpy (excepting T4'), two signals with the relative integral (number of ligands x number of equivalent protons x statistical weighting) = (2 x 2 x 1) : (1 x 2 x 2) = 4:4. For the special case of T4' the relative integral would be (2 x 1 x 1) : (1 x 1 x 2) = 2:2. For each of the aromatic proton of terpy-CH₃, always assuming a statistical mixture, the number of signals would also be two, with the relative integral (2 x 1 x 1) : (1 x 1 x 2) = 2:2.

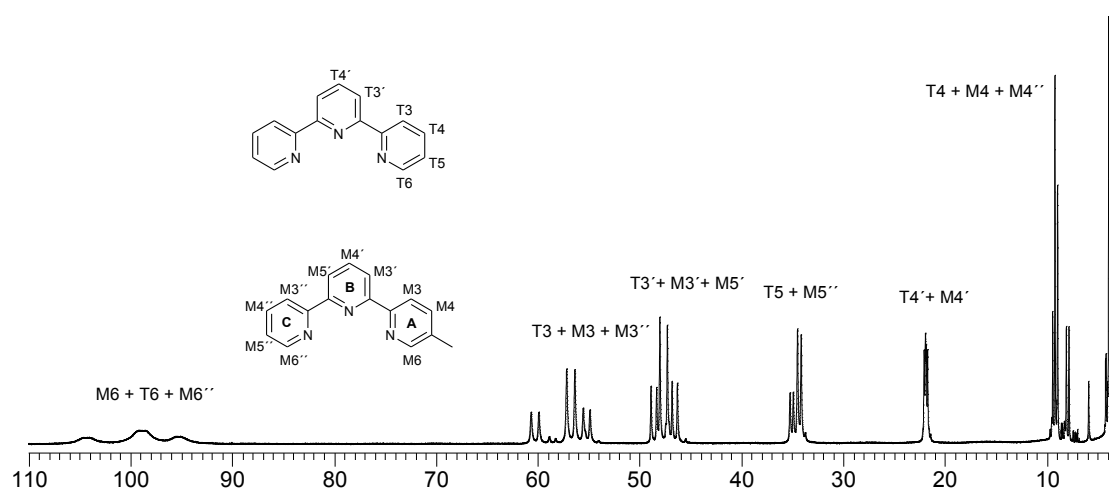
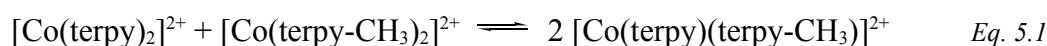


Figure 5.22: 250 MHz ¹H-NMR spectrum of the 1:1 mixture of [Co(terpy)₂][PF₆]₂ and [Co(terpy-CH₃)₂][PF₆]₂ (CD₃CN) in the region δ 110-6 ppm.

Figure 5.22 shows the ¹H-NMR spectrum of a 1:1 mixture of [Co(terpy)₂][PF₆]₂ and [Co(terpy-CH₃)₂][PF₆]₂. It was clearly visible how, within each group of signals, the peaks for terpy were twice as intense as the others, this confirming the establishment of the statistical composition of the library. The equilibrium constant of this library was calculated.

The equilibrium constant *K* for the reaction



is given by the equation (here [] is used to mean concentration and the use of square brackets to designate a complex is ignored):

$$K = \frac{[\text{Co}(\text{terpy})(\text{terpy}-\text{CH}_3)^{2+}]^2}{[\text{Co}(\text{terpy})_2^{2+}][\text{Co}(\text{terpy}-\text{CH}_3)_2^{2+}]} \quad \text{Eq. 5.2}$$

In the 1:1 mixture, where the relative concentrations are $[\text{Co}(\text{terpy})_2^{2+}] : [\text{Co}(\text{terpy}-\text{CH}_3)_2^{2+}] : [\text{Co}(\text{terpy})(\text{terpy}-\text{CH}_3)^{2+}] = 1:1:2$, the equilibrium constant K becomes

$$K = \frac{2^2}{1 \cdot 1} = 4 \quad \text{Eq. 5.3}$$

and

$$\log K = 0.60 \quad \text{Eq. 5.4}$$

The full assignment of the $^1\text{H-NMR}$ spectrum was possible by comparison with the spectra of the homoleptic complexes and with the help of the integrals of the peaks. The chemical shifts for the signals of the homoleptic species were already known and could be simply picked out from the spectrum. Of the remaining peaks, those with relative integral 2 were attributed to the terpy ligand, while those with relative integral 1 were attributed to terpy- CH_3 for the symmetry reasons explained above. Figure 5.23 shows the clusters of peaks between δ 54 and 30 ppm and how they were assigned. The 2:1 ratio in the integrals is clearly visible. The full assignment of the library is presented in Table 5.2.

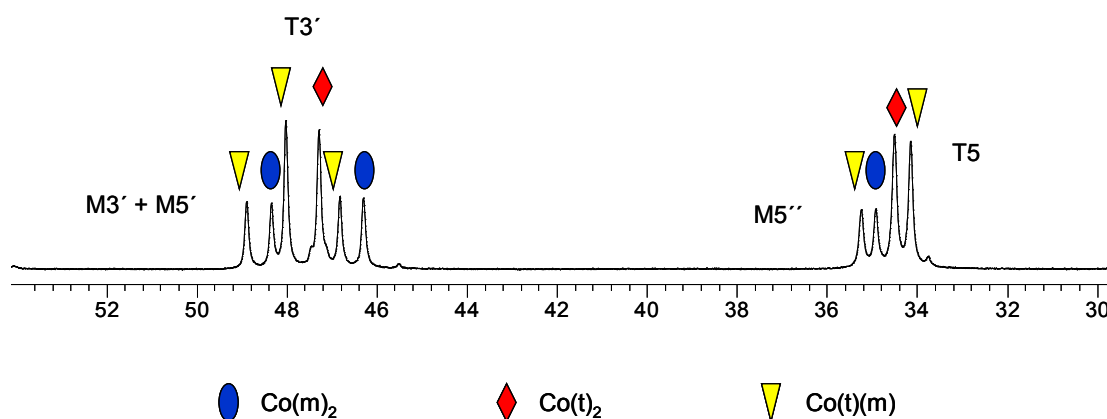


Figure 5.23: 250 MHz $^1\text{H-NMR}$ resonances (in CD_3CN) of the protons $\text{M3}'$, $\text{M5}'$ and $\text{M5}''$ of terpy- CH_3 and $\text{T3}'$ and T5 of terpy in the 1:1 mixture of $[\text{Co}(\text{terpy})_2]^{2+}$ and $[\text{Co}(\text{terpy}-\text{CH}_3)_2]^{2+}$. $m = \text{terpy}-\text{CH}_3$, $t = \text{terpy}$.

A 1:1 mixture of $[\text{Fe}(\text{terpy})_2][\text{PF}_6]_2$ and $[\text{Fe}(\text{terpy-CH}_3)_2][\text{PF}_6]_2$ in CD_3CN was prepared in an NMR tube. The $^1\text{H-NMR}$ spectrum was measured immediately after mixing, but did not suggest any ligand exchange. This was deduced from the presence of only one peak with a relative integral of 3 in the region where the signals for CH_3 were expected. The sample was heated to $80\text{ }^\circ\text{C}$ for about one hour and another spectrum was measured. If there were any new signals, these could not be identified as there was a general broadening of the peaks which prevented us from interpreting the spectrum.

terpy-CH ₃	CH ₃	-	-	3.95	3.89
	H6''	-	-	**	***
	H5''	-	-	34.91	35.23
	H4''	-	-	8.10	7.85
	H3''	-	-	54.89	55.55
	H4'	-	-	21.86	*
	H3'+H5'†	-	-	48.33, 46.28	48.88, 46.82
	H6	-	-	**	***
	H4	-	-	9.44	9.22
	H3	-	-	59.91	60.65
terpy	H4'	21.94	-	-	*
	H3'	48.02	-	-	47.28
	H6	99.63	-	-	***
	H5	34.50	-	-	34.14
	H4	8.96	-	-	9.22
	H3	51.17	-	-	56.36
	terpy		terpy-CH ₃		terpy-CH ₃
	terpy		terpy-CH ₃		terpy

Table 5.2: 250 MHz ¹H-NMR peaks (δ / ppm) of the homoleptic and binary complexes in the 1:1 mixture of [Co(terpy)₂][PF₆]₂ and [Co(terpy-CH₃)₂][PF₆]₂ in CD₃CN.

† Distinction between H3' and H5' ambiguous.

* δ 21.72, 22.07 ppm, ambiguous.

** δ 103.87, 94.84 ppm, ambiguous.

*** Overlapping of the peaks and line broadening did not allow an unambiguous assignment.

After having confirmed the ligand exchange between the Co(II)/terpy complexes used in this chapter, we investigated the exchange behaviour between a complex and a free ligand.

For this reaction, the equation for the exchange between a general complex MA_2 and a general ligand B is



and the equilibrium constant K is given by the equation

$$K = \frac{[MB_2][MAB][A]^3}{[MA_2]^2[B]^3} \quad \text{Eq. 5.6}$$

where $[\]$ means concentration, ignoring their function to designate a complex.

A way to calculate the statistical composition for a 1:1 mixture of $[MA_2]$ and B is shown in Figure 5.24. Knowing the rapidity of the ligand exchange, mixing $[MA_2]$ and B in 1:1 ratio can be considered to be the same as mixing M, A and B in 1:2:1 ratio. The pyramid is similar to the one explained in Chapter 2 for the 2:1 mixture of $[MA_3]$ and $[MB_3]$, only one layer shorter because here the metal binds only two ligands. The pyramid yields the relative concentrations of the complexes in the mixture, but this time there will be some free ligands next to the complexes. To find the relative concentrations of the free ligands, the following calculation was made. It was known that at equilibrium the complexes were present in ratio $[MA_2] : [MAB] : [MB_2] = 4:4:1$. If we considered these weighting as number of molecules, we could say that the total number of M in the mixture was $4 + 4 + 1 = 9$. The initial conditions were a M : A : B ratio of 1:2:1, i.e. 9:18:9 molecules of M, A and B. The M's and the necessary number of A and B were used to form the nine complexes obtained through the pyramid, leaving us with 3 B's and 6 A's remaining as free ligands. A statistical 1:1 mixture of $[MA_2]$ and B will then contain the products $[MA_2]$, $[MAB]$, $[MB_2]$, A and B in the ratio 4:4:1:6:3.

The same calculations were carried out for the case when $[MA_2]$ and B are mixed in 1:2 ratio. The result gave a mixture of $[MA_2]$, $[MAB]$, $[MB_2]$, A and B in the ratio 1:2:1:4:4.

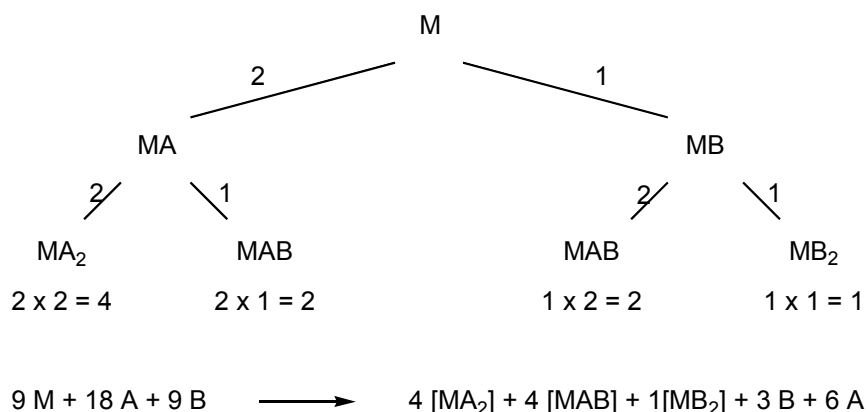


Figure 5.24: Statistical distribution of the complexes in the library with $M : A : B = 1 : 2 : 1$.

To two CD_3CN solutions of $[\text{Co}(\text{terpy-CH}_3)_2][\text{PF}_6]_2$ were added 1 and 2 equivalents of free terpy. In a similar way, to two CD_3CN solutions of $[\text{Co}(\text{terpy})_2][\text{PF}_6]_2$ were added 1 and 2 equivalents of free terpy- CH_3 . The $^1\text{H-NMR}$ spectra of these mixtures were measured and analysed. Figures 5.25 and 5.26 show the peaks for the aromatic protons of the coordinated ligands. The peaks for the free ligands, as well as for the protons T4, M4 and M4'' of the coordinated ligands, were appearing in the region δ 10-7 ppm. These signals were overlapping and were rather poorly resolved, so that an analysis of the composition of the mixture from these peaks was not possible.

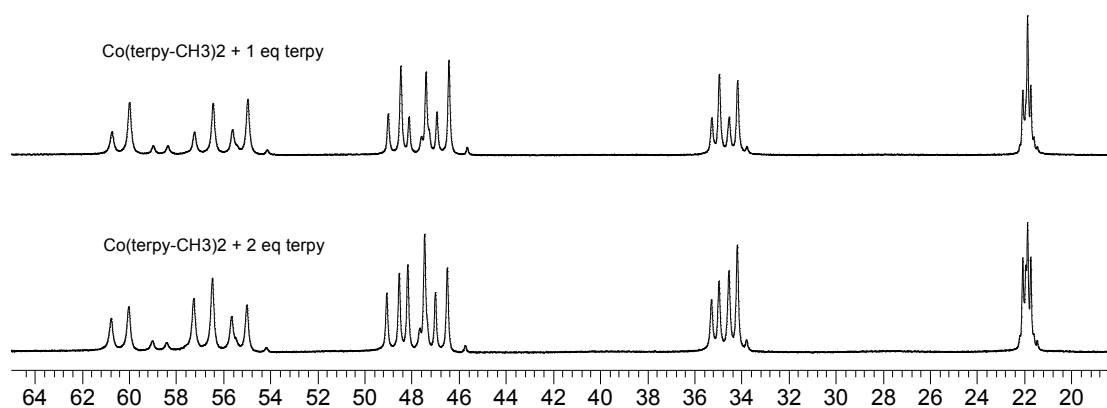


Figure 5.25: 250 MHz $^1\text{H-NMR}$ spectra (in CD_3CN) of the mixtures of $[\text{Co}(\text{terpy-CH}_3)_2][\text{PF}_6]_2$ with different equivalents of free terpy in the region δ 65-18 ppm.

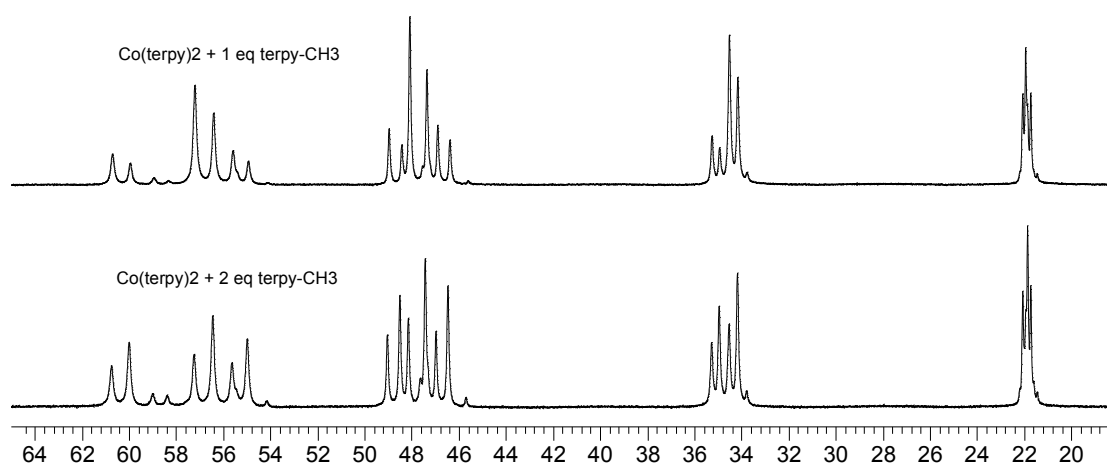


Figure 5.26: 250 MHz $^1\text{H-NMR}$ spectra (in CD_3CN) of the mixtures of $[\text{Co}(\text{terpy})_2][\text{PF}_6]_2$ with different equivalents of free terpy-CH_3 in the region δ 65-18 ppm.

In Figures 5.25 and 5.26, we could recognise the same peaks already encountered in the $^1\text{H-NMR}$ of the mixture of $[\text{Co}(\text{terpy})_2]^{2+}$ and $[\text{Co}(\text{terpy-CH}_3)_2]^{2+}$. This was not a surprise as the ligands used were the same in all three cases, and when these were mixed with Co(II) ions in whichever ratio, the resulting Co(II) species were the same. The relative integrals changed according to the starting concentrations of complex and free ligand. From the integrals, the relative concentrations of the Co(II) species could be calculated with [concentration = integral / (number of ligands x number of equivalent protons)]. The integrals of the peaks for the single free ligands in the region δ 10-7 ppm could not be read, but the concentrations could be derived from the values calculated for the Co(II) complexes. How this was done is illustrated in Figure 5.27 with the case of the 1:1 mixture of $[\text{Co}(\text{terpy-CH}_3)_2]^{2+}$ and terpy .

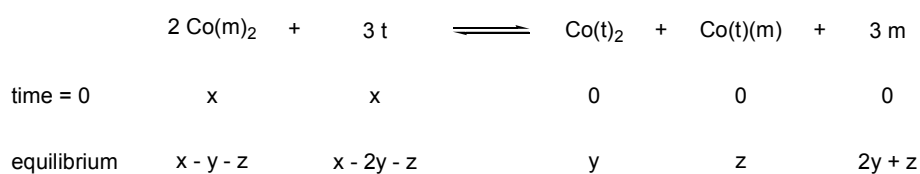


Figure 5.27: System for the calculation of the relative integrals of free terpy and terpy-CH_3 in the 1:1 mixture of $[\text{Co}(\text{terpy-CH}_3)_2][\text{PF}_6]_2$ and terpy . $m = \text{terpy-CH}_3$, $t = \text{terpy}$.

At the moment of mixing (time = 0) the real amounts of material were known, but not the volume of the solution, so that the concentrations of $[\text{Co}(\text{terpy-CH}_3)_2]^{2+}$ and terpy were set to equal x . At equilibrium, a certain amount y of $[\text{Co}(\text{terpy})_2]^{2+}$ and a certain amount z of $[\text{Co}(\text{terpy-CH}_3)(\text{terpy})]^{2+}$ had formed. The remaining $[\text{Co}(\text{terpy-CH}_3)_2]^{2+}$ was given then by the starting concentration minus what had undergone ligand exchange to form the new Co(II) species, i.e. $x-y-z$. The remaining amount of terpy was given by the starting concentration (x) minus the amount needed to form the two new complexes: two terpy for every $[\text{Co}(\text{terpy})_2]^{2+}$ ($2y$) and one for every $[\text{Co}(\text{terpy-CH}_3)(\text{terpy})]^{2+}$ (z). The concentration of free terpy-CH₃ was the sum of the ligands set free to form the new complexes, i.e. two terpy-CH₃ for every $[\text{Co}(\text{terpy})_2]^{2+}$ and one for every $[\text{Co}(\text{terpy-CH}_3)(\text{terpy})]^{2+}$, for a total of $2y+z$. The relative concentrations at equilibrium of $[\text{Co}(\text{terpy-CH}_3)(\text{terpy})]^{2+}$ ($= z$) and $[\text{Co}(\text{terpy})_2]^{2+}$ ($= y$) were known from the ¹H-NMR spectrum. The relative concentration of $[\text{Co}(\text{terpy-CH}_3)_2]^{2+}$ was also known from the spectrum; with that and the numerical values of y and z , the value of x could be calculated. Once we had all the numerical values for x , y and z , it was easy to calculate the relative concentrations of each free ligand.

A similar calculation was carried out for the 1:2 mixture, with the difference that the initial concentrations of complex and free ligand were set to x and $2x$ respectively. With the concentrations of all the species, the experimental equilibrium constants for the 1:1 and 1:2 mixtures were calculated according to Equation 5.6. The results are summarised in Table 5.3.

$[\text{Co}(\text{t})_2]^{2+}:\text{m}$	$[\text{Co}(\text{t})_2]^{2+}$	$[\text{Co}(\text{t})(\text{m})]^{2+}$	$[\text{Co}(\text{m})_2]^{2+}$	t	m	K	$\log K$
1:1	0.38	0.48	0.15	0.78	0.23	19.4 ± 4.8	1.29
1:2	0.25	0.72	0.61	1.9	1.2	33.0 ± 8.1	1.52
$[\text{Co}(\text{m})_2]^{2+}:\text{t}$	$[\text{Co}(\text{t})_2]^{2+}$	$[\text{Co}(\text{t})(\text{m})]^{2+}$	$[\text{Co}(\text{m})_2]^{2+}$	t	m	K	$\log K$
1:1	0.25	1.1	1.3	1.1	1.6	0.5 ± 0.1	-0.30
1:2	0.23	0.62	0.42	1.5	1.1	0.3 ± 0.1	-0.50

Table 5.3: Relative concentrations of each species in different mixtures, and equilibrium constants for the mixtures. The concentrations were calculated from the ¹H-NMR integrals with an estimated error of 5% and rounded to two significant digits. The error in K was calculated with the error propagation formula. $m = \text{terpy-CH}_3$, $t = \text{terpy}$.

The statistical composition of a 1:1 mixture of [MA₂] and B was shown to be [MA₂] : [MAB] : [MB₂] : A : B = 4:4:1:6:3. Inserting these values in Equation 5.6, the equilibrium constant K is obtained:

$$K = \frac{1 \cdot 4 \cdot 6^3}{4^2 \cdot 3^3} = 2 \quad \text{Eq. 5.7}$$

and

$$\log K = 0.30 \quad \text{Eq. 5.8}$$

For the case when [MA₂] and B are mixed in 1:2 ratio, the final composition was calculated to be [MA₂] : [MAB] : [MB₂] : A : B = 1:2:1:4:4. The reaction conditions are the same as in the previous mixture, therefore the equilibrium constant K should reach the same value as in Equation 5.7. This is confirmed by inserting the final concentrations calculated for the 1:2 mixture in Equation 5.6, which gives Equation 5.9:

$$K = \frac{1 \cdot 2 \cdot 4^3}{1^2 \cdot 4^3} = 2 \quad \text{Eq. 5.9}$$

The results shown in Table 5.3 differed slightly from the equilibrium constant calculated for a statistical distribution of the products. In the first two entries the equilibrium constant was higher than the predicted value of $K = 2$ for a statistical mixture. This suggested that the equilibrium was slightly favouring the formation of [Co(terpy-CH₃)₂]²⁺ and free terpy, at the expense of the starting materials. This trend was confirmed in the last two entries. A K smaller than 1 indicated that, this time, the equilibrium was shifted to the side of the starting materials, which were [Co(terpy-CH₃)₂]²⁺ and terpy again. This behaviour was quite unexpected, after having seen that in the case where the two Co(II) complexes were mixed, the composition of the library followed the expected statistical distribution, regardless of any eventual difference in the stability of the single complexes. The reason for the equilibrium shifting in the complex/free ligand mixtures must lie in the different stability of the free ligands with respect to each other. A possible explanation could be the different solubility of terpy and terpy-CH₃ in acetonitrile. While terpy-CH₃ was found to be

reasonably soluble in CH_3CN , at least at the mM scale needed for these NMR experiments, terpy remained partially insoluble. This surely drove the equilibrium to the side where free terpy was present, as its precipitation was removing it from the equilibrium.

5.6. Ligand exchange at two metal centres

So far, we have studied libraries that possessed one level of exchange, which was between ligand and Co(II) . In this section, studies will be presented of the attempt to add a second level of exchange by introducing another metal ion into the library. A 1:1 mixture of $[\text{Co(terpy)}_2][\text{PF}_6]_2$ and $[\text{Fe(terpy-CH}_3)_2][\text{PF}_6]_2$ in CD_3CN was prepared in an NMR tube. The $^1\text{H-NMR}$ spectrum was measured immediately after mixing and a different times thereafter. The spectra showed the sum of the peaks of the pure substances, revealing that no ligand exchange occurred between the two metal centres. The sample was then heated to about $80\text{ }^\circ\text{C}$ for one hour, and the NMR spectrum was measured again. This time a range of new peaks were observed (Figure 5.28). The peaks for the Co(II) species were easily recognised to be the same already observed in the previous section with the mixtures containing the cobalt(II) ion and the two ligands terpy and terpy- CH_3 . This indicated the presence of the complexes $[\text{Co(terpy)(terpy-CH}_3)]^{2+}$ and $[\text{Co(terpy-CH}_3)_2]^{2+}$, which can only have formed by ligand exchange with the Fe(II) complex.

The observation of the NMR spectrum in the range δ 10-0 ppm, where the signals for the Fe(II) are visible, confirmed this exchange (Figure 5.29). These peaks did not profit from the paramagnetic shifting due to the Co(II) ion, so that most of them overlapped and were difficult to assign. However, the triplet of doublets around δ 7.9 ppm assigned to M4'' of $[\text{Fe(terpy-CH}_3)_2]^{2+}$, which was still distinguishable in the spectrum at $t = 0$, became a broad multiplet after heating. The signal for T4 in pure $[\text{Fe(terpy)}_2]^{2+}$ was a multiplet around the same chemical shift, therefore the broad multiplet in the spectrum of the mixture was considered evidence for the presence of this complex.

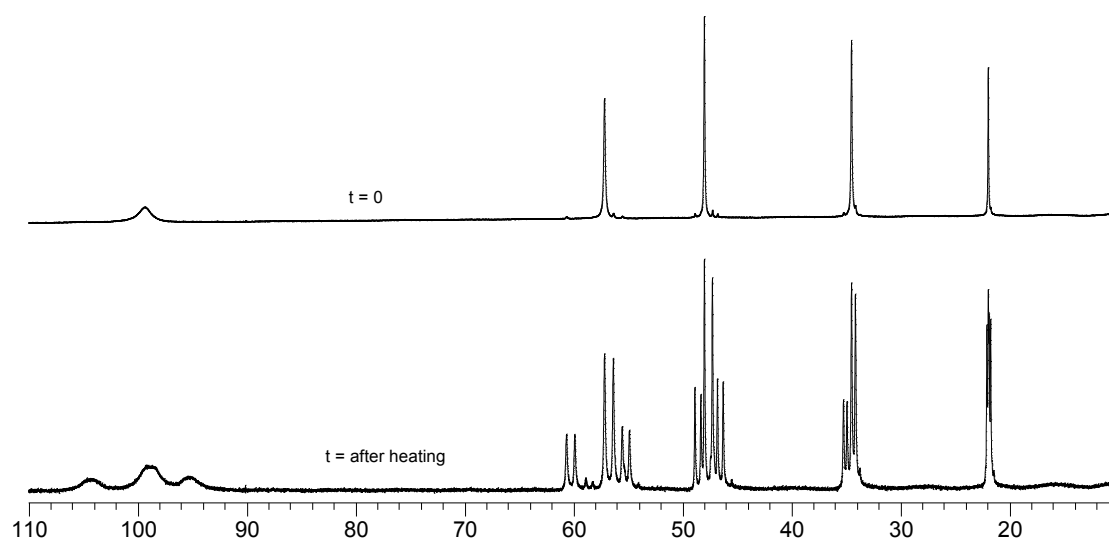


Figure 5.28: 250 MHz ¹H-NMR spectra (in CD₃CN) of the 1:1 mixture of [Co(terpy)₂][PF₆]₂ and [Fe(terpy-CH₃)₂][PF₆]₂ at different times showing the peaks for the Co(II) species.

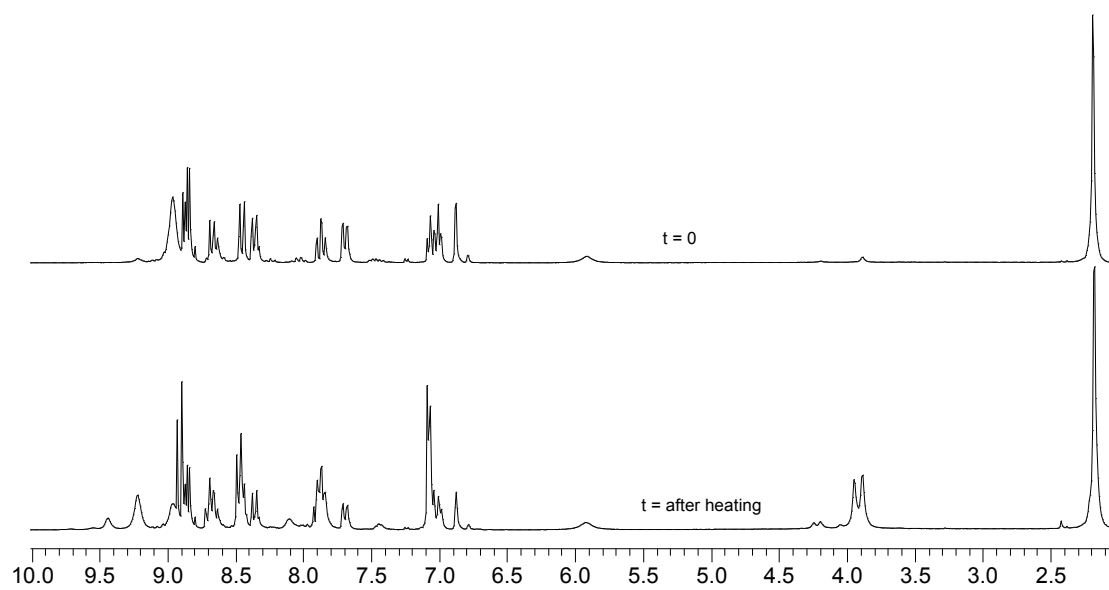
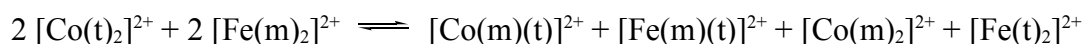


Figure 5.29: 250 MHz ¹H-NMR spectra (in CD₃CN) of the 1:1 mixture of [Co(terpy)₂][PF₆]₂ and [Fe(terpy-CH₃)₂][PF₆]₂ at different times showing the peaks for the Fe(II) species.

The chemical equation for this exchange is



Eq. 5.10

with $t = \text{terpy}$ and $m = \text{terpy-CH}_3$.

The equilibrium constant K is given by

$$K = \frac{[\text{Co}(m)(t)]^{2+} [\text{Fe}(m)(t)]^{2+} [\text{Co}(m)_2]^{2+} [\text{Fe}(t)_2]^{2+}}{[\text{Fe}(m)_2]^{2+} [\text{Co}(t)_2]^{2+}}$$

Eq. 5.11

where $[\]$ means concentration, ignoring their function to designate a complex.

The statistical weighting of each member of the library would be 1 for every homoleptic species and 2 for the heteroleptic $[\text{Co}(\text{terpy})(\text{terpy-CH}_3)]^{2+}$ and $[\text{Fe}(\text{terpy})(\text{terpy-CH}_3)]^{2+}$. When these relative concentrations are inserted in Equation 5.11, the equilibrium constant for the statistical mixture is given by Equation 5.12:

$$K = \frac{2 \cdot 2 \cdot 1 \cdot 1}{1^2 \cdot 1^2} = 4$$

Eq. 5.12

The experimental relative concentrations of the three Co(II) complexes in the mixture were calculated from the integrals of the NMR peaks. Among the many signals that overlapped in the region δ 10-0 ppm, the singlet for M6 at δ 6.9 ppm and the doublet for M4 at δ 7.7 ppm of $[\text{Fe}(\text{terpy-CH}_3)_2]^{2+}$ remained clean and their integrals could also be used to calculate the concentration of this Fe(II) species. The concentrations of the remaining complexes were derived from the known values in a similar way as was presented in the previous section (Figure 5.30).

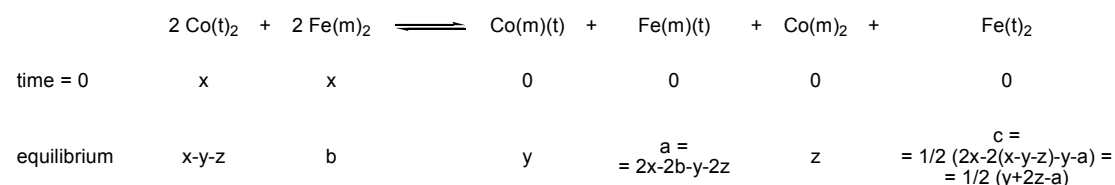


Figure 5.30: System for the calculation of the relative concentrations of $[\text{Fe}(\text{terpy-CH}_3)(\text{terpy})]^{2+}$ and $[\text{Fe}(\text{terpy})_2]^{2+}$ in the 1:1 mixture of $[\text{Co}(\text{terpy})_2][\text{PF}_6]_2$ and $[\text{Fe}(\text{terpy-CH}_3)_2][\text{PF}_6]_2$. $m = \text{terpy-CH}_3$, $t = \text{terpy}$.

As has just been said, the values of b , y and z could readily be calculated from the integrals of the NMR peaks. The value of $(x-y-z)$ could also be derived from the NMR spectrum and, with it, the value of x . To find a , an expression was found using the total number of terpy-CH₃ ligands, which was given by the initial concentration of [Fe(terpy-CH₃)₂]²⁺ multiplied by two, i.e. $2x$. At equilibrium, of these $2x$ molecules of terpy-CH₃, $2b$ were used in [Fe(terpy-CH₃)₂]²⁺, y were used in [Co(terpy)(terpy-CH₃)]²⁺, and $2z$ were used in [Co(terpy-CH₃)₂]²⁺. The rest was equal to the number of [Fe(terpy-CH₃)(terpy)]²⁺. In a similar way, an expression was found to calculate c by using the total number of terpy ligands. The results are shown in Table 5.4.

[Co(t) ₂] ²⁺	[Fe(m) ₂] ²⁺	[Co(m)(t)] ²⁺	[Fe(m)(t)] ²⁺	[Co(m) ₂] ²⁺	[Fe(t) ₂] ²⁺	K	$\log K$
0.23	0.15	0.41	0.56	0.19	0.12	4.4 ± 0.7	0.64

Table 5.4: Relative concentrations of each species in the 1:1 mixture of [Co(terpy)₂][PF₆]₂ and [Fe(terpy-CH₃)₂][PF₆]₂ and equilibrium constant for the mixture. The concentrations were calculated from the ¹H-NMR integrals with an estimated error of 5% and rounded to two significant digits. The error in K was calculated with the error propagation formula. m = terpy-CH₃, t = terpy.

A 1:1 mixture of [Co(terpy-CH₃)₂][PF₆]₂ and [Fe(terpy)₂][PF₆]₂ in CD₃CN was prepared in an NMR tube. The ¹H-NMR spectrum of the mixture was measured right after mixing and then after heating at about 80 °C for one hour. The NMR spectrum at $t = 0$ in Figure 5.31 could induce to think that some ligand exchange had occurred already before heating. In fact, the small peaks next to the signals of [Co(terpy-CH₃)₂]²⁺ are unfortunately due to an impurity in the sample and were already present in the spectrum of the “pure” [Co(terpy-CH₃)₂][PF₆]₂.

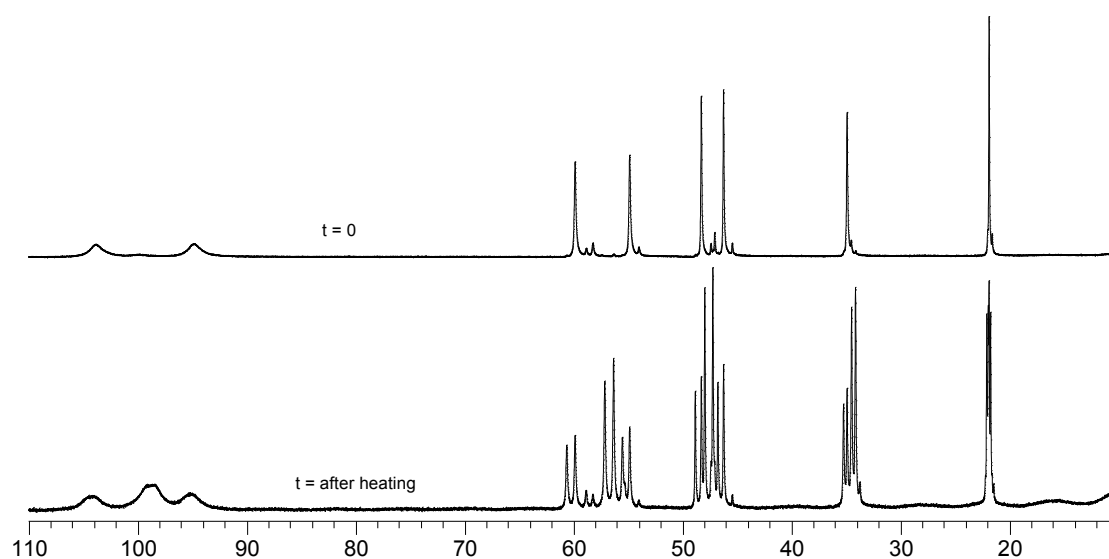


Figure 5.31: 250 MHz $^1\text{H-NMR}$ spectra (in CD_3CN) of the 1:1 mixture of $[\text{Co}(\text{terpy-CH}_3)_2][\text{PF}_6]_2$ and $[\text{Fe}(\text{terpy})_2][\text{PF}_6]_2$ at different times showing the peaks for the Co(II) species.

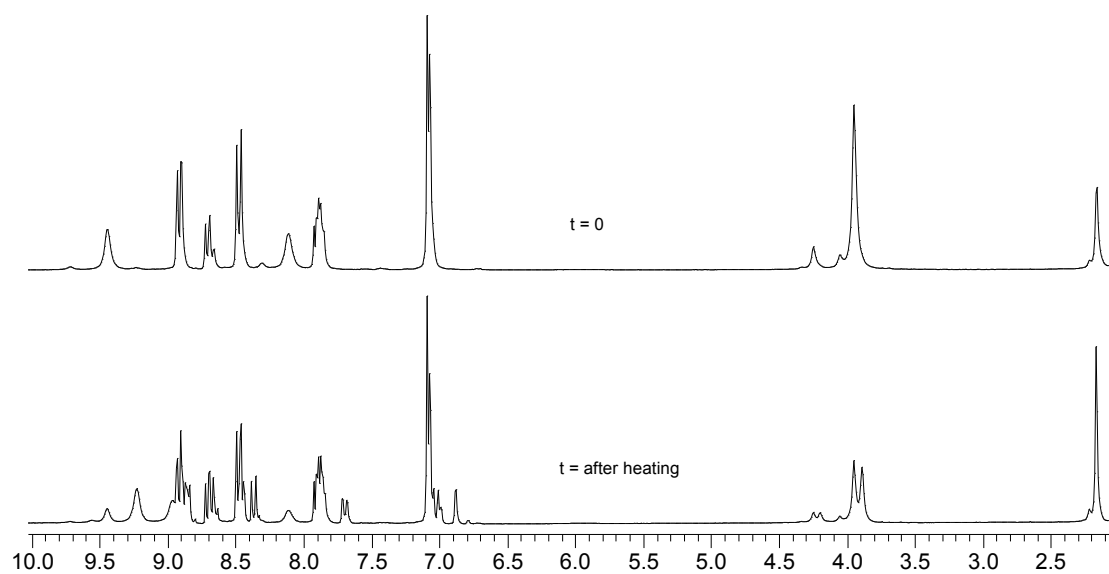


Figure 5.32: 250 MHz $^1\text{H-NMR}$ spectra (in CD_3CN) of the 1:1 mixture of $[\text{Co}(\text{terpy-CH}_3)_2][\text{PF}_6]_2$ and $[\text{Fe}(\text{terpy})_2][\text{PF}_6]_2$ at different times showing the peaks for the Fe(II) species.

Ligand exchange occurred only after heating, as was confirmed by the range δ 10-0 ppm of the NMR spectrum, shown in Figure 5.32. Here it was possible to see how the few signals characteristic of $[\text{Fe}(\text{terpy-CH}_3)_2]^{2+}$ (a singlet at δ 6.9 ppm, a doublet at δ 7.7 ppm) have arisen upon heating. Again, the relative concentration of each species

in the mixture was calculated, and with it the equilibrium constant of the mixture. The results are summarised in Table 5.5.

The results reported in Table 5.4 and 5.5 approximately reflect a statistical mixture.

$[\text{Co(m)}_2]^{2+}$	$[\text{Fe(t)}_2]^{2+}$	$[\text{Co(m)(t)}]^{2+}$	$[\text{Fe(m)(t)}]^{2+}$	$[\text{Co(t)}_2]^{2+}$	$[\text{Fe(m)}_2]^{2+}$	K	$\log K$
0.27	0.25	0.53	0.56	0.23	0.22	3.3 ± 0.5	0.52

Table 5.5: Relative concentrations of each species in the 1:1 mixture of $[\text{Co(terpy-CH}_3)_2][\text{PF}_6]_2$ and $[\text{Fe(terpy)}_2][\text{PF}_6]_2$ and equilibrium constant for the mixture. The concentrations were calculated from the $^1\text{H-NMR}$ integrals with an estimated error of 5% and rounded to two significant digits. The error in K was calculated with the error propagation formula. $m = \text{terpy-CH}_3$, $t = \text{terpy}$.

5.7. Conclusions

In this chapter, a synthetic route was described for the synthesis of 5-formyl-2,2':6',2''-terpyridine (terpy-CHO, **36**) and 5-carboxy-2,2':6',2''-terpyridine (terpy-COOH, **39**).

The Co(II) complexes of these two ligands and of 5-methyl-2,2':6',2''-terpyridine (terpy-CH₃, **34**) were prepared and the $^1\text{H-NMR}$ spectra of their $[\text{PF}_6]^-$ salts in CD_3CN were studied. The spectrum of $[\text{Co(terpy-CHO)}_2][\text{PF}_6]_2$ showed many more peaks than expected and could not be interpreted. For the case of $[\text{Co(terpy-COOH)}_2][\text{PF}_6]_2$ and $[\text{Co(terpy-CH}_3)_2][\text{PF}_6]_2$, a full assignment of the NMR peaks could be made with the help of the $^1\text{H-}^1\text{H}$ COSY spectra.

The complex $[\text{Fe(terpy-CH}_3)_2][\text{PF}_6]_2$ was prepared and its $^1\text{H-NMR}$ spectrum was fully assigned with the help of the $^1\text{H-}^1\text{H}$ COSY spectrum.

Three bis-amine templates, 1,2-diaminoethane (ED), 1,4-diaminobutane (TD) and 1,6-diaminohexane (HD), were separately added to three sample of $[\text{Co(terpy-COOH)}_2][\text{PF}_6]_2$ in CD_3CN . It was shown that the three templates interacted with the complex by forming hydrogen bonds.

A 1:1 mixture of $[\text{Co(terpy-CH}_3)_2][\text{PF}_6]_2$ and $[\text{Co(terpy)}_2][\text{PF}_6]_2$ was prepared and analysed by $^1\text{H-NMR}$. The solution contained the starting and mixing products in the ratio predicted for a statistical mixture.

$[\text{Co}(\text{terpy-CH}_3)_2][\text{PF}_6]_2$ and terpy on one side, and $[\text{Co}(\text{terpy})_2][\text{PF}_6]_2$ and terpy-CH₃ on the other side, were mixed in different ratios, and their ¹H-NMR spectra analysed. It was shown that the complexes were exchanging their ligands with the free terpys in solution to form a mixture of 3 different complexes and both free ligands. The product distribution was slightly different from the predicted statistical composition, revealing a light shifting of the equilibrium to the side where free terpy was present. This was probably due to the limited solubility of terpy in the solvent used for the experiments (CD₃CN).

While a 1:1 mixture of two different Fe(II) complexes could not be investigated because the ¹H-NMR peaks were too broad, two 1:1 mixtures of one Fe(II) and one Co(II) complex with different ligands revealed ligand exchange. This ligand exchange occurred only upon heating of the mixtures, providing in fact a tool that allowed us to easily switch on and off one of the two levels of dynamicity of the library (exchange at the Fe(II) centre). In Chapter 3 it was already shown that it was possible to switch off the second level of exchange (ligand exchange at the Co(II) centre) by oxidation of the metal centre. The product distribution at equilibrium of the Co(II) complex / Fe(II) complex mixtures reflected the statistics. This confirmed the suitability of the Co(II)/Fe(II)/terpy system to form dynamic combinatorial libraries.

6. Self-assembly of polynuclear macrocycles containing 2,2':6',2''-terpyridine- and sandwich-complexes

6.1. Introduction

So far we have formed new dynamic combinatorial libraries of Co(II) complexes by exchanging their ligands between each other and with free ligands. In these cases the exchange was limited to one moiety: the Co(II)/bpy or Co(II)/terpy moiety. The exchange could be switched off if all the Co(II) centres were oxidised to Co(III), virtually at the same time.

When Co(II) and Fe(II) complexes were mixed, it was shown that ligand exchange between the two metals could occur only upon heating. This added a second level of exchange, which could be controlled by changing the temperature of the mixture.

In both cases, the resulting products were complexes containing only one metal centre. In this chapter, it will be discussed how attempts were made to combine two kinds of exchange within the same molecule. The idea was to form macrocycles containing more than one metal centre with two different complexing sites, where the exchange could be controlled by independent actions influencing only one complex. Initially it was thought possible to combine a bis- 2,2':6',2''-terpyridine complex and a bis- η^6 -arene complex. Arene exchange reactions of bis-arene complexes of chromium(0) were known to take place under relatively mild conditions, by heating in the absence or presence of a catalyst [101, 102, 103]. The new ligand 5-(4-phenylbutyl)-2,2':6',2''-terpyridine (terpy-C4-Ph, **47**) was synthesised from terpy-CH₃ (**34**) and 1-bromo-3-phenylpropane, and its Co(II) and Fe(II) complexes were prepared. However, no reports were found about the formation of the sandwich bis(benzene)chromium(0) complex by simple mixing of benzene and Cr(0). In fact, the reported synthetic pathways for this complex involve several steps starting from Cr(III) with the subsequent reduction of the metal, or even metal-vapour synthesis

[104]. Indeed, our attempts to form a sandwich bis-arene complex with Cr(0) and other d^6 metals such as molybdenum(0), tungsten(0) and rhodium(III), in different solvents and under different reaction conditions, were all unsuccessful. These experiments are described schematically in Figure 6.2 but will not be discussed further. The synthetic procedure and the characterisation of terpy-C4-Ph and its Co(II) and Fe(II) complexes are reported in the experimental chapter.

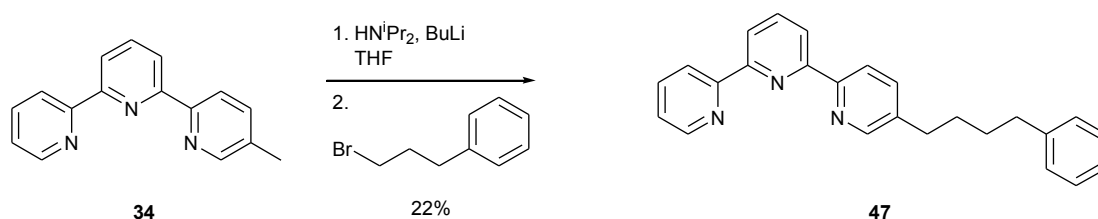


Figure 6.1: Synthesis of 5-(4-phenylbutyl)-2,2':6',2''-terpyridine (terpy-C4-Ph, 47).

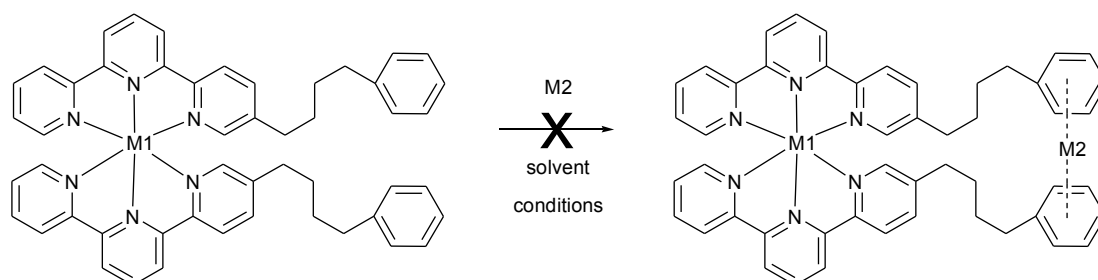


Figure 6.2: Schematic representation of the unsuccessful attempts to add a sandwich bis-arene complex next to the bis-terpy complex. M1 = Co(II), Fe(II); M2 = Cr(0), Mo(0), W(0), Rh(III); solvent = CD_3CN , acetone- d_6 , THF- d_8 ; conditions = room temperature, heating, hv.

A publication was found, describing the formation of a dimeric Ru(II)/arene complex by heating an ethanolic solution of RuCl_3 with the corresponding cyclohexa-1,3-diene or cyclohexa-1,4-diene [105].

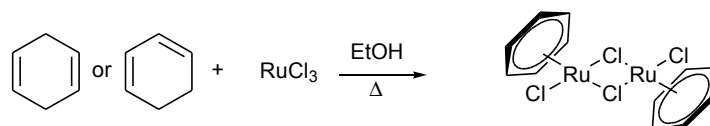


Figure 6.3: Formation of the dimeric Ru(II) complex after the redox reaction between Ru(III) and cyclohexadiene.

Inspired by this model, the synthesis of 5-(4-cyclohexa-1,4-dienylbutyl)-2,2':6',2''-terpyridine (terpy-C4-chd, **53**) was developed. The ligand was similar to **47** but with a cyclohexadiene instead of the phenyl ring. After preparing the Co(II) or Fe(II)/terpy complex, this would be mixed with RuCl₃ in the hope of forming the polynuclear macrocycle as shown in Figure 6.4.

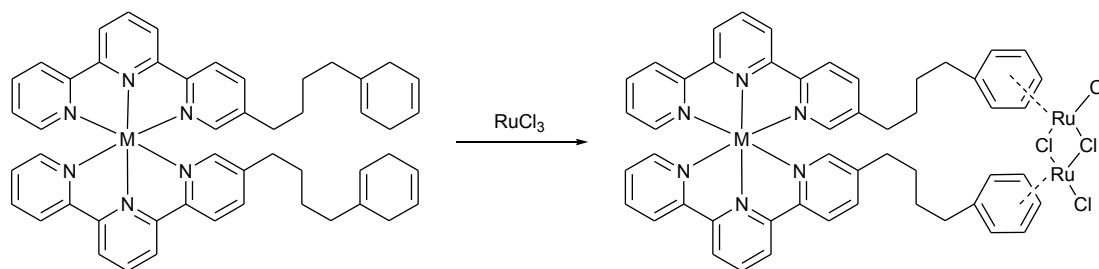


Figure 6.4: Structure of the polynuclear complex expected from the reaction of $[M(\text{terpy-C4-chd})_2]^{2+}$ with Ru(III). $M = \text{Co(II)}, \text{Fe(II)}$.

6.2. Synthesis of the ligand

The first step of the synthesis involved a Birch reduction of the commercially available 3-phenylpropanol (**48**) to obtain the substituted cyclohexadiene ring (Figure 6.5). The procedure was adapted from the one published for the reduction of *t*-butylbenzene [106]. The reaction yielded the 2,5-dihydro product **49** as a single product. This was identified from the presence of two ¹H-NMR peaks with the relative integrals 2 and 1 in the region δ 6-5 ppm, corresponding to the three protons attached to the double bonds (Figure 6.6). For the symmetrical 1,4-dihydro product (**50**), only one peak of relative integral 4 would have been expected for these protons.

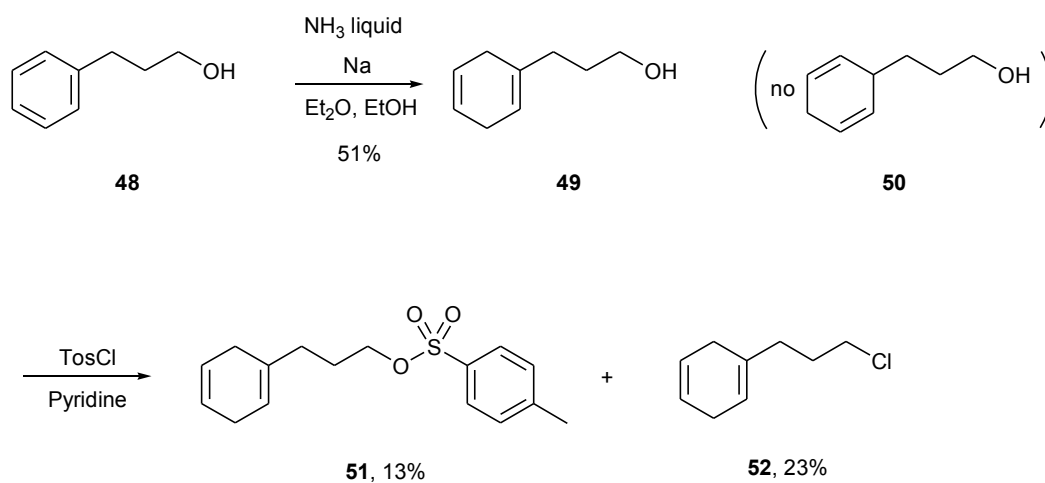


Figure 6.5: Synthesis of the first precursor of terpy-C4-chd, **51**.

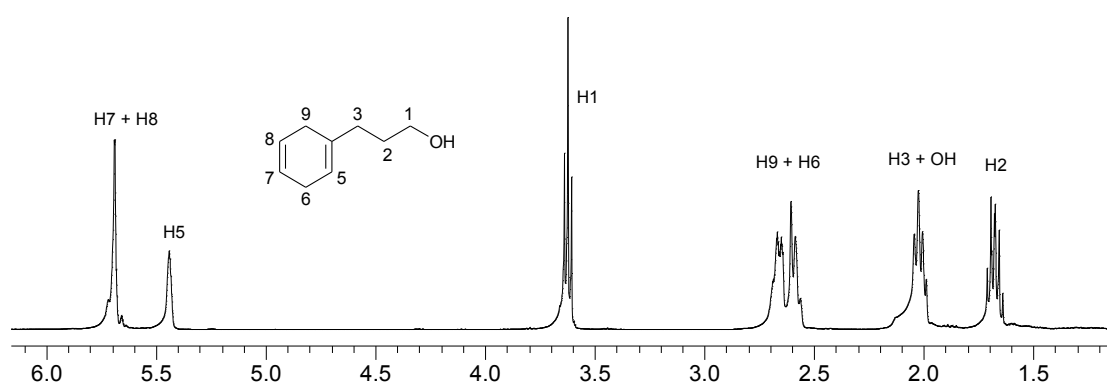


Figure 6.6: 400 MHz $^1\text{H-NMR}$ spectrum (in CDCl_3) of 3-cyclohexa-1,4-dienylpropan-1-ol (**49**).

The hydroxyl group of **49** was then activated by tosylation with *p*-toluenesulfonyl chloride (TosCl) in cold pyridine (Figure 6.5). The reaction worked only with a modest yield of 13%, probably because of a previous partial decomposition of an old batch of TosCl into TosOH and HCl. Indeed, as the side product of the reaction, the product of the substitution of the hydroxyl group by chloride, **52**, was obtained in significant yield (23%).

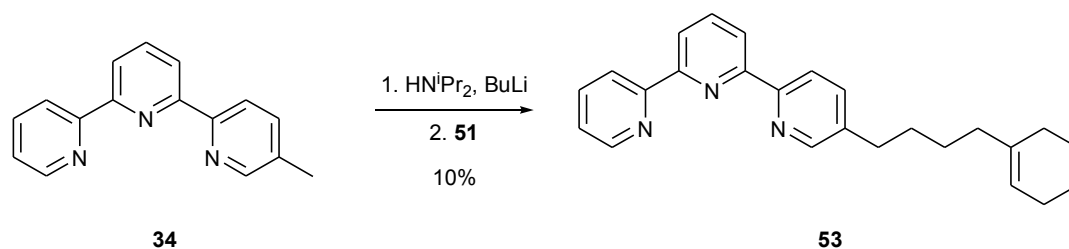


Figure 6.7: Last step of the synthesis of terpy-C4-chd (**53**).

The desired ligand, terpy-C4-chd (**53**), was obtained by the reaction of the precursor **51** with terpy- CH_3 (**34**), whose synthesis was presented in Chapter 5. The chloride **52** could have been used as well, but unfortunately it was identified after the completion of the synthesis.

The procedure for the last step followed a model proposed by Holbrey [51]. The methyl group of terpy- CH_3 was deprotonated by lithium diisopropylamide, which was prepared *in situ* from diisopropylamine and butyl lithium. The resulting carbanion then substituted the tosylate leaving group of **51** to give the desired product. The yield was rather low, probably due to the very low acidity of the methyl group, but enough material was obtained for characterisation and preparation of the complexes.

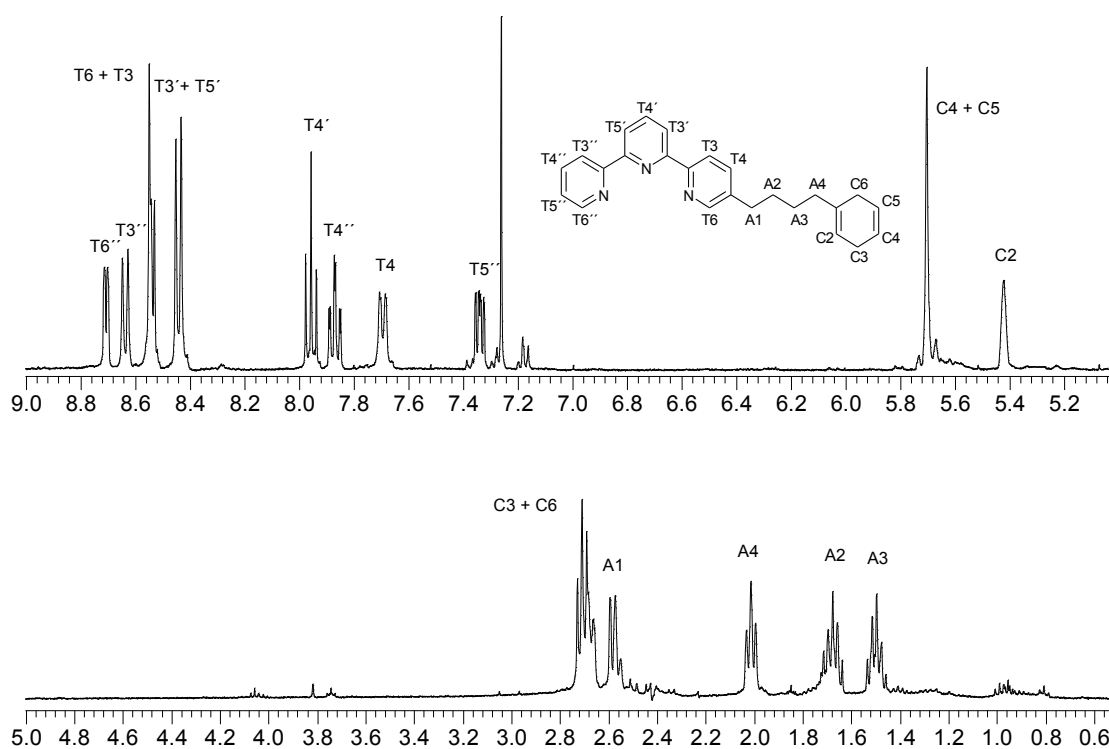


Figure 6.8: 400 MHz $^1\text{H-NMR}$ spectrum (in CDCl_3) of terpy-C4-chd (**53**).

Figure 6.8 shows the $^1\text{H-NMR}$ spectrum of terpy-C4-chd. The assignments of the terpy signals were made by comparison with the spectrum of terpy- CH_3 . As expected, the different length of the alkyl chain had hardly any influence on the chemical shifts of the aromatic protons. Three signals with distinct coupling patterns were expected for protons C2, C4 and C5, because of their vicinity to C3, C6 and to each other, but unfortunately the peaks were not well resolved and they appeared only as broad singlets. The coupling pattern was more visible in the signals for C3 and C6, but these overlapped, so that only a poorly defined multiplet could be seen. The remaining peaks for the alkyl chain, A1, A2, A3 and A4, were assigned by comparison with the chemical shifts calculated with the help of spectral reference tables [107].

6.3. Synthesis of the complexes

$[\text{Co}(\text{terpy-C4-chd})_2][\text{PF}_6]_2$ and $[\text{Fe}(\text{terpy-C4-chd})_2][\text{PF}_6]_2$ were prepared by mixing cobalt(II) acetate and iron(II) sulfate respectively with two equivalents of the ligand,

followed by precipitation of the $[\text{PF}_6]^-$ salts. The $^1\text{H-NMR}$ spectra of the two complexes in CD_3CN are shown in Figures 6.9 and 6.10.

For both complexes, the peaks of the aromatic protons showed hardly any change in chemical shifts from the corresponding terpy- CH_3 -complex, as was the case with the free ligand.

In the spectrum of $[\text{Fe}(\text{terpy-C4-chd})_2]^{2+}$ (Figure 6.9) it was observed that the complexation of the terpy moiety caused a small upfield shifting of the signals for the aliphatic protons. It was assumed that all signals were similarly affected, so that the signals were assigned to the protons in the same order as for the free ligand.

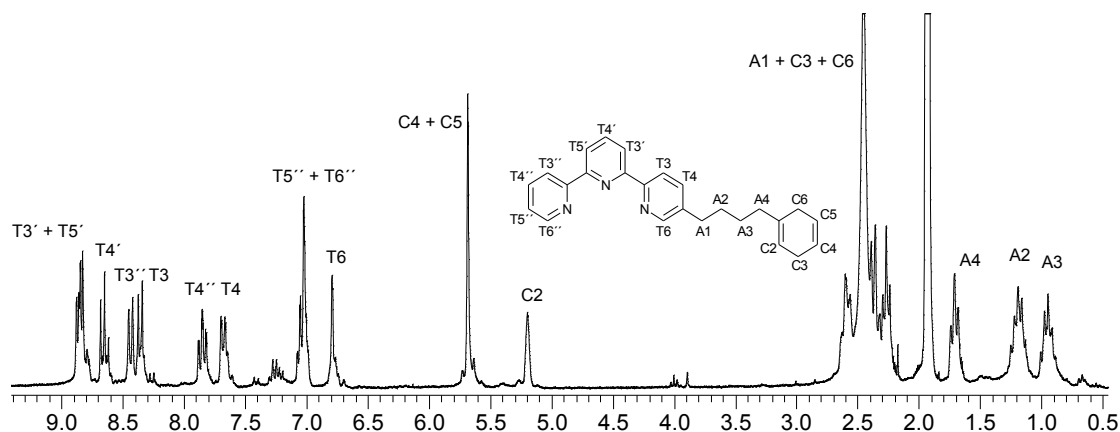


Figure 6.9: 250 MHz $^1\text{H-NMR}$ spectrum (in CD_3CN) of $[\text{Fe}(\text{terpy-C4-chd})_2][\text{PF}_6]_2$ (54).

In the spectrum of $[\text{Co}(\text{terpy-C4-chd})_2]^{2+}$ (Figure 6.10) the shifting of the peaks due to complexation with Co(II) was greater than with Fe(II) , because of the paramagnetism of cobalt(II). The shifting was relevant also for the peaks of the alkyl protons. The signals between δ 6 and 4 ppm and the intense signal around δ 2.2 ppm were assigned to the protons of cyclohexadiene in the same order as for the free ligand. The ring was still relatively far from the paramagnetic centre and it was assumed that the influence of the metal was comparable in every position of the ring. The signals for the protons of the butyl chain were possibly in the same order as for the free ligand as well. However, the protons A1 could have felt the proximity of the Co(II) more than the others and their peak could have been shifted differently. No more investigation was made of this issue, and a precise assignment was not made.

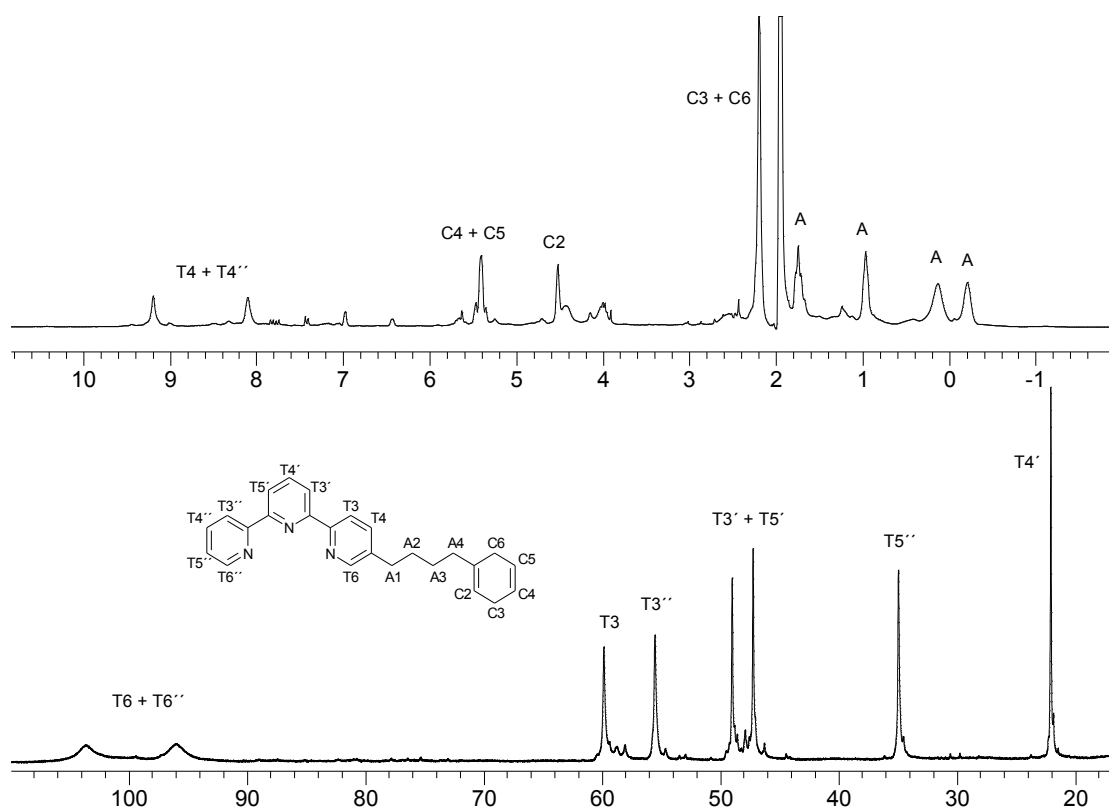


Figure 6.10: 250 MHz $^1\text{H-NMR}$ spectrum (in CD_3CN) of $[\text{Co}(\text{terpy-C4-chd})_2][\text{PF}_6]_2$ (**55**).

6.4. Attempts at the formation of the macrocycles

To a CD_3CN solution of $[\text{Co}(\text{terpy-C4-chd})_2][\text{PF}_6]_2$ were added 2 equivalents of RuCl_3 for every cobalt. The $^1\text{H-NMR}$ spectrum of the mixture was measured immediately after mixing, and is shown in Figure 6.11. It was immediately noticed that all the paramagnetically shifted peaks had disappeared. In the expansion of the δ 11 to -1 ppm region (Figure 6.12) we could see that the peaks are much too broad to give any real information. However, the two signals of relatively intensity 2:1 between δ 6 and 5 ppm, characteristic of the cyclohexadiene ring, suggested that no reaction occurred between the rings and Ru(III) . If a reaction had occurred, the aromatisation of the rings would have caused these two peaks to disappear, and a new peak in the aromatic region to appear.

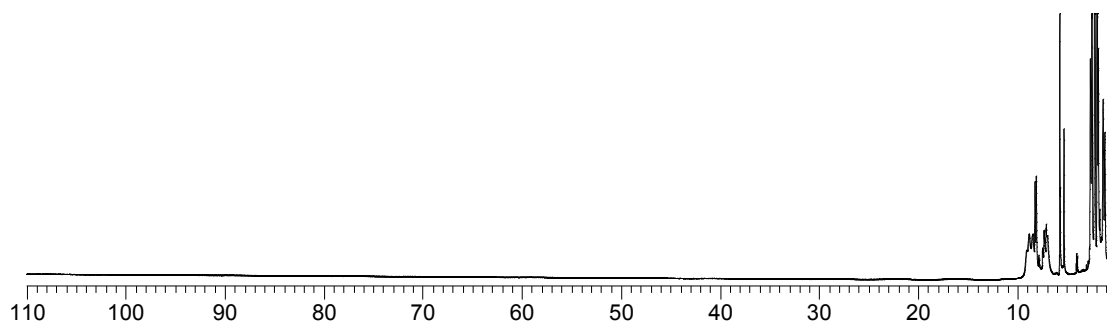


Figure 6.11: 250 MHz $^1\text{H-NMR}$ spectrum (in CD_3CN) of $[\text{Co}(\text{terpy-C4-chd})_2]^{2+}$ after addition of 2 equivalents of RuCl_3 .

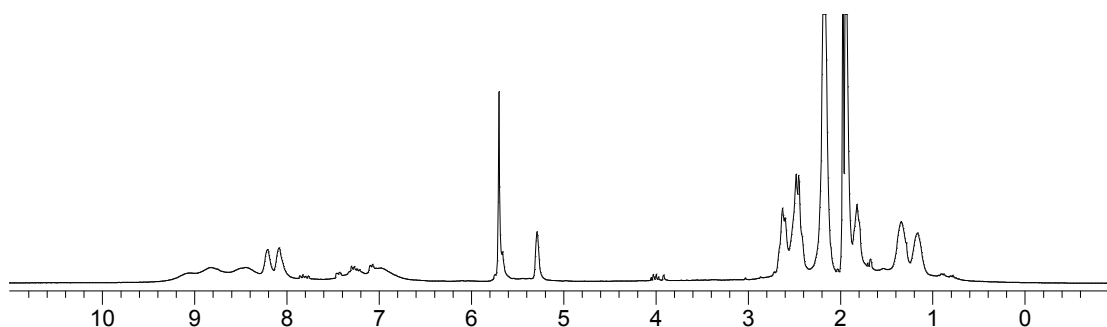


Figure 6.12: Expansion of the 250 MHz $^1\text{H-NMR}$ spectrum (in CD_3CN) of $[\text{Co}(\text{terpy-C4-chd})_2]^{2+}$ after addition of 2 equivalents of RuCl_3 .

A transfer of the ligand from the cobalt(II) complex to ruthenium to form $[\text{Ru}(\text{terpy-C4-chd})]\text{Cl}_3$ could formally be possible. However, Ru(III), with the electronic configuration d^5 , is paramagnetic and would cause a shifting of the peaks as is observed for Co(II). Another possible explanation for this result could be a redox reaction between Ru(III) and Co(II). Although the standard reduction potential for this couple of metals is negative ($E^0 = E^0_{\text{Ru(III)/Ru(II)}} - E^0_{\text{Co(III)/Co(II)}} = -1.952 \text{ V}$), this value is measured in an aqueous solution. The change in solvent and the presence of the ligand maybe render this reaction possible.

These considerations remain, however, speculations, as this issue was not investigated further.

A similar experiment was carried out by mixing one equivalent of $[\text{Fe}(\text{terpy-C4-chd})_2]^{2+}$ with two equivalents of RuCl_3 in CD_3CN . The $^1\text{H-NMR}$ spectra of the

complex and the mixture right after addition of Ru(III) and after different times of heating at 80 °C are shown in Figure 6.13.

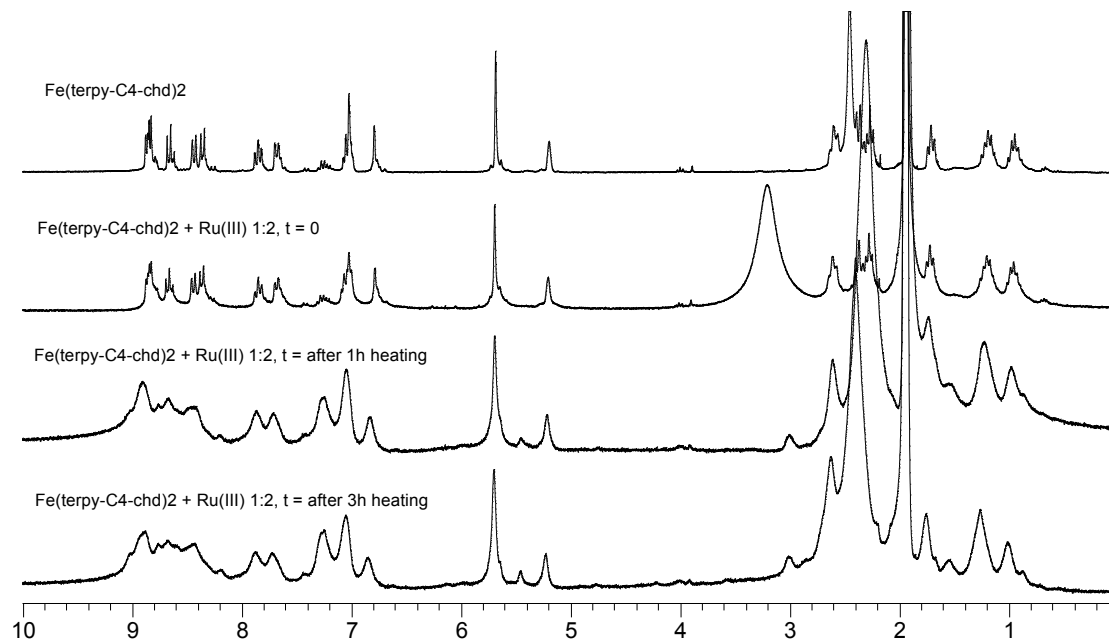


Figure 6.13: Comparison of the 250 MHz ¹H-NMR spectra (in CD₃CN) of [Fe(terpy-C4-chd)₂]²⁺ and of the mixture of [Fe(terpy-C4-chd)₂]²⁺ and RuCl₃ at different times after mixing.

Over all the spectra shown in the figure, a general observation is the broadening of the signals and the continuous presence of the two peaks at δ 5.7 and 5.2 ppm. Nothing could really be concluded from the pattern in the aromatic region, but the two peaks in the middle of the spectrum indicated that, again, the cyclohexadiene ring did not undergo any transformation. Our attempt at the formation of a polynuclear macrocycle failed again.

A third attempt was carried out, to form the dimeric Ru(II)/phenyl complex with the ligand used in this section. To a CDCl₃ solution of the free terpy-C4-chd were added 2 equivalents of RuCl₃ in CD₃CN. In fact, the right stoichiometry would have needed only one equivalent of Ru(III), but the experiment could not be repeated because no more ligand was available. Figure 6.14 shows the ¹H-NMR spectra of the free ligand and of the mixture at different times after mixing. The slight shifting of the signals observable upon addition of Ru(III) is probably due to the presence of a second solvent.

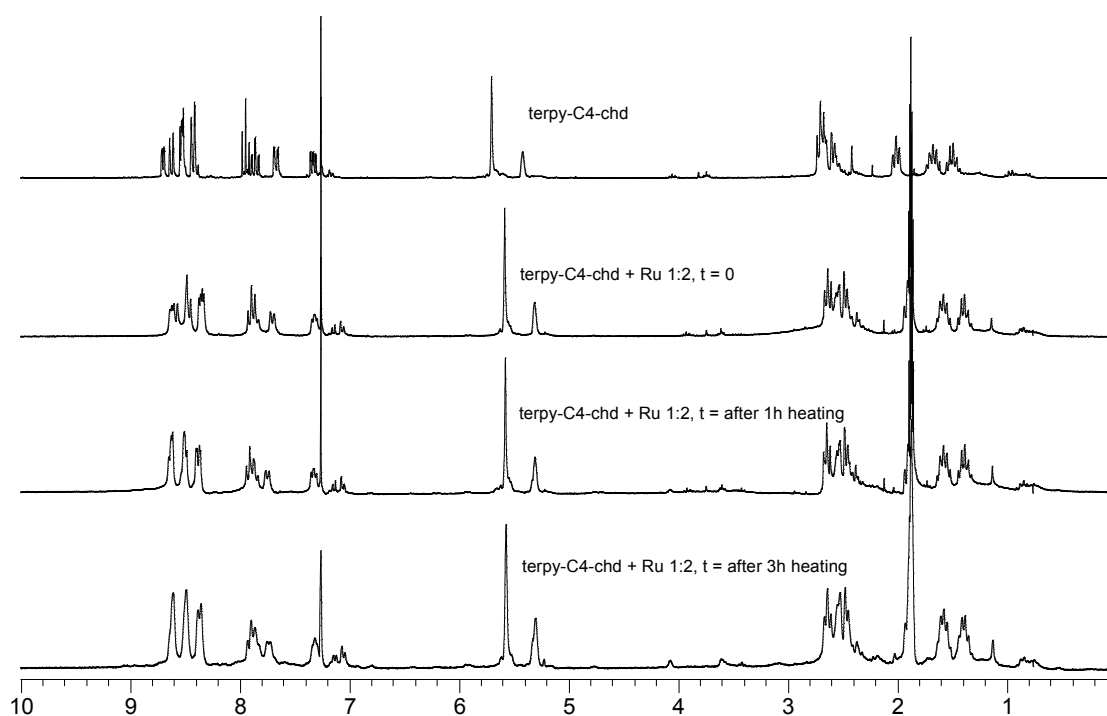


Figure 6.14: Comparison of the 250 MHz $^1\text{H-NMR}$ spectra (in CDCl_3) of terpy-C4-chd and of the mixture of terpy-C4-chd and RuCl_3 at different times after mixing.

As with the Co(II) and the Fe(II) complex, the peaks for the olefinic protons around δ 5.5 ppm neither moved nor decreased after addition of Ru(III), even after several hours at 80 °C. This indicated for the third time that the cyclohexadiene of our ligand was not being oxidised to form the desired dimeric complex with Ru(II). After these unsuccessful results, this project was abandoned and another system was developed.

6.5. Synthesis of new ferrocene complexes

The new approach for the preparation of polynuclear macrocycles consisted of forming the sandwich moiety first. For this purpose, ferrocene was chosen for its stability and its facile preparation. An alkyl chain would be attached to the ferrocene ring, and a terpy at the other end of the chain. The resulting structure will be abbreviated with $\text{Fe}(\text{Cp-C}_n\text{-terpy})_2$, where n is the number of carbons of the alkyl chain. The macrocycle would then be built upon addition of a metal binding with two terpys (Figure 6.15). The ligand exchange between two terpy complexes has now

been established and demonstrated several times in the previous chapter. Concerning the ring exchange in ferrocene, Bublitz reported the ring migration in alkylated ferrocene to easily happen in refluxing dichloromethane with aluminium chloride as catalyst [75].

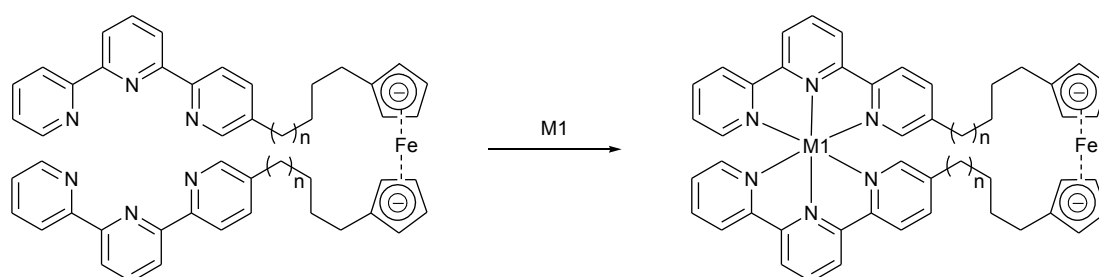


Figure 6.15: Structure of the polynuclear complex expected from the reaction of $\text{Fe}(\text{Cp-Cn-terpy})_2$ with M1. M1 = Co(II), Fe(II).

One part of the synthesis consisted of the preparation of an alkylated ferrocene with a leaving group at the end of the alkyl chain. In another step, 5-methyl-2,2':6',2''-terpyridine was synthesised as described in Chapter 5. Finally, the deprotonated terpy- CH_3 would substitute the leaving group on the alkyl chain attached to the ferrocene.

A procedure for the preparation of 1,1'-bis-(ω -hydroxyalkyl)ferrocenes has been published by Lindner and co-workers [66]. Our attempt to reproduce the published procedure was unsuccessful, therefore the synthetic pathway was slightly modified. The synthesis is shown in Figure 6.16. 3-Bromopropan-1-ol (**56**) and 4-chlorobutan-1-ol (**57**) were chosen as starting materials because of their cheap commercial availability. Their hydroxyl groups were protected by forming the tetrahydropyranyl ether following a procedure published by Mori [108]. Cyclopentadiene was obtained by thermal cracking of dicyclopentadiene (**60**) immediately before use. Adapting a published procedure [109], cyclopentadiene was then deprotonated by butyl lithium in cold tetrahydrofuran and mixed with the halide **58** or **59** to obtain the substitution products. Two isomers were formed at this stage, corresponding to the 1- and 2-substituted cyclopentadiene. These two isomers were visible on the TLC plate, although their spots were too close to be separated. This was not a problem, since the

two isomers would yield the same product after the aromatisation of the cyclopentadiene ring during the formation of the ferrocene. The sandwich complexes were readily prepared by mixing **61** or **62**, respectively, with anhydrous iron(II) chloride and a base, adapting the standard procedure reported for the synthesis of unsubstituted ferrocene [110].

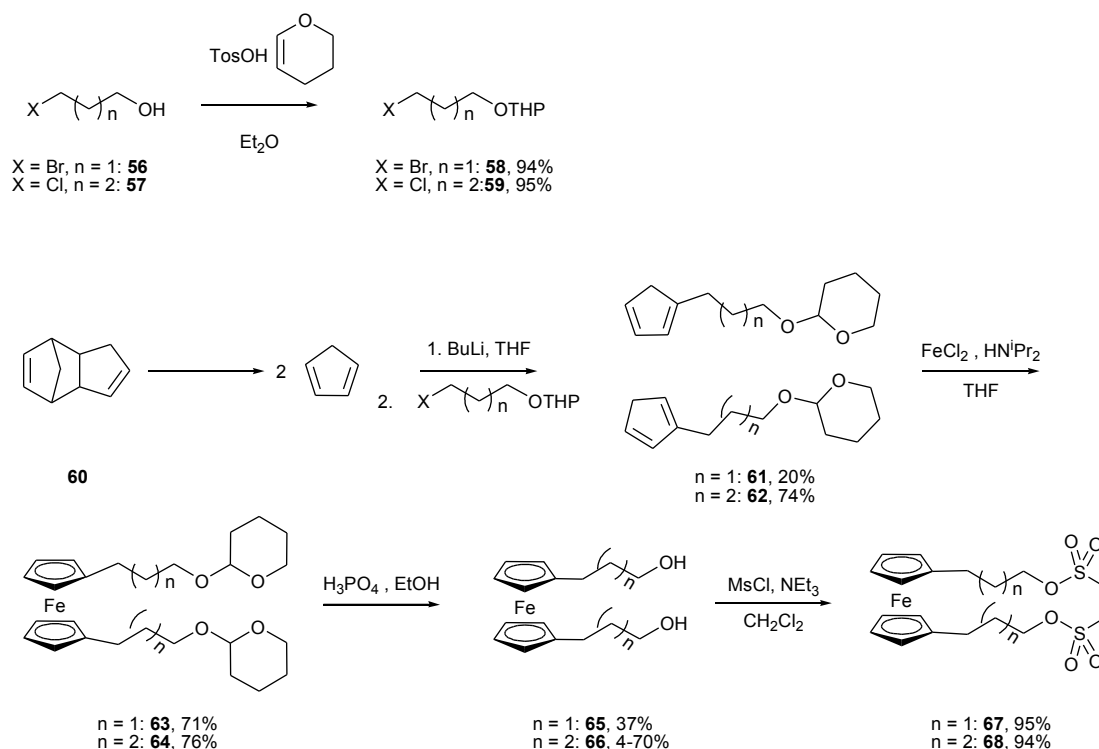


Figure 6.16: Synthesis of the mesylate precursor of $\text{Fe}(\text{Cp}-\text{C}_n\text{-terpy})_2$.

The cleavage of the tetrahydropyranyl protecting groups was one of the main problems encountered in this synthesis. Lindner used a 2% ethanolic solution of phosphoric acid [66], but in our case this procedure gave the desired product in yields ranging from 4 to 70% for the same substrate, with no recovery of any unreacted starting material. Other methods were tried with **64** (Figure 6.17). A 4:2:1 mixture of acetic acid, tetrahydrofuran and water, as proposed by Weiss [111], gave the bis-alcohol **66** with a very poor yield, and loss of the starting material. Finally, with the use of pyridinium *p*-toluenesulfonate (PPTS, easily prepared by mixing *p*-

toluenesulfonic acid and pyridine) [112], the deprotected product could be obtained in acceptable yield, and any unreacted starting material could be recovered.

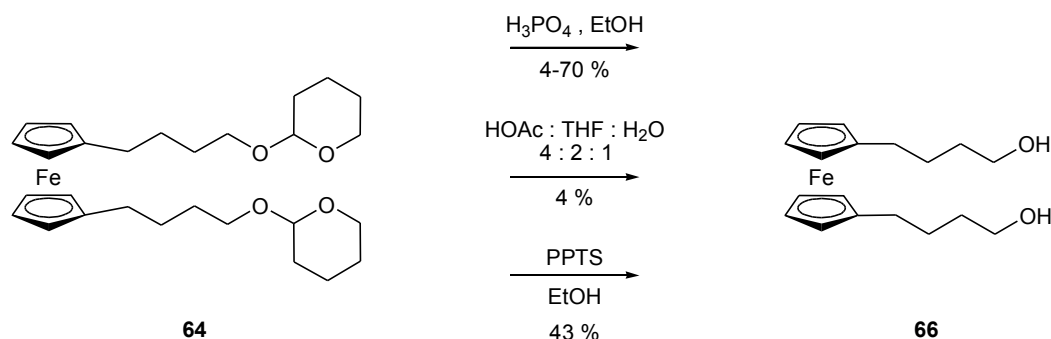


Figure 6.17: Different reagents tried for the cleavage of the tetrahydropyranyl protecting group. PPTS = pyridinium *p*-toluenesulfonate.

Going back to the synthesis shown in Figure 6.16, the hydroxyl groups of **65** and **66** needed to be activated to become good leaving groups. A first attempt was carried out with *p*-toluenesulfonyl chloride, but it was unsuccessful. The second attempt, consisting in the mesylation of the starting material with methanesulfonylchloride (MsCl), was carried out adapting a general procedure already known [113] and worked in a few minutes of reaction in nearly quantitative yields.

The reaction used to bind terpy- CH_3 and the substituted ferrocene was the same as described previously for the synthesis of terpy-C4-Ph and terpy-C4-chd. Terpy- CH_3 (**34**) was deprotonated by lithium diisopropylamide, then the activated ferrocene **67** was added (Figure 6.18). Unfortunately, this reaction did not give the desired **69**, but a mixture of the two starting materials with other unidentified products. The mesylate leaving groups of **67** and **68** were therefore converted into bromides. This was easily obtained by mixing the bis-mesylate with lithium bromide in acetone [114]. The two anions exchanged and lithium mesylate precipitated, leaving the bis-bromide in solution. The reaction with terpy- CH_3 was tried with the newly activated ferrocene, and this time the desired 1,1'-bis(4-(2,2':6',2''-terpyridin-5-yl)butyl)ferrocene ($\text{Fe}(\text{Cp-C4-terpy})_2$, **69**) and 1,1'-bis(5-(2,2':6',2''-terpyridin-5-yl)pentyl)ferrocene ($\text{Fe}(\text{Cp-C5-terpy})_2$, **72**) were obtained.

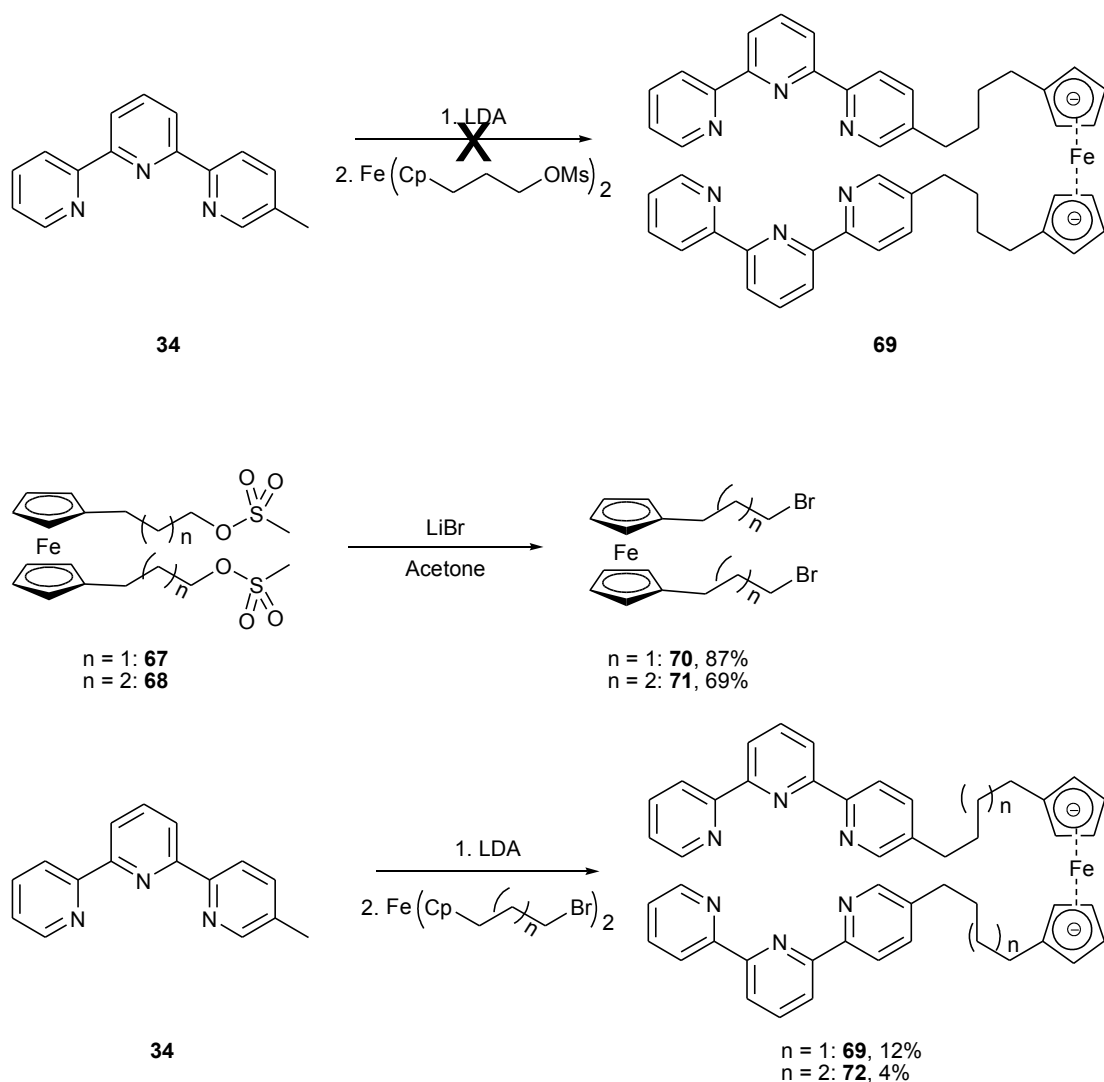


Figure 6.18: Last steps in the synthesis of $\text{Fe}(\text{Cp-Cn-terpy})_2$.

The $^1\text{H-NMR}$ spectra of the final products are shown in Figures 6.19 and 6.20. The signals for the terpy moieties were assigned by comparison with the spectrum of terpy- CH_3 . The two expected doublets for protons Cp2 and Cp3 overlap around δ 4 ppm. The signals for the alkyl chain were not precisely assigned. However, from their multiplicities, it could be said that the two triplets between δ 2.8 and 2.2 ppm must arise from the protons attached to the external carbons of the chain (A1 and A4/A5), coupling with only one pair of neighbouring protons. The remaining multiplets resulted then from the central protons of the alkyl chain, A2, A3, and A4 (for **72**).

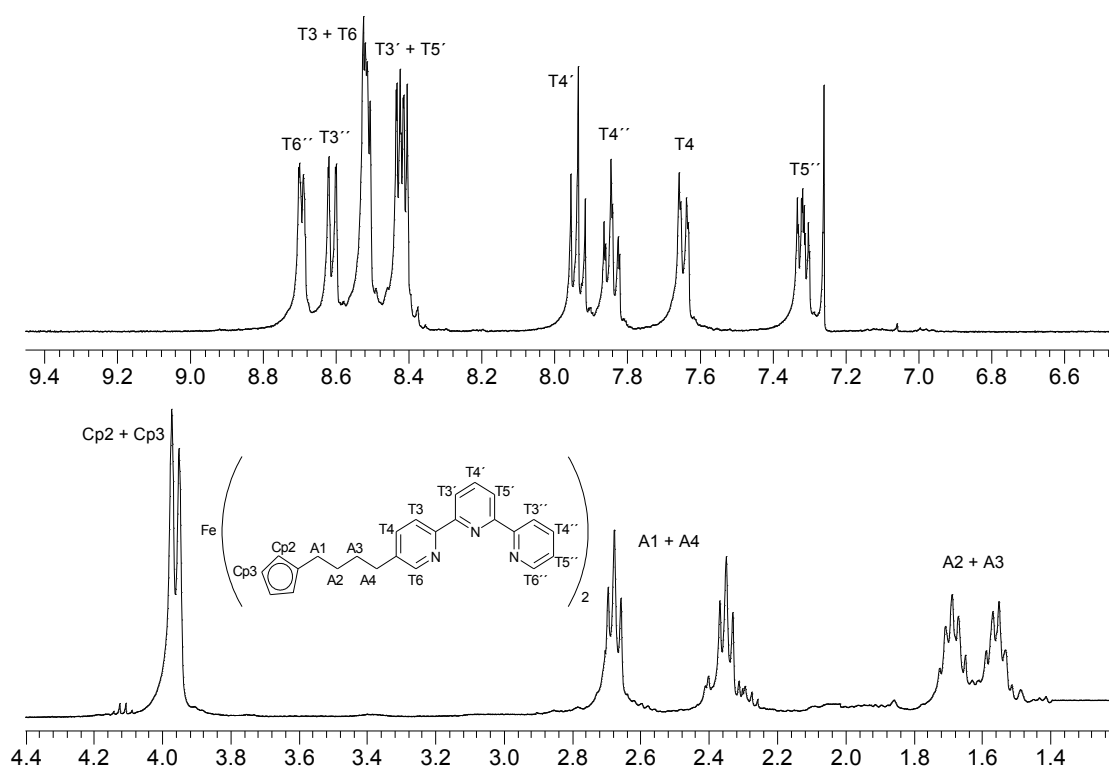


Figure 6.19: 400 MHz $^1\text{H-NMR}$ spectrum (in CDCl_3) of $\text{Fe}(\text{Cp-C4-terpy})_2$ (**69**).

In the spectrum of **72**, the less shifted multiplet around δ 1.4 ppm was assigned to A3 because it was the only signal absent in the spectrum of **69**, and this pair of protons was the only difference between the two molecules.

The preparation of $\text{Fe}(\text{Cp-Cn-Br})_2$ presented so far involved seven synthetic steps, some of which influenced heavily the total yield of the synthesis. For this reason, a new synthetic strategy was developed which was less time-consuming and could eventually yield a larger amount of material. The reaction scheme for this new synthesis is presented in Figure 6.21. A similar synthesis had already been reported, but was applied on only one ring of the ferrocene, while the second ring was deactivated by the presence of an electron-withdrawing group [64].

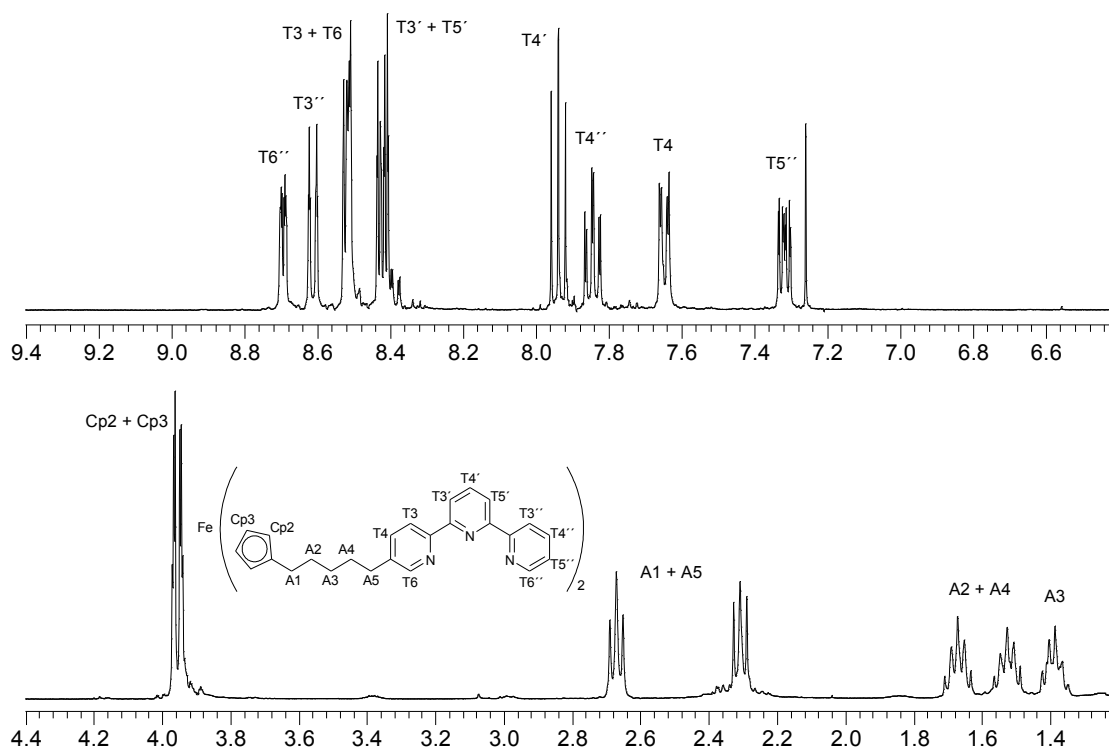


Figure 6.20: 400 MHz $^1\text{H-NMR}$ spectrum (in CDCl_3) of $\text{Fe}(\text{Cp-C5-terpy})_2$ (**72**).

The starting material was the commercially available ferrocene (**73**). It was reacted with different bromo-substituted acid chlorides in the presence of aluminium chloride to yield the products of the Friedel-Craft acylation, **74**, **75** and **76**. The following Clemmensen reduction with zinc dust, mercury(II) chloride and hydrochloric acid gave the already presented $\text{Fe}(\text{Cp-C4-Br})_2$ (**71**) and the new $\text{Fe}(\text{Cp-C6-Br})_2$ (**77**). The synthesis with bromoacetyl chloride to give **74** first, and its reduction product second, gave some problems in the first step. The reaction mixture became worryingly black, even before the addition of the AlCl_3 catalyst, and the yield was significantly lower

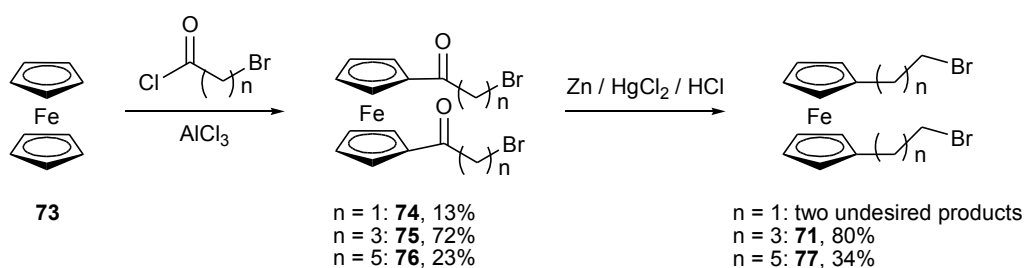


Figure 6.21: New synthetic strategy for the synthesis of $\text{Fe}(\text{Cp-C}_n\text{-Br})_2$.

than in the two other cases. In the reduction step, in the case when the reaction mixture was stirred overnight, both the carbonyl and the bromide substituents were cleaved, giving 1,1'-diethylferrocene. When the reaction was repeated, the disappearance of the starting product was followed by TLC, so that the reaction was stopped after 15 minutes. In spite of that, the reaction gave a mixture of 1,1'-diethylferrocene and 1-acetyl-1'-ethylferrocene. Apparently, the vicinity of the carbonyl group renders the bromide-substituted carbon more electrophilic, so that it is attacked by the reducing hydride.

In the new synthesis of $\text{Fe}(\text{Cp-Cn-terpy})_2$, another problem needed to be addressed. The last step of the synthesis of **69** and **72** gave the desired product with $\leq 12\%$ yield (Figure 6.18). The problem was already known from the synthesis of terpy-C4-chd (**53**), obtained in 10% yield. The main reason for these low yields was probably the incomplete deprotonation of terpy- CH_3 . Therefore, we thought of replacing the methyl group by a more acidic hydroxyl group.

A synthesis was developed to prepare 5-methoxy-2,2':6',2''-terpyridine (terpy- OCH_3 , Figure 6.22) which would then be converted to 5-hydroxy-2,2':6',2''-terpyridine. As was explained in Chapter 5, to prepare an asymmetrically substituted terpy, we need a properly substituted acetylpyridine on one side, and the enaminone **31** on the other side. The precursor for the acetylpyridine needed here was 2-bromo-5-methoxypyridine (**83**), whose synthesis was reproduced from the literature [115]. The synthesis began with the electrophilic iodination of the commercially available 2-aminopyridine (**78**). This was performed following the procedure published by Ogura [116], with a small modification in the workup. After removal of the unreacted iodine, Ogura first extracted the product with ether and then basified the extract with NaOH. When following the proposed workup, the product was obtained in only 5% yield. Therefore NaOH was added to the aqueous phase remaining from the extraction and the precipitate thus forming was collected with a second extraction. This brought the yield to 58%. The amino group of **79** was then protected by forming a pyrrole ring (**80**) with 2,5-hexanedione under continuous removal of the forming water. The iodine could then be replaced by a methoxy group, in a substitution reaction catalysed by copper(I) chloride, to give **81**. Deprotection of the amino group gave 2-amino-5-

methoxypyridine **82**. It was now the amino group that had to be substituted, using bromine in hydrobromic acid, and then sodium nitrite, following a procedure published by Leeson and Emmett [117]. The obtained **83** was treated with butyl lithium and *N,N*-dimethylacetamide, in the same way as had already been done with 2-bromo-5-methylpyridine (**27**, Chapter 5), to obtain **84**. This was used with **31** to build terpy-OCH₃, but in fact the reaction did not yield the desired product. Instead, the disubstituted **86** was collected in 37% yield.

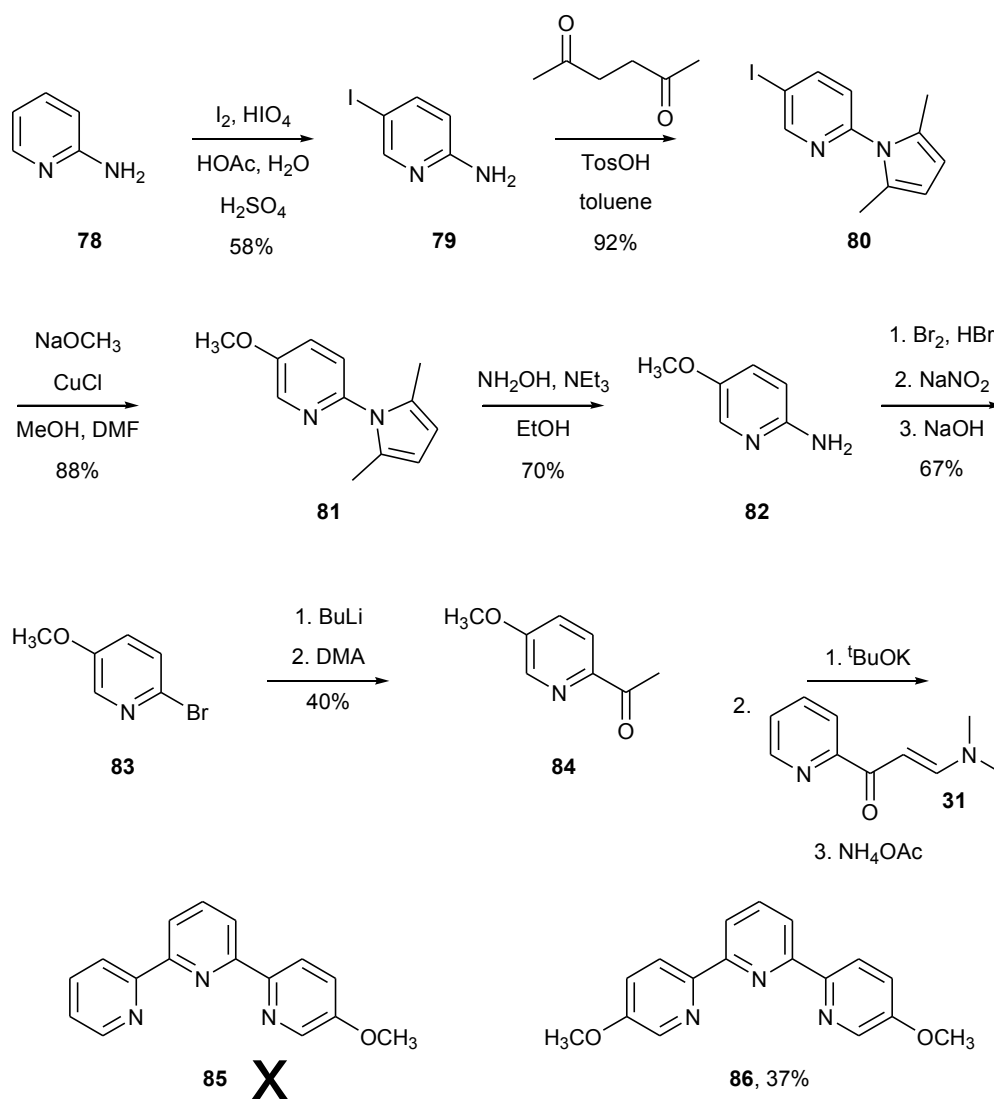


Figure 6.22: Attempt at the synthesis of 5-methoxy-2,2':6',2''-terpyridine (**85**).

Since a doubly functionalised terpy was not desired for this project, **86** was not used further, and 4'-hydroxy-2,2':6',2''-terpyridine (terpy-OH, **89**) was synthesised instead. The preparation of terpy-OH is a well established procedure published by Constable and Ward [118] (Figure 6.23). In the first step, acetone was deprotonated by sodium hydride and attacked the electrophilic carbon of ethyl 2-pyridine-carboxylate (**87**). The yellow 1,3,5-trione **88** was thus obtained. This was not purified, but was used further for the cyclisation reaction in the presence of ammonium acetate, to give 2,6-bis(2'-pyridyl)-4-pyridone, which tautomerised to the aromatic terpy-OH (**89**).

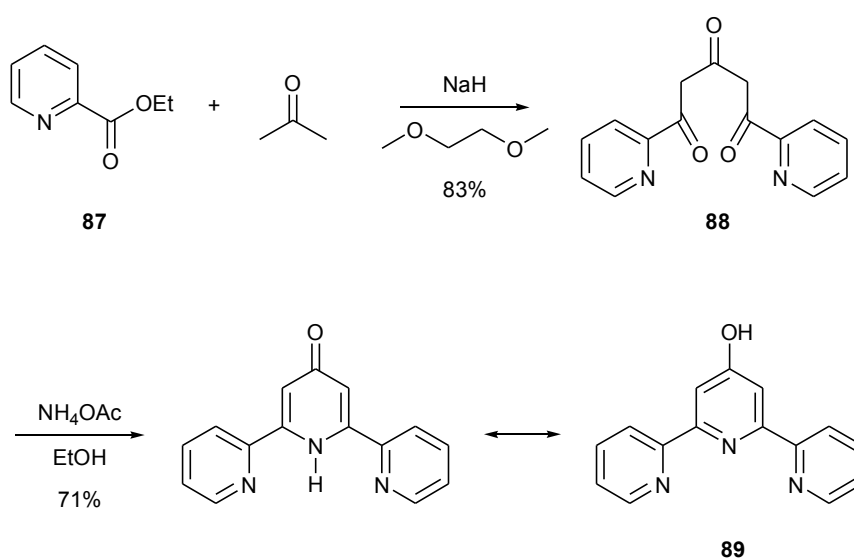


Figure 6.23: Synthesis of 4'-hydroxy-2,2':6',2''-terpyridine (**89**).

Terpy-OH and Fe(Cp-Cn-Br)₂ could finally be put together to form the desired terpy-functionalised ferrocene (Fe(Cp-Cn-O-terpy)₂, Figure 6.24). The first attempt at this synthesis was carried out by mixing Fe(Cp-C4-Br)₂ (**71**), potassium carbonate and terpy-OH in acetonitrile, and then heating the mixture [119]. The desired **90** was obtained, but with a modest 15% yield. For the second attempt, terpy-OH was first heated in acetonitrile in presence of potassium carbonate, and only later was Fe(Cp-C6-Br)₂ (**77**) added. In this way, the yield could be increased to 28%. A few attempts were carried out to react **75**, the precursor of Fe(Cp-C4-Br)₂, with terpy-OH, but they were all unsuccessful.

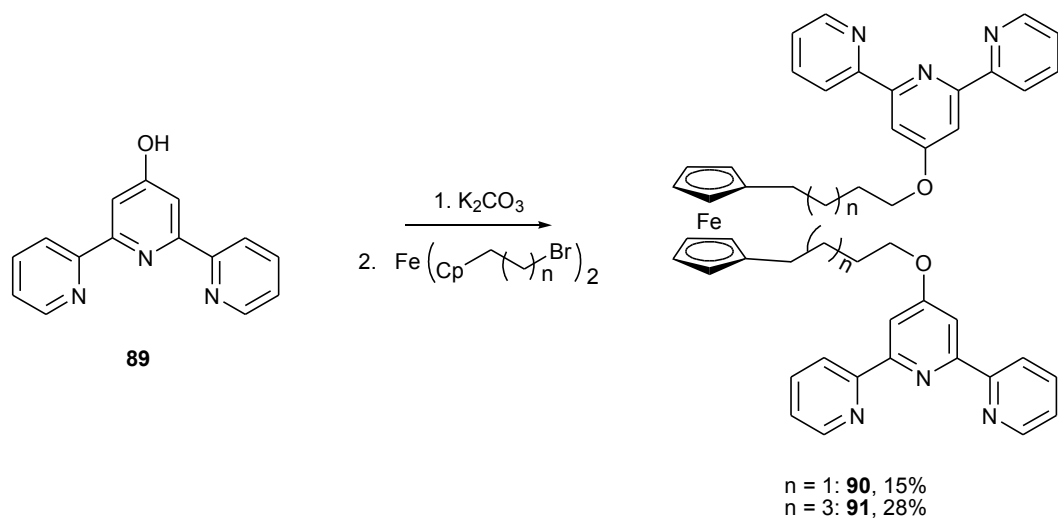


Figure 6.24: Last step in the synthesis of $\text{Fe}(\text{Cp-Cn-O-terpy})_2$.

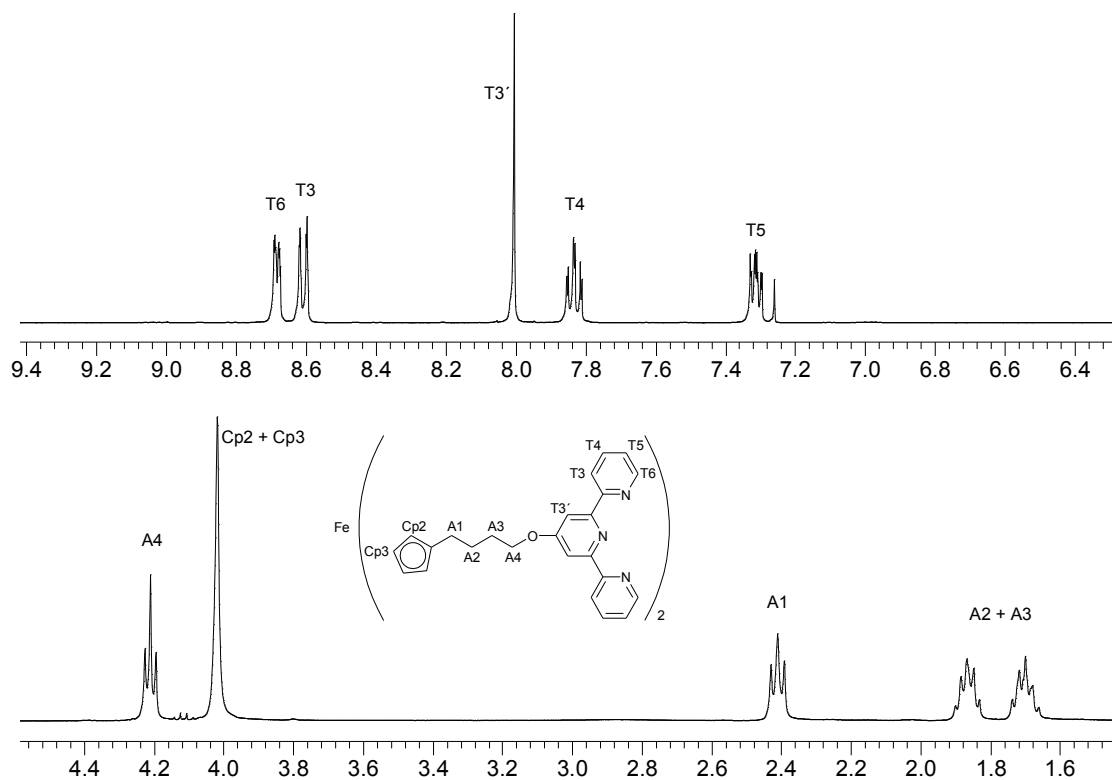


Figure 6.25: 400 MHz $^1\text{H-NMR}$ spectrum (in CDCl_3) of $\text{Fe}(\text{Cp-C4-O-terpy})_2$ (**90**).

Figures 6.25 and 6.26 show the $^1\text{H-NMR}$ spectra of $\text{Fe}(\text{Cp-C4-O-terpy})_2$ (**90**) and $\text{Fe}(\text{Cp-C6-O-terpy})_2$ (**91**). The signals for the terpy have now decreased to five

compared with the spectra encountered so far, because of the symmetry of the structure. The chemical shifts of the signals for T6, T3, T4 and T5 hardly changed from the shifts of the protons on the corresponding position in the asymmetric terpy. These signals were therefore assigned by comparison with the spectrum of $\text{Fe}(\text{Cp-C4-terpy})_2$ (**69**). The singlet around δ 8 ppm could be unambiguously assigned to T3', the only proton not able to show any coupling. The shifting of the triplet around δ 4.2 ppm, next to the signal for Cp2 and Cp3, was attributed to the proximity of the oxygen, so that this signal was assigned to A4 in **90** and A6 in **91**. The second triplet was then assigned to the couple of protons at the other end of the alkyl chain, A1 in both molecules, which were closest to the ferrocene ring. The remaining multiplets in the region δ 2.0-1.2 ppm were assigned to the remaining protons of the alkyl chain, although the single positions were not distinguished.

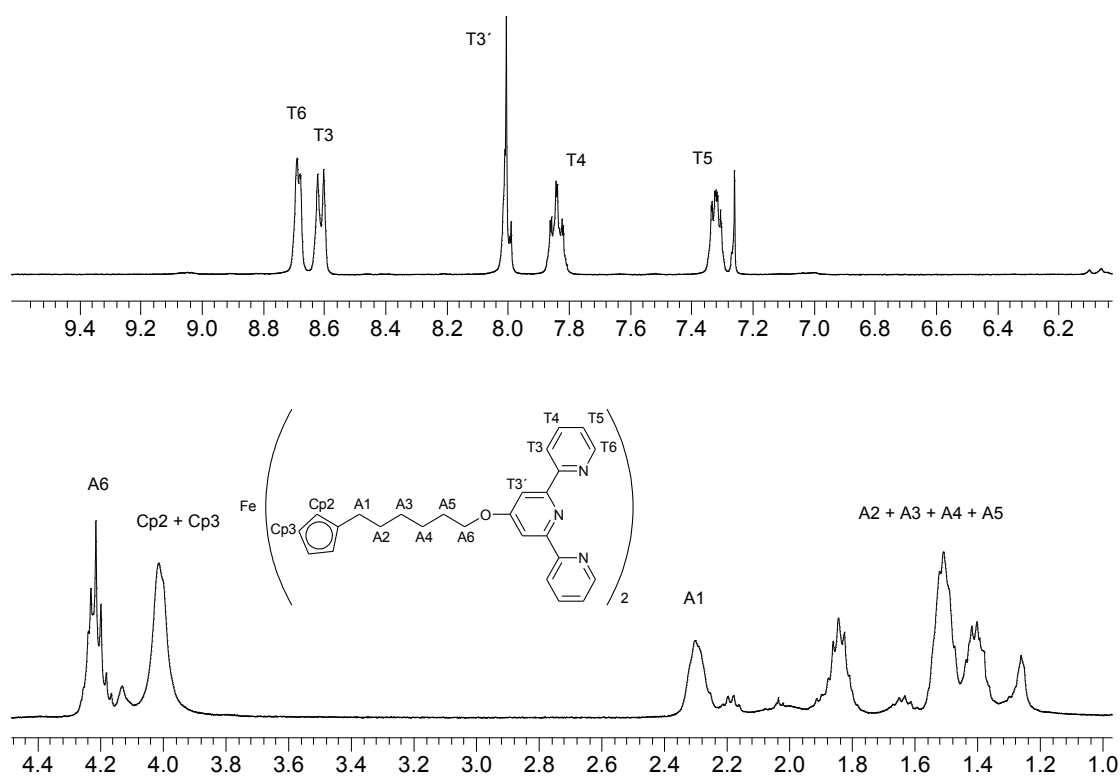


Figure 6.26: 400 MHz $^1\text{H-NMR}$ spectrum (in CDCl_3) of $\text{Fe}(\text{Cp-C6-O-terpy})_2$ (**91**).

The comparison of the spectra of **69** and **72** (Figures 6.19 and 6.20) with the ones just discussed helped to assign the two triplets in the region δ 2.8-2.2 ppm, which had so

far remained ambiguous. The less shifted signal at about δ 2.3 ppm, which is found in Figure 6.25 and again 6.26, could be assumed to arise from the protons closest to the ferrocene. Consequently, the second, slightly more shifted triplet, could be assigned to the protons closest to the pyridine ring (Figure 6.27).

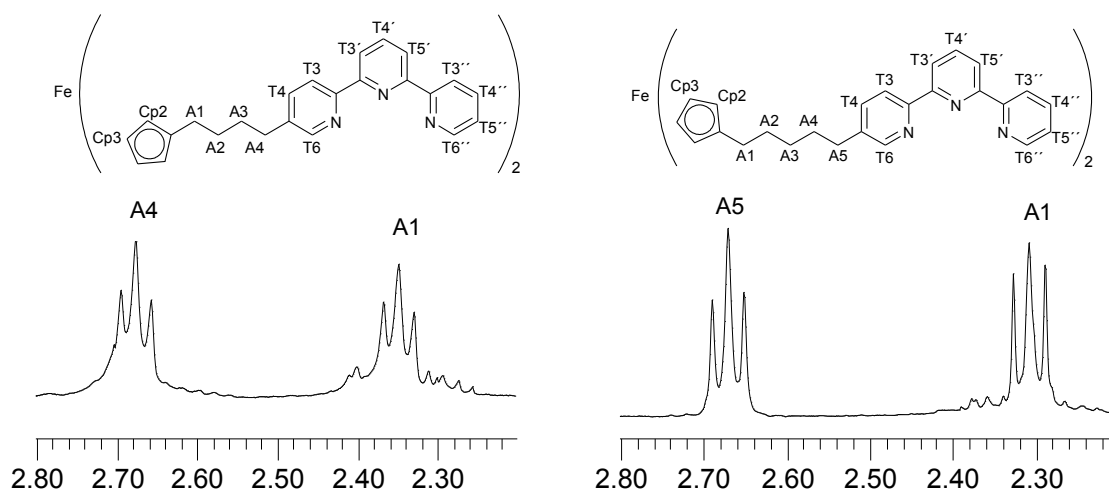


Figure 6.27: Expansions of the 400 MHz $^1\text{H-NMR}$ spectra of $\text{Fe}(\text{Cp-C4-terpy})_2$ (**69**, left) and $\text{Fe}(\text{Cp-C5-terpy})_2$ (**72**, right), showing the assignments of the triplet signals.

6.6. Synthesis of the polynuclear macrocycles

The syntheses of four new complexes containing one metal and two other coordinating sites have just been described. In the following experiments, a second metal will be added to separate solutions of $\text{Fe}(\text{Cp-C4-terpy})_2$, $\text{Fe}(\text{Cp-C5-terpy})_2$, $\text{Fe}(\text{Cp-C4-O-terpy})_2$ and $\text{Fe}(\text{Cp-C6-O-terpy})_2$. The resulting mixtures will be studied to try and understand if any polynuclear macrocycle was formed, and how many metal centres it contained. Depending on several factors, for example the length of the alkyl chain, or the anion present in the mixture, [1+1], [2+2] or even larger macrocycles can theoretically be formed.

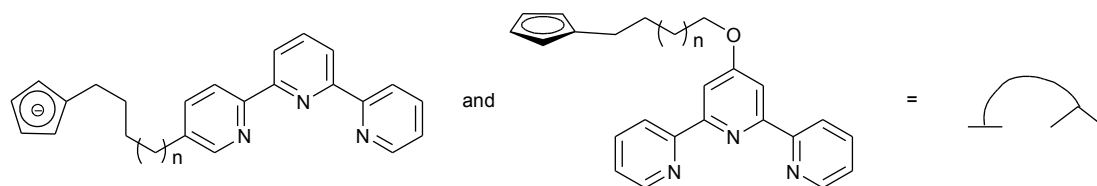


Figure 6.28: Schematic representation used for the ligands Cp-Cn-terpy and Cp-Cn-O-terpy .

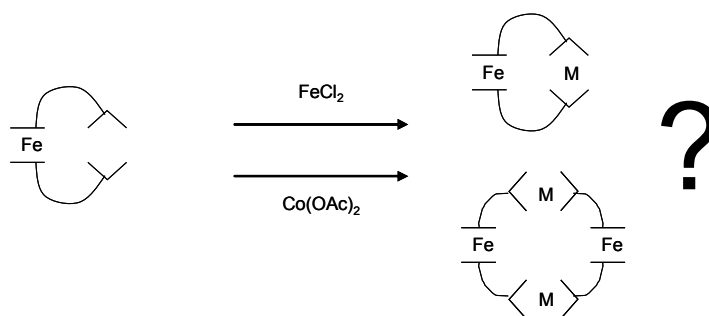


Figure 6.29: Possible macrocyclic products of the reaction between $\text{Fe}(\text{Cp-R-terpy})_2$ and a second metal.

To a CDCl_3 solution of $\text{Fe}(\text{Cp-C4-terpy})_2$ in an NMR tube was added one equivalent of anhydrous cobalt(II) acetate, which was obtained by heating $\text{Co}(\text{OAc})_2 \cdot 4\text{H}_2\text{O}$ under vacuum. A few drops of deuterated methanol were also added to improve the solubility of $\text{Co}(\text{OAc})_2$. The $^1\text{H-NMR}$ spectrum of the mixture was measured immediately after mixing and at intervals during several days while the mixture was kept at room temperature. No change occurred during this time, and the spectrum is shown in Figure 6.30.

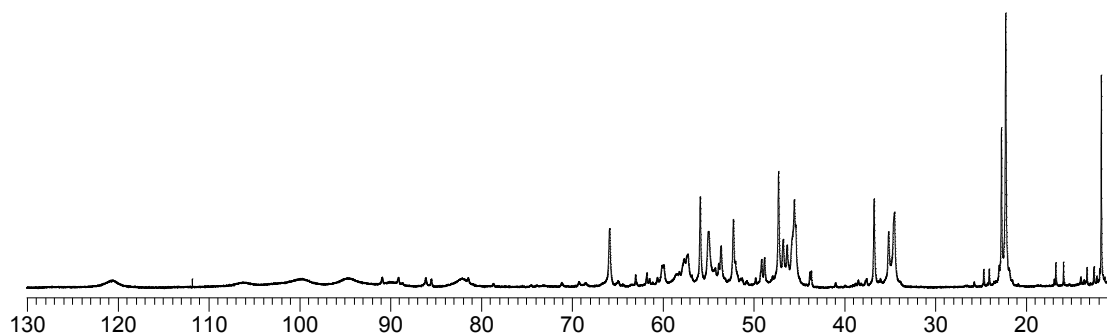


Figure 6.30: 250 MHz $^1\text{H-NMR}$ spectrum (in $\text{CDCl}_3/\text{CD}_3\text{OD}$) of the 1:1 mixture of $\text{Fe}(\text{Cp-C4-terpy})_2$ and $\text{Co}(\text{II})$ in the region δ 130-10 ppm.

The $^1\text{H-NMR}$ spectrum showed a range of peaks with the characteristic paramagnetic shift due to the coordination with $\text{Co}(\text{II})$. This confirmed the expected binding of cobalt with the terpy moieties. However, the high number of peaks seemed to indicate a large number of different products. To try and identify the products

present in this mixture, the ESI mass spectrum of the solution was measured. The ESI-MS peaks obtained, with their corresponding fragments, are listed in Figure 6.31.

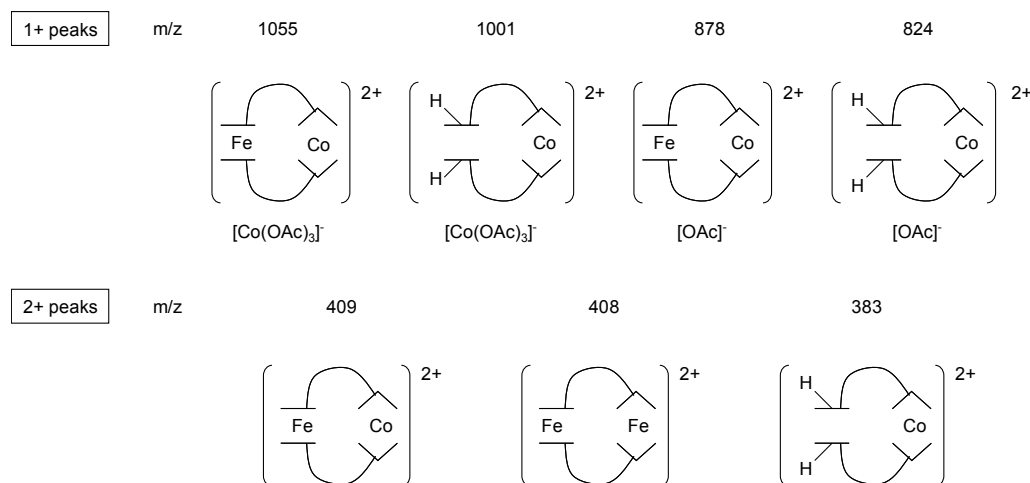


Figure 6.31: ESI-MS peaks of the 1:1 mixture of $\text{Fe}(\text{Cp-C4-terpy})_2$ and $\text{Co}(\text{OAc})_2$. The mixture was prepared in CDCl_3 and CD_3OD and the ESI-MS sample was diluted with CHCl_3 .

Surprisingly, mass peaks were observed which belonged to fragments where the iron had been displaced from the ferrocene. The free Fe^{2+} was then captured by two terpys to form the macrocycle containing two Fe(II) centres but no Co(II). However, we assumed this behaviour was caused by the electric potential in the spectrometer, and that these unexpected species were actually absent in the NMR sample. With this assumption, the only coordination sphere for Co(II) would be the one for the $[\text{Fe}(\text{Cp-C4-terpy})_2\text{Co}]^{2+}$ macrocycle. Why did the NMR spectrum then show so many signals? A possible reason could be the poor ability of CDCl_3 to solubilise ions, so that the doubly charged complex and its anions are present as ion clusters in solution. It was explained in the previous chapters that MA_3 and MB_2 complexes are chiral, when A is a general bidentate ligand and B is an asymmetrically substituted tridentate ligand. In the solution studied here, we had two enantiomers of the macrocycle $[\text{Fe}(\text{Cp-C4-terpy})_2\text{Co}]^{2+}$ and a second couple of enantiomers of the anion $[\text{Co}(\text{OAc})_3]^-$. Considering the neutral cluster $[\text{Fe}(\text{Cp-C4-terpy})_2\text{Co}][\text{Co}(\text{OAc})_3][\text{OAc}]$, where two enantiomeric species were combined, four possible combinations could be obtained. These are the $\Delta\Lambda$, $\Delta\Delta$, $\Lambda\Delta$, and $\Lambda\Lambda$ diastereomers (Figure 6.32). Since the NMR spectrum was measured in an achiral solvent, the enantiomers could not be

distinguished, but the two couples of diastereomers (identified with the oval and the hexagon in the figure) would give two sets of NMR peaks.

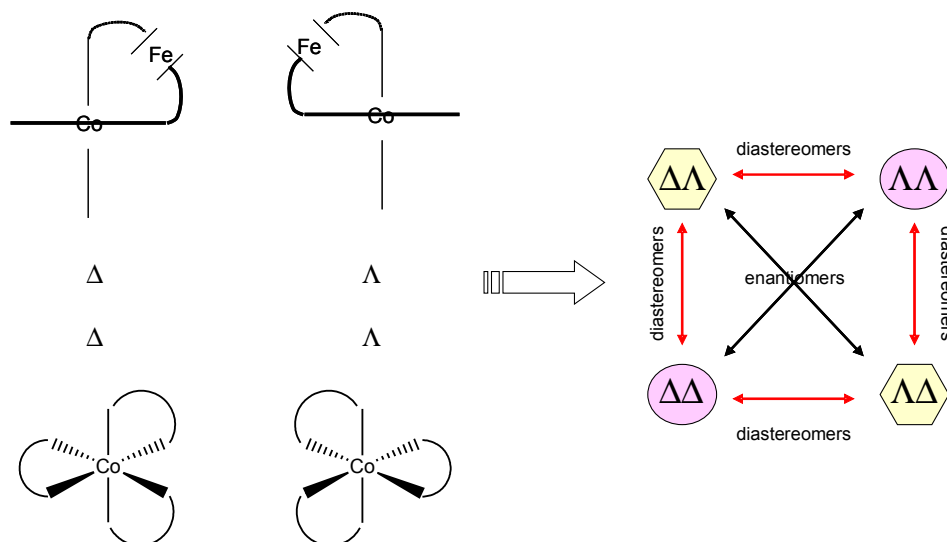


Figure 6.32: Stereoisomers obtained from the different combinations of the chiral binuclear cation $[Fe(Cp-C4-terpy)_2Co]^{2+}$ and the chiral anion $[Co(OAc)_3]^-$.

If we consider a cluster containing the chiral cation and two of the chiral anions $[Co(OAc)_3]^-$, four other diastereomeric pairs of enantiomers are found (Figure 6.33)

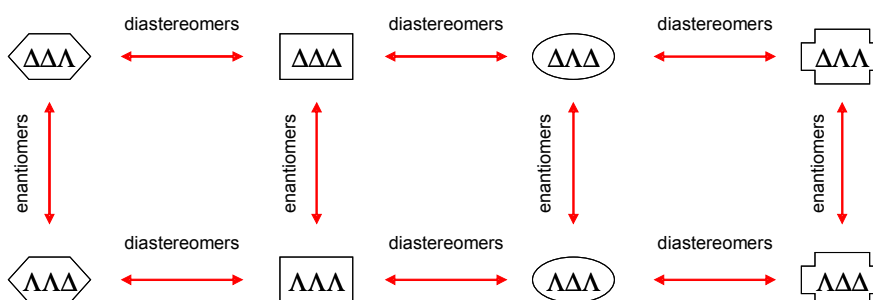


Figure 6.33: Stereoisomers obtained from the different combinations of the chiral binuclear cation $[Fe(Cp-C4-terpy)_2Co]^{2+}$ and two chiral anions $[Co(OAc)_3]^-$.

This would give a total of at least six different environments for each unique proton of the terpy, to which could be added a seventh environment for the complex coupled with two achiral $[OAc]^-$ anions.

If all this was true, the addition to the NMR sample of a solvent better suited for the solubility of ions should cause the dissociation of cations and anions, and the NMR spectrum should show a single set of peaks.

A few drops of CD_3CN were added to the sample studied so far. The ^1H -NMR spectrum of the sample was measured right after mixing and then after 9 days of equilibration (Figure 6.34).

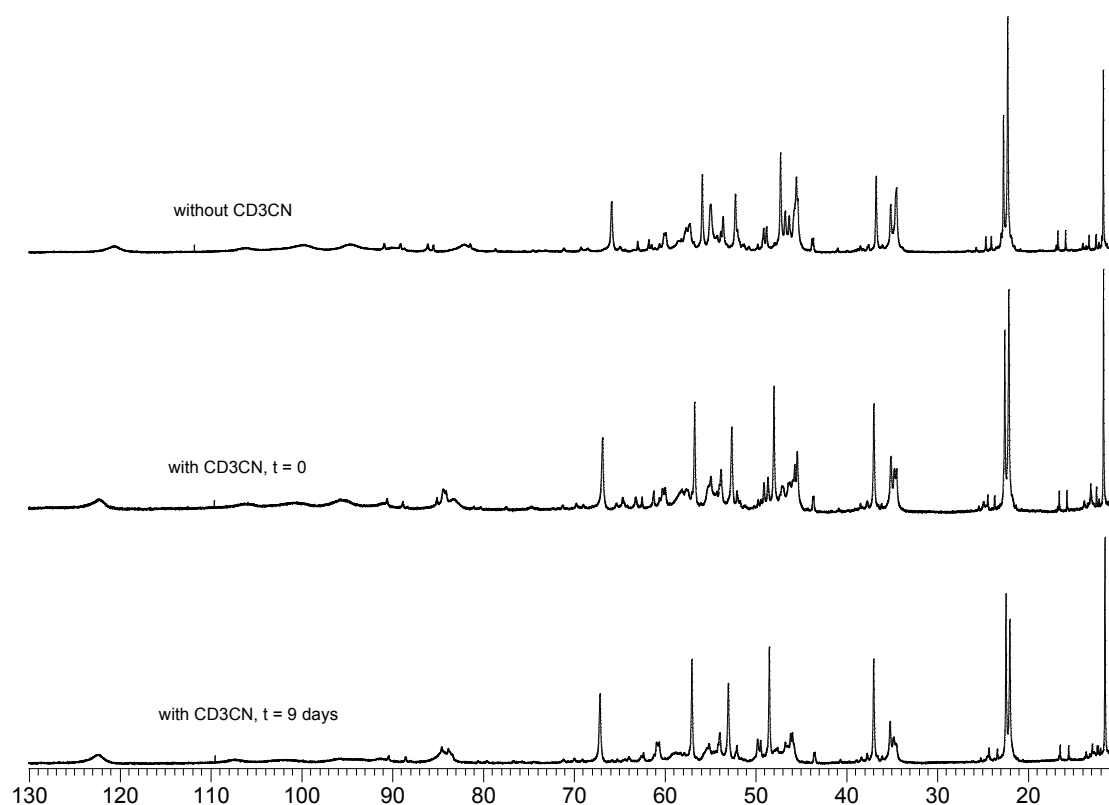


Figure 6.34: 250 MHz ^1H -NMR spectra (in $\text{CDCl}_3/\text{CD}_3\text{OD}$) of the 1:1 mixture of $\text{Fe}(\text{Cp-C4-terpy})_2$ and $\text{Co}(\text{II})$ before and after the addition of CD_3CN , in the region δ 130-10 ppm.

From the figure it could be observed how, already at time $t = 0$, one species seemed to be dominant. After 9 days this species was clearly predominant, although still not the only one present. This problem could probably be solved by adding more CD_3CN , but the results obtained here were considered enough evidence for the explanation made above, so that no more experiments were carried out with this sample.

To a CDCl_3 solution of $\text{Fe}(\text{Cp-C4-terpy})_2$ in an NMR tube was added one equivalent of anhydrous iron(II) chloride. A few drops of deuterated methanol were also added

to allow FeCl_2 to dissolve. The $^1\text{H-NMR}$ spectrum of the mixture was measured right after mixing and at intervals during several days while the mixture was kept at room temperature. The solution had turned from orange-red to purple immediately after the addition of Fe(II) , indicating the formation of a Fe(terpy-R)_2 complex, but the NMR signals were all very broad and could not confirm the presence of this complex. The confirmation of the formation of the [1+1] macrocycle came with ESI-MS (Figure 6.35). Again, fragments resulting from the decomposition of the ferrocene were identified, and again, they were assumed to form only in the spectrometer and not to be present in the NMR tube. The $[\text{OAc}]^-$ anion used to assign the peak at m/z 875 was probably a residue leaking from the sample measured before.

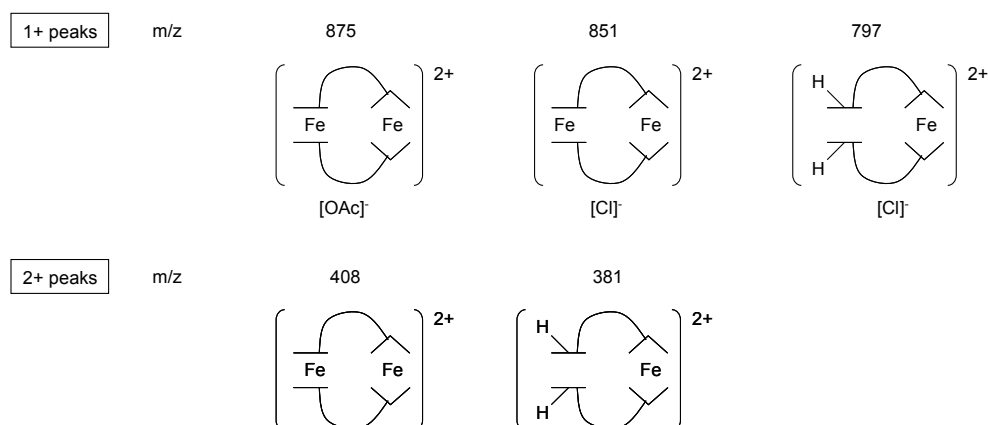


Figure 6.35: ESI-MS peaks of the 1:1 mixture of Fe(Cp-C4-terpy)_2 and FeCl_2 . The mixture was prepared in CDCl_3 and CD_3OD and the ESI-MS sample was diluted with CHCl_3 .

The $^1\text{H-NMR}$ spectrum of the 1:1 mixture of Fe(Cp-C5-terpy)_2 and Co(OAc)_2 in CDCl_3 and CD_3OD is shown in Figure 6.36. Unlike the case with Fe(Cp-C4-terpy)_2 and Co(II) , this time the mixture revealed mainly a single Co(II) species. The reason could be the larger amount of methanol added to the sample, which solubilised the ions well. This prevented the formation of all the diastereomers encountered with $[\text{Fe(Cp-C4-terpy)}_2\text{Co}]^{2+}$. From the NMR spectrum it could not be deduced whether the Co(terpy-R)_2 complex formed is part of a [1+1], [2+2] or other macrocycle.

Therefore, the sample was analysed by ESI mass spectrometry. The peaks reported in Figure 6.37 confirmed the formation of the [1+1] species. The presence in the ESI-MS of the chloride counterion was probably due to a residue from a previous sample.

It was interesting to notice the absence of any peak for the decomposed ferrocene. A possible explanation could be that the macrocycle with the longer arms is more “comfortable” and has less tendency to open and break a strained position.

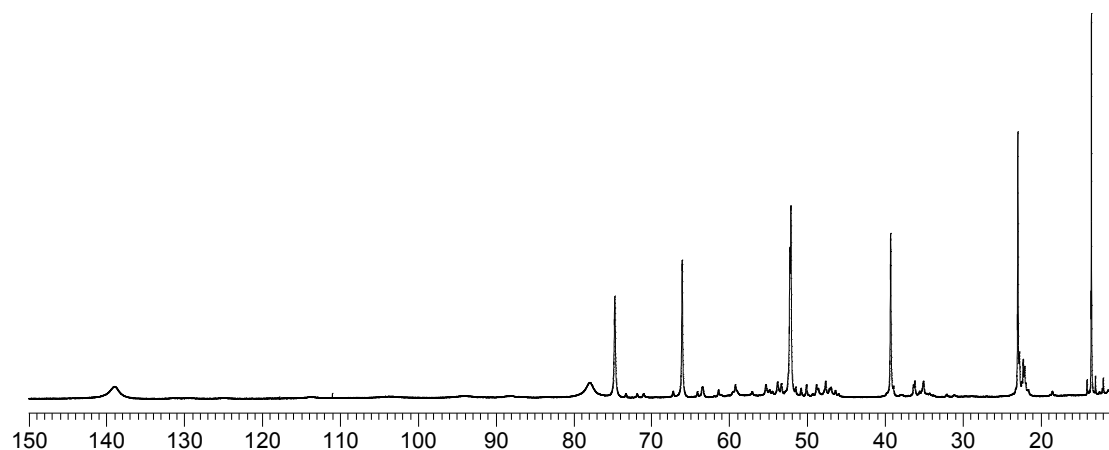


Figure 6.36: 250 MHz $^1\text{H-NMR}$ spectrum (in $\text{CDCl}_3/\text{CD}_3\text{OD}$) of the 1:1 mixture of $\text{Fe}(\text{Cp-C5-terpy})_2$ and Co(II) in the region δ 150-10 ppm.

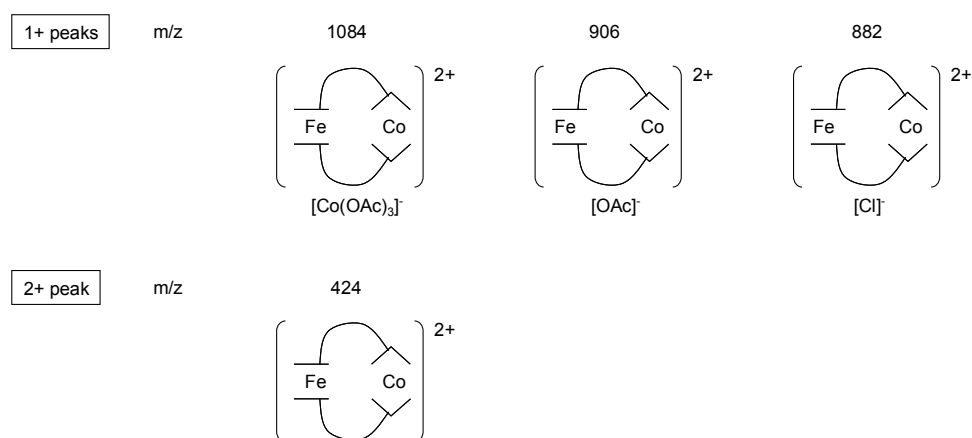


Figure 6.37: ESI-MS peaks of the 1:1 mixture of $\text{Fe}(\text{Cp-C5-terpy})_2$ and $\text{Co}(\text{OAc})_2$. The mixture was prepared in CDCl_3 and CD_3OD and the ESI-MS sample was diluted with CHCl_3 .

The $^1\text{H-NMR}$ spectrum of the 1:1 mixture of $\text{Fe}(\text{Cp-C5-terpy})_2$ and FeCl_2 in CDCl_3 and CD_3OD in the region δ 9.5-6.5 ppm showed the pattern typical for a $\text{Fe}(\text{terpy-R})_2$ complex (Figure 6.38). However, the signals are relatively broad and badly resolved, so that it cannot be determined whether the reaction had worked quantitatively and to which product.

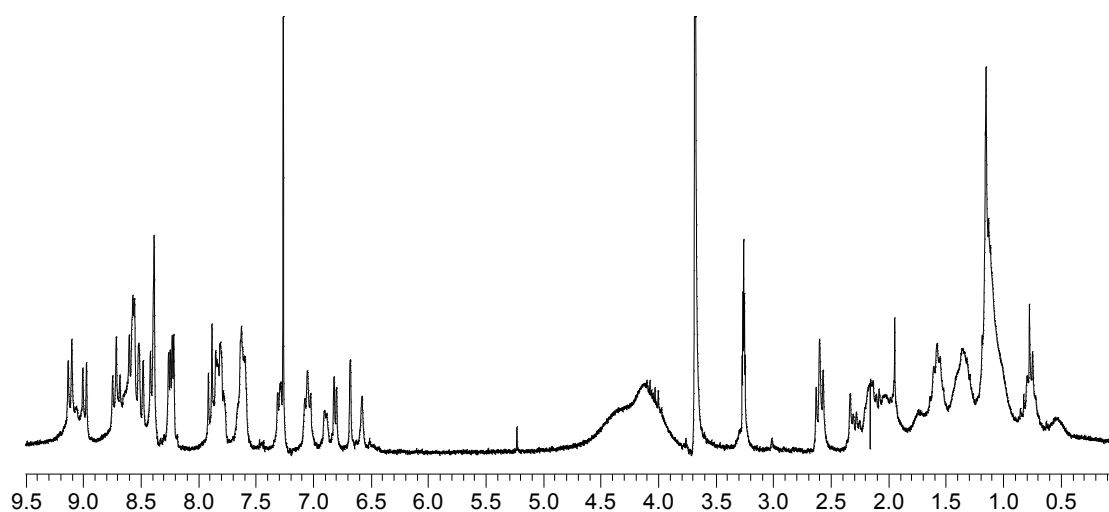


Figure 6.38: 250 MHz $^1\text{H-NMR}$ spectrum (in $\text{CDCl}_3/\text{CD}_3\text{OD}$) of the 1:1 mixture of $\text{Fe}(\text{Cp-C5-terpy})_2$ and $\text{Fe}(\text{II})$.

The ESI mass spectrum of the NMR sample showed only two peaks, corresponding to the same fragment with and without a chloride counterion (Figure 6.39). As with $\text{Co}(\text{II})$ before, there is no decomplexation of the ferrocene, for the same reason suggested above. Finally, in this fourth case as well, the [1+1] dimetallic macrocycle was selectively formed.

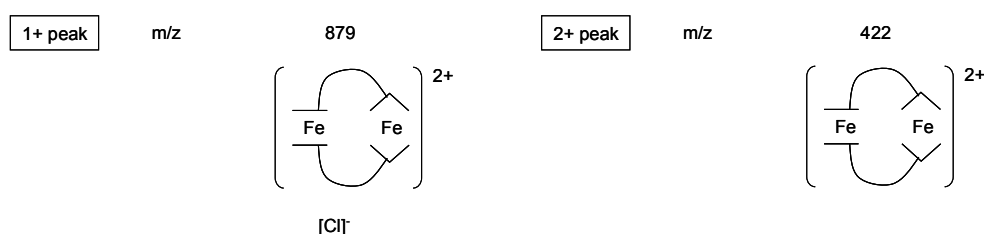


Figure 6.39: ESI-MS peaks of the 1:1 mixture of $\text{Fe}(\text{Cp-C5-terpy})_2$ and FeCl_2 . The mixture was prepared in CDCl_3 and CD_3OD and the ESI-MS sample was diluted with CHCl_3 .

The same experiments were carried out with the ligands obtained from the combination of the bis-substituted ferrocene and the symmetrical 4'-hydroxy-2,2':6',2''-terpyridine: $\text{Fe}(\text{Cp-C4-O-terpy})_2$ and $\text{Fe}(\text{Cp-C6-O-terpy})_2$. The presence of an oxygen atom at the junction between the alkyl chain and the terpy was not expected to change the outcome of the experiments, compared to $\text{Fe}(\text{Cp-C4-terpy})_2$ or $\text{Fe}(\text{Cp-C5-}$

terpy)₂. Rather, the fact that the alkyl chain was attached in position 4' of the terpy, instead of position 5, could have some influence in the formation of the macrocycles. To a CDCl₃ solution of Fe(Cp-C4-O-terpy)₂ in an NMR tube was added one equivalent of anhydrous cobalt(II) acetate. Deuterated methanol was also added to allow the solubility of the ions. The ¹H-NMR spectrum of the mixture, measured right after mixing, is shown in Figure 6.40.

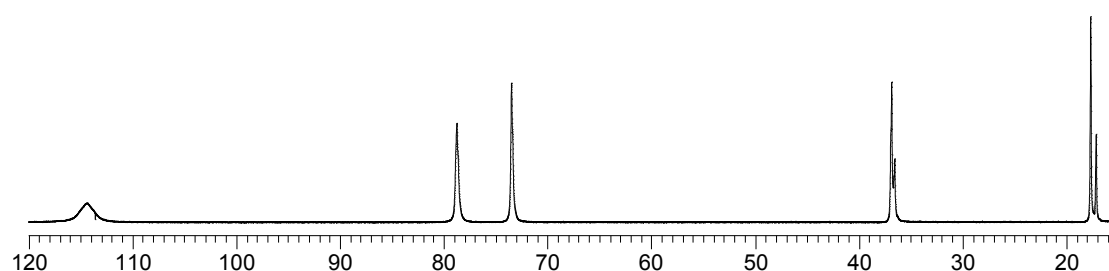


Figure 6.40: 250 MHz ¹H-NMR spectrum (in CDCl₃/CD₃OD) of the 1:1 mixture of Fe(Cp-C4-O-terpy)₂ and Co(II) in the region δ 120-15 ppm.

The NMR spectrum clearly revealed the complexation of terpy by Co(II). Initially it looked as though a single compound was formed. However, the smaller peaks next to the signals at δ 36.8 and 17.7 ppm suggested the presence of a second macrocycle, rather than being just the result of an impurity in the starting material. Furthermore, the two peaks at δ 78.7 and 73.5 ppm were broad enough to each hide a second signal. Indeed, the ESI mass spectrum of the NMR sample, revealed the presence of a [2Fe + 1Co] adduct in significant amount next to the now usual [1+1] macrocycle (Figure 6.41).

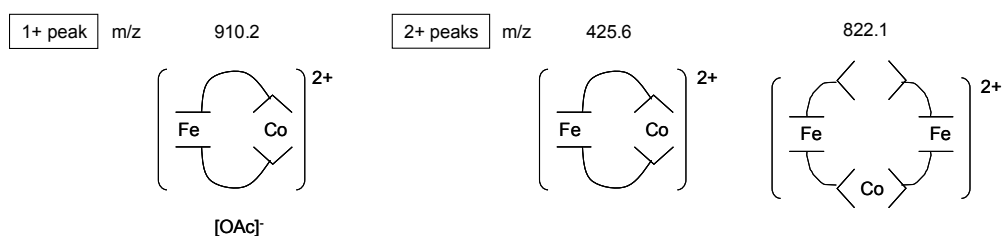


Figure 6.41: ESI-MS peaks of the 1:1 mixture of Fe(Cp-C4-O-terpy)₂ and Co(OAc)₂. The mixture was prepared in CDCl₃ and CD₃OD and the ESI-MS sample was diluted with MeOH.

Apparently, the $[2\text{Fe} + 1\text{Co}]$ product did not lose the second Co(II) in the spectrometer, but was already present as such in solution. This was suggested by the presence of a set of signals in the aromatic region of the $^1\text{H-NMR}$ spectrum. These signals were too broad to be properly compared with those of $\text{Fe}(\text{Cp-C4-O-terpy})_2$, but they could arise from the two terminal free terpys of a $[2\text{Fe} + 1\text{Co}]$ oligomer. The corresponding oligomer with three Fe(II) ions was obtained again with the 1:1 mixture of $\text{Fe}(\text{Cp-C4-O-terpy})_2$ and FeCl_2 , as it is shown in Figure 6.42. This time, the mass peak corresponding to this fragment was even the most intense, with the peaks for the $[1+1]$ macrocycle reaching only about 40% of the relative intensity. With this mixture, the $^1\text{H-NMR}$ did not yield any information, because the signals were very broad.

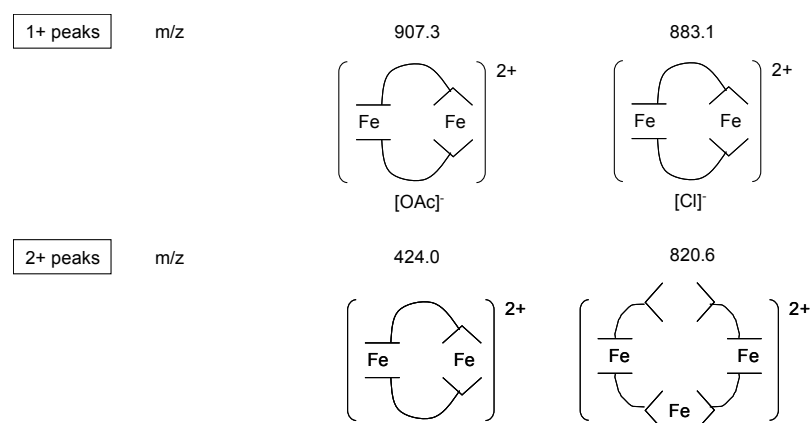


Figure 6.42: ESI-MS peaks of the 1:1 mixture of $\text{Fe}(\text{Cp-C4-O-terpy})_2$ and FeCl_2 . The mixture was prepared in CDCl_3 and CD_3OD and the ESI-MS sample was diluted with MeOH .

When $\text{Fe}(\text{Cp-C6-O-terpy})_2$ was mixed with 1 equivalent of $\text{Co}(\text{OAc})_2$, the resulting $^1\text{H-NMR}$ spectrum was very similar to the one obtained with the shorter $\text{Fe}(\text{Cp-C4-O-terpy})_2$ (Figure 6.43). Less intense peaks were visible close to the main signals, although the difference in chemical shift was smaller here than in the previous case. In the aromatic region, the signals were weaker and much broader than with $\text{Fe}(\text{Cp-C4-O-terpy})_2$, so that they were not helpful to properly identify a free terpy. The ESI mass spectrum, however, confirmed the presence of both the $[1+1]$ macrocycle and the $[2\text{Fe} + 1\text{Co}]$ oligomer (Figure 6.44). The cyclic product seemed to be the main product, its mass peak being the most intense. However, although the

NMR spectrum did not suggest such a ratio, the peak for the oligomer showed a significant relative intensity of about 65%.

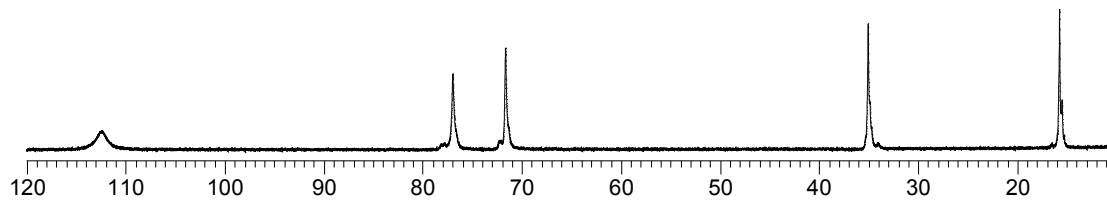


Figure 6.43: 250 MHz ¹H-NMR spectrum (in CDCl₃/CD₃OD) of the 1:1 mixture of Fe(Cp-C6-O-terpy)₂ and Co(II) in the region δ 120-10 ppm.

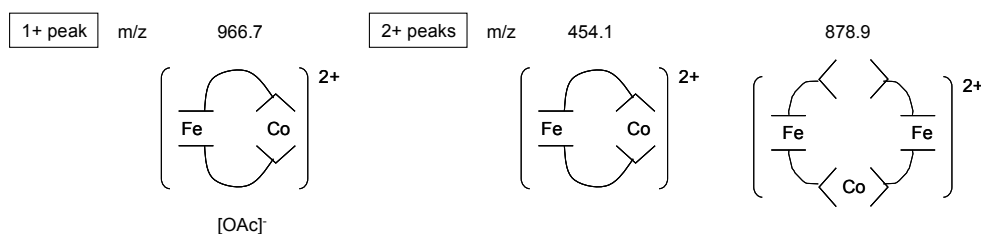


Figure 6.44: ESI-MS peaks of the 1:1 mixture of Fe(Cp-C6-O-terpy)₂ and Co(OAc)₂. The mixture was prepared in CDCl₃ and CD₃OD and the ESI-MS sample was diluted with MeOH.

The last experiment of this series was the mixing of Fe(Cp-C6-O-terpy)₂ and FeCl₂ in 1:1 ratio. As often happened, when Fe(II) was added as the second metal, the ¹H-NMR signals were too broad to be studied.

The ESI mass spectrum indicated the [2Fe + 1Fe] oligomer as the main product, next to the [1+1] cycle (Figure 6.45), as was already the case when Fe(Cp-C4-O-terpy)₂ was used.

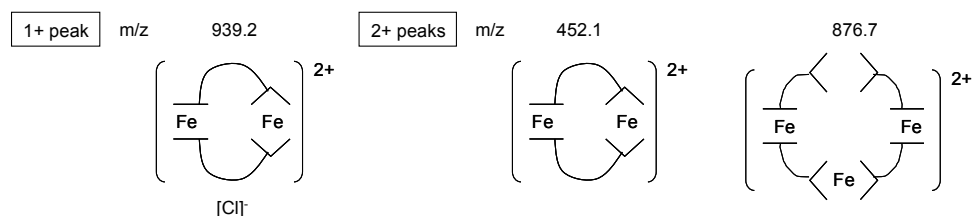


Figure 6.45: ESI-MS peaks of the 1:1 mixture of Fe(Cp-C6-O-terpy)₂ and FeCl₂. The mixture was prepared in CDCl₃ and CD₃OD and the ESI-MS sample was diluted with MeOH.

6.7. Exchange between macrocycles

In the previous section it was established that when the ferrocene complexes $\text{Fe}(\text{Cp-Cn-terpy})_2$ and $\text{Fe}(\text{Cp-Cn-O-terpy})_2$ were mixed with $\text{Co}(\text{II})$ or $\text{Fe}(\text{II})$, the system chose to form only one (or sometimes two) of the virtually infinite number of possible products. In all cases one of the preferred products was the [1+1] bimetallic macrocycle. In some mixtures, this macrocycle was accompanied by a [2Fe + 1M] oligomer. This choice represented the first level of exchange of a new dynamic combinatorial library. A second level of exchange is represented by the possibility for the metal bound to the terpy moiety to swap its ligands with another bis-terpy complex. The third level of exchange will be the swapping of ligands for the metal bound to the cyclopentadienyl rings.

In this section we will study the exchange at the terpy moiety. To obtain evidence for the ligand exchange between the terpy complex within the macrocycle and another terpy complex, it was necessary that the metals bound in the two complexes were different to recognise the formation of new products. For this purpose, the macrocycle $[\text{Fe}(\text{Cp-C4-terpy})_2\text{Co}]^{2+}$ and $[\text{Fe}(\text{terpy})_2]^{2+}$ were chosen. The possible products of the ligand exchange between these two starting materials are the [2Fe + 1Co] trimetallic linear product or the [1+1] homometallic cycle next to $[\text{Co}(\text{terpy})_2]^{2+}$ (Figure 6.46).

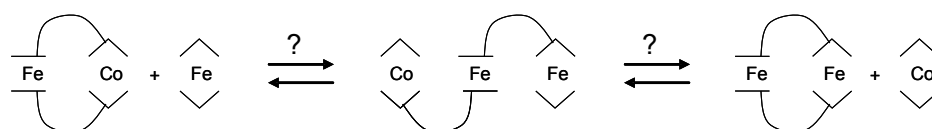


Figure 6.46: Schematic representation of the terpy exchange between $[\text{Fe}(\text{Cp-C4-terpy})_2\text{Co}]^{2+}$ and $[\text{Fe}(\text{terpy})_2]^{2+}$.

$\text{Fe}(\text{Cp-C4-terpy})_2$ and $\text{Co}(\text{OAc})_2$ were first mixed in 1:1 ratio in CDCl_3 , CD_3OD and CD_3CN to obtain the mixture that was previously identified as $[\text{Fe}(\text{Cp-C4-terpy})_2\text{Co}]^{2+}$ containing different anions. One equivalent of $[\text{Fe}(\text{terpy})_2][\text{PF}_6]_2$ was then added to the NMR sample. The $^1\text{H-NMR}$ spectrum measured right after mixing showed already a range of new signals arising for the $\text{Co}(\text{II})$ species. However, it was only after one day of equilibrating at room temperature that the spectrum revealed a clear change in the nature of the $\text{Co}(\text{II})$ complex, and this remained constant for a longer time (Figure

6.47). The comparison of the chemical shifts of the signals of this spectrum with those known for $[\text{Co}(\text{terpy})_2]^{2+}$ [120] confirmed the formation of this complex.

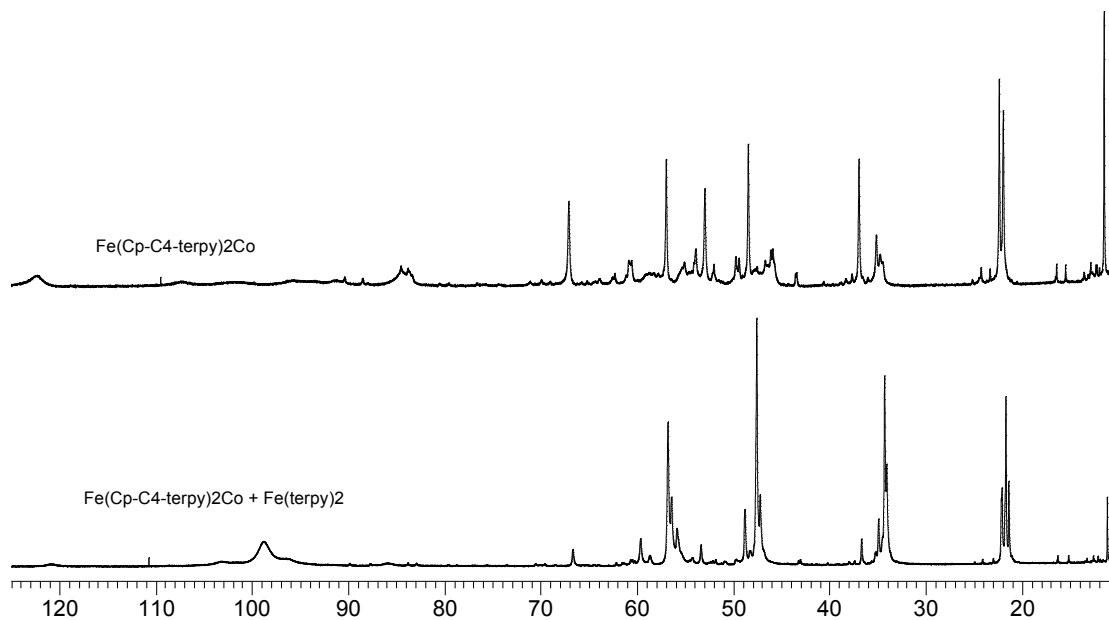


Figure 6.47: 250 MHz ^1H -NMR spectra (in $\text{CDCl}_3/\text{CD}_3\text{OD}/\text{CD}_3\text{CN}$) of $[\text{Fe}(\text{Cp-C4-terpy})_2\text{Co}]^{2+}$ before and after the addition of 1 equivalent of $[\text{Fe}(\text{terpy})_2]^{2+}$, in the region δ 125-10 ppm. The bottom spectrum was measured after two days of equilibrating.

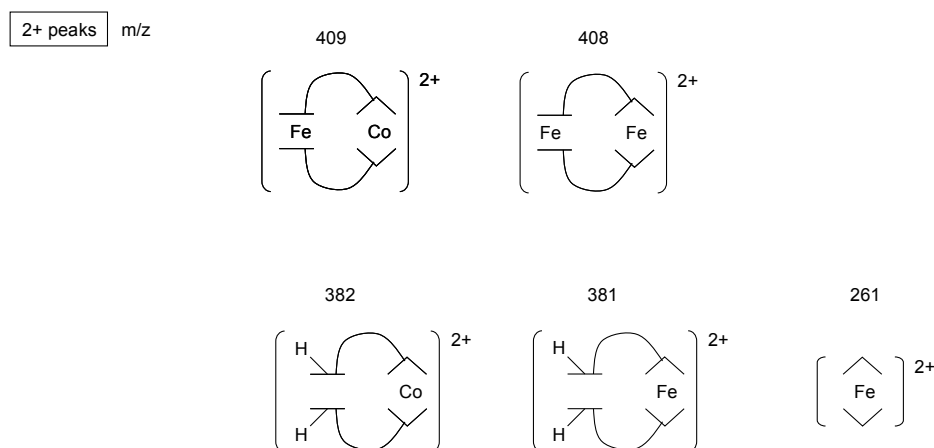


Figure 6.48: ESI-MS peaks of the 1:1 mixture of $[\text{Fe}(\text{Cp-C4-terpy})_2\text{Co}]^{2+}$ and $[\text{Fe}(\text{terpy})_2]^{2+}$. The mixture was prepared in CDCl_3 , CD_3OD and CD_3CN and the ESI-MS sample was diluted with CH_3CN .

The ESI mass spectrum of the mixture was measured. The fragments assigned to the observed peaks are listed in Figure 6.48. Next to the starting materials, the new macrocycle $[\text{Fe}(\text{Cp-C4-terpy})_2\text{Fe}]^{2+}$ could be observed, as well as the corresponding fragments after decomplexation of the ferrocene. Curiously, no mass peak was observed for the fragment $[\text{Co}(\text{terpy})_2]^{2+}$, although its presence in the mixture was unambiguous from the $^1\text{H-NMR}$ spectrum, and it was the clear consequence of the formation of the $[\text{Fe} + \text{Fe}]$ macrocycle.

After this experiment confirmed the feasibility of the ligand exchange at the terpy level, a similar mixture was prepared with two macrocycles of different size and with different metals to study its behaviour. This time, the range of possible products was larger than for the mixture containing a simple, non-functionalised terpy, as is shown in Figure 6.49.

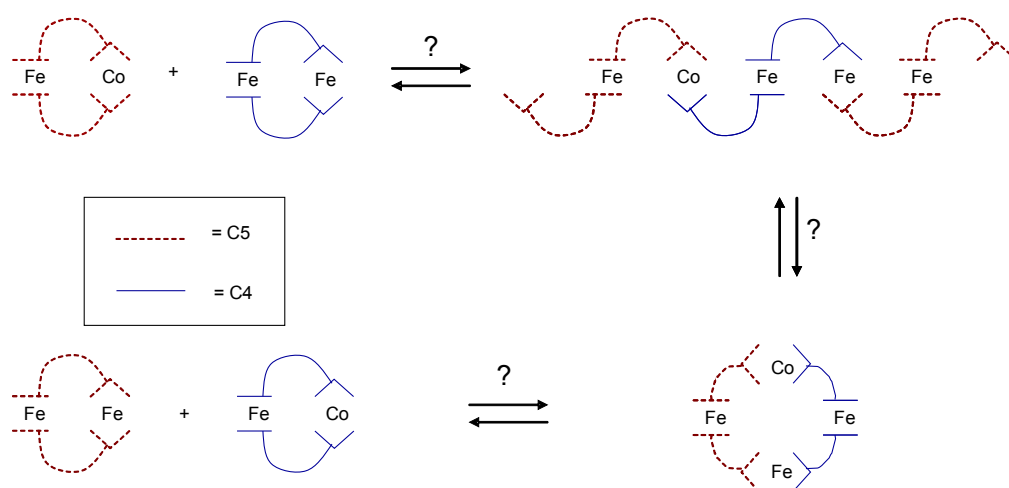


Figure 6.49: Schematic representation of the terpy exchange between $[\text{Fe}(\text{Cp-C4-terpy})_2\text{Fe}]^{2+}$ and $[\text{Fe}(\text{Cp-C5-terpy})_2\text{Co}]^{2+}$.

The two initial macrocycles $[\text{Fe}(\text{Cp-C5-terpy})_2\text{Co}]^{2+}$ and $[\text{Fe}(\text{Cp-C4-terpy})_2\text{Fe}]^{2+}$ were separately prepared in CDCl_3 and CD_3OD . They were then mixed in a 1:1 ratio, and the $^1\text{H-NMR}$ spectrum of the mixture was measured. Unlike in the previous experiment, $^1\text{H-NMR}$ spectroscopy was not very helpful in the analysis of the mixture. After one day of equilibrating at room temperature, and even after heating, the signals for the new $\text{Co}(\text{II})$ species that arose were too weak and too broad to be compared with any known spectrum.

The ESI mass spectrum, on the other hand, showed a whole range of peaks revealing exchange of metals between the two initial macrocycles (Figure 6.50). Every mass peak appeared as a kind of “doublet” with a characteristic separation which was the difference in mass between Co and Fe.

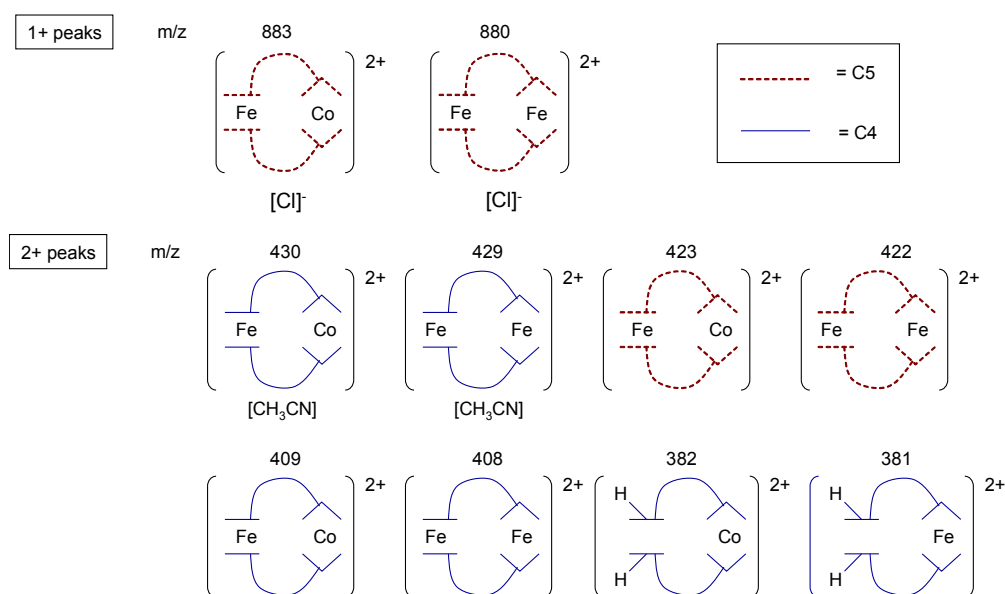


Figure 6.50: ESI-MS peaks of the 1:1 mixture of $[\text{Fe}(\text{Cp-C5-terpy})_2\text{Co}]^{2+}$ and $[\text{Fe}(\text{Cp-C4-terpy})_2\text{Fe}]^{2+}$. The mixture was prepared in CDCl_3 , and CD_3OD , and the ESI-MS sample was diluted with CH_3CN .

The experiments just described established terpy exchange as a second level of freedom for this kind of dynamic combinatorial libraries. The next step consists of trying and exchanging the cyclopentadienyl rings of the ferrocene moiety, to see whether it is possible to add a third level of freedom to the dynamic combinatorial library.

An example was found in the literature, reporting the ring migration in alkylated ferrocenes by simple heating in presence of aluminium chloride in a nitrogen atmosphere [75]. We tried to reproduce this experiment by mixing $\text{Fe}(\text{Cp-C4-O-terpy})_2$ with one equivalent of ferrocene (FeCp_2) in dichloromethane, in presence of 1.1 equivalents of AlCl_3 and under a nitrogen atmosphere. The mixture was refluxed overnight. The TLC analysis of the mixture of products obtained after 21 h of reaction

showed three spots, which were assumed to correspond to the two starting materials and the mixing product $\text{Fe}(\text{Cp})(\text{Cp-C4-O-terpy})$ (Figure 6.51).

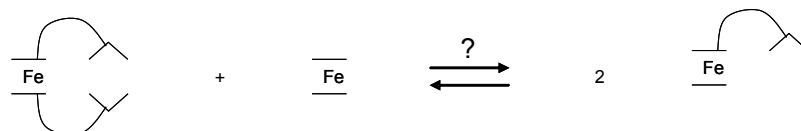


Figure 6.51: Schematic representation of the cyclopentadienyl exchange between $[\text{Fe}(\text{Cp-C4-O-terpy})_2]$ and FeCp_2 .

After separation of the products by column chromatography, the two starting materials were easily identified from their $^1\text{H-NMR}$ spectra. The $^1\text{H-NMR}$ peaks of the third product were too weak and broad to be interpreted, and the amount of material available was too small to try and improve the quality of the spectrum. Assuming that this product was the desired $\text{Fe}(\text{Cp})(\text{Cp-C4-O-terpy})$, half an equivalent of $\text{Co}(\text{OAc})_2$ was added to the NMR sample to try and form the complex shown in Figure 6.52. This trimetallic complex would bear a 2+ charge and could therefore be identified by ESI-MS.

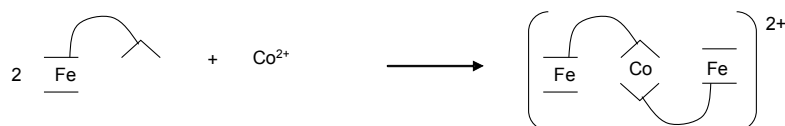


Figure 6.52: Schematic representation of the reaction used to characterise the mixing product $\text{Fe}(\text{Cp})(\text{Cp-C4-O-terpy})$.

Many of the peaks observed in the ESI mass spectrum of the mixture could not be assigned to any fragments (Figure 6.53). However, two of them confirmed the presence of the desired product, $\text{Fe}(\text{Cp})(\text{Cp-C4-O-terpy})$, before and after reacting with $\text{Co}(\text{II})$.

Two of the observed peaks corresponded to the mass of the fragment resulting from the cleavage of one terpy-O from $\text{Fe}(\text{Cp-C4-O-terpy})_2$. The breaking of the C-O ether bond could have occurred under the reaction conditions for the exchange, but no experiment was carried out to give evidence for this behaviour.

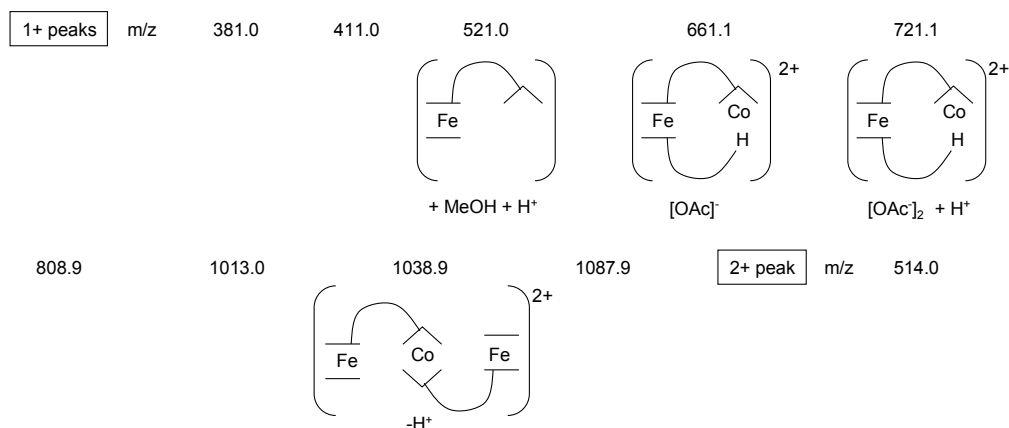


Figure 6.53: ESI-MS peaks of the mixture between the hypothetical $\text{Fe}(\text{Cp})(\text{Cp-C4-O-terpy})$ and $\text{Co}(\text{OAc})_2$. The mixture was prepared in CDCl_3 , and CD_3OD , and the ESI-MS sample was diluted with CH_3OH .

6.8. Conclusions and outlook

In this chapter, the synthesis of a new ligand composed of a 2,2':6'-2''-terpyridine bound to a cyclohexadiene ring was presented. Its $\text{Co}(\text{II})$ and $\text{Fe}(\text{II})$ complexes were prepared. Attempts to form a polynuclear macrocycle by reaction of the $\text{Co}(\text{II})$ and $\text{Fe}(\text{II})$ complex with RuCl_3 were unsuccessful, as was the attempt to form the desired dimeric $\text{Ru}(\text{II})/\text{arene}$ complex by reacting RuCl_3 with the free ligand.

The syntheses of four new bis-2,2':6'-2''-terpyridine ligands containing a ferrocene moiety were then described. These were called $\text{Fe}(\text{Cp-Cn-terpy})_2$ and $\text{Fe}(\text{Cp-Cn-O-terpy})_2$, where n corresponded to the number of carbon atoms composing the alkyl chain binding the cyclopentadienyl ring and the terpy moiety.

The four new ferrocene complexes were each mixed with one equivalent of $\text{Co}(\text{II})$ and $\text{Fe}(\text{II})$ and the resulting products were identified by ESI-MS. In all cases, among the virtually infinite number of possible products, the [1+1] dimetallic macrocycle was formed. With $\text{Fe}(\text{Cp-C4-O-terpy})_2$ and $\text{Fe}(\text{Cp-C6-O-terpy})_2$, the $[2\text{Fe} + 1\text{M}]$ linear oligomer was also obtained, where $\text{M} = \text{Co}(\text{II})$ or $\text{Fe}(\text{II})$. This possibility for the ferrocene complex to choose which product to form upon addition of a second metal, represented the first level of exchange of a dynamic combinatorial library.

The second level of exchange was represented by the possibility for the formed $\text{M}(\text{terpy})_2$ complex to exchange its ligands with another complex. One $[1\text{Fe} + 1\text{Co}]$

dimetallic macrocycle was mixed with one equivalent of $[\text{Fe}(\text{terpy})_2]^{2+}$, and two dimetallic macrocycles with different alkyl chain length and different metals in the terpy moiety were mixed in equimolar ratio. In both mixtures, the products resulting from the exchange of the terpy ligands were identified by ESI-MS. These experiments confirmed the second level of exchange of the dynamic combinatorial library.

An experiment was carried out to try and establish a third level of exchange, namely the ring exchange in the ferrocene moiety. The substituted ferrocene $\text{Fe}(\text{Cp-C4-O-terpy})_2$ was mixed with one equivalent of FeCp_2 and was submitted to the conditions supposed to allow the ring exchange. However, the main compounds obtained in the mixture of products were the two starting materials. What seemed to be the third product revealed itself as a mixture of the desired mixing product $\text{Fe}(\text{Cp})(\text{Cp-C4-O-terpy})$ and the unexpected $\text{Fe}(\text{Cp-C4-H})(\text{Cp-C4-O-terpy})$. No investigations were made to understand if the cleavage of the ether bond was caused by the reaction conditions used for the ring exchange. This experiment did not give enough evidence for the feasibility of the third level of exchange. Nevertheless, the fact that we could obtain the product of the ring exchange, although in very small quantities, is encouraging enough to consider another attempt worthwhile.

To avoid the problem of ether cleavage, it would be better to use a $\text{Fe}(\text{Cp-Cn-terpy})_2$ system. The synthesis proposed here for these systems, however, is rather inconvenient in terms of yields, so that another synthetic pathway should be developed.

Another experiment that would be interesting is to look for a template that would drive the $\text{Fe}(\text{Cp-Cn-terpy})_2$ system to form a product other than the [1+1] dimetallic macrocycle (Figure 6.54). An example could be an anion filling the cavity of a larger macrocycle, in a similar way as was obtained by Lehn and co-workers [121, 122].

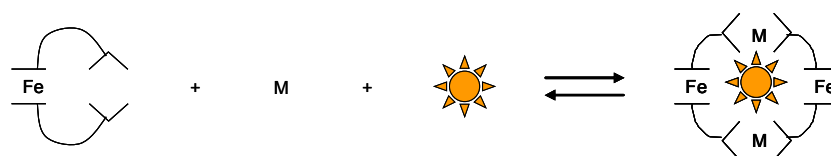


Figure 6.54: Schematic representation of the templating experiment to form a macrocycle other than the [1+1] species obtained in this chapter without any template.

7. Experimental

7.1. General experimental

Materials

All commercially available chemicals were of reagent grade and used without further purification.

Dry solvents were obtained as follows:

Pyridine, diisopropylamine and triethylamine were refluxed with potassium hydroxide then distilled.

N,N-Dimethylformamide was purchased as dry solvent stored over molecular sieves under a crown cap.

Tetrahydrofuran was refluxed with sodium and benzophenone then distilled under a nitrogen atmosphere.

Diethyl ether was refluxed with sodium hydride then distilled under a nitrogen atmosphere.

Dichloromethane was refluxed with phosphorus pentoxide then distilled under a nitrogen atmosphere.

Ethanol was refluxed with sodium then distilled under a nitrogen atmosphere.

Methanol was refluxed with magnesium turnings then distilled under a nitrogen atmosphere.

Instrumentation

¹H-NMR spectra were recorded on Bruker AM-250 (250 MHz), AV-400 (400 MHz) or DRX-500 (500 MHz) instruments at a temperature of 300 K. **¹³C-NMR** were recorded at 125 MHz on Bruker DRX-500 or at 100 MHz on AV-400 instruments. Chemical shifts are given in parts per million (ppm) with respect to TMS = δ 0 ppm and referenced with respect to residual protons of the deuterated solvent. The multiplicities are described as s (singlet), d (doublet), t (triplet) and m (multiplet).

FAB-MS spectra were recorded on a Finnigan MAT312 instrument with 3-nitrobenzyl alcohol as supporting matrix.

EI-MS spectra were recorded on a Finnigan MAT95Q instrument with a potential of 70 eV.

ESI-MS spectra were recorded on a Finnigan MAT LCQ instrument.

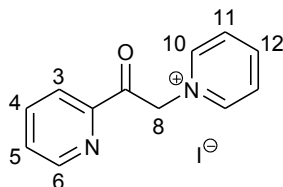
IR absorption spectra were recorded on a Shimadzu FTIR-8400S spectrophotometer.

UV/Vis absorption spectra were recorded on a Varian Cary 5000 UV-Vis-NIR spectrophotometer.

Melting points were measured with an Electrothermal or a Gallenkamp digital melting point apparatus.

7.2. Organic syntheses

1-(2-Pyridylacetyl)pyridinium iodide (M = 326.15) (PPI, 12) [82]



A solution of iodine (40.49 g, 159.5 mmol) in dry pyridine (140 ml) was heated to 60 °C under a nitrogen atmosphere. This solution was added to 2-acetylpyridine (54 ml, 480 mmol) while it was still warm, and the mixture was stirred at 85-90 °C under N₂ for 4 h. When the mixture had cooled to room temperature the black precipitate was filtered and washed with dry pyridine; it was then recrystallised from ethanol (11 for half of the crude product) with addition of activated charcoal to give golden brown crystals. Yield: 50.58 g, 97.5%.

¹H-NMR (250 MHz, DMSO-d₆): δ / ppm 9.02 (2H, dd, *J* = 6.8, 1.3 Hz, H10), 8.89 (1H, ddd, *J* = 4.5, 1.5, 1.0 Hz, H6), 8.75 (1H, tt, *J* = 7.8, 1.3 Hz, H12), 8.29 (2H, dd, *J* = 8.0, 6.8 Hz, H11), 8.16 (1H, td, *J* = 7.5, 1.8 Hz, H4), 8.09 (1H, ddd, *J* = 7.8, 1.7, 0.9 Hz, H3), 7.86 (1H, ddd, *J* = 7.3, 4.8, 1.6 Hz, H5), 6.52 (2H, s, H8).

¹³C-NMR (100 MHz, DMSO-d₆): δ / ppm 192.3, 151.3, 150.4, 147.2, 139.0, 128.6, 128.0, 122.9, 67.5.

5-Methyl-2,2'-bipyridine (M = 170.23) (9)

a) The method followed that in the literature. [41]

1-(2-Pyridylacetyl)pyridinium iodide (8.14 g, 24.9 mmol), methacrolein (3.0 ml, 36 mmol) and ammonium acetate (5.92 g, 76.8 mmol) were dissolved in *N,N*-dimethylformamide (15 ml) and stirred at 80 °C for 6 h. The mixture was cooled to room temperature, then water (20 ml) was added. The solution was extracted with

ether (2 x 50 ml, 5 x 20 ml), the combined organic phases were dried over sodium sulfate, and the solvent evaporated. The yellow liquid residue was dried *in vacuo*. Yield: 2.81 g, 66.3%.

b)

1-(2-Pyridylacetyl)pyridinium iodide (8.16 g, 25.0 mmol), methacrolein (3 ml, 36 mmol) and ammonium acetate (5.81 g, 75.4 mmol) were dissolved in methanol (70 ml) and refluxed at 65 °C for 3.5 h. The solution was concentrated and the residue was extracted with hexane (6 x 30 ml). The combined organic layers were washed with brine (2 x 70 ml), dried over sodium sulfate, and the solvent evaporated. The yellow liquid residue was dried *in vacuo*. Yield: 3.10 g, 72.8%.

¹H-NMR (250 MHz, CDCl₃): δ / ppm 8.61 (1H, ddd, *J* = 4.9, 1.9, 1.0 Hz, H6'), 8.45 (1H, m, H6), 8.31 (1H, dt, *J* = 8.3, 1.0 Hz, H3'), 8.24 (1H, d, *J* = 7.5 Hz, H3), 7.72 (1H, td, *J* = 7.6, 1.9 Hz, H4'), 7.54 (1H, m, H4), 7.19 (1H, ddd, *J* = 7.4, 4.9, 1.1 Hz, H5'), 2.29 (3H, s, CH₃).

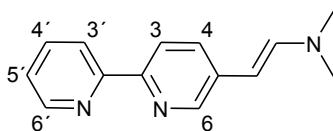
¹³C-NMR (100 MHz, CDCl₃): δ / ppm 156.6, 153.9, 149.9, 149.4, 137.8, 137.2, 133.7, 123.7, 121.1, 120.9, 18.6.

ESI-MS: *m/z* 250.8 [M + Na + acetone]⁺, 193.2 [M + Na]⁺.

IR (solid, cm⁻¹): 3047w, 3001w, 2923w, 2869w, 1558m, 1458s, 1434m, 1380m, 1249w, 1218w, 1126w, 1095w, 1064w, 1033m, 987m, 848m, 786s, 740s, 648w.

Elem. an.: % calc. C 77.62, H 5.92, N 16.46; found C 75.61, H 6.43, N 16.14.

5-[2-(*N,N*-Dimethylamino)vinyl]-2,2'-bipyridine (M = 225.32) (13)



A solution of 5-methyl-2,2'-bipyridine (1.32 g, 7.8 mmol) and *t*-butoxybis(dimethylamino)methane (Bredereck's reagent, 4.5 ml, 22 mmol) in dry

N,N-dimethylformamide (25 ml) was degassed with argon for 15 min. The solution was then heated to 140 °C under argon for 17 h. The reaction mixture was cooled to room temperature and water (200 ml) was added. The solution was extracted with dichloromethane (5 x 100 ml), the combined organic layers were dried over sodium sulfate and the solvent evaporated. Purification of the crude product by column chromatography (aluminium oxide 90 standardised, toluene : diethylamine 40:1) gave the final product as a yellow oil. Yield: 0.53 g, 30.4%.

¹H-NMR (250 MHz, CDCl₃): δ / ppm 8.65 (1H, ddd, *J* = 4.9, 1.9, 1.0 Hz, H6'), 8.48 (1H, d, *J* = 2.0 Hz, H6), 8.33 (1H, dt, *J* = 8.0, 1.3 Hz, H3), 8.22 (1H, d, *J* = 8.5 Hz, H3'), 7.78 (1H, td, *J* = 7.8, 1.9 Hz, H4), 7.60 (1H, dd, *J* = 8.3, 2.3 Hz, H4'), 7.23 (1H, m, H5'), 6.92 (1H, d, *J* = 13.8 Hz, H8), 5.13 (1H, d, *J* = 13.8 Hz, H7), 2.88 (6H, s, N(CH₃)₂).

¹³C-NMR (100 MHz, CDCl₃): δ / ppm 157.0, 150.9, 149.4, 145.6, 142.0, 137.2, 130.1, 125.7, 123.1, 121.3, 120.7, 93.8, 41.0.

R_f (Al₂O₃, toluene : diethylamine 40:1): 0.47.

5-Formyl-2,2'-bipyridine (M = 184.21) (10)

5-[2-(*N,N*-Dimethylamino)vinyl]-2,2'-bipyridine (0.46 g, 2.0 mmol) was dissolved in water : tetrahydrofuran 1:1 (130 ml) and sodium periodate (1.72 g, 8.04 mmol) was added. The solution was stirred at room temperature for 4 h. The insoluble products were filtered off and washed with tetrahydrofuran, then the solvent was evaporated. The residue was dissolved in dichloromethane (100 ml) and washed with saturated sodium hydrogencarbonate (4 x 50 ml). The organic phase was dried over sodium sulfate and evaporated to give the product as a yellow-brown solid. Yield: 0.32 g, 86.9%.

An analytically pure sample of white solid was obtained after purification by column chromatography (Alox 90 standardised, CH₂Cl₂).

$^1\text{H-NMR}$ (250 MHz, CDCl_3): δ / ppm 10.20 (1H, s, CHO), 9.16 (1H, dd, $J = 2.1, 0.9$ Hz, H6), 8.76 (1H, ddd, $J = 4.8, 1.8, 1.1$ Hz, H6'), 8.65 (1H, d, $J = 8.0$ Hz, H3), 8.54 (1H, dt, $J = 8.0, 1.1$ Hz, H3'), 8.32 (1H, dd, $J = 8.1, 2.1$ Hz, H4), 7.90 (1H, td, $J = 7.8, 1.7$ Hz, H4'), 7.42 (1H, ddd, $J = 7.4, 4.6, 1.4$ Hz, H5').

$^{13}\text{C-NMR}$ (100 MHz, CDCl_3): δ / ppm 190.9, 161.1, 155.2, 152.0, 149.9, 137.5, 137.3, 131.5, 125.2, 122.6, 121.7.

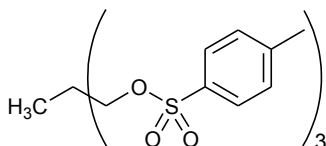
EI-MS: m/z 184.1 $[\text{M}]^+$, 155.1 $[\text{M} - \text{CHO}]^+$.

IR (solid, cm^{-1}): 3379w, 3055w, 2916w, 2840w, 2715w, 1697m, 1589m, 1550m, 1450m, 1434m, 1357m, 1303w, 1249w, 1203m, 1141w, 1087w, 1064w, 995w, 840m, 794s, 740s, 663w, 624w.

R_f (Al_2O_3 , CH_2Cl_2): 0.39.

Elem. an.: % calc. C 71.73, H 4.38, N 15.21, O 8.69; found C 71.45, H 4.63, N 14.95. m. p.: 91.8-93.0 $^\circ\text{C}$.

1,1,1-Tris(*p*-toluenesulfonyloxymethyl)ethane (M = 582.77) (20) [87]



1,1,1-Tris(hydroxymethyl)ethane (6.02 g, 50.1 mmol) was dissolved in pyridine (17 ml) and cooled to 0 $^\circ\text{C}$. To this solution was added dropwise a cold solution of *p*-toluenesulfonyl chloride (28.75 g, 150.8 mmol) in pyridine (45-50 ml), while keeping the reaction mixture in an ice bath. After addition was complete the mixture was left to stand overnight at room temperature. Pyridine was evaporated and the residue dissolved in chloroform (100 ml) and water (200 ml). After separation of the phases, the organic layer was washed with sulphuric acid 0.1 M (50 ml) and water (1 x 100 ml, then 3 x 200 ml), then dried over sodium sulfate and concentrated to about half the volume. Upon cooling in an ice bath, addition of little methanol and

scratching with a glass rod the white product crystallized in the solution. It was filtered, washed with ether and dried *in vacuo*. Yield: 19.45 g, 66.6%.

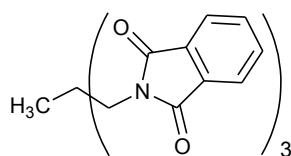
$^1\text{H-NMR}$ (250 MHz, CDCl_3): δ / ppm 7.34 (6H, d, $J = 8.5$ Hz, H-Ar), 7.39 (6H, d, $J = 8.3$ Hz, H-Ar), 3.79 (6H, s, CH_2), 2.50 (9H, s, CH_3 -Ar), 0.92 (3H, s, CH_3).

$^{13}\text{C-NMR}$ (100 MHz, CDCl_3): δ / ppm 145.8, 132.4, 130.5, 128.3, 70.2, 39.8, 22.1, 16.5.

IR (solid, cm^{-1}): 1599w, 1354m, 1189m, 1176s, 1096w, 1038w, 1004m, 981m, 961s, 865m, 837s, 813s, 788m, 667s, 621m.

m. p. : 91.3-94.6 °C.

1,1,1-Tris(phthalimidomethyl)ethane (M = 507.53) (21)



a) The method followed that in the literature. [88]

1,1,1-Tris(*p*-toluenesulfonyloxymethyl)ethane (10.81 g, 18.55 mmol) was dissolved in dry *N,N*-dimethylformamide (20 ml) under nitrogen atmosphere and potassium phthalimide (12.02 g, 64.89 mmol) was added. The mixture was heated to 170 °C for 3 h and the colour changed from white to orange-brown. After cooling to room temperature the solid precipitate was filtered off and washed with methanol : *N,N*-dimethylformamide 1:1 (20 ml), then thoroughly with water, methanol and ether. The white residue was dried *in vacuo*. Yield: 1.03 g, 10.9%.

$^1\text{H-NMR}$ (250 MHz, CDCl_3): δ / ppm 7.89 (6H, dd, $J = 5.8, 3.0$ Hz, H-Ar), 7.77 (6H, dd, $J = 5.5, 3.0$ Hz, H-Ar), 3.85 (6H, s, CH_2), 1.02 (3H, s, CH_3).

$^{13}\text{C-NMR}$ (100 MHz, CDCl_3): δ / ppm 169.4, 134.6, 132.3, 123.9, 45.3, 45.2, 19.7.

b) The method followed that in the literature. [87]

1,1,1-Tris(*p*-toluenesulfonyloxymethyl)ethane (9.71 g, 16.7 mmol) and potassium phthalimide (9.33 g, 50.4 mmol) were crushed with *p*-xylene (10 ml) and the mixture was heated to 140 °C with an electromantel for 1 h. More *p*-xylene (50 ml) was added and the solution was heated at 160 °C during 4 h, until all the solvent had distilled off. The residue was crushed with hot water (50 ml at 80 °C) and the mixture was left to cool at room temperature. The solution was filtered and the filtrate washed with water and dried in a desiccator. The dry residue was crushed with methanol (25 ml), filtered and washed with methanol, it was then recrystallised from ethyl acetate. The brown product was not the desired compound.

c)

A mixture of potassium phthalimide (8.45 g, 45.6 mmol), potassium carbonate (19.08 g, 138.0 mmol) and benzyltriethylammonium bromide (1.29 g, 4.74 mmol) in acetone (200 ml) was refluxed for 40 min. A solution of 1,1,1-tris(*p*-toluenesulfonyloxymethyl)ethane (8.5 g, 15 mmol) in acetone (25 ml) was added dropwise to the mixture and refluxed for additional 5.5 h. The precipitate was filtered and washed with acetone, and the solution evaporated to leave a yellow sticky residue, which was dissolved in dichloromethane (100 ml) and washed with sodium hydroxide 2% (2 x 50 ml) and water (2 x 70 ml). The organic phase was dried over sodium sulfate and the solvent evaporated. The yellow liquid residue solidified in the air to give a white compound with yellow impurities. The crude final product turned out to be the starting material.

1,1,1-Tris(aminomethyl)ethane hydrochloride (M = 226.61) (23) [87]

1,1,1-Tris(phthalimidomethyl)ethane (5.15 g, 10.1 mmol) was suspended in an aqueous solution of potassium hydroxide (6.77 g, in 20 ml) and stirred at room temperature for 14 days during which time evaporated water was replenished regularly. Water was distilled, to the residue was added more water (20 ml) and the

distillation repeated. The combined distillates were neutralised with diluted hydrochloric acid and evaporated. The pale pink residue was not the desired product.

1,1,1-Tris(azidomethyl)ethane (M = 195.23) (22) [91]

A mixture of 1,1,1-tris(*p*-toluenesulfonyloxymethyl)ethane (8.00 g, 13.7 mmol) and sodium azide (4.51 g, 69.4 mmol) in ethylene glycol (40 ml) was stirred under nitrogen at 135 °C for 23 h. The yellow clear solution was cooled to room temperature and poured into water (55 ml), the resulting solution was extracted with diethyl ether (2 x 100 ml) and the combined ether layers washed with water (50 ml). The ether phase was treated with activated charcoal, dried with sodium sulfate and evaporated. The yellow oily product was dried *in vacuo*. Yield: 1.58 g, 59.1%.

¹H-NMR (250 MHz, CDCl₃): δ / ppm 3.26 (6H, s, CH₂), 0.98 (3H, s, CH₃).

¹³C-NMR (100 MHz, CDCl₃): δ / ppm 55.9, 41.0, 19.3.

IR (liquid, cm⁻¹): 2970w, 2931w, 2869w, 2090s, 1442w, 1288m.

1,1,1-Tris(aminomethyl)ethane (M = 117.23) (17) [91]

A solution of 1,1,1-tris(azidomethyl)ethane (1.45 g, 7.43 mmol) in dry tetrahydrofuran (5 ml) was added slowly to a suspension of lithium aluminium hydride (1.08 g, 28.4 mmol) in dry tetrahydrofuran (20 ml) under a nitrogen atmosphere. When the addition was complete, the mixture was refluxed for 7 h, and after cooling to room temperature water (5 ml), sodium hydroxide 25% (about 3 ml) and water again (5 ml) were added. The white precipitate was collected and extracted in a Soxhlet apparatus with tetrahydrofuran (70 ml) for 20 h. The solvent was evaporated and to the resulting oil was added benzene (5 ml). The solution was distilled, collecting the water in a Dean-Stark trap. Final distillation of the benzene gave the product as a colourless oil. Yield: 0.03g, 3.4%.

¹H-NMR (250 MHz, CDCl₃): δ / ppm 2.61 (6H, s, CH₂), 1.61 (12H, s, NH₂), 0.82 (3H, s, CH₃).

^{13}C -NMR (100 MHz, CDCl_3): δ / ppm 128.7, 47.6.

2-Acetyl-5-methylpyridine (M = 135.18) (29)

a)

A solution of *N,N*-dimethylethanolamine (2.4 ml, 24 mmol) in hexane (10 ml) was cooled to 0 °C. *n*-Butyl lithium (1.6 M in hexane, 30 ml, 48 mmol) was added dropwise while keeping the temperature below 10 °C. After the addition was complete the mixture was stirred until the temperature regained 0 °C, then a solution of 3-methylpyridine (0.8 ml, 8.2 mmol) in hexane (10 ml) was added dropwise. Stirring at 0 °C continued for 1 h, then the mixture was cooled to -78 °C before adding dropwise a solution of *N,N*-dimethylacetamide (2.6 ml, 28 mmol) in THF (50 ml). The reaction was stirred at -78 °C for 1 h, then it was allowed to warm up at room temperature overnight.

The mixture was cooled to 0 °C and cold water (0 °C, 30 ml) was added. The layers were separated and the aqueous phase was extracted with diethyl ether (2 x 40 ml). The combined organic layers were dried over Na_2SO_4 and the solvent evaporated. The oily residue was purified by column chromatography (silica gel, hexane : EtOAc 3:2), but none of the three collected products was the desired compound.

b)

A solution of 2-bromo-5-methylpyridine (16.20 g, 94.17 mmol) in dry diethyl ether (200 ml) was cooled to -78 °C under nitrogen atmosphere. A solution of *n*-butyl lithium (1.7 M in hexanes, 57 ml, 97 mmol, 1.03 eq) was added dropwise over 35 min, then the dark red mixture was stirred at -78 °C for another 10 min. A solution of *N,N*-dimethylacetamide (9.2 ml, 99 mmol, 1.06 eq) in dry ether (10 ml) was prepared under nitrogen and added to the reaction mixture over 15 min. The temperature tended to increase during the addition but it was kept around -70 °C. After addition was complete, the mixture was stirred at -78 °C for 30 min, then it was allowed to warm up slowly to room temperature (about 3 h) and it was finally stirred at room temperature overnight, during which time the solution became turbid and

orange-pink in colour. Water was added (30 ml) making the mixture clear and yellow. The two phases were separated and the aqueous layer was extracted with EtOAc (3 x 30 ml). All the combined organic layers were washed with brine (2 x 50 ml), then dried over Na₂SO₄ and evaporated yielding a golden yellow liquid. Yield: 11.28 g, 88.62%. The product was used crude for the next synthesis, but for proper characterisation a sample was purified by column chromatography (silica gel, CH₂Cl₂ : EtOAc 85:15).

¹H-NMR (250 MHz, CDCl₃): δ / ppm 8.26 (1H, broad s, H6), 7.70 (1H, d, *J* = 7.8 Hz, H3), 7.39 (1H, dd, *J* = 8.1, 2.4 Hz, H4), 2.47 (3H, s, OCH₃), 2.19 (3H, s, CH₃).

¹³C-NMR (100 MHz, CDCl₃): δ / ppm 199.9, 151.6, 149.6, 137.7, 137.3, 121.5, 25.9, 18.8.

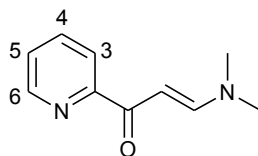
ESI-MS: *m/z* 136.2 [M + H]⁺, 138.7 [M + 3]⁺.

IR (liquid, cm⁻¹): 3001w, 2923w, 1689s, 1589w, 1566w, 1419w, 1380w, 1350m, 1288m, 1242m, 1218m, 1126w, 1087w, 1026m, 956m, 833m, 748w, 678m, 640w.

R_f (silica gel, CH₂Cl₂ : EtOAc 85:15): 0.66.

Elem. an.: % calc. C 71.09, H 6.71, N 10.31, O 11.84; found C 70.02, H 6.70, N 10.24.

2-(3'-(*N,N*-Dimethylamino)-1'-oxoprop-2'-en-1'-yl)pyridine (M = 176.24) (31)



A mixture of 2-acetylpyridine (3.7 ml, 33 mmol) and *N,N*-dimethylformamide dimethylacetal (5.4 ml, 40 mmol, 1.2 eq) was heated at reflux under nitrogen for 20 h. The dark green solid that formed when the mixture was cooled to room temperature was recrystallised from hexane:EtOAc 1:1 (about 200 ml) and activated charcoal. The product was obtained as dark yellow needles. Yield: 4.45g, 76.5%.

¹H-NMR (250 MHz, CDCl₃): δ / ppm 8.60 (1H, d, *J* = 4.5 Hz, H6), 8.12 (1H, d, *J* = 8.0 Hz, H3), 7.89 (1H, d, *J* = 12.8 Hz, COCH), 7.77 (1H, td, *J* = 7.7, 1.8 Hz, H4), 7.33 (1H, ddd, *J* = 7.6, 4.6, 1.2 Hz, H5), 6.43 (1H, d, *J* = 12.5 Hz, CHNMe₂), 3.15 (3H, s, CH₃), 2.97 (3H, s, CH₃).

¹³C-NMR (100 MHz, CDCl₃): δ / ppm 187.2, 156.6, 155.2, 148.6, 137.2, 125.8, 122.5, 91.6, 45.6, 37.9.

ESI-MS: *m/z* 136.2 [M + H]⁺, 138.7 [M + 3]⁺.

IR (solid, cm⁻¹): 2993w, 1635s, 1527s, 1427s, 1357s, 1257s, 1234s, 1126m, 1056s, 987s, 894s, 671s.

Elem. an.: % calc. C 68.16, H 6.86, N 15.90, O 9.08; found C 68.22, H 6.90, N 15.97.
m. p.: 127-131 °C.

5-Methyl-2,2':6',2''-terpyridine (M = 247.32) (34) [97]

To a solution of 2-acetyl-5-methylpyridine (3.00 g, 22.2 mmol) in dry THF (20 ml) at 0 °C under nitrogen atmosphere was added ^tBuOK (4.84 g, 43.1 mmol). After 3 h at 0 °C, 2-(3'-(*N,N*-dimethylamino)-1'-oxoprop-2'-en-1'-yl)-pyridine (3.57 g, 20.3 mmol) in dry THF (50 ml) was added. The mixture was allowed to warm up to room temperature and stirred overnight. NH₄OAc (16.14 g, 209.4 mmol) and HOAc (30 ml) were added and the mixture was heated to reflux for 2 h. The solvent was evaporated, then water (140 ml) was added. The solution was basified with a concentrated solution of NaOH until pH 8-9, then it was divided into two portions, each of which was extracted with CH₂Cl₂ (3 x 50 ml). Another 100 ml of CH₂Cl₂ were used to wash the flask containing the neutralised mixture. The combined organic layers were combined, dried over MgSO₄ and evaporated. The dark brown oily residue was purified by column chromatography (Alox 90 standardised, CH₂Cl₂) to yield a cream coloured solid. Yield: 1.50 g, 29.9%.

¹H-NMR (400 MHz, CDCl₃): δ / ppm 8.70 (1H, dt, *J* = 5.6, 1.0 Hz, H6''), 8.62 (1H, d, *J* = 8.0 Hz, H3''), 8.53 (1H, s broad, H6), 8.50 (1H, d, *J* = 8.0 Hz, H3), 8.43 (1H, d, *J* = 7.6 Hz, H3' or H5'), 8.42 (1H, d, *J* = 7.6 Hz, H3' or H5'), 7.94 (1H, t, *J* = 8.0 Hz,

H4'), 7.86 (1H, td, $J = 7.7, 1.9$ Hz, H4''), 7.67 (1H, dd, $J = 8.2, 1.4$ Hz, H4), 7.33 (1H, ddd, $J = 7.6, 4.8, 1.2$ Hz, H5''), 2.41 (3H, s, CH₃).

¹³C-NMR (100 MHz, CDCl₃): δ / ppm 156.6, 155.6, 155.5, 153.9, 149.7, 149.5, 138.3, 138.1, 137.3, 134.0, 124.2, 121.6, 121.2, 121.1, 18.8.

ESI-MS: m/z 270.3 [M + Na]⁺.

IR (solid, cm⁻¹): 3055w, 3001w, 2916w, 2854w, 1558s, 1481m, 1450m, 1427s, 1380m, 1257w, 1149w, 1126w, 1095w, 1080w, 1026w, 987w, 864w, 817m, 779s, 748s, 694w.

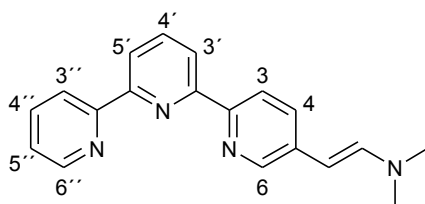
R_f (Al₂O₃, CH₂Cl₂), 0.32.

Elem. an.: % calc. C 77.71, H 5.30, N 16.99; found C 77.80, H 5.45, N 16.75.

m. p.: 79.1-80.4 °C.

Comment: if the reaction mixture with 2-acetyl-5-methylpyridine and ^tBuOK is allowed to warm at room temperature an "isomerisation" of the starting products occurs and this leads to a mixture of final products: 2,2':6',2''-terpyridine, 5-methyl-2,2':6',2''-terpyridine and 5,5'-dimethyl-2,2':6',2''-terpyridine. These products are difficult to separate at this stage (single spot on the TLC), so the mixture was used for the next reaction and the 3 products were separated only then.

5-[2-(*N,N*-Dimethylamino)vinyl]- 2,2':6',2''-terpyridine (M = 302.41) (35)



A solution of 5-methyl-2,2':6',2''-terpyridine (1.00 g, 4.04 mmol) and *t*-butoxybis(dimethylamino)methane (Bredereck's reagent, 2.4 ml, 11 mmol) in dry *N,N*-dimethylformamide (10 ml) was degassed with nitrogen for 20 min. The solution was then heated to 140 °C under nitrogen for 20 h. The reaction mixture was cooled to room temperature and water (75 ml) was added. The solution was extracted with

dichloromethane (4 x 30 ml), the combined organic layers were dried over magnesium sulfate and the solvent evaporated. Purification of the crude product needed two column chromatographies (Alox 90 standardised, toluene : diethylamine 50:1). Yield: 0.22 g, 18.0%.

$^1\text{H-NMR}$ (250 MHz, CDCl_3): δ / ppm 8.69 (1H, ddd, $J = 4.8, 1.7, 0.9$ Hz, $\text{H6}''$), 8.63 (1H, dt, $J = 8.0, 1.0$ Hz, $\text{H3}''$), 8.48-8.35 (4H, m, $\text{H3}, \text{H6}, \text{H3}', \text{H5}'$), 7.90 (1H, t, $J = 7.9$ Hz, $\text{H4}'$), 7.85 (1H, td, $J = 7.7, 1.8$ Hz, $\text{H4}''$), 7.60 (1H, dd, $J = 8.5, 2.3$ Hz, H4), 7.32 (1H, ddd, $J = 7.5, 4.7, 1.3$ Hz, $\text{H5}''$), 6.92 (1H, d, $J = 13.5$ Hz, CHN), 5.13 (1H, d, $J = 13.7$ Hz, CHPy), 2.88 (6H, s, CH_3).

$^{13}\text{C-NMR}$ (100 MHz, CDCl_3): δ / ppm 156.9, 155.5, 149.9, 149.5, 145.4, 141.9, 138.1, 137.8, 137.2, 136.5, 130.2, 124.0, 121.6, 121.4, 120.6, 120.4, 93.9, 41.0.

R_f (Al_2O_3 , toluene : diethylamine 50:1): 0.27.

Comment: characterisation of 5,5'-bis-[2-(*N,N*-dimethylamino)vinyl]-2,2':6',2''-terpyridine

$^1\text{H-NMR}$ (250 MHz, CDCl_3): δ / ppm 8.47 (1H, d, $J = 2.3$ Hz, H6), 8.42 (1H, d, $J = 8.5$ Hz, H3), 8.27 (1H, d, $J = 8.0$ Hz, $\text{H3}'$), 7.85 (1H, t, $J = 7.6$ Hz, $\text{H4}'$), 7.60 (1H, dd, $J = 8.4, 2.4$ Hz, H4), 6.91 (1H, d, $J = 13.8$ Hz, CHN), 5.13 (1H, d, $J = 13.8$ Hz, CHPy), 2.89 (6H, s, CH_3).

$^{13}\text{C-NMR}$ (100 MHz, CDCl_3): δ / ppm 115.9, 151.4, 145.5, 141.8, 137.9, 136.2, 130.1, 121.4, 119.6, 94.0, 41.0 (2C).

R_f (Al_2O_3 , toluene : diethylamine 50:1): 0.31.

5-Formyl-2,2':6',2''-terpyridine (M = 261.30) (36)

5-[2-(*N,N*-Dimethylamino)vinyl]-2,2':6',2''-terpyridine (0.13 g, 0.43 mmol) was dissolved in tetrahydrofuran (15 ml) and sodium periodate (0.36 g, 1.7 mmol) in water (15 ml) was added. The solution was stirred at room temperature for 4 h. The

insoluble products were filtered off and washed with tetrahydrofuran, then the solvent was evaporated.

When all THF had evaporated a pale yellow precipitate formed in the aqueous phase. It was filtered and dried in a desiccator (silica blue). Yield: 0.09 g, 80.1%.

$^1\text{H-NMR}$ (250 MHz, CDCl_3): δ / ppm 10.20 (1H, s, CHO), 9.15 (1H, s broad, H6), 8.84 (1H, d, $J = 8.5$ Hz, H3), 8.74 (1H, d broad, $J = 5.8$ Hz, H6'), 8.64-8.51 (3H, m, H3'', H3', H5'), 8.33 (1H, dd, $J = 7.9, 2.1$ Hz, H4), 8.02 (1H, t, $J = 7.7$ Hz, H4'), 7.91 (1H, td, $J = 7.7, 1.7$ Hz, H4''), 7.38 (1H, dd, $J = 7.3, 4.8$ Hz, H5'').

$^{13}\text{C-NMR}$ (100 MHz, CDCl_3): δ / ppm 171.3, 160.2, 155.2, 153.7, 151.3, 149.0, 137.9, 137.1, 136.7, 130.9, 124.0, 122.1, 121.7, 121.5, 121.3, 120.9.

FAB-MS: m/z 276 $[\text{M} + 15]^+$, 262 $[\text{M} + \text{H}]^+$.

IR (solid, cm^{-1}): 1689s, 1589s, 1558s, 1473m, 1427m, 1365m, 1265m, 1203s, 1141w, 1080m, 1018m, 987m, 856m, 817s, 786s, 756s, 717w, 648w.

m. p.: decomposes >114.3 °C.

5,5'-Diformyl-2,2':6',2''-terpyridine (M = 261.30)

5,5'-Bis-[2-(*N,N*-dimethylamino)vinyl]- 2,2':6',2''-terpyridine (0.05 g, 0.1 mmol) was dissolved in tetrahydrofuran (20 ml) and sodium periodate (0.28 g, 1.3 mmol) in water (20 ml) was added. The solution was stirred at room temperature for 4 h. The insoluble products were filtered off and washed with tetrahydrofuran, then the solvent was evaporated. The residue was dried in a desiccator. Yield: 0.252 g.

This product was still crude and not completely soluble in CDCl_3 , but after filtration the sample was good enough for NMR characterisation. It was not purified further.

$^1\text{H-NMR}$ (250 MHz, CDCl_3): δ / ppm 10.21 (1H, s, CHO), 9.16 (1H, d, $J = 1.5$ Hz, H6), 8.82 (1H, d, $J = 8.0$ Hz, H3), 8.64 (1H, d, $J = 7.8$ Hz, H3'), 8.35 (1H, dd, $J = 8.2, 2.3$ Hz, H4), 8.07 (1H, t, $J = 7.8$ Hz, H4').

5-Carboxy-2,2':6',2''-terpyridine (M =277.30) (39)

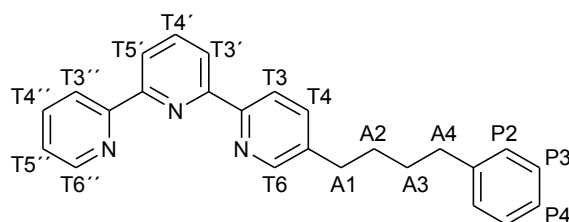
5-Methyl-2,2':6',2''-terpyridine (0.85 g, 3.4 mmol) and KMnO_4 (1.14 g, 7.22 mmol) were mixed in water (25 ml) and heated to reflux for 5.5 h, then it was left to cool overnight. The brown precipitate was filtered off and washed with Et_2O . After the two phases were separated, the aqueous phase was extracted with ether (10 ml). The pH of the aqueous phase was brought to ~ 3 with HCl , when a white precipitate formed. It was filtered, washed with water and dried in the desiccator (silica blue). Yield: 0.07g, 7.4%.

$^1\text{H-NMR}$ (400 MHz, $\text{D}_2\text{O} + \text{CF}_3\text{COOD}$): δ / ppm 9.06 (1H, d, $J = 1.6$ Hz, H6), 8.82 (1H, dd, $J = 8.2, 1.8$ Hz, H3), 8.57 (1H, d, $J = 5.6$ Hz, H6''), 5.53 (1H, d, $J = 8.4$ Hz, H3'), 8.72-8.37 (2H, m, H3', H5'), 8.25 (1H, d, $J = 7.6$ Hz, H4 or H4''), 8.21 (1H, d, $J = 8.0$ Hz, H4 or H4''), 8.03 (1H, t, $J = 7.8$ Hz, H4'), 7.79-7.75 (1H, m, H5'').

Elem. an.: (product·2HCl) % calc. C 54.87, H 3.75, N 12.00; found C 55.25, H 4.19, N 11.94.

b)

5-Methyl-2,2':6',2''-terpyridine (0.40 g, 1.6 mmol) was dissolved in concentrated sulfuric acid (1.44 ml, 96%). While cooling in an ice bath chromium trioxide (0.50 g, 5.0 mmol, 3 eq) was added. After 1 h, when all the chromium had dissolved, the mixture was stirred for 4 h at room temperature, then it was poured over ice (5 g). The precipitate was filtered off, the solution was basified with NaOH conc, until a bright orange precipitate formed. This was filtered off and the solution was basified further to pH 5-6 when another white-greenish solid precipitated. This was filtered and dried in a desiccator. The characterisation of this compound did not succeed, but after reacting it to form the cobalt complex, it turned out to be the same as the starting material.

5-(4-Phenylbutyl)-2,2':6',2''-terpyridine (M = 365.51) (47)

For this synthesis it is important to have perfectly dry glasswares, solvents and reagents.

To a solution of diisopropylamine (0.95 ml, 6.8 mmol) in THF (3 ml) cooled to 0 °C under a nitrogen atmosphere was added *n*-BuLi (1.6 M in hexanes, 4.4 ml, 7.0 mmol), the mixture was then stirred for 1 h at 0 °C. A solution of 5-methyl-2,2':6',2''-terpyridine (1.4 g, 5.6 mmol) in THF (10 ml) was added and stirred for 1.5 h at 0 °C, followed by the addition of 1-bromo-3-phenylpropane (0.85 ml, 5.6 mmol) in THF (30 ml). The mixture was stirred at 0 °C for another hour, allowed to come to room temperature and then stirred at room temperature for 18 h. Water was added (100 ml), then the mixture was extracted with CHCl₃ (3 x 50 ml). The combined organic phases were dried over MgSO₄ and evaporated to leave a brown oily residue that was purified by column chromatography (Alox 90 standardised, CH₂Cl₂). The product is a yellowish oil that eventually solidifies to a creamy coloured solid. Yield: 0.45 g, 22.0%.

¹H-NMR (500 MHz, CDCl₃): δ / ppm 8.71 (1H, ddd, *J* = 4.8, 1.8, 0.9 Hz, T6''), 8.63 (1H, dt, *J* = 7.9, 1.0 Hz, T3''), 8.53-8.52 (2H, m, T3, T6), 8.45 (1H, dd, *J* = 7.8, 1.0 Hz, T3' or T5'), 8.43 (1H, dd, *J* = 7.8, 1.0 Hz, T3' or T5'), 7.95 (1H, t, *J* = 7.8 Hz, T4'), 7.85 (1H, td, *J* = 7.7, 1.8 Hz, T4''), 7.65 (1H, dd, *J* = 8.2, 2.1 Hz, T4), 7.32 (1H, ddd, *J* = 7.5, 4.8, 1.2 Hz, T5''), 7.30-7.26 (2H, m, P3), 7.20-7.17 (3H, m, P2, P4), 2.71 (2H, t, *J* = 7.1 Hz, A1), 2.66 (2H, t, *J* = 7.1 Hz, A4), 1.71 (4H, m, A2, A3).

¹³C-NMR (125 MHz, CDCl₃): δ / ppm 156.3, 155.2, 155.3, 153.9, 149.2, 149.1, 142.2, 138.1, 137.9, 136.9 (2C), 128.4, 128.3, 125.8, 123.8, 121.2, 120.9, 120.8, 120.7, 35.7, 32.8, 30.9, 30.7.

EI-MS: m/z 365.2 $[M]^+$, 364.2 $[M - H]^+$, 274.2 $[\text{terpy-CH}_2\text{CH}_2\text{CH}_2]^+$, 260.1 $[\text{terpy-CH}_2\text{CH}_2]^+$, 246.1 $[\text{terpy=CH}_2]^+$.

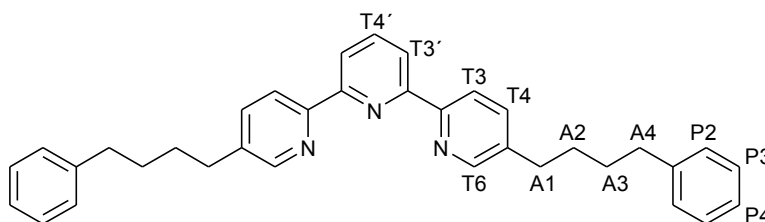
IR (solid, cm^{-1}): 3063w, 3020w, 2994w, 2929w, 2853w, 1583m, 1557m, 1485w, 1451s, 1430m, 1409m, 1383w, 1260w, 1147w, 1101m, 1078m, 1039w, 1022m, 989m, 898w, 863w, 824m, 784s, 760s, 742s, 700s, 652m, 622w, 617w.

R_f (Al_2O_3 , CH_2Cl_2): 0.60.

Elem. an.: % calc. C 82.16, H 6.34, N 11.50; found C 81.72, H 6.54, N 11.57.

m. p.: 59.2-62.8 °C.

Comment: as side product, the double substituted 5,5''-bis(4-phenylbutyl)-2,2':6',2''-terpyridine was isolated from the column chromatography.



$^1\text{H-NMR}$ (400 MHz, CDCl_3): δ / ppm 8.59-8.57 (4H, m, T3, T6), 8.47 (2H, d, $J = 7.6$ Hz, T3'), 7.98 (1H, t, $J = 7.8$ Hz, T4'), 7.73 (2H, d, $J = 8$ Hz, T4), 7.30-7.16 (10H, m, P2, P3, P4), 2.74 (4H, t, $J = 6.8$ Hz, A1), 2.67 (4H, t, $J = 6.8$ Hz, A4), 1.72 (8H, t, $J = 3.6$ Hz, A2, A3).

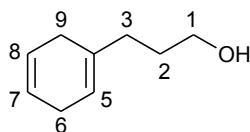
$^{13}\text{C-NMR}$ (100 MHz, CDCl_3): δ / ppm 155.1, 153.9, 149.1, 142.6, 138.7, 138.4, 137.8, 128.8, 128.7, 126.2, 121.6, 121.2, 36.1, 33.2, 31.3, 31.1.

EI-MS: m/z 497 $[M]^+$, 364 $[\text{terpy}-(\text{CH}_2)_4\text{-Ph}]^+$, 274 $[\text{terpy-CH}_2\text{CH}_2\text{CH}_3]^+$, 260 $[\text{terpy-CH}_2\text{CH}_3]^+$, 246 $[\text{terpy-CH}_3]^+$, 219, 91, 44 $[\text{CH}_3\text{CH}_2\text{CH}_3]^+$.

R_f (Al_2O_3 , CH_2Cl_2): 0.71.

Elem. an.: % calc. C 84.45, H 7.10, N 8.45; found C 84.17, H 7.19, N 8.44.

m. p.: 97.8-98.0 °C.

3-Cyclohexa-1,4-dienylpropan-1-ol (M = 138.23) (Birch reduction) (49)

The glasswares were dried in an oven for at least one night. The reaction flask was marked at the level of 300 ml for ammonia. It was fitted with a mechanical stirrer and a dry ice condenser. The overpressure of gaseous ammonia in the condenser was led into water to form ammonium hydroxide.

Gaseous ammonia was condensed on dry ice/ acetone and collected in the reaction flask under nitrogen atmosphere up to the 300 ml mark. The flask was also cooled in a dry ice/ acetone bath. Dry diethyl ether (40 ml), dry ethanol (48 ml) and 3-phenylpropanol (20.0 ml, 147 mmol) were added under nitrogen flow, then sodium (17 g, 0.74 mol) was cut into small pieces and added over 55 min under nitrogen flow. The dark blue solution was stirred at $-78\text{ }^{\circ}\text{C}$ for 3 h, then it was left to warm at room temperature with the open top to allow the evaporation of ammonia. To the white solid residue was added water (150 ml) while cooling in an ice bath.

The product was extracted with ether (3 x 50 ml), the combined organic layers dried over MgSO_4 and evaporated. Purification by column chromatography (silica gel, hexane : EtOAc 3:2, TLC coloured with KMnO_4) gave a colourless liquid. Yield: 10.46 g, 51.5 %.

$^1\text{H-NMR}$ (400 MHz, CDCl_3): δ / ppm 5.69 (2H, s, H7, H8), 5.44 (1H, s, H5), 3.62 (2H, t, $J = 6.6$ Hz, H1), 2.67-2.64 (2H, m, H6 or H9), 2.59 (2H, d, $J = 7.6$ Hz, H6 or H9), 2.02 (2H, t, $J = 7.6$ Hz, H3), 1.99 (1H, s, OH), 1.71-1.64 (2H, m, H2).

$^{13}\text{C-NMR}$ (100 MHz, CDCl_3): δ / ppm 134.4, 124.2, 124.1, 118.6, 62.6, 33.6, 30.1, 28.8, 26.6.

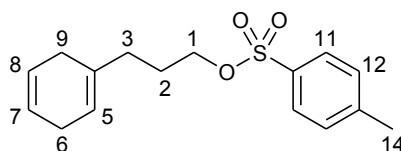
ESI-MS: m/z 196.6 $[\text{M} + \text{CH}_3\text{COOH}]^+$, 138.7 $[\text{M} + \text{H}]^+$.

IR (liquid, cm^{-1}): 3299br, 3025w, 2935m, 2876m, 2850m, 2818m, 1428m, 1169w, 1057s, 955s, 741m, 699m, 657s.

R_f (silica gel, hexane : EtOAc 3:2): 0.47.

Elem. an.: % calc. C 78.20, H 10.23, O 11.57; found C 77.15, H 10.16, O 12.70.

Toluene-4-sulfonic acid 3-cyclohexa-1,4-dienyl-propyl ester (M = 292.43) (51)



3-Cyclohexa-1,4-dienylpropan-1-ol (6.48 g, 46.9 mmol) was diluted in pyridine (35 ml) and cooled to 0 °C. To this solution was added dropwise a cold solution of *p*-toluenesulfonyl chloride (10.00 g, 52.45 mmol) in pyridine (30ml), while keeping the reaction mixture in an ice bath. After addition was complete the mixture was left to stand overnight at room temperature. Water (100 ml) and CHCl₃ (50 ml) were added and the layers separated. The aqueous phase was extracted with CHCl₃ (1 x 50 ml) then the combined organic phases were washed with sulphuric acid (22 ml H₂SO₄ in 100 ml H₂O) and water (2 x 50 ml), dried over MgSO₄ and evaporated. Purification by column chromatography (silica gel, hexane until the first fraction was eluted, then hexane : EtOAc 3:2) gave a yellow oil. Yield: 1.78 g, 13.0 %.

¹H-NMR (400 MHz, CDCl₃): δ / ppm 7.77 (2H, d, *J* = 8.8 Hz, H11 or H12), 7.33 (2H, d, *J* = 8.0 Hz, H11 or H12), 5.65 (2H, s, H7, H8), 5.28 (1H, s, H5), 4.01 (2H, t, *J* = 6.2 Hz, H1), 2.63-2.57 (2H, m, H6 or H9), 2.48 (2H, t, *J* = 8.8 Hz, H6 or H9), 2.43 (3H, s, H14), 1.96 (2H, t, *J* = 7.8 Hz, H3), 1.78-1.71 (2H, m, H2).

¹³C-NMR (100 MHz, CDCl₃): δ / ppm 144.6, 133.0, 132.8, 129.7, 127.8, 124.1, 123.9, 119.4, 70.0, 32.8, 28.6, 26.5, 26.3, 21.5.

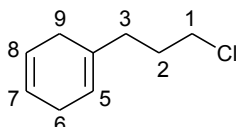
ESI-MS: *m/z* 350.4 [M + CH₃COOH]⁺, 336.1 [M + 44]⁺, 318.4 [M + 26]⁺.

IR (liquid, cm⁻¹): 3027w, 2956w, 2922w, 2880w, 2851w, 2819w, 1597w, 1494w, 1445w, 1429w, 1354s, 1306w, 1291w, 1188m, 1171s, 1096m, 1004w, 956m, 928s, 833m, 812s, 774m, 748m, 704w, 688w, 659s.

R_f (silica gel, hexane : EtOAc 3:2): 0.74.

Elem. an.: % calc. C 65.71, H 6.91, O 16.41, S 10.97; found C 64.89, H 6.76.

Comment: As a side product, 1-chloro-3-cyclohexa-1,4-dienylpropane (**52**, M = 156.67) was isolated from the column chromatography as a colourless oil in significant yield: 1.73 g, 23.4 %.



$^1\text{H-NMR}$ (400 MHz, CDCl_3): δ / ppm 5.70 (4H, s, H7, H8), 5.46 (2H, s, H5), 3.52 (4H, t, $J = 6.8$ Hz, H1), 2.71-2.66 (4H, m, H6 or H9), 2.58 (4H, t, $J = 8.8$ Hz, H6 or H9), 2.11 (4H, t, $J = 7.6$ Hz, H3), 1.92-1.85 (4H, m, H2).

$^{13}\text{C-NMR}$ (100 MHz, CDCl_3): δ / ppm 133.1, 124.1, 124.0, 119.4, 44.5, 34.3, 30.1, 28.7, 26.6.

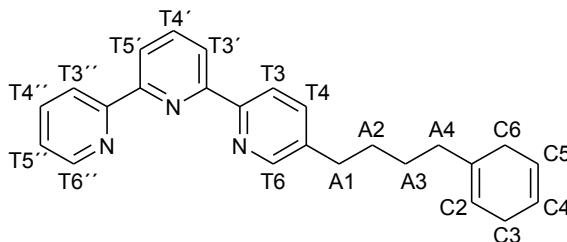
EI-MS: m/z 156 $[\text{M}]^+$, 91 $[\text{M} - 65]^+$, 79 $[\text{CH}_2\text{CHCHCH}_2\text{CHC}]^+$.

IR (liquid, cm^{-1}): 3026w, 2954w, 2879w, 2850w, 2819m, 1649w, 1496w, 1441m, 1429m, 1302w, 1288w, 956s, 891w, 866w, 817w, 771w, 743m, 716m, 700m, 652s.

R_f (silica gel, hexane): 0.40.

Elem. an.: % calc. C 68.99, H 8.38; found C 69.01, H 8.40.

5-(4-Cyclohexa-1,4-dienyl-butyl)-2,2':6',2''-terpyridine (M = 367.53) (**53**)



For this synthesis it is important to have perfectly dry glasswares, solvents and reagents.

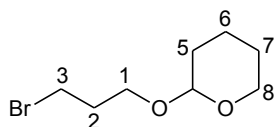
To a solution of diisopropylamine (0.75 ml, 5.3 mmol) in THF (3 ml) cooled to 0 °C under a nitrogen atmosphere was added *n*-BuLi (1.6 M in hexanes, 4.6 ml, 7.3 mmol). The mixture was then stirred for 1 h at 0 °C. A solution of 5-methyl-2,2':6',2''-terpyridine (1.1 g, 4.5 mmol) in THF (10 ml) was added and stirred for 1.5 h at 0 °C, followed by the addition of toluene-4-sulfonic acid 3-cyclohexa-1,4-dienyl-propyl ester (1.33 g, 4.55 mmol) in THF (30 ml). The mixture was stirred at 0 °C for another hour, allowed to come to room temperature and then stirred at room temperature for 2 days. Water was added (100 ml), then the mixture was extracted with CHCl₃ (3 x 50 ml). The combined organic phases were dried over MgSO₄ and evaporated to leave a brown oily residue that was purified by column chromatography (Alox 90 standardised, CH₂Cl₂). The product is a yellowish oil. Yield: 0.17 g, 10.3%.

¹H-NMR (400 MHz, CDCl₃): δ / ppm 8.71 (1H, d, *J* = 4.4 Hz, T6''), 8.64 (1H, d, *J* = 8.0 Hz, T3''), 8.55-8.53 (2H, m, T3, T6), 8.44 (2H, d, *J* = 7.6 Hz, T3', T5'), 7.96 (1H, t, *J* = 7.8 Hz, T4'), 7.87 (1H, td, *J* = 7.6, 1.7 Hz, T4''), 7.69 (1H, dd, *J* = 8.4, 2.0 Hz, T4), 7.34 (1H, ddd, *J* = 7.4, 4.6, 1.0 Hz, T5''), 5.70 (2H, s, C4, C5), 5.42 (1H, s, C2), 2.73-2.66 (4H, m, C3, C6), 2.58 (2H, d, *J* = 8.0 Hz, A1), 2.01 (2H, t, *J* = 7.6 Hz, A4), 1.71-1.64 (2H, m, A2 or A3), 1.53-1.46 (2H, m, A2 or A3).

¹³C-NMR (100 MHz, CDCl₃): δ / ppm 156.6, 155.7, 149.5, 149.3, 138.8, 138.4, 137.6, 137.4, 135.1, 128.8, 124.7, 124.2, 121.7, 121.4, 121.3, 119.0, 37.6, 33.2, 31.1, 29.3, 27.2.

R_f (Al₂O₃, CH₂Cl₂): 0.58.

2-(3-Bromopropanoxy)tetrahydropyran (M = 233.13) (58)



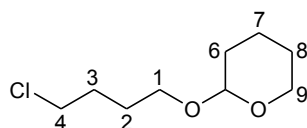
To a solution of 3-bromopropan-1-ol (15.00 g, 107.9 mmol) and dihydropyran (16.5 ml, 180 mmol) in dry ether (50 ml) was added *p*-toluic acid (225 mg,

1.62 mmol). The mixture was stirred at room temperature for about 4 h, then it was washed with saturated Na_2CO_3 (3 x 50 ml), dried over MgSO_4 and evaporated. The product is a colourless liquid that was used further without any purification. Yield: 22.50 g, 93.5%.

$^1\text{H-NMR}$ (250 MHz, CDCl_3): δ / ppm 4.51 (1H, t, H4), 3.82-3.75 (2H, m, H1), 3.46-3.34 (4H, m, H3, H8), 2.03 (2H, q, $J = 6.3$ Hz, H2), 1.80-1.41 (4H, m, H5, H6 or H7), 1.11 (2H, t, $J = 7.0$ Hz, H6 or H7).

IR (liquid, cm^{-1}): 2940m, 2868w, 1440w, 1383w, 1352w, 1323w, 1283w, 1256w, 1200m, 1184w, 1132m, 1116s, 1075m, 1028s, 982s, 965m, 868m, 815m, 769w, 650w.

2-(4-Chlorobutoxy)tetrahydropyran (M = 192.71) (59)



To a solution of 4-chlorobutan-1-ol (9.2 ml, 92 mmol) and dihydropyran (14.0 ml, 153 mmol) in dry ether (50 ml) was added *p*-toluic acid (188 mg, 1.38 mmol). The mixture was stirred at room temperature for 4 h 40 min, then it was washed with saturated Na_2CO_3 (3 x 50 ml), dried over MgSO_4 and evaporated. The product is a colourless liquid that was used further without any purification. Yield: 16.87 g, 95.2%.

$^1\text{H-NMR}$ (400 MHz, CDCl_3): δ / ppm 4.58-4.56 (1H, m, H5), 3.87-3.74 (2H, m, H1 or H9), 3.58 (2H, t, $J = 6.4$ Hz, H4), 3.53-3.39 (2H, m, H1 or H9), 1.92-1.50 (10H, m, H2, H3, H6, H7, H8).

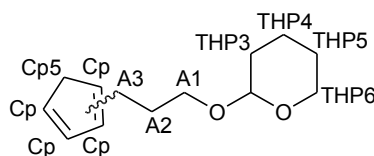
$^{13}\text{C-NMR}$ (100 MHz, CDCl_3): δ / ppm 98.8, 66.6, 62.3, 44.9, 30.7, 29.6, 27.1, 25.4, 19.6.

EI-MS: m/z 191.1 $[M]^+$, 91.0 $[Cl-CH_2CH_2CH_2CH_2]^+$, 85.1 $[O(CH_2)_5]^+$, 55.1 $[CH_2CH_2CH_2CH_2]^+$, 41.0.

IR (liquid, cm^{-1}): 2940m, 2868w, 1440w, 1352w, 1322w, 1275w, 1259w, 1199m, 1134m, 1118s, 1074s, 1032s, 1020s, 985m, 966s, 904m, 868m, 813m, 758w, 728w, 650m.

b. p.: 51 °C at 0.02 mbar.

2-[3-(1,3-Cyclopentadienyl)propoxy]tetrahydro-2H-pyran (**M** = 208.33) (**61**)



Cyclopentadiene was obtained immediately before the reaction by the thermal cracking of its dimer (distillation fitted with a Vigreux column).

Freshly distilled cyclopentadiene (11.12 g, 168.2 mmol) was diluted in freshly distilled THF (200 ml) and cooled to 0 °C under nitrogen atmosphere. *n*-BuLi (1.5 M, 113 ml, 170 mmol) was added dropwise over 40 min while the temperature was kept below 10 °C, the reaction mixture turned from colourless to clear red-brown, then turbid white. The mixture was stirred in an ice bath for 2.5 h, then a solution of 2-(3-bromopropoxy)tetrahydropyran (10.05 g, 45.04 mmol) in dry THF (100 ml) was added dropwise over 35 min. The yellow-orange mixture was left to stir in the ice bath until it melted and then overnight at room temperature, during which time the colour became red. Water was added (200 ml), then the layers were separated and the aqueous phase extracted with CH_2Cl_2 (2 x 100 ml). The combined organic layers were washed with water (2 x 100 ml) and brine (1 x 100 ml), dried over $MgSO_4$ and evaporated.

The crude product was purified by column chromatography (silica gel, hexane : diethyl ether 49:1 until the first fraction was eluted, then hexane : EtOAc 4:1), then by fractional distillation (b. p. 140 °C at 0.21 mbar). Yield: 1.88 g, 20.0 %.

$^1\text{H-NMR}$ (400 MHz, CDCl_3): δ / ppm 6.46-6.41 (3H, m, Cp), 6.25 (1H, d, $J = 5.2$ Hz, Cp), 6.17 (1H, broad s, Cp), 6.02 (1H, broad s, Cp), 4.59-4.57 (2H, m, THP2), 3.89-3.84 (2H, m, THP6 or A1), 3.80-3.74 (2H, m, THP6 or A1), 3.52-3.45 (2H, m, THP6 or A1), 3.44-3.39 (2H, m, THP6 or A1), 2.95 (2H, s, Cp5), 2.91 (4H, d, $J = 22.8$ Hz, Cp5), 2.50-2.44 (4H, m, A3), 1.88-1.83 (6H, m, A2 or THP3 or THP4 or THP5), 1.75-1.69 (2H, m, A2 or THP3 or THP4 or THP5), 1.60-1.52 (8H, m, A2 or THP3 or THP4 or THP5).

$^{13}\text{C-NMR}$ (100 MHz, CDCl_3): δ / ppm 149.7, 147.0, 135.1, 134.2, 132.8, 130.9, 126.8, 126.4, 99.3, 99.2, 67.6, 67.5, 62.8, 62.7, 43.7, 41.7, 31.2 (2C), 30.1, 29.3, 27.8, 26.9, 25.9 (2C), 20.1, 20.0.

EI-MS: m/z 208.1 $[\text{M}]^+$, 177.1, 139.1, 101.1 $[(\text{O}(\text{CH}_2)_4\text{CH})\text{O}]^+$, 41.0.

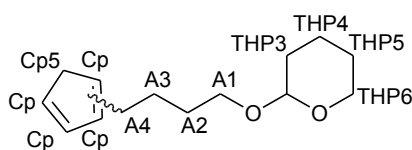
IR (liquid, cm^{-1}): 2936m, 2868w, 1717w, 1465w, 1453w, 1440w, 1381w, 1352w, 1344w, 1259w, 1199m, 1180w, 1158w, 1120s, 1074s, 1020s, 965s, 903m, 867m, 811m, 603w.

R_f (silica gel, hexane : EtOAc 4:1): 0.65.

Elem. an.: % calc. C 74.96, H 9.68; found C 72.72, H 9.68.

b. p.: 140 °C at 0.21 mbar.

2-[4-(1,3-Cyclopentadienyl)butoxy]tetrahydro-2H-pyran ($M = 222.36$) (62)



Cyclopentadiene was obtained immediately before the reaction by the thermal cracking of its dimer (distillation fitted with a Vigreux column).

Freshly distilled cyclopentadiene (6.11 g, 92.4 mmol) was diluted in freshly distilled THF (135 ml) and cooled to 0 °C under nitrogen atmosphere. *n*-BuLi (1.6 M, 61 ml, 98 mmol) was added dropwise over 25 min while the temperature was kept below 10 °C, the reaction mixture turned from colourless to clear red-brown, then turbid white. The mixture was stirred in an ice bath for 2.5 h, then a solution of 2-(4-

chlorobutoxy)tetrahydropyran (5.43 g, 28.2 mmol) in dry THF (60 ml) was added dropwise over 25 min. The mixture was heated to 45 °C for 20 h, then water was added (200 ml), the layers were separated and the aqueous phase extracted with Et₂O (2 x 100 ml). The combined organic layers were washed with brine (2 x 100 ml) and water (1 x 100 ml), dried over MgSO₄ and evaporated.

The crude product was purified by column chromatography (silica gel, hexane : diethyl ether 49:1 until the first fraction was eluted, then hexane : EtOAc 4:1) to give the product as a yellow liquid. Yield: 4.62 g, 73.7 %.

¹H-NMR (400 MHz, CDCl₃): δ / ppm 6.39-6.37 (1.5H, m, Cp), 6.18-6.16 (0.5H, m, Cp), 6.09 (0.5H, s, Cp), 5.94 (1H, s, Cp), 4.52-4.51 (6.5H, m, THP2), 3.80-3.68 (12H, m, A1 or THP6), 3.51 (6H, t, *J* = 6.4 Hz, A4), 3.45-3.33 (12H, m, A1 or THP6), 2.87 (2H, d, *J* = 1.6 Hz, Cp5), 2.81 (2H, d, *J* = 1.2 Hz, Cp5), 2.38-2.33 (3H, m, A3 or THP3), 1.86-1.44 (67H, m, THP4, THP5, A2, A3 or THP3).

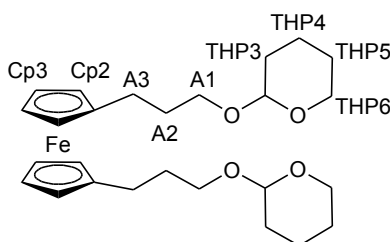
¹³C-NMR (100 MHz, CDCl₃): δ / ppm 150.0, 147.3, 135.0, 133.9, 132.7, 130.7, 126.8, 126.3, 99.1, 67.7, 66.9, 63.1, 62.6, 45.2, 41.5, 31.1, 31.1, 30.0, 27.5, 25.9, 25.8, 20.0, 19.9.

ESI-MS: *m/z* 467.3 [2M + Na]⁺, 245.3 [M + Na]⁺.

IR (liquid, cm⁻¹): 2938m, 2866m, 1452w, 1440w, 1352w, 1274w, 1282w, 1260w, 1200m, 1184w, 1135m, 1118s, 1075m, 1031s, 1020s, 985m, 904m, 867m, 813m, 724w, 649w.

R_f (silica gel, hexane : EtOAc 4:1): 0.59.

1,1'-Bis[3(2-pyranoxy)propyl]ferrocene (M = 470.49) (63)



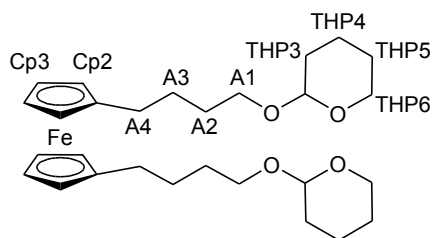
Anhydrous FeCl_2 (2.10 g, 16.5 mmol) was suspended in freshly distilled THF (10 ml) under nitrogen atmosphere. 2-[3-(1,3-Cyclopentadienyl)propoxy]tetrahydro-2*H*-pyran (6.96 g, 33.4 mmol) was mixed with diisopropylamine (9.3 ml, 66 mmol) and added to the suspension while cooling in an ice bath. The reaction mixture was heated to 70 °C for 20 h. After cooling to room temperature CH_2Cl_2 was added (100 ml). After washing with water (50 ml) the mixture could be separated into two small aqueous and organic phases and a large volume of emulsion. The emulsion was extracted with more CH_2Cl_2 (2 x 50 ml), then the combined organic layers were washed with water (2 x 50 ml) dried over MgSO_4 and evaporated to yield a yellow-brown oil.

The crude product was purified by column chromatography (silica gel, hexane : EtOAc 4:1). Yield: 5.52 g, 71.1 %.

$^1\text{H-NMR}$ (250 MHz, CDCl_3): δ / ppm 4.57 (1H, broad s, THP2), 3.97 (1.2H, s, Cp2 and Cp3), 3.89-3.70 (2H, m, THP6 or A1), 3.52-3.34 (2H, m, THP6 or A1), 2.42-2.36 (1H, m, THP3), 1.83-1.47 (9H, m, THP3, THP5, THP4, A3, A2).

R_f (silica gel, hexane : EtOAc 4:1): 0.53.

1,1'-Bis[4-(2-pyranoxy)butyl]ferrocene (M = 498.55) (64)



Anhydrous FeCl_2 (1.65 g, 13.0 mmol) was suspended in freshly distilled THF (10 ml) under nitrogen atmosphere. 2-[4-(1,3-Cyclopentadienyl)butoxy]tetrahydro-2*H*-pyran (5.89 g, 26.5 mmol) was mixed with di-isopropylamine (7.5 ml, 53 mmol) and added to the suspension while cooling in an ice bath. The reaction mixture was heated to 70 °C for about 7.5 h then stirred at room temperature overnight. To the mixture was added water (50 ml) and CH_2Cl_2 (50 ml). and the layers were separated without any

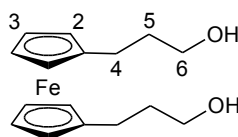
shaking. The aqueous phase was extracted with CH_2Cl_2 (2 x 50 ml, with only light shaking). The combined organic layers were washed with water (50 ml), dried over MgSO_4 and evaporated to yield a yellow-brown oil. The crude product was purified by column chromatography (silica gel, hexane : EtOAc 4:1). Yield: 4.94 g, 76.2 %.

$^1\text{H-NMR}$ (400 MHz, CDCl_3): δ / ppm 4.58-4.56 (1H, m, THP2), 3.96 (1H, s, Cp2 and Cp3), 3.87-3.71 (2H, m, A1 or THP6), 3.58 (1H, t, $J = 6.4$ Hz, A4), 3.51-3.35 (2H, m, A1 or THP6), 1.92-1.52 (10H, m, A2, A3, THP3, THP4, THP5).

$^{13}\text{C-NMR}$ (100 MHz, CDCl_3): δ / ppm 99.3, 68.1, 67.8, 67.0, 62.7, 45.4, 31.1, 30.1, 27.5, 25.9, 20.1.

R_f (silica gel, hexane : EtOAc 4:1): 0.49.

1,1'-Bis(3-hydroxypropyl)ferrocene (M = 302.23) (65) [66]

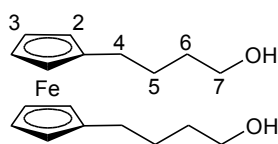


1,1'-Bis[3(2-pyranoxy)propyl]ferrocene (5.52 g, 11.7 mmol) was dissolved in ethanol (100 ml) and phosphoric acid was added (85%, 2 ml). The mixture was refluxed for 15 h, then ethanol was evaporated and the residue redissolved in ether (100 ml). After washing with water (3 x 50 ml), the ether phase was dried over MgSO_4 and evaporated. The crude product was purified by column chromatography (silica gel, CH_2Cl_2 : EtOAc 1:1). Yield: 1.34 g, 37.9%. This yield was not reproducible, so that other methods for the deprotection were tried on other compounds.

$^1\text{H-NMR}$ (400 MHz, CDCl_3): δ / ppm 4.12 (4H, s, H2, H3), 3.67 (2H, t, $J = 6.0$ Hz, H6), 2.35 (2H, t, $J = 6.8$ Hz, H4), 1.75 (2H, broad s, H5), 1.62 (1H, s, OH).

$^{13}\text{C-NMR}$ (100 MHz, CDCl_3): δ / ppm 90.1, 69.9, 69.1, 63.0, 34.4, 26.0.

R_f (silica gel, CH_2Cl_2 : EtOAc 1:1): 0.23.

1,1'-Bis(4-hydroxybutyl)ferrocene (M = 330.29) (66)

a) The method followed that in the literature. [66]

1,1'-Bis[4-(2-pyranoxy)butyl]ferrocene (6.86 g, 13.8 mmol) was dissolved in ethanol (100 ml) and phosphoric acid was added (85%, 2 ml). The mixture was refluxed for 10.5 h, then ethanol was evaporated and the residue redissolved in ether (100 ml). After washing with water (3 x 50 ml), the ether phase was dried over MgSO_4 and evaporated. The crude product was purified by column chromatography (silica gel, CH_2Cl_2 : EtOAc 1:1). Yield: 1.03 g, 22.6%. This yield was not reproducible, so that other methods for the deprotection were tried.

b)

1,1'-Bis[4-(2-pyranoxy)butyl]ferrocene (4.99 g, 10.0 mmol) was dissolved in THF (15 ml). A mixture of acetic acid (98%, 28 ml) and water (7 ml) was added and the reaction mixture was stirred at 45 °C overnight. In the morning a TLC analysis revealed that significant starting material remained and so another portion of acetic acid (98%, 28 ml) in water (7 ml) and THF (15 ml) was added, and the mixture stirred at 45 °C for another 2 h. After cooling to room temperature the mixture was neutralized with potassium carbonate, then water (50 ml) and ether (50 ml) were added and the layers separated. The aqueous phase was extracted once with ether (50 ml), then the combined organic layers were washed with saturated NaHCO_3 (50 ml) and water (50 ml), dried over MgSO_4 and evaporated. The dark yellow oily residue was purified by column chromatography (silica gel, EtOAc : hexane 1:1). Yield: 0.14 g, 4.2%.

c)

1,1'-Bis[4-(2-pyranoxy)butyl]ferrocene (3.0 g, 6.0 mmol) and PPTS (0.30 g, 1.2 mmol) were dissolved in EtOH (60 ml) and heated to 55 °C for 1.5 h. The solvent was evaporated and the crude product was purified by column chromatography (silica gel, EtOAc : hexane 1:1). Yield: 0.85 g, 42.9 %.

¹H-NMR (400 MHz, CDCl₃): δ / ppm 4.04 (4H, s, H2, H3), 3.63 (2H, t, *J* = 6.2 Hz, H7), 2.31 (2H, t, *J* = 6.8 Hz, H4), 1.73 (1H, s, OH), 1.60-1.48 (4H, m, H5, H6).

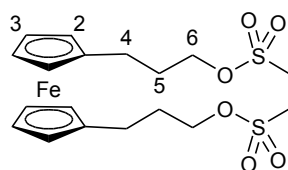
¹³C-NMR (100 MHz, CDCl₃): δ / ppm 90.1, 69.7, 68.6, 63.2, 33.0, 29.6, 27.8.

R_f (silica gel, CH₂Cl₂ : EtOAc 1:1): 0.24.

Pyridinium *p*-toluenesulfonate (PPTS) (M = 251.33) [112]

p-Toluenesulfonic acid monohydrate (5.73 g, 30.1 mmol) was added to pyridine (12.1 ml, 150 mmol) and stirred at room temperature for 20 min. Excess pyridine was evaporated under vacuum, and the residue recrystallised from acetone to give white crystals. Yield: 5.11 g, 67.5%.

1,1'-Bis(3-(methylsulfonyloxy)propyl)ferrocene (M = 458.43) (67)



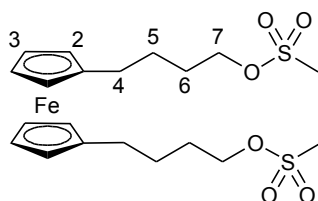
1,1'-Bis(3-hydroxypropyl)ferrocene (1.87 g, 6.19 mmol) was dissolved in CH₂Cl₂ (60 ml) and dry triethylamine (2.5 ml, 18 mmol) and cooled to 0 °C.

Methanesulfonylchloride (1.1 ml, 14 mmol) was added, then the reaction mixture was stirred at room temperature for 2 h. The mixture was washed with ice water, followed by 10% HCl, saturated sodium bicarbonate solution and brine (each 1 x 75 ml). The organic phase was dried over MgSO₄ and evaporated to give a yellow oily product. Yield: 2.70 g, 95.1%. The product did not need further purification.

$^1\text{H-NMR}$ (400 MHz, CDCl_3): δ / ppm 4.22 (2H, t, $J = 6.0$ Hz, H6), 4.03 (4H, d, $J = 6.8$ Hz, H2 and H3), 3.01 (3H, s, CH_3), 2.44 (2H, t, $J = 7.2$ Hz, H4), 1.96-1.89 (2H, m, H5).

$^{13}\text{C-NMR}$ (100 MHz, CDCl_3): δ / ppm 87.6, 69.9, 69.4, 68.8, 37.8, 31.1, 25.7.

1,1'-Bis(4-(methylsulfonyloxy)butyl)ferrocene (M = 486.49) (68)

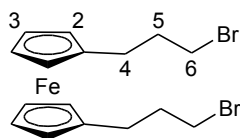


1,1'-Bis(4-hydroxybutyl)ferrocene (1.26 g, 3.81 mmol) was dissolved in CH_2Cl_2 (38 ml) and dry triethylamine (1.6 ml, 11 mmol) and cooled to 0°C .

Methanesulfonylchloride (0.65 ml, 8.4 mmol) was added, then the reaction mixture was stirred at room temperature for 3 h. The mixture was washed with ice water (50 ml), followed by HCl (10%, 50 ml), saturated sodium bicarbonate solution (50 ml) and brine (50 ml). The organic phase was dried over MgSO_4 and evaporated to give a yellow oily product. Yield: 1.74 g, 93.9%. The product did not need further purification.

$^1\text{H-NMR}$ (400 MHz, CDCl_3): δ / ppm 4.20 (2H, t, $J = 5.8$ Hz, H7), 4.06 (4H, broad s, H2 and H3), 3.00 (3H, s, CH_3), 2.31 (2H, broad s, H4), 1.76 (2H, broad s, H5 or H6), 1.58 (2H, broad s, H5 or H6).

$^{13}\text{C-NMR}$ (100 MHz, CDCl_3): δ / ppm 70.4, 66.7, 37.9, 29.3, 27.5.

1,1'-Bis(3-bromopropyl)ferrocene (M = 428.01) (70)

1,1'-Bis(3-(methylsulfonyloxy)propyl)ferrocene (2.33 g, 5.08 mmol) was dissolved in acetone (50 ml), LiBr (1.75 g, 20.1 mmol) was added and the solution was refluxed for 17 h. A precipitate started to form almost immediately upon heating, but the mixture was nevertheless left to reflux overnight. The mixture was then poured over ice (200 ml) and extracted with ether (3 x 75 ml). The organic phase was dried over MgSO₄ and evaporated to yield a yellow oil that was used for the next step without purification. Yield: 1.89 g, 86.9%.

A sample was purified by column chromatography for better characterisation (silica gel, hexane : EtOAc 10:1).

¹H-NMR (250 MHz, CDCl₃): δ / ppm 4.06 (4H, s, H2, H3), 3.41 (2H, t, *J* = 6.2 Hz, H6), 2.46 (2H, t, *J* = 6.6 Hz, H4), 2.05-2.00 (2H, m, H5).

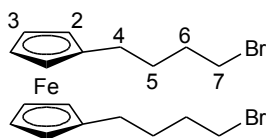
¹³C-NMR (100 MHz, CDCl₃): δ / ppm 71.1, 70.4, 33.9, 33.6, 27.7.

EI-MS: *m/z* 427.8 [M]⁺, 345.8 [Fe(Cp-(CH₂)₃-Br)(Cp-(CH₂)₃)]⁺, 188.0 [Cp-(CH₂)₃-Br + 2H]⁺, 160.9, 134.9, 105.0, 91.0, 79.0.

IR (liquid, cm⁻¹): 3084w, 2928m, 2844w, 1648w br, 1470w, 1433m, 1344w, 1321w, 1271m, 1250s, 1227m, 1203m, 1112w, 957w, 924m, 906w, 856m, 823s, 806s, 765m, 718w, 640m.

UV/Vis (CHCl₃): λ_{max}, nm (ε_{max}, M⁻¹cm⁻¹): 276 (1601), 279 (1543), 282 (1497), 467 (168).

R_f (silica gel, hexane : EtOAc 10:1): 0.61.

1,1'-Bis(4-bromobutyl)ferrocene (M = 456.07) (71)

1,1'-Bis(4-(methylsulfonyloxy)butyl)ferrocene (0.96 g, 1.9 mmol) was dissolved in acetone (20 ml), LiBr (0.66 g, 7.6 mmol) was added and the solution was refluxed for 3 h. The mixture was then poured over ice (100 ml) and extracted with ether (2 x 30 ml). The organic phase was dried over MgSO₄ and evaporated to yield a yellow-brown oil that was purified by column chromatography (silica gel, hexane : EtOAc 10:1). Yield: 0.60 g, 69.2%.

¹H-NMR (400 MHz, CDCl₃): δ / ppm 4.00 (4H, d, *J* = 6.0 Hz, H2, H3), 3.41 (2H, t, *J* = 6.6 Hz, H7), 2.34 (2H, t, *J* = 7.2 Hz, H4), 1.92-1.85 (2H, m, H5 or H6), 1.68-1.60 (2H, m, H5 or H6).

¹³C-NMR (100 MHz, CDCl₃): δ / ppm 89.1, 69.2, 68.5, 34.2, 32.9, 30.1, 28.9.

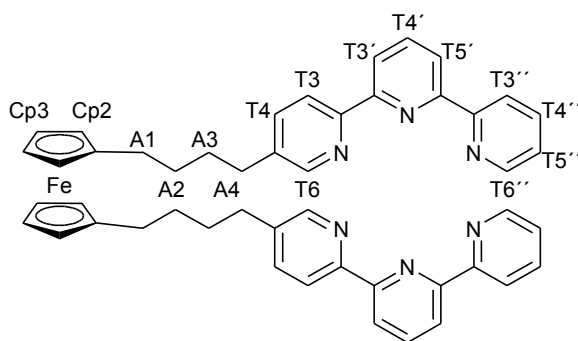
EI-MS: *m/z* 456 [M]⁺.

IR (liquid, cm⁻¹): 3084w, 2928m, 2853m, 1634w br, 1455m, 1435m, 1394w, 1354w, 1323w, 1284m, 1244m, 1038m, 1021m, 920w, 822s, 805s, 768m, 735m, 644m.

UV/Vis (CHCl₃): λ_{max}, nm (ε_{max}, M⁻¹cm⁻¹): 282 (2148), 469 (290).

R_f (silica gel, hexane : EtOAc 10:1): 0.60.

Elem. an.: % calc. C 47.41, H 5.30, found C 48.26, H 5.51.

1,1'-Bis(4-(2,2':6',2''-terpyridin-5-yl)butyl)ferrocene (M = 760.83) (69)

For this synthesis it is important to have perfectly dry glasswares, solvents and reagents.

To a solution of diisopropylamine (1.2 ml, 8.4 mmol) in THF (3 ml) cooled to 0 °C under a nitrogen atmosphere was added *n*-BuLi (1.6 M in hexanes, 5.2 ml, 8.4 mmol), the mixture was then stirred for 45 min at 0 °C. A solution of 5-methyl-2,2':6',2''-terpyridine (1.7 g, 6.9 mmol) in THF (10 ml) was added and stirred for 3.5 h at 0 °C, followed by the addition of 1,1'-bis(3-bromopropyl)ferrocene (1.5 g, 3.5 mmol) in THF (18 ml). The mixture was allowed to warm to room temperature and then stirred at room temperature for 2 days. Water was added (50 ml), then the mixture was extracted with ether (3 x 50 ml). The combined organic phases were dried over MgSO₄ and evaporated to leave a golden yellow oily residue that was purified with column chromatographies (first column: Alox 90 standardised, CH₂Cl₂ until the fraction with R_f = 0.42 was eluted fully, then CH₂Cl₂ : EtOAc 5:1. The product with R_f = 0.07 on Alox, CH₂Cl₂ was purified with a second column : Alox 90 standardised, hexane : EtOAc 3:1). The product is a yellow-orange solid. Yield: 0.32 g, 12.1%.

¹H-NMR (400 MHz, CDCl₃): δ / ppm 8.69 (1H, d, *J* = 4.0 Hz, T6''), 8.61 (1H, dd, *J* = 8.2, 1.0 Hz, T3''), 8.52-8.51 (2H, m, T6, T3), 8.42 (1H, dd, *J* = 7.8, 1.0 Hz, T3'), 8.41 (1H, d, *J* = 7.6 Hz, T5'), 7.93 (1H, t, *J* = 7.8 Hz, T4'), 7.84 (1H, td, *J* = 7.9, 1.5 Hz, T4''), 7.65 (1H, dd, *J* = 8.0, 2.0 Hz, T4), 7.32 (1H, ddd, *J* = 7.5, 5.1, 1.3 Hz, T5''),

3.96 (4H, d, $J = 8.4$ Hz, Cp2, Cp3), 2.68 (2H, t, $J = 7.6$ Hz, A4 or A1), 2.35 (2H, t, $J = 7.4$ Hz, A4 or A1), 1.72-1.65 (2H, m, A2 or A3), 1.59-1.51 (2H, m, A2 or A3).

^{13}C -NMR (100 MHz, CDCl_3): δ / ppm 156.2, 155.3, 155.2, 153.9, 149.1, 149.0, 138.1, 137.8, 136.8, 136.7, 123.7, 121.1, 120.8, 120.7, 120.6, 68.7, 67.8, 32.7, 30.9, 30.8, 29.2.

ESI-MS: m/z 783.5 $[\text{FeL}_2 + \text{Na}]^+$, 760.3 $[\text{FeL}_2 + \text{H}]^+$, 729.5, 656.5, 467.4 $[\text{L} + \text{CH}_2\text{Cl}_2 + \text{CH}_3\text{OH} + \text{H}]^+$, 412.6 $[\text{FeL}_2 + 2\text{CH}_3\text{OH}]^{2+}$, 385.1 $[\text{L} + \text{CH}_3\text{OH} + 3\text{H}]^{2+}$.

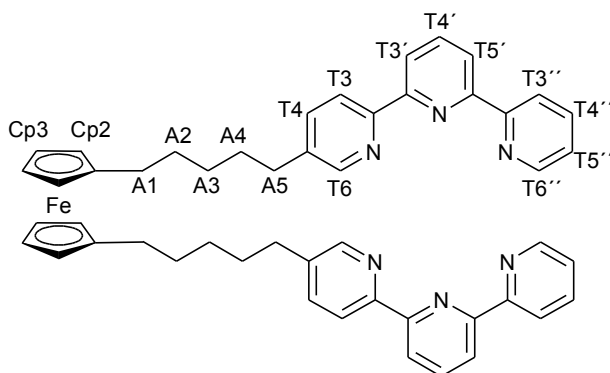
IR (solid, cm^{-1}): 3063w, 2928m, 2850w, 1582m, 1557s, 1451m, 1427s, 1393m, 1264w, 1145w, 1131w, 1100m, 1075w, 1037m, 1019m, 990m, 855w, 823s, 813s, 786s, 770s, 703w, 650m, 619m, 601s.

UV/Vis (CHCl_3): λ_{max} , nm (ϵ_{max} , $\text{M}^{-1}\text{cm}^{-1}$): 292 (43894), 299 (34887), 302 (40165).

R_f (Al_2O_3 , hexane : EtOAc 3:1): 0.30.

m. p.: 132.2-138.1 $^\circ\text{C}$.

1,1'-Bis(5-(2,2':6',2''-terpyridin-5-yl)pentyl)ferrocene (M = 788.89) (72)



For this synthesis it is important to have perfectly dry glasswares, solvents and reagents.

To a solution of lithium diisopropylamide (2 M, 0.7 ml, 1.4 mmol) cooled to 0 $^\circ\text{C}$ under a nitrogen atmosphere was added a solution of 5-methyl-2,2':6',2''-terpyridine (0.29 g, 1.2 mmol) in THF (8 ml) and the mixture was stirred for 1 h at 0 $^\circ\text{C}$. 1,1'-Bis(4-bromobutyl)ferrocene (0.27 g, 0.59 mmol) in THF (4 ml) was added, and the mixture was heated to 50 $^\circ\text{C}$ overnight. After cooling to room temperature water was

added (50 ml), and the organic solvent evaporated. The residual water suspension was extracted with CH_2Cl_2 (2 x 50 ml), the combined organic phases were dried over MgSO_4 and evaporated to leave a golden yellow oily residue that was purified by column chromatography (Alox 90 standardised, hexane : EtOAc 3:1). The product is a yellow oil. Yield: 20.4 mg, 4.4%.

$^1\text{H-NMR}$ (400 MHz, CDCl_3): δ / ppm 8.69 (1H, dt, $J = 4.0, 1.0$ Hz, T6''), 8.61 (1H, dt, $J = 8.0, 1.0$ Hz, T3'), 8.53-8.51 (2H, m, T6, T3), 8.43 (1H, dd, $J = 7.6, 0.8$ Hz, T3'), 8.42 (1H, dd, $J = 7.8, 1.4$ Hz, T5'), 7.94 (1H, t, $J = 7.8$ Hz, T4'), 7.85 (1H, td, $J = 7.7, 1.9$ Hz, T4''), 7.65 (1H, dd, $J = 8.4, 2.4$ Hz, T4), 7.32 (1H, ddd, $J = 7.3, 4.7, 1.3$ Hz, T5''), 3.97-3.94 (4H, m, Cp2, Cp3), 2.67 (2H, t, $J = 7.6$ Hz, A1 or A5), 2.31 (2H, t, $J = 7.6$ Hz, A1 or A5), 1.67 (2H, q, $J = 7.7$ Hz, A2 or A4), 1.53 (2H, q, $J = 7.6$ Hz, A2 or A4), 1.39 (2H, q, $J = 7.4$ Hz, A3).

$^{13}\text{C-NMR}$ (100 MHz, CDCl_3): δ / ppm 156.2, 155.3, 155.2, 153.8, 149.1, 149.0, 138.2, 137.8, 136.8 (2C), 123.7, 121.1, 120.8, 120.7, 120.6, 88.9, 68.6, 67.7, 32.8, 31.1, 31.0, 29.3, 29.0.

EI-MS: m/z 788.4 [FeL_2]⁺, 422.2 [FeL]⁺.

IR (solid, cm^{-1}): 3070w, 3011w, 2926m, 2852w, 1581m, 1575m, 1557s, 1485w, 1470m, 1451s, 1428s, 1393m, 1323w, 1298w, 1262m, 1223w, 1145w, 1133w, 1101m, 1077m, 1038m, 1022m, 990m, 924w, 893w, 864w, 826m, 784s, 760s, 703w, 651m, 622m.

UV/Vis (CHCl_3): λ_{max} , nm (ϵ_{max} , $\text{M}^{-1}\text{cm}^{-1}$): 282 (46811), 373 (1884), 475 (4347), 523 (1184).

R_f (Al_2O_3 , hexane : EtOAc 3:1): 0.33.

m. p.: 91.4-96.9 °C.

2-Amino-5-iodopyridine (M = 220.02) (79) [116]

2-Aminopyridine (47.16 g, 0.5011 mol), periodic acid dehydrate (22.84 g, 0.1002 mol), and iodine (51.00 g, 0.2009 mol) were added to a mixture of acetic acid (98%, 300 ml), water (60 ml) and sulfuric acid (*conc.*, 9 ml) and heated to 80 °C for

4 h. After that the reaction mixture was poured over aqueous sodium thiosulfate (200 ml) and then extracted with ether (2 x 200 ml). The combined ether layers were washed once more with aqueous Na₂S₂O₃ then with aqueous NaOH. The organic phase was dried over MgSO₄ and evaporated to yield a yellow-orange solid. The residue was purified by column chromatography (silica gel, hexane : EtOAc 2:1 until the first fraction was eluted, then EtOAc) and then recrystallised from ethanol to give white flakes. Yield: 5.35 g, 4.9%.

The aqueous phase remaining from after the extraction was treated with NaOH, which caused the precipitation of a white compound. It was extracted with CH₂Cl₂, the organic layer was dried over MgSO₄ and evaporated to yield a pale yellow solid that was used for the next step without purification. Overall yield: 63.39 g, 57.5%.

¹H-NMR (250 MHz, CDCl₃): δ / ppm 8.20 (1H, d, *J* = 2.3 Hz, H6), 7.61 (1H, dd, *J* = 8.5, 2.3 Hz, H4), 6.34 (1H, d, *J* = 8.5 Hz, H3), 4.52 (2H, broad s, NH₂).

¹³C-NMR (100 MHz, CDCl₃): δ / ppm 157.2, 153.5, 145.3, 110.9, 77.7.

ESI-MS: *m/z* 261.6 [M + CH₃CN]⁺, 221.1 [M + H]⁺.

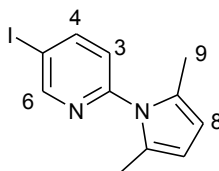
IR (solid, cm⁻¹): 3385w, 3295w, 3134w, 1634m, 1580w, 1547m, 1480m, 1379m, 1256w, 1140w, 923w, 819s, 613s.

R_f (silica gel, hexane : EtOAc 2:1): 0.22.

Elem. an.: % calc. C 27.30, H 2.29, N 12.73, found C 27.17, H 2.17, N 12.48.

m. p.: 130.7-132.0 °C.

1-(5-Iodopyridin-2-yl)-2,5-dimethyl-1*H*-pyrrole (M = 298.14) (80) [115]



2-Amino-5-iodopyridine (51.71 g, 0.2350 mol), 2,5-hexanedione (33 ml, 0.28 mol) and *p*-toluenesulfonic acid monohydrate (0.32 g, 1.7 mmol) were dissolved in toluene

(200 ml) and heated in a Dean-Stark apparatus at 115 °C overnight. After cooling, the reaction mixture was washed with NaHCO₃ sat. (200 ml), water (4 x 100 ml) and NaCl sat. (100 ml). After drying over MgSO₄, the organic phase was evaporated to yield a light brown solid. Yield: 64.19 g, 91.6%.

The product was used for the next step without purification. An analytically pure sample was obtained after column chromatography (silica gel, hexane : EtOAc 1:1) and recrystallisation from hexane and activated charcoal to give yellow needles.

¹H-NMR (250 MHz, CDCl₃): δ / ppm 8.81 (1H, d, *J* = 2.4 Hz, H6), 8.11 (1H, dd, *J* = 8.3, 2.3 Hz, H4), 7.03 (1H, dd, *J* = 10.9, 0.6 Hz, H3), 5.91 (2H, s, CCH), 2.14 (6H, s, CH₃).

¹³C-NMR (100 MHz, CDCl₃): δ / ppm 155.4, 151.1, 146.1, 128.5, 123.5, 107.4, 90.9, 13.2.

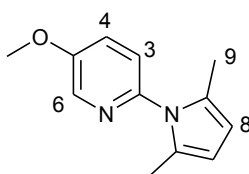
ESI-MS: *m/z* 299.2 [M + H]⁺.

R_f (silica gel, hexane : EtOAc 1:1): 0.90.

Elem. an.: % calc. C 44.32, H 3.72, N 9.40, found C 44.33, H 3.72, N 9.35.

m. p.: 120.5-121.2 °C.

1-(5-Methoxypyridin-2-yl)-2,5-dimethyl-1*H*-pyrrole (M = 202.28) (81) [115]



Metallic sodium (6.6 g, 0.29 mol) was added slowly to dry methanol (100 ml), then a solution of 1-(5-iodopyridin-2-yl)-2,5-dimethyl-1*H*-pyrrole (27 g, 90 mmol) in dry DMF (70 ml) was added to the sodium methoxide solution. A precipitate formed immediately. Copper(I) chloride (1.35 g, 13.6 mmol) was added and the reaction mixture was heated to 80 °C overnight. After cooling to room temperature the reaction was quenched with diethyl ether (180 ml), aqueous NH₄Cl (5%, 100 ml) and

water (125 ml). After stirring for 1 h at room temperature the mixture was filtered over celite and the filtrate extracted with CH_2Cl_2 (1 x 300 ml, then 4 x 100 ml). The combined organic layers were washed with NH_3 (10%, 3 x 300 ml), filtered through silica gel, dried over MgSO_4 , and evaporated to give a brown solid. Yield: 16.02 g, 88.0%.

The product was used for the next step without purification. An analytically pure sample was obtained after column chromatography (silica gel, hexane : EtOAc 1:1) and recrystallisation from hexane to give a brown solid.

$^1\text{H-NMR}$ (400 MHz, CDCl_3): δ / ppm 8.28 (1H, d, $J = 2.8$ Hz, H6), 7.34 (1H, dd, $J = 8.6, 3.0$ Hz, H3), 7.17 (1H, d, $J = 8.8$ Hz, H4), 5.88 (2H, s, CCH), 3.93 (3H, s, OCH_3), 2.09 (6H, s, CH_3).

$^{13}\text{C-NMR}$ (100 MHz, CDCl_3): δ / ppm 154.7, 144.8, 136.0, 128.7, 122.7, 122.4, 106.3, 55.9, 12.9.

ESI-MS: m/z 203.3 $[\text{M}+\text{H}]^+$.

R_f (silica gel, hexane : EtOAc 1:1): 0.65

Elem. an.: % calc. C 71.26, H 6.98, N 13.85, O 7.91; found C 71.32, H 6.94, N 13.88, O 7.79.

m. p.: 72-73 °C.

2-Amino-5-methoxypyridine (M = 124.16) (82) [115]

A solution of 1-(5-methoxypyridin-2-yl)-2,5-dimethyl-1*H*-pyrrole (14.25 g, 70.45 mmol) in ethanol (120 ml), a solution of hydroxylamine hydrochloride (48.66 g, 700.2 mmol) in water (60 ml), and triethylamine (19.7 ml, 140 mmol) were mixed and heated to reflux for 16 h. After cooling to room temperature the reaction mixture was treated with cold HCl (*conc.*, 200 ml), which caused the formation of a precipitate. The suspension was washed with Et_2O , then basified to pH 9-10 with aqueous NaOH which redissolved the precipitate. The resulting mixture was extracted several times with CH_2Cl_2 , the combined organic layers dried over MgSO_4 , and

evaporated. The resulting brown oil was purified by distillation to yield the product as a pale yellow oil (b. p. 114-120 °C at 0.16 mbar). Yield: 6.12 g, 70.0%.

¹H-NMR (400 MHz, CDCl₃): δ / ppm 7.75 (1H, d, *J* = 2.8 Hz, H6), 7.08 (1H, dd, *J* = 9.0, 3.0 Hz, H4), 6.47 (1H, d, *J* = 8.4 Hz, H3), 4.32 (2H, broad s, NH₂), 3.76 (3H, s, OCH₃).

¹³C-NMR (100 MHz, CDCl₃): δ / ppm 152.9, 149.4, 132.7, 125.9, 109.5, 56.3.

ESI-MS: *m/z* 125.3 [M + H]⁺.

b. p.: 114-120 °C at 0.16 mbar.

2-Bromo-5-methoxypyridine (M = 188.03) (83) [117]

2-Amino-5-methoxypyridine (6 g, 50 mmol) was dissolved in HBr (62%, 62 ml) and cooled to -10 °C in an ice-salt bath. Bromine (6.2 ml, 120 mmol) was added dropwise while keeping the temperature between -10 and -5 °C. The bromine fumes that formed during the reaction were led into a sodium thiosulfate solution to be absorbed. To the yellow turbid reaction mixture was then added very slowly a solution of NaNO₂ (8.3 g, 120 mmol) in water (16 ml) while the temperature was kept below 0 °C. After the addition was complete, the mixture was allowed to warm to room temperature, stirred for 30 min, then it was cooled to 0 °C again. A solution of NaOH (48.06 g, 1.201 mol) in water (45 ml) was slowly added to the reaction mixture, causing an exothermic reaction and forming a white turbid solution with insoluble brown droplets. After cooling, the mixture was extracted with ether (3 x 100 ml), the combined organic layers dried over MgSO₄ and the solvent evaporated to give an orange oil. Yield: 6.31 g, 67.1%.

The product was used for the next step without purification. An analytically pure yellow oil was obtained after column chromatography (silica gel, CH₂Cl₂ : EtOAc 85:15).

¹H-NMR (400 MHz, CDCl₃): δ / ppm 8.05 (1H, d, *J* = 3.2 Hz, H6), 7.36 (1H, d, *J* = 13.2 Hz, H3), 7.09 (1H, dd, *J* = 8.6, 3.0 Hz, H4), 3.84 (3H, s, OCH₃).

^{13}C -NMR (100 MHz, CDCl_3): δ / ppm 155.4, 136.9, 132.0, 128.1, 124.3, 55.9.

R_f (silica gel, CH_2Cl_2 : EtOAc 85:15): 0.68.

Elem. an.: % calc. C 38.33, H 3.22, N 7.45, O 8.51; found C 36.23, H 3.08, N 7.51, O 12.57.

2-Acetyl-5-methoxypyridine (M = 151.18) (84)

2-Bromo-5-methoxypyridine (6.0 g, 32 mmol) was dissolved in dry diethyl ether and cooled to $-78\text{ }^\circ\text{C}$. $n\text{-BuLi}$ (1.6 M in hexanes, 22 ml, 35 mmol) was added dropwise, then the resulting brown-red mixture was stirred at $-78\text{ }^\circ\text{C}$ for 25 min. A solution of N,N -dimethylacetamide (3.4 ml, 37 mmol) in dry ether (5 ml) was added dropwise, the mixture was stirred for another hour at $-78\text{ }^\circ\text{C}$, then it was left to warm to room temperature overnight. After addition of water (10 ml) and separation of the layers, the aqueous phase was extracted with EtOAc (3 x 30 ml). The combined organic layers were washed with brine (100 ml), dried over MgSO_4 and evaporated. The brown liquid residue was purified by column chromatography (silica gel, CH_2Cl_2 : EtOAc 85:15) to give a yellow oil. Yield: 1.95 g, 40.3%.

^1H -NMR (400 MHz, CDCl_3): δ / ppm 8.32 (1H, d, $J = 2.8$ Hz, H6), 8.04 (1H, d, $J = 8.4$ Hz, H3), 7.25 (1H, dd, $J = 9.0, 2.6$ Hz, H4), 3.92 (3H, s, OCH_3), 2.67 (3H, s, CH_3).

^{13}C -NMR (100 MHz, CDCl_3): δ / ppm 199.4, 158.8, 147.3, 137.3, 123.7, 120.2, 56.2, 26.1.

ESI-MS: m/z 152.2 $[\text{M} + \text{H}]^+$.

R_f (silica gel, CH_2Cl_2 : EtOAc 85:15): 0.67.

Attempt at 5-methoxy-2,2':6',2''-terpyridine (M = 263.32) (85)

To a solution of 2-acetyl-5-methoxypyridine (1.95 g, 12.9 mmol) in freshly distilled THF (15 ml) at $0\text{ }^\circ\text{C}$ under a nitrogen atmosphere was added a solution of potassium tert-butoxide (3.33 g, 29.7 mmol) in cold, dry THF (65 ml). The mixture was stirred for 3 h while cooling in an ice bath, then a solution of 2-(3'-(N,N -dimethylamino)-

1'-oxoprop-2'-en-1'-yl)pyridine (2.30 g, 13.1 mmol) in dry THF (30 ml) was added and the mixture was allowed to come to room temperature. After stirring overnight, a mixture of ammonium acetate (10.06 g, 130.1 mmol) and acetic acid (98%, 20 ml) was added and the reaction mixture was heated to reflux for 2 h. The THF was evaporated and water (100 ml) was added to the residue, followed by aqueous NaOH until pH 9-10 was reached. The mixture was extracted with CH₂Cl₂ (3 x 100 ml), the organic layers were dried over MgSO₄ and the solvent evaporated to yield a brown-black residue that was purified by column chromatography (Alox 90 standardised, CH₂Cl₂ : hexane 1:1 until the fraction with R_f = 0.23 was eluted fully, then CH₂Cl₂). The collected product was 5,5''-dimethoxy-2,2':6',2''-terpyridine (**86**) rather than the desired 5-methoxy-2,2':6',2''-terpyridine. Yield: 0.70 g, 36.7%.

¹H-NMR (400 MHz, CDCl₃): δ / ppm 8.61 (1H, d, *J* = 8.4 Hz, H3), 8.43 (1H, d, *J* = 2.0 Hz, H6), 8.36 (1H, d, *J* = 8.0 Hz, H3'), 7.93 (0.5H, t, *J* = 7.8 Hz, H4'), 7.43 (1H, dd, *J* = 8.6, 2.6 Hz, H4), 3.96 (3H, s, OCH₃).

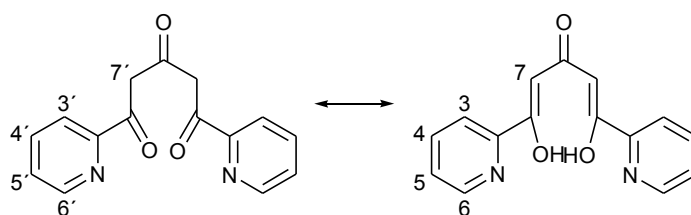
¹³C-NMR (100 MHz, CDCl₃): δ / ppm 156.6, 155.33, 149.4, 138.2, 136.9, 122.2, 121.6, 120.0, 56.1.

EI-MS: 293.1 [M]⁺, 263.1 [terpy-CH₃]⁺, 251.1, 180.1, 146.6.

IR (solid, cm⁻¹): 3056w, 3007w, 2972w, 2944w, 2841w, 1558s, 1481m, 1452m, 1435m, 1333w, 1263m, 1248m, 1228s, 1216m, 1184m, 1133m, 1079w, 1059m, 1021s, 902w, 848m, 827m, 809s, 780m, 752s, 737m, 673m, 645m.

R_f (Al₂O₃, CH₂Cl₂): 0.56.

m. p.: 152.9-160.5 °C.

1,5-Bis(2'-pyridyl)pentane-1,3,5-trione (M = 268.29) (88) [118]

A solution of acetone (1.86 ml, 25.3 mmol) and ethyl 2-pyridine-carboxylate (10.2 ml, 74.9 mmol) in 1,2-dimethoxyethane (50 ml) was added to a suspension of sodium hydride (60% dispersion in mineral oil, 5.09 g, 106 mmol) in 1,2-dimethoxyethane (50 ml) under a nitrogen atmosphere. The mixture was stirred at room temperature; it slowly became yellow, then turned suddenly orange after about 2 h. It was then heated to reflux overnight. The solvent was evaporated, then water (100 ml) was added to the yellow residue. The suspension was filtered through celite, and the filtrate treated with diluted HCl until pH 7. This caused a thick yellow precipitate to form. The solid was collected by filtration, washed with water, then redissolved in Et₂O and CH₂Cl₂. This solution was dried over MgSO₄ and evaporated to yield a yellow solid. Yield: 5.60g, 82.5%.

¹H-NMR (250 MHz, CDCl₃): δ / ppm 14.55 (0.5H, broad s, OH), 8.69 (1H, d, *J* = 4.5 Hz, H6), 8.02 (1H, d, *J* = 8.0 Hz, H3), 7.85 (1H, td, *J* = 7.8, 1.4 Hz, H4), 7.40 (1H, ddd, *J* = 7.6, 4.7, 1.2 Hz, H5), 6.83 (1H, s, H7), 4.44 (0.3H, s, H7').

4'-Hydroxy-2,2':6',2''-terpyridine (M = 249.29) (89) [118]

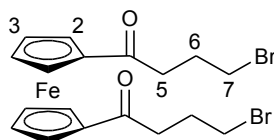
A mixture of 1,5-bis(2'-pyridyl)pentane-1,3,5-trione (5.6 g, 21 mmol) and ammonium acetate (11.72 g, 152.0 mmol) in ethanol (140 ml) was heated to reflux overnight. The resulting brown solution was concentrated to half its volume, then cooled in the fridge. A precipitate formed that was collected by filtration and washed with Et₂O to yield a fluffy light grey compound. Yield: 3.71 g, 70.9%.

$^1\text{H-NMR}$ (400 MHz, $\text{CDCl}_3 + \text{CD}_3\text{OD}$): δ / ppm 8.61 (1H, d, $J = 4.4$ Hz, H6), 7.89 (1H, d, $J = 8.0$ Hz, H3), 7.76 (1H, td, $J = 7.9, 1.5$ Hz, H4), 7.31 (1H, dd, $J = 7.6, 5.2$ Hz, H5), 6.98 (1H, s, H3'), 4.42 (6H, s, OH), 1.79 (3.5H, s, H3'').

$^{13}\text{C-NMR}$ (100 MHz, $\text{CDCl}_3 + \text{CD}_3\text{OD}$): δ / ppm 176.0, 149.2, 137.6, 125.3, 120.5, 112.3, 21.5.

ESI-MS: m/z 250.1 $[\text{M} + \text{H}]^+$, 521.9 $[2\text{M} + \text{Na}]^+$.

1,1'-Bis(4-bromobutanoyl)ferrocene (M = 484.03) (75)



To a solution of ferrocene (8.03 g, 43.1 mmol) and 4-bromobutanoyl chloride (10.0 ml, 86.3 mmol) in CH_2Cl_2 (100 ml) was added slowly anhydrous AlCl_3 (15.03 g, 112.7 mmol). The mixture was left to stir at room temperature for 2.5 h, then it was poured over ice-water (200 ml). After separation of the layers, the aqueous phase was extracted with CH_2Cl_2 (2 x 50 ml). The combined organic phases were washed with dilute NaHCO_3 (50 ml NaHCO_3 sat. + 50 ml H_2O) and brine (100 ml), then dried over MgSO_4 and concentrated. The solid black residue was purified by column chromatography (silica gel, hexane : EtOAc 5:3) to give a red-brown solid. Yield: 14.95 g, 71.7%.

A sample was recrystallised from hexane and activated charcoal to yield bright red crystals.

$^1\text{H-NMR}$ (250 MHz, CDCl_3): δ / ppm 4.83 (2H, s, H2 or H3), 4.53 (2H, s, H2 or H3), 3.58 (2H, t, $J = 6.1$ Hz, H7), 2.88 (2H, t, $J = 6.9$ Hz, H5), 2.26 (2H, q, $J = 6.6$ Hz).

$^{13}\text{C-NMR}$ (100 MHz, CDCl_3): δ / ppm 202.0, 80.0, 73.6, 70.6, 37.5, 33.9, 26.5.

ESI-MS: m/z 555.4 $[\text{M} + 71]^+$, 507.1 $[\text{M} + \text{Na}]^+$.

IR (solid, cm^{-1}): 3095w, 3081w, 2932w, 2914w, 2900w, 1651s, 1456s, 1441m, 1418m, 1407m, 1401m, 1377m, 1355m, 1278m, 1244s, 1161w, 1135w, 1091w, 1054s, 1031w, 992w, 957w, 895w, 866m, 833m, 805m, 700w, 649w, 625w, 614w.

UV/Vis (CHCl_3): λ_{max} , nm (ϵ_{max} , $\text{M}^{-1}\text{cm}^{-1}$): 281 (4390), 333 (1960), 476 (1080).

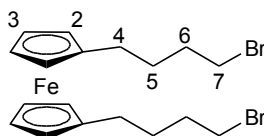
R_f (silica gel, hexane : EtOAc 5:3): 0.46.

Elem. an.: % calc. C 44.67, H 4.16, O 6.61, found C 44.86, H 4.17, O 6.77.

m. p.: 74.0-75.0 °C.

Crystal structure: see appendix

1,1'-Bis(4-bromobutyl)ferrocene (M = 456.07) (71)



1,1'-Bis(4-bromobutanoyl)ferrocene (10 g, 21 mmol) was dissolved in toluene (200 ml). To this solution was added zinc dust (63.44 g, 970.3 mmol), mercury(II) chloride (5.92 g, 21.8 mmol) and water (120 ml), followed by dropwise addition of HCl (36%, 120 ml). After the mixture was stirred at room temperature for about 2 h, the two phases were separated; the zinc dust was filtered off the aqueous phase and washed with CH_2Cl_2 . The aqueous phase was also extracted with CH_2Cl_2 (2 x 100 ml). The combined organic phases were washed with dilute NaHCO_3 (50 ml NaHCO_3 sat. + 50 ml H_2O) and brine (100 ml), then dried over MgSO_4 and concentrated. The brown oily residue was purified by column chromatography (silica gel, hexane : EtOAc 10:0.5) to give a yellow oil. Yield: 7.67 g, 80.1%.

For the characterisation see the synthesis of the same product starting from 1,1'-bis(4-(methylsulfonyloxy)butyl)ferrocene (68).

1,1'-Bis(4-(2,2':6',2''-terpyridin-4'-yl)butanoyl)ferrocene (M = 820.79)

a)

4'-Hydroxy-2,2':6',2''-terpyridine (1.01 g, 4.05 mmol) and K₂CO₃ (1.11 g, 8.03 mmol) were mixed in dry DMF (8 ml) and heated to 90 °C for 45 min. Then a solution of 1,1'-bis(4-bromobutanoyl)ferrocene (0.97 g, 2.0 mmol) in dry DMF (10 ml) was added dropwise and the purple reaction mixture was stirred at 90 °C overnight. After cooling, water (50 ml) was added. The addition of CH₂Cl₂ for the extraction resulted only in the formation of a small amount of aqueous phase, an emulsion and a precipitate. The precipitate was filtered off, the emulsion was treated with water and could be separated. The brown organic phase was washed once with water, dried over MgSO₄ and evaporated to give a red-brown liquid. After purification by column chromatography (Alox 90 standardised, hexane : EtOAc 3:1) only tiny amounts of three materials were collected, that could not be identified.

The purple aqueous phase remaining from the extraction was concentrated to half the volume. The white precipitate that formed was filtered off, and the filtrate was treated with an aqueous solution of NH₄PF₆, causing the formation of a purple precipitate. It was filtered through celite, but then it became more soluble in water than in CH₃CN. After complete evaporation of the solvent a dark purple solid was collected. From the NMR spectroscopic and ESI-MS analyses the compound was identified as Fe(terpy-OH)₂.

¹H-NMR (250 MHz, CD₃CN, D₂O): δ / ppm 8.98 (1H, d, *J* = 10.3 Hz, H3), 8.96 (1H, s, H3'), 8.45 (1H, t, *J* = 7.5 Hz, H4), 7.77 (1H, d, *J* = 5.3, H6), 7.67 (1H, t, *J* = 6.5 Hz, H5).

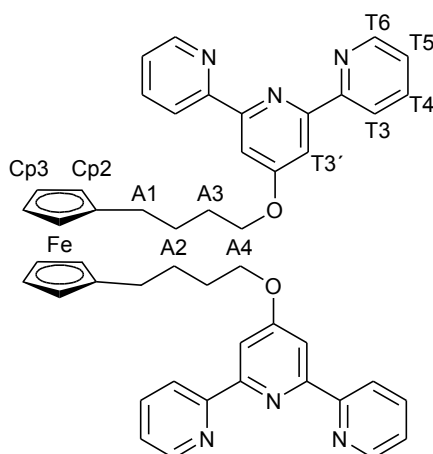
ESI-MS: *m/z* 553.3 [Fe(terpy-OH)(terpy-O⁻)]⁺, 277 [Fe(terpy-OH)₂]²⁺.

b)

4'-Hydroxy-2,2':6',2''-terpyridine (1.01 g, 4.05 mmol) was suspended in CH₃CN (about 30 ml) under a nitrogen atmosphere. 1,1'-Bis(4-bromobutanoyl)ferrocene (0.97 g, 2.00 mmol) was dissolved in CH₃CN and added to the suspension of terpy to give a total volume of 100 ml of solvent. Unlike the previous reaction, this time the

mixture did not become purple. K_2CO_3 (3.30 g, 23.9 mmol) was added and the reaction mixture was heated to 65 °C under nitrogen overnight. The red-brown solution was concentrated, the residue was redissolved in water (100 ml) and CH_2Cl_2 (60 ml), and the layers separated. The brown organic phase was dried over $MgSO_4$ and evaporated. The red-brown sticky residue was purified by column chromatography (Alox 90 standardised, hexane : EtOAc 3:1 until first two fractions were eluted, then 1:3). Neither of the three products collected could be identified.

1,1'-Bis(4-(2,2':6',2''-terpyridin-4'-yl)butoxy)ferrocene (M = 792.83) (90)



1,1'-Bis(4-bromobutyl)ferrocene (0.83 g, 1.8 mmol) was dissolved in CH_3CN (about 50 ml) under a nitrogen atmosphere. A suspension of 4'-hydroxy-2,2':6',2''-terpyridine (1.03 g, 4.13 mmol) in CH_3CN was added, to give a total volume of 100 ml of solvent. The mixture became immediately purple, even at room temperature. K_2CO_3 (3.33 g, 24.1 mmol) was added and the mixture was heated to 65 °C under nitrogen overnight. The purple solution was concentrated, the residue was redissolved in water (100 ml) and CH_2Cl_2 (50 ml), and the layers separated. The brown organic phase was washed once with water (50 ml), then dried over $MgSO_4$ and evaporated. The brown sticky residue was purified by column chromatography (Alox 90 standardised, hexane : EtOAc 3:1) then recrystallised from hexane to give a bright yellow solid. Yield: 0.21 g, 14.7%.

$^1\text{H-NMR}$ (400 MHz, CDCl_3): δ / ppm 8.68 (2H, dt, $J = 5.6, 1.0$ Hz, T6), 8.61 (2H, dd, $J = 8.0, 0.8$ Hz, T3), 8.00 (2H, s, T3'), 7.83 (2H, td, $J = 7.6, 1.5$ Hz, T4), 7.31 (2H, ddd, $J = 7.4, 4.8, 1.0$ Hz, T5), 4.21 (2H, t, $J = 6.4$ Hz, A4), 4.02 (4H, s, Cp2, Cp3), 2.41 (2H, t, $J = 7.6$ Hz, A1), 1.90-1.83 (2H, m, A2 or A3), 1.74-1.66 (2H, m, A2 or A3).

$^{13}\text{C-NMR}$ (100 MHz, CDCl_3): δ / ppm 167.3, 156.9, 156.0, 148.9, 136.8, 123.8, 121.3, 107.4, 68.7, 68.0, 67.9, 29.0, 28.8, 27.6.

EI-MS: m/z 792.2 $[\text{M}]^+$, 561.2 $[\text{Fe}(\text{Cp-CH}_2\text{CH}_2\text{CH}_2\text{CH}_2\text{-O-terpy})(\text{Cp-CH}_2\text{CH}_2\text{CH}_2\text{CH}_2\text{-OH})]^+$, 545.1 $[\text{Fe}(\text{Cp-CH}_2\text{CH}_2\text{CH}_2\text{CH}_2\text{-O-terpy})(\text{Cp-CH}_2\text{CH}_2\text{CH}_2\text{CH}_2)]^+$, 424.1 $[\text{Fe}(\text{Cp-CH}_2\text{CH}_2\text{CH}_2\text{CH}_2\text{-O-terpy})]^+$, 369.2, 351.1, 304 $[\text{Fe}(\text{terpy-O})]^+$, 250.1, 221.1, 91.1.

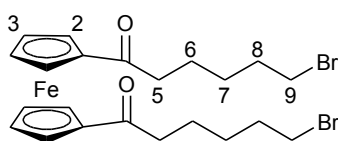
IR (solid, cm^{-1}): 3060w, 2947w, 2841w, 1579m, 1561s, 1466m, 1443m, 1406m, 1358m, 1252w, 1203s, 1088m, 1036m, 1024m, 1008m, 986m, 921m, 890w, 863m, 824m, 792s, 733m, 658m.

UV/Vis (CHCl_3): λ_{max} , nm (ϵ_{max} , $\text{M}^{-1}\text{cm}^{-1}$): 279 (85300), 284 (53900).

R_f (Al_2O_3 , hexane : EtOAc 3:1): 0.37.

m. p.: 139.3-141.9 $^\circ\text{C}$.

1,1'-Bis(6-bromohexanoyl)ferrocene (M = 540.15) (76)



To a solution of ferrocene (4.36 g, 23.4 mmol) and 6-bromohexanoyl chloride (10.0 g, 46.8 mmol) in CH_2Cl_2 (50 ml) was added slowly anhydrous AlCl_3 (8.16 g, 61.2 mmol). The mixture was left to stir at room temperature overnight, then it was poured over ice-water (100 ml). After separation of the layers, the aqueous phase was extracted with CH_2Cl_2 (25 ml). The combined organic phases were washed with diluted NaHCO_3 (25 ml NaHCO_3 sat. + 25 ml H_2O) and brine (50 ml), then dried over

MgSO₄ and concentrated. The residue was purified by column chromatography (silica gel, hexane : EtOAc 5:3) to give a brown oil. Yield: 2.87 g, 22.7%.

¹H-NMR (400 MHz, CDCl₃): δ / ppm 4.74 (2H, s, H2 or H3), 4.47 (2H, s, H2 or H3), 3.42 (2H, t, *J* = 6.6 Hz, H9), 2.64 (2H, t, *J* = 7.2 Hz, H5), 1.93-1.89 (2H, m, H6 or H7 or H8), 1.74-1.68 (2H, m, H6 or H7 or H8), 1.54-1.51 (2H, m, H6 or H7 or H8).

¹³C-NMR (100 MHz, CDCl₃): δ / ppm 203.0, 80.1, 73.2, 70.4, 39.4, 33.6, 32.5, 27.8, 23.0.

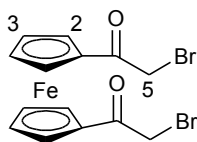
EI-MS: *m/z* 539.9 [M]⁺, 458 [M - Br]⁺, 416.

IR (liquid, cm⁻¹): 3097w, 2928w, 2857w, 1664s, 1452s, 1407w, 1397w, 1375m, 1346w, 1291w, 1253s, 1230m, 1122w, 1078m, 1052m, 1026m, 984w, 891m, 828m, 746m, 731m, 640w.

UV/Vis (CHCl₃): λ_{max}, nm (ε_{max}, M⁻¹cm⁻¹): 349 (260), 477 (220), 545 (520).

R_f (silica gel, hexane : EtOAc 5:3): 0.49.

1,1'-Bis(bromoacetyl)ferrocene (M = 427.91) (74)



To a solution of ferrocene (5.58 g, 30.0 mmol) in CH₂Cl₂ (80 ml) was added bromoacetyl chloride (5.0 ml, 60 mmol). The mixture became immediately green-black. Anhydrous AlCl₃ (8.16 g, 61.2 mmol) was added slowly, the mixture was left to stir at room temperature for 4.5 h, then it was poured over ice-water (200 ml). After separation of the layers, the aqueous phase was extracted with CH₂Cl₂ (4 x 50 ml, shaking only very lightly because it tends to form an emulsion). The combined organic phases were washed with diluted NaHCO₃ (50 ml NaHCO₃ sat. + 50 ml H₂O) and brine (2 x 100 ml), then dried over MgSO₄ and concentrated. The residue was purified by column chromatography (silica gel, CH₂Cl₂) to give a dark red solid. Yield: 1.63 g, 12.7%.

$^1\text{H-NMR}$ (400 MHz, CDCl_3): δ / ppm 4.88 (2H, s, H2 or H3), 4.64 (2H, s, H2 or H3), 4.11 (2H, s, H5).

$^{13}\text{C-NMR}$ (100 MHz, CDCl_3): δ / ppm 195.0, 77.5, 74.5, 71.7, 31.4.

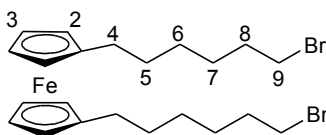
IR (solid, cm^{-1}): 3106w, 2990w, 2943w, 2921w, 2850w, 1682s, 1447s, 1386s, 1372s, 1284s, 1214s, 1062s, 1027m, 988m, 878s, 841s, 830s, 809m, 715w, 661s, 639s.

UV/Vis (CHCl_3): λ_{max} , nm (ϵ_{max} , $\text{M}^{-1}\text{cm}^{-1}$): 279 (10700), 282 (7100), 334 (2000), 340 (2000), 476 (1380).

R_f (silica gel, CH_2Cl_2): 0.13.

m. p.: 79.5-81.8 °C.

1,1'-Bis(6-bromohexyl)ferrocene ($M = 512.19$) (77)



1,1'-Bis(6-bromohexanoyl)ferrocene (1.14 g, 2.11 mmol) was dissolved in toluene (25 ml). To this solution was added zinc dust (6.36 g, 97.3 mmol), mercury(II) chloride (0.60 g, 2.21 mmol) and water (15 ml), followed by dropwise addition of HCl (36%, 15 ml). The Zn dust almost immediately formed small pellets. After 3 h of stirring at room temperature a TLC analysis did not show the formation of any new product, so the mixture was heated to reflux and a spatula of Zn turnings was added. A TLC analysis at this point showed that a new compound had started to form. The mixture was heated for 1.5 h while new zinc turnings were added every 20 min, then the residual zinc was filtered off the aqueous phase and washed with CH_2Cl_2 . The two phases were separated, and the aqueous phase was extracted with toluene (30 ml). The combined organic phases were washed with dilute NaHCO_3 (30 ml NaHCO_3 sat. + 30 ml H_2O) and brine (50 ml), then dried over MgSO_4 and concentrated. The yellow oily residue was purified by column chromatography (silica gel, CH_2Cl_2) to give a yellow oil. Yield: 0.37 g, 34.2%.

$^1\text{H-NMR}$ (400 MHz, CDCl_3): δ / ppm 4.05 (4H, broad s, H2, H3), 3.41 (2H, t, $J = 6.8$ Hz, H9), 2.26 (2H, broad s, H4), 1.88-1.84 (2H, m, H5 or H6 or H7 or H8), 1.47-1.30 (10H, m, three between H5, H6, H7, H8).

$^{13}\text{C-NMR}$ (100 MHz, CDCl_3): δ / ppm 69.2, 68.3, 34.0, 32.7, 31.0, 28.6, 28.0, 22.6.

EI-MS: 512.0 $[\text{M}]^+$, 466.0, 430.1 $[\text{Fe}(\text{Cp}-(\text{CH}_2)_6\text{-Br})(\text{Cp}-(\text{CH}_2)_6)]^+$, 201.0.

IR (liquid, cm^{-1}): 3083w, 2925s, 2853s, 1712w, 1456m, 1437m, 1256w, 1227w, 1039m, 1021m, 960w, 921w, 821s, 805s, 726m, 645m.

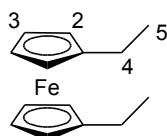
UV/Vis (CHCl_3): λ_{max} , nm (ϵ_{max} , $\text{M}^{-1}\text{cm}^{-1}$): 285 (4750), 474 (470).

R_f (silica gel, CH_2Cl_2): 0.89.

1,1'-Bis(2-bromoethyl)ferrocene (M = 399.95)

1,1'-Bis(bromoacetyl)ferrocene (1.58 g, 3.69 mmol) was dissolved in toluene (30 ml). To this solution was added zinc dust (11.18 g, 171.0 mmol), mercury(II) chloride (1.04 g, 3.83 mmol) and water (15 ml), followed by dropwise addition of HCl (36%, 15 ml). After the mixture was stirred at room temperature for 15 min, the Zn was decanted and washed with toluene. The two layers were separated, and the aqueous phase was extracted with toluene (30 ml). The combined organic phases were washed with dilute NaHCO_3 (25 ml NaHCO_3 sat. + 25 ml H_2O) and brine (50 ml), then dried over MgSO_4 and concentrated. The yellow oily residue was purified by column chromatography (silica gel, hexane : EtOAc 5:2). Neither of the two products was the desired compound.

The first product to be collected was 1,1'-diethylferrocene: 0.16 g, 17.9%.

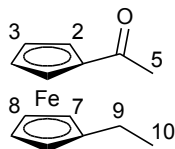


$^1\text{H-NMR}$ (400 MHz, CDCl_3): δ / ppm 4.0 (4H, s, H2, H3), 2.33 (2H, q, $J = 7.5$ Hz, H4), 1.15 (3H, t, $J = 7.6$ Hz, H5).

$^{13}\text{C-NMR}$ (100 MHz, CDCl_3): δ / ppm 91.3, 68.2, 67.8, 22.1, 14.8.

R_f (silica gel, hexane : EtOAc 5:2): 0.91.

The second product to be collected was 1-acetyl-1'-ethylferrocene: 0.33 g, 34.9%.



$^1\text{H-NMR}$ (400 MHz, CDCl_3): δ / ppm 4.70 (2H, d, $J = 2.0$ Hz, H2 or H3), 4.45 (2H, d, $J = 1.2$ Hz, H2 or H3), 4.09 (4H, s, H7, H8), 2.38 (3H, s, H5), 2.27 (2H, q, $J = 7.6$ Hz, H9), 1.13 (3H, t, $J = 7.6$ Hz, H10).

$^{13}\text{C-NMR}$ (100 MHz, CDCl_3): δ / ppm 202.0, 92.8, 79.4, 72.9, 70.0, 69.1, 69.0, 27.4, 21.5, 14.7.

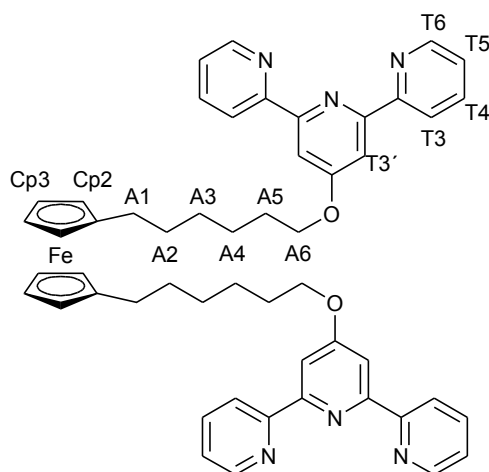
EI-MS: m/z 256 $[\text{M}]^+$, 213 $[\text{M} - \text{COCH}_3]^+$.

IR (liquid, cm^{-1}): 3084w, 2963w, 2925w, 1663s, 1451s, 1396w, 1372m, 1352m, 1314w, 1274s, 1111m, 1035m, 1019m, 957w, 906m, 891, 821m, 617m.

UV/Vis (CHCl_3): λ_{max} , nm (ϵ_{max} , $\text{M}^{-1}\text{cm}^{-1}$): 282 (4080), 334 (1340), 451 (650).

R_f (silica gel, hexane : EtOAc 5:2): 0.50.

If the mixture is left to react overnight the only product obtained is 1,1'-diethylferrocene in 62% yield.

1,1'-Bis(6-(2,2':6',2''-terpyridin-4'-yl)hexoxy)ferrocene (M = 848.95) (91)

4'-Hydroxy-2,2':6',2''-terpyridine (0.34 g, 1.4 mmol) was suspended in CH₃CN (30 ml) and flushed with nitrogen. K₂CO₃ (1.13 g, 8.18 mmol) was added and the mixture was heated to 80 °C under nitrogen for 1 h. To the reaction mixture was added a solution of 1,1'-bis(6-bromohexylferrocene) (0.35 g, 0.68 mmol) in CH₃CN (20 ml), and it was heated to 80 °C overnight. The orange solution was concentrated, the residue was redissolved in water (100 ml) and CH₂Cl₂ (60 ml), and the layers separated. The slightly purple aqueous phase was extracted with CH₂Cl₂, then the combined yellow organic layers were washed once with water (60 ml), dried over MgSO₄ and evaporated. The residue was purified by column chromatography (silica gel, hexane : EtOAc 3:1 until the first two fractions had been eluted, then 1:1). The third product that was eluted was then recrystallised from toluene/hexane to give a bright yellow solid. Yield: 0.16 g, 13.5%.

¹H-NMR (400 MHz, CDCl₃): δ / ppm 8.69 (2H, d, *J* = 3.6 Hz, T6), 8.61 (2H, d, *J* = 7.2 Hz, T3), 8.00 (2H, s, T3'), 7.84 (2H, td, *J* = 7.8, 1.6 Hz, T4), 7.34-7.31 (2H, m, T5), 4.21 (2H, t, *J* = 6.6 Hz, A6), 4.01 (4H, broad s, Cp2, Cp3), 2.30 (2H, broad s, A1), 1.86-1.82 (2H, m, A2 or A3 or A4 or A5), 1.51-1.98 (6H, m, three between A2, A3, A4, A5).

^{13}C -NMR (100 MHz, CDCl_3): δ / ppm 167.3, 156.9, 156.1, 148.9, 136.8, 123.8, 121.3, 107.4, 68.2, 31.2, 29.2, 29.0, 25.8.

EI-MS: m/z 848.2 $[\text{M}]^+$, 659.3, 601.3 $[\text{Fe}(\text{Cp}-(\text{CH}_2)_6\text{-O-terpy})(\text{Cp}-(\text{CH}_2)_6\text{-H})]^+$, 452.1 $[\text{Fe}(\text{Cp}-(\text{CH}_2)_6\text{-O-terpy})]^+$, 304 $[\text{Fe}(\text{terpy-O})]^+$, 250.1, 221.1.

IR (solid, cm^{-1}): 2921w, 2856w, 1596m, 1579s, 1557s, 1465s, 1442s, 1404s, 1359s, 1252m, 1200s, 1089m, 1029s, 1016s, 922m, 887m, 866m, 828m, 792s, 745m, 733m, 698m, 658s, 621m.

UV/Vis (CHCl_3): λ_{max} , nm (ϵ_{max} , $\text{M}^{-1}\text{cm}^{-1}$): 280 (88400).

R_f (Al_2O_3 , hexane : EtOAc 3:1): 0.48.

m. p.: 145.1-148.6 $^\circ\text{C}$.

7.3. Inorganic syntheses

General method for synthesising $[\text{CoL}_3][\text{PF}_6]_2$ complexes

$\text{Co}(\text{OAc})_2 \cdot 4\text{H}_2\text{O}$ (1 equivalent) and the ligand (3 equivalents) were mixed in methanol (about 10 ml). The reaction mixture changed colour immediately. Excess aqueous NH_4PF_6 was added to the solution to precipitate the complex that was collected by filtration and washed with water. When the precipitate was particularly fine, it was filtered over celite, washed out with CH_3CN , and dried under reduced pressure.

$[\text{Co}(\text{bpy})_3][\text{PF}_6]_2$ ($M = 817.44$) (4)

bpy = 2,2'-bipyridine

$\text{Co}(\text{OAc})_2 \cdot 4\text{H}_2\text{O}$ (0.25 g, 1.00 mmol) and 2,2'-bipyridine (0.47 g, 3.01 mmol) were used. Yield: 0.81 g, 99.1%.

^1H -NMR (500 MHz, CD_3CN): δ / ppm 87.96 (1H, s, H6), 84.48 (1H, s, H3), 46.25 (1H, s, H5), 14.58 (1H, s, H4).

IR (solid, cm^{-1}): 3105w, 1600m, 1576w, 1567w, 1492w, 1471w, 1441m, 1315w, 1245w, 1162w, 1107w, 1062w, 1045w, 1021w, 903w, 876w, 827s, 756s, 734s, 652m.

UV/Vis (CH₃CN): λ_{max} , nm (ϵ_{max} , M⁻¹cm⁻¹): 282 (31800), 294 (35600), 301 (33900).
Elem. an.: % calc. C 44.08, H 2.96, N 10.28; found C 44.03, H 3.01, N 10.17.
m. p.: decomposes >251 °C.

[Co(Me₂bpy)₃][PF₆]₂ (M = 901.62) (5)

Me₂bpy = 4,4'-dimethyl-2,2'-bipyridine

Co(OAc)₂·4H₂O (0.25 g, 1.00 mmol) and 4,4'-dimethyl-2,2'-bipyridine (0.55 g, 2.99 mmol) were used. Yield: 0.90 g, 99.8%.

¹H-NMR (500 MHz, CD₃CN): δ / ppm 89.74 (1H, s, H6), 81.52 (1H, s, H3), 44.50 (1H, s, H5), 0.40 (3H, s, CH₃).

IR (solid, cm⁻¹): 3670w, 3595w, 1615m, 1557w, 1485w, 1407w, 1243w, 1042w, 1018w, 821s, 639w, 619w.

UV/Vis (CH₃CN): λ_{max} , nm (ϵ_{max} , M⁻¹cm⁻¹): 292 (30500).

Elem. an.: % calc. C 47.96, H 4.02, N 9.32; found C 47.30, H 4.21, N 9.15.

m. p.: decomposes >254 °C.

[Co(phen)₃][PF₆]₂ (M = 889.50) (6)

phen = 1,10-phenanthroline

Co(OAc)₂·4H₂O (0.25 g, 1.00 mmol) and 1,10-phenanthroline (0.60 g, 3.03 mmol) were used. Yield: 0.88 g, 98.9%.

¹H-NMR (500 MHz, CD₃CN): δ / ppm 107.20 (1H, s, H2), 50.18 (1H, s, H3), 33.43 (1H, s, H5), 17.33 (1H, s, H4).

IR (solid, cm⁻¹): 1626w, 1580w, 1518m, 1495w, 1424m, 1337w, 1302w, 1222w, 1146w, 1104w, 823s, 722s, 644m.

UV/Vis (CH₃CN): λ_{max} , nm (ϵ_{max} , M⁻¹cm⁻¹): 286 (37000), 283 (36400), 342 (3600).

Elem. an.: % calc. C 48.61, H 2.72, N 9.45; found C 48.53, H 2.76, N 9.33.

m. p.: >272 °C.

[Co(bpy-CH₃)₃][PF₆]₂ (M = 859.11) (15)bpy-CH₃ = 5-methyl-2,2'-bipyridine

Co(OAc)₂·4H₂O (50 mg, 0.20 mmol) and 5-methyl-2,2'-bipyridine (108 mg, 0.635 mmol) were used. Yield: 170 mg, 98.9%.

¹H-NMR (250 MHz, CD₃CN): δ / ppm 93 (1H, broad, H6 or H6'), 91 (1H, broad, H6 or H6'), 89 (1H, broad, H6 or H6'), 87 (1H, broad, H6 or H6'), 86.61 (1H, s, H3 or H3'), 86.37 (1H, s, H3 or H3'), 86.15 (1H, s, H3 or H3'), 85.45 (1H, s, H3 or H3'), 84 (1H, broad, H6 or H6'), 84.04 (1H, s, H3 or H3'), 83.65 (2H, s, H3 or H3'), 82.86 (1H, s, H3 or H3'), 46.43 (1H, s, H5'), 46.03 (1H, s, H5'), 45.72 (2H, s, H5'), 14.6 (1H, s, H4 or H4'), 14.4 (1H, s, H4 or H4'), 14.4 (1H, s, H4 or H4'), 14.3 (1H, s, H4 or H4'), 14.0 (1H, s, H4 or H4'), 14.0 (1H, s, H4 or H4'), 14.0 (1H, s, H4 or H4'), 13.6 (1H, s, H4 or H4'), 2.0 (12H overlap with solvent peak, s, CH₃), 1.8 (6H, s, CH₃), 1.7 (3H, s, CH₃).

IR (solid, cm⁻¹): 3040w br, 1602w, 1473w, 1440w, 1317w, 1244w, 1230w, 1172w, 1053w, 829s, 783m, 732m, 666w.

UV/Vis (CH₃CN): λ_{max}, nm (ε_{max}, M⁻¹cm⁻¹): 282 (41900), 284 (41200), 288 (40000), 295 (39000).

m. p.: decomposes >240 °C.

[Co(bpy-CHO)₃][PF₆]₂ (M = 901.50) (14)

bpy-CHO = 5-formyl-2,2'-bipyridine

Co(OAc)₂·4H₂O (79 mg, 0.32 mmol) and 5-formyl-2,2'-bipyridine (176 mg, 0.955 mmol) were used. Yield: 287 mg, 99.5%.

¹H-NMR (500 MHz, CD₃CN): δ / ppm 105 (1H, broad, H6 or H6'), 99 (1H, broad, H6 or H6'), 96 (1H, broad, H6 or H6'), 91.5 (1H, broad, H6 or H6'), 91 (1H, broad, H6 or H6'), 90.20 (1H, s, H3'), 87.86 (1H, s, H3'), 86 (1H, broad, H6 or H6'), 85.66 (1H, s, H3'), 84 (1H, broad, H6 or H6'), 82.69 (1H, s, H3'), 82.32 (1H, s, H3), 80.21 (1H, s, H3), 80 (1H, broad, H6 or H6'), 77.53 (1H, s, H3), 74.81 (1H, s, H3), 51.80

(1H, s, H5'), 51.66 (1H, s, H5'), 46.40 (1H, s, H5'), 46.29 (1H, s, H5'), 18.32 (1H, s, H4'), 16.99 (1H, s, H4'), 16.12 (1H, s, H4), 15.08 (1H, s, H4), 14.54 (1H, s, H4'), 13.71 (1H, s, CHO), 13.10 (1H, s, H4'), 12.41 (1H, s, H4), 11.25 (1H, s, H4), 10.97 (1H, s, CHO), 9.66 (1H, s, CHO), 7.24 (1H, s, CHO).

IR (solid, cm^{-1}): 3318w br, 1695w, 1607w, 1579w, 1470w, 1428m, 1368w, 1246w, 1215w, 821s, 745s.

UV/Vis (CH_3CN): λ_{max} , nm (ϵ_{max} , $\text{M}^{-1}\text{cm}^{-1}$): 304 (30700).

General method for synthesising $[\text{CoL}_3][\text{PF}_6]_3$ complexes

The Co(II) complex was suspended in water (40 ml), and an aqueous solution of bromine (about 5 ml) was added until a noticeable change of colour of the suspension occurred. Excess of aqueous NH_4PF_6 was added to precipitate any possible dissolved bromide complex. The precipitate was filtered, washed with water and dried.

$[\text{Co}(\text{bpy})_3][\text{PF}_6]_3$ ($\text{M} = 962.41$) (7)

bpy = 2,2'-bipyridine

$[\text{Co}(\text{bpy})_3][\text{PF}_6]_2$ (148 mg, 0.181 mmol) was used. Yield: 99 mg, 56.8%

$^1\text{H-NMR}$ (250 MHz, CD_3CN): δ / ppm 8.72 (1H, d, $J = 8.3$ Hz, H3), 8.50 (1H, t, $J = 7.6$ Hz, H4), 7.76 (1H, t, $J = 6.8$ Hz, H5), 7.30 (1H, d, $J = 6.0$ Hz, H6).

IR (solid, cm^{-1}): 3097w br, 1607m, 1503w, 1469w, 1450s, 1320w, 1244w, 1168w, 1112w, 1076w, 985m, 879w, 834s, 760s, 722s, 637m, 622w.

UV/Vis (CH_3CN): λ_{max} , nm (ϵ_{max} , $\text{M}^{-1}\text{cm}^{-1}$): 306 (14100), 316 (12900).

Elem. an.: % calc. for $[\text{Co}(\text{bpy})_3][\text{PF}_6]_2[\text{Br}_3] \cdot 3\text{H}_2\text{O}$ C 32.43, H 2.72, N 7.56; found C 32.50, H 2.87, N 7.60.

m. p.: 214.7-218.5 °C.

$[\text{Co}(\text{Me}_2\text{bpy})_3][\text{PF}_6]_3$ ($\text{M} = 1046.59$)

Me_2bpy = 4,4'-dimethyl-2,2'-bipyridine

$[\text{Co}(\text{Me}_2\text{bpy})_3][\text{PF}_6]_2$ (150 mg, 0.166 mmol) was used. Yield: 93 mg, 53.5%

$^1\text{H-NMR}$ (250 MHz, CD_3CN): δ / ppm 8.51 (1H, d, $J = 2.0$ Hz, H3), 7.54 (1H, dd, $J = 6.0, 1.5$ Hz, H5), 7.08 (1H, d, $J = 7.1$ Hz, H6), 2.65 (3H, s, CH_3).

IR (solid, cm^{-1}): 3083w br, 1619m, 1557w, 1484w, 1435w, 1306w, 1273w, 1250w, 1223w, 1079w, 1032w, 1001w, 931w, 821s, 624w.

UV/Vis (CH_3CN): λ_{max} , nm (ϵ_{max} , $\text{M}^{-1}\text{cm}^{-1}$): 301 (22900), 312 (22700).

Elem. an.: % calc. for $[\text{Co}(\text{Me}_2\text{bpy})_3][\text{PF}_6]_{1.5}[\text{Br}_3]_{1.5}\cdot 4\text{H}_2\text{O}$ C 34.30, H 3.52, N 6.67; found C 34.48, H 3.42, N 6.69.

m. p.: 213.8-216.3 $^\circ\text{C}$.

$[\text{Co}(\text{phen})_3][\text{PF}_6]_3$ (M = 1034.47) (8)

phen = 1,10-phenanthroline

$[\text{Co}(\text{phen})_3][\text{PF}_6]_2$ (107 mg, 0.120 mmol) was used. Yield: 91 mg, 73.3%

$^1\text{H-NMR}$ (250 MHz, CD_3CN): δ / ppm 9.03 (1H, d, $J = 8.3$ Hz, H4), 8.48 (1H, d, $J = 1.0$ Hz, H5), 7.91 (1H, dd, $J = 8.0, 6.3$ Hz, H3), 7.53 (1H, d, $J = 5.3$ Hz, H2).

IR (solid, cm^{-1}): 1605w, 1583w, 1519w, 1494w, 1460w, 1427m, 1345w, 1317w, 1226w, 1149w, 1040w, 881w, 823s, 771w, 749w, 709m, 622w.

UV/Vis (CH_3CN): λ_{max} , nm (ϵ_{max} , $\text{M}^{-1}\text{cm}^{-1}$): 283 (48900).

Elem. an.: % calc. for $[\text{Co}(\text{phen})_3][\text{PF}_6]_2[\text{Br}_3]\cdot 2\text{H}_2\text{O}$ C 37.11, H 2.42, N 7.21; found C 36.71, H 2.34, N 7.11.

m. p.: 227.9-230.5 $^\circ\text{C}$.

General method for synthesising $[\text{CoL}_2][\text{PF}_6]_2$ complexes

$\text{Co}(\text{OAc})_2\cdot 4\text{H}_2\text{O}$ (1 equivalent) and the ligand (2 equivalents) were mixed in methanol (5 ml). The reaction mixture changed colour immediately. Excess aqueous NH_4PF_6 was added to the solution to precipitate the complex that was filtered over celite, washed out with CH_3CN , and dried under reduced pressure.

[Co(terpy)₂][PF₆]₂ (M = 815.43) (44)

terpy = 2,2':6',2''-terpyridine

Co(OAc)₂·4H₂O (25 mg, 0.10 mmol) and 2,2':6',2''-terpyridine (47 mg, 0.20 mmol) were used. Yield: 71 mg, 87.1%.

¹H-NMR (250 MHz, CD₃CN): δ / ppm 100 (1H, broad, s, H6), 57.27 (1H, s, H3), 48.18 (1H, s, H3'), 34.56 (1H, s, H5), 21.96 (1H, s, H4'), 8.97 (1H, s, H4).

[Co(terpy-CHO)₂][PF₆]₂ (M = 871.47) (38)

terpy-CHO = 5-formyl-2,2':6',2''-terpyridine

Co(OAc)₂·4H₂O (25 mg, 0.10 mmol) and 5-formyl-2,2':6',2''-terpyridine (52 mg, 0.20 mmol) were used. Yield: 62 mg, 71.1%.

¹H-NMR (250 MHz, CD₃CN): δ / ppm 108 (1H, broad, H6 or H6''), 95 (1H, broad, H6 or H6''), 59.64 (1H, s, H3 or H3'' or H3' or H5'), 58.69 (0.5H, s, H3 or H3'' or H3' or H5'), 56.39 (2H, s, H3 or H3'' or H3' or H5'), 56.19 (2H, s, H3 or H3'' or H3' or H5'), 55.68 (1H, s, H3 or H3'' or H3' or H5'), 55.24 (1H, s, H3 or H3'' or H3' or H5'), 54.40 (1H, s, H3 or H3'' or H3' or H5'), 53.84 (0.5H, s, H3 or H3'' or H3' or H5'), 50.80 (3H, s, H3 or H3'' or H3' or H5'), 49.95 (1H, s, H3 or H3'' or H3' or H5'), 49.32 (1H, s, H3 or H3'' or H3' or H5'), 48.66 (0.5H, s, H3 or H3'' or H3' or H5'), 48.07 (1H, s, H3 or H3'' or H3' or H5'), 47.25 (3H, s, H3 or H3'' or H3' or H5'), 46.30 (1H, s, H3 or H3'' or H3' or H5'), 35.32 (2H, s, H5''), 34.95 (1H, s, H5''), 22.17 (4H, s, H4'), 22.03 (2H, s, H4'), 14.29 (2H, s, H4 or H4'' or CHO), 13.70 (4H, s, H4 or H4'' or CHO), 11.13 (1H, s, H4 or H4'' or CHO), 10.81 (3H, s, H4 or H4'' or CHO), 9.94 (0.5H, s, H4 or H4'' or CHO), 9.59 (1H, s, H4 or H4'' or CHO), 7.93 (0.5H, s, H4 or H4'' or CHO), 7.76 (1H, s, H4 or H4'' or CHO), 7.61 (1H, s, H4 or H4'' or CHO), 7.39 (3H, s, H4 or H4'' or CHO), 4.17 (2H, s, H4 or H4'' or CHO), 4.08 (4H, s, H4 or H4'' or CHO).

[Co(terpy-COOH)₂][PF₆]₂ (M = 903.47) (40)

Terpy-COOH = 5-carboxy-2,2':6',2''-terpyridine

Co(OAc)₂·4H₂O (22 mg, 0.088 mmol) and 5-carboxy-2,2':6',2''-terpyridine dihydrochloric acid (50 mg, 0.14 mmol) were used. Yield: 40 mg, 50.3%.

¹H-NMR (500 MHz, CD₃CN): δ / ppm 110 (1H, broad, H6 or H6''), 99 (1H, broad, H6 or H6''), 58.66 (1H, s, H3), 57.98 (1H, s, H3''), 53.61 (1H, s, H3' or H5'), 50.34 (1H, s, H3' or H5'), 35.78 (1H, s, H5''), 22.46 (1H, s, H4'), 10.27 (1H, s, H4), 7.33 (1H, s, H4').

IR (solid, cm⁻¹): 3661w, 3381w br, 3088w, 1605m, 1622w, 1509w, 1482w, 1452w, 1361w, 1330w, 1302w, 1276w, 1249w, 1100w, 1048m, 1025w, 827s, 766m, 723m, 601m.

UV/Vis (CH₃CN): λ_{max}, nm (ε_{max}, M⁻¹cm⁻¹): 282 (26500), 284 (30700), 287 (28000), 290 (24500), 342 (18900).

Elem. an.: % calc. for [Co(terpy-COOH)₂][PF₆]₂·3H₂O C 40.14, H 2.95, N 8.78; found C 39.66, H 3.04, N 8.78.

m. p.: >250 °C.

[Co(terpy-CH₃)₂][PF₆]₂ (M = 843.51) (37)

terpy-CH₃ = 5-methyl-2,2':6',2''-terpyridine

Co(OAc)₂·4H₂O (26 mg, 0.10 mmol) and 5-methyl-2,2':6',2''-terpyridine (50 mg, 0.20 mmol) were used. Yield: 68 mg, 80.6%.

¹H-NMR (500 MHz, CD₃CN): δ / ppm 104 (1H, broad, H6 or H6''), 95 (1H, broad, H6 or H6''), 59.90 (1H, s, H3), 54.87 (1H, s, H3''), 48.31 (1H, s, H3' or H5'), 46.26 (1H, s, H3' or H5'), 34.90 (1H, s, H5''), 21.85 (1H, s, H4'), 9.42 (1H, s, H4), 8.08 (1H, s, H4'), 3.92 (3H, s, CH₃).

IR (solid, cm⁻¹): 1599w, 1574w, 1562w, 1477w, 1451m, 1404w, 1318w, 1249w, 1232w, 1190w, 1163w, 1047w, 1027w, 827s, 776s, 751m, 738m, 703w.

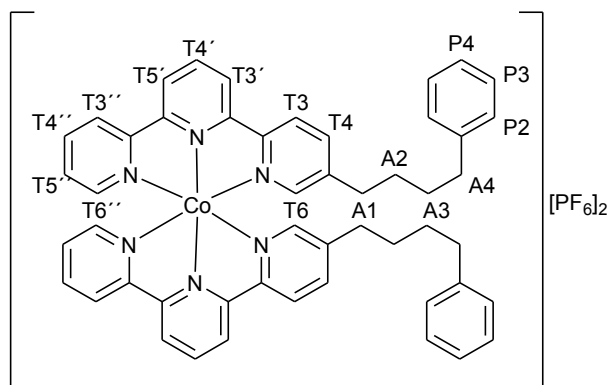
UV/Vis (CH₃CN): λ_{max}, nm (ε_{max}, M⁻¹cm⁻¹): 282 (23800), 314 (25500).

Elem. an.: % calc. C 45.57, H 3.11, N 9.96; found C 45.28, H 3.00, N 9.74.

m. p.: >250 °C.

[Co(terpy-C4-Ph)₂][PF₆]₂ (M = 1079.89)

terpy-C4-Ph = 5-(4-phenylbutyl)-2,2':6',2''-terpyridine



Co(OAc)₂·4H₂O (11 mg, 0.044 mmol) and 5-(4-phenylbutyl)-2,2':6',2''-terpyridine (37 mg, 0.10 mmol) were used. Yield: 43 mg, 90.5%.

¹H-NMR (250 MHz, CD₃CN): δ / ppm 102 (1H, broad, s, T6 or T6'), 97 (1H, broad, s, T6 or T6'), 59.29 (1H, s, T3), 55.73 (1H, s, T3'), 48.62 (1H, s, T3' or T5'), 47.33 (1H, s, T3' or T5'), 34.76 (1H, s, T5'), 21.98 (1H, s, T4'), 8.89 (1H, s, T4), 8.28 (1H, s, T4'), 6.98 (3H, s, P2, P4), 6.44 (2H, s, P3), 4.3 (2H, d, *J* = 105.3 Hz, A1), 2.16 (2H, s, A2 or A3 or A4), 1.68 (2H, s, A2 or A3 or A4), 0.2 (2H, broad, s, A2 or A3 or A4).

IR (solid, cm⁻¹): 2926w, 2855w, 1599w, 1557w, 1478w, 1451m, 1389w, 1318w, 1248w, 1188w, 1163w, 1028w, 827s, 778m, 751m, 736m.

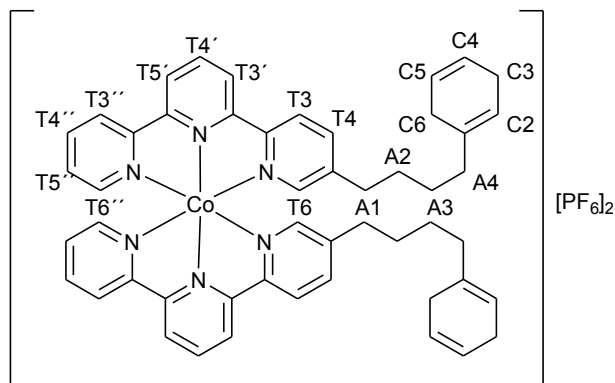
UV/Vis (CH₃CN): λ_{max}, nm (ε_{max}, M⁻¹cm⁻¹): 282 (38400), 317 (38100).

Elem. an.: % calc. C 55.62, H 4.29, N 7.78; found C 56.05, H 4.48, N 7.65.

m. p.: decomposes >84.9 °C.

[Co(terpy-C4-chd)₂][PF₆]₂ (M = 1083.93) (55)

terpy-C4-chd = 5-(4-cyclohexa-1,4-dienylbutyl)-2,2':6',2''-terpyridine



Co(OAc)₂·4H₂O (25 mg, 0.10 mmol) and 5-(4-cyclohexa-1,4-dienylbutyl)-2,2':6',2''-terpyridine (70 mg, 0.19 mmol) were used. Yield: 65 mg, 60.0%.

¹H-NMR (250 MHz, CD₃CN): δ / ppm 104 (1H, broad, T6 or T6''), 96 (1H, broad, T6 or T6''), 59.81 (1H, s, T3), 55.50 (1H, s, T3''), 48.97 (1H, s, T3' or T5'), 47.20 (1H, s, T3' or T5'), 34.91 (1H, s, T5''), 22.03 (1H, s, T4'), 9.19 (1H, s, T4 or T4'), 8.10 (1H, s, T4 or T4'), 5.40 (2H, s, C4, C5), 4.52 (1H, s, C2), 2.2 (overlap with water, s, C3, C6), 1.74 (2H, s, A1), 0.96 (2H, s, A4), 0.13 (2H, s, A2 or A3), -0.22 (2H, s, A2 or A3).

IR (solid, cm⁻¹): 3083w, 2924w, 2856w, 1599w, 1562w, 1478w, 1451m, 1248w, 1046s, 1024s, 818w, 782m, 753m, 700m, 600m.

UV/Vis (CH₃CN): λ_{max}, nm (ε_{max}, M⁻¹cm⁻¹): 283 (24800), 317 (26900).

m. p.: decomposes >59.0 °C.

General method for synthesising [FeL₂][PF₆]₂ complexes

FeSO₄·7H₂O (1 equivalent) and the ligand (2 equivalents) were mixed in methanol (about 5 ml). The reaction mixture changed colour immediately. Excess aqueous NH₄PF₆ was added to the solution to precipitate the complex that was filtered over celite, washed out with CH₃CN, and dried under reduced pressure.

[Fe(terpy)₂][PF₆]₂ (M = 812.37) (45)

terpy = 2,2':6',2''-terpyridine

FeSO₄·7H₂O (28 mg, 0.10 mmol) and 2,2':6',2''-terpyridine (47 mg, 0.20 mmol) were used. Yield: 71 mg, 87.4%.

¹H-NMR (500 MHz, CD₃CN): δ / ppm 8.89 (1H, d, *J* = 8.1 Hz, H3'), 8.67 (0.5 H, t, *J* = 8.3, 7.8 Hz, H4'), 8.46 (1H, dt, *J* = 8.0, 1.1 Hz, H3), 7.89-7.85 (1H, m, H4), 7.07-7.05 (2H, m, H5, H6).

IR (solid, cm⁻¹): 3116w br, 1605w, 1466w, 1450m, 1396w, 1285w, 1244w, 1164w, 826s, 766s, 673w, 646m.

UV/Vis (CH₃CN): λ_{max}, nm (ε_{max}, M⁻¹cm⁻¹): 317 (67500), 549 (30600).

Elem. an.: % calc. C 44.36, H 2.73, N 10.35; found C 44.38, H 2.68, N 10.25.

m. p.: >250 °C.

[Fe(terpy-CH₃)₂][PF₆]₂ (M = 840.43) (46)

terpy-CH₃ = 5-methyl-2,2':6',2''-terpyridine

FeSO₄·7H₂O (28 mg, 0.10 mmol) and 5-methyl-2,2':6',2''-terpyridine (50 mg, 0.20 mmol) were used. Yield: 70 mg, 83.3%.

¹H-NMR (500 MHz, CD₃CN): δ / ppm 8.85 (1H, dd, *J* = 8.1, 0.9 Hz, H3' or H5'), 8.83 (1H, dd, *J* = 8.3, 0.9 Hz, H3' or H5'), 8.64 (1H, t, *J* = 8.0 Hz, H4'), 8.43 (1H, ddd, *J* = 8.1, 1.3, 0.9 Hz, H3''), 8.35 (1H, d, *J* = 8.2 Hz, H3), 7.85 (1H, ddd, *J* = 8.0, 7.6, 1.5 Hz, H4'), 7.68 (1H, ddd, *J* = 8.2, 1.9, 0.8 Hz, H4), 7.05 (1H, ddd, *J* = 7.5, 5.6, 1.3 Hz, H5''), 6.98 (1H, ddd, *J* = 5.6, 1.5, 0.3 Hz, H6''), 6.87-6.86 (1H, m, H6).

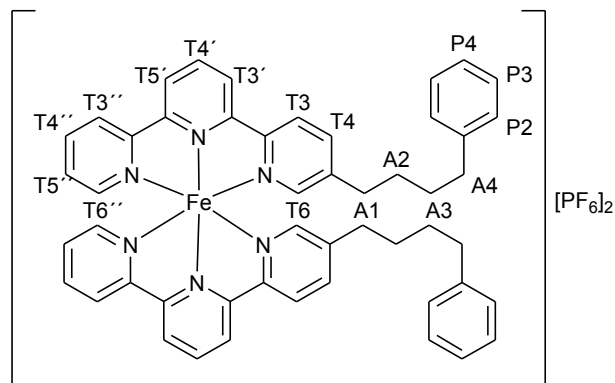
IR (solid, cm⁻¹): 1604w, 1450w, 1244w, 826s, 772m, 757m, 751m, 637w, 622m.

UV/Vis (CH₃CN): λ_{max}, nm (ε_{max}, M⁻¹cm⁻¹): 282 (48500), 320 (58000), 550 (7500).

Elem. an.: % calc. C 45.74, H 3.12, N 10.00; found C 45.20, H 3.29, N 9.83.

[Fe(terpy-C4-Ph)₂][PF₆]₂ (M = 1076.81)

terpy-C4-Ph = 5-(4-phenylbutyl)-2,2':6',2''-terpyridine



FeSO₄·7H₂O (14 mg, 0.050 mmol) and 5-(4-phenylbutyl)-2,2':6',2''-terpyridine (36 mg, 0.098 mmol) were used. Yield: 49 mg, 91.0%.

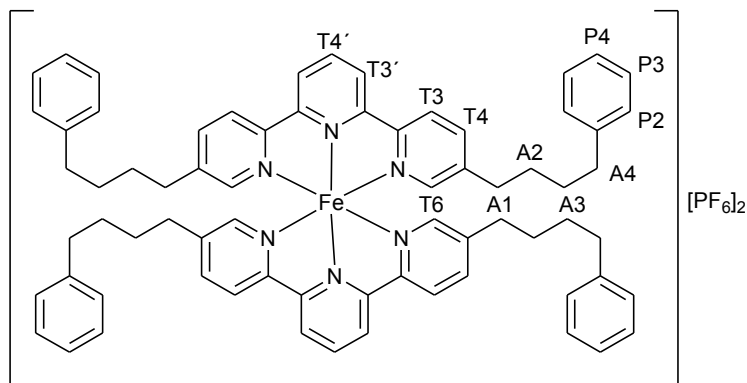
¹H-NMR (500 MHz, CD₃CN): δ / ppm 8.80 (1H, dd, *J* = 8.3, 1.3 Hz, T5'), 8.78 (1H, dd, *J* = 8.0, 0.5 Hz, T3'), 8.64 (1H, t, *J* = 8.0 Hz, T4'), 8.36 (1H, d, *J* = 8.0 Hz, T3''), 8.25 (1H, d, *J* = 8.0 Hz, T3), 7.82 (1H, td, *J* = 7.8, 1.5 Hz, T4''), 7.61 (1H, dd, *J* = 8.0, 2.0 Hz, T4), 7.28 (2H, t, *J* = 7.3 Hz, P3), 7.21 (1H, t, *J* = 7.3 Hz, T6''), 7.05-7.00 (4H, m, T5'', P2, P4), 6.75 (1H, d, *J* = 1.5 Hz, T6), 2.36 (2H, t, *J* = 7.5 Hz, A4), 2.28 (2H, td, *J* = 7.0, 1.5 Hz, A1), 1.26-1.20 (2H, m, A2), 1.16-1.10 (2H, m, A3).

IR (solid, cm⁻¹): 2923w, 2855w, 1603w, 1450w, 1386w, 1245w, 828s, 776m, 752m, 699w.

UV/Vis (CH₃CN): λ_{max}, nm (ε_{max}, M⁻¹cm⁻¹): 282 (32800), 321 (46100), 550 (10300).

Elem. an.: % calc. C 55.78, H 4.31, N 7.81; found C 55.55, H 4.24, N 7.74.

m. p.: decomposes >83.1 °C.

[Fe(terpy-(C4-Ph)₂)₂][PF₆]₂ (M = 1341.21)terpy-(C4-Ph)₂ = 5,5''-bis-(4-phenylbutyl)-2,2':6',2''-terpyridine

FeSO₄·7H₂O (9 mg, 0.03 mmol) and 5,5''-bis-(4-phenylbutyl)-2,2':6',2''-terpyridine (31 mg, 0.062 mmol) were used. Yield: 39 mg, 96.9%.

¹H-NMR (400 MHz, CD₃CN): δ / ppm 8.67 (1H, d, *J* = 8.8 Hz, T3'), 8.59 (0.5H, dd, *J* = 8.8, 6.8 Hz, T4'), 8.12 (1H, d, *J* = 8.0 Hz, T3), 7.54 (1H, dd, *J* = 8.0, 2.0 Hz, T4), 7.29 (2H, t, *J* = 7.4 Hz, P3), 7.22 (1H, t, *J* = 7.4 Hz, P4), 7.00 (2H, d, *J* = 7.2 Hz, P2), 6.68 (1H, s, T6), 2.34 (2H, t, *J* = 8.0 Hz, A1 or A4), 2.26 (2H, t, *J* = 7.2 Hz, A1 or A4), 1.25-1.12 (2H, m, A2 or A3), 1.10-1.05 (2H, m, A2 or A3).

IR (solid, cm⁻¹): 2921w, 2855w, 1601w, 1453w, 1383w, 829s, 740m, 699m, 637s, 621s.

UV/Vis (CH₃CN): λ_{max}, nm (ε_{max}, M⁻¹cm⁻¹): 285 (28300), 324 (65400), 550 (15900).

Elem. an.: % calc. C 62.69, H 5.26, N 6.27; found C 61.70, H 5.13, N 6.35.

m. p.: decomposes >72 °C.

[Fe(terpy-CHO)₂][PF₆]₂ (M = 868.39)

terpy-CHO = 5-formyl-2,2':6',2''-terpyridine

FeSO₄·7H₂O (16 mg, 0.058 mmol) and 5-formyl-2,2':6',2''-terpyridine (30 mg, 0.11 mmol) were used. Yield: 39 mg, 77.2%.

$^1\text{H-NMR}$ (250MHz, CD_3CN): δ / ppm 9.62 (1H, s, CHO), 9.07-8.97 (2H, m, H3', H5'), 8.76 (1H, t, $J = 8.0$ Hz, H4'), 8.63 (1H, d, $J = 8.8$ Hz, H3''), 8.48 (1H, d, $J = 6.8$ Hz, H3), 8.24 (1H, dd, $J = 8.3, 1.8$ Hz, H4), 7.89 (1H, td, $J = 7.8, 1.8$ Hz, H4''), 7.44 (1H, s, H6), 7.11 (2H, m, H5'', H6'').

IR (solid, cm^{-1}): 3121w, 3085w, 1703m, 1605w, 1568w, 1454m, 1401w, 1366w, 1253m, 1214m, 828s, 811s, 774s, 752s, 706w, 675w.

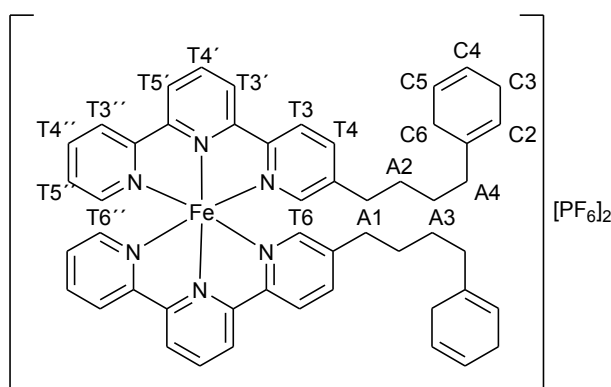
UV/Vis (CH_3CN): λ_{max} , nm (ϵ_{max} , $\text{M}^{-1}\text{cm}^{-1}$): 283 (44300), 325 (52300), 550 (11100).

Elem. an.: % calc. C 44.26, H 2.55, N 9.68; found C 44.05, H 2.43, N 9.52.

m. p.: >250 °C.

[Fe(terpy-C4-chd) $_2$][PF $_6$] $_2$ (M = 1080.85) (54)

terpy-C4-chd = 5-(4-cyclohexa-1,4-dienylbutyl)-2,2':6',2''-terpyridine



$\text{FeSO}_4 \cdot 7\text{H}_2\text{O}$ (28 mg, 0.10 mmol) and 5-(4-cyclohexa-1,4-dienylbutyl)-2,2':6',2''-terpyridine (74 mg, 0.20 mmol) were used. Yield: 97 mg, 89.7%.

$^1\text{H-NMR}$ (400 MHz, CD_3CN): δ / ppm 8.84 (2H, t, $J = 7.6$ Hz, T3', T5'), 8.65 (1H, t, $J = 7.8$ Hz, T4'), 8.43 (1H, d, $J = 8.0$ Hz, T3''), 8.35 (1H, d, $J = 8.0$ Hz, T3), 7.85 (1H, td, $J = 7.6, 1.5$ Hz, T4''), 7.68 (1H, dd, $J = 8.2, 1.8$ Hz, T4), 7.07-6.78 (2H, m, T5'', T6''), 6.79 (1H, d, $J = 2.0$ Hz, T6), 5.69 (2H, d, $J = 1.2$ Hz, C4, C5), 5.20 (1H, s, C2), 2.63-2.58 (2H, m, A1), 2.30 (overlap with H_2O peak, C3, C6), 1.71 (2H, t, $J = 7.6$ Hz, A4), 1.23-1.16 (2H, m, A2), 0.99-0.91 (2H, m, A3).

IR (solid, cm^{-1}): 3075w, 2923w, 2853w, 1602w, 1450m, 1386w, 1285w, 1245w, 1050s, 1027s, 779w, 747w, 702w, 639s, 621m.

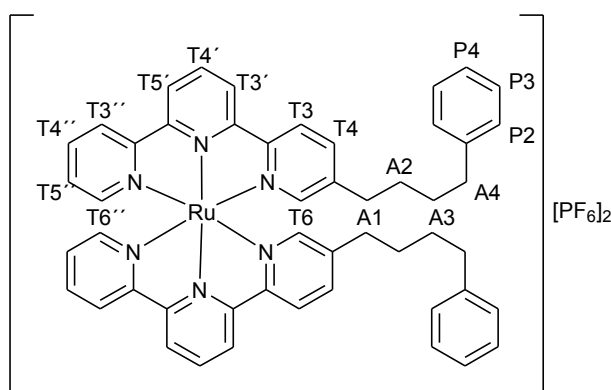
UV/Vis (CH_3CN): λ_{max} , nm (ϵ_{max} , $\text{M}^{-1}\text{cm}^{-1}$): 283 (22700), 321 (43600), 554 (9500).

Elem. an.: % calc. for $[\text{Fe}(\text{terpy-C4-chd})_2][\text{PF}_6]_2 \cdot \text{H}_2\text{O}$ C 54.66, H 4.77, N 7.65; found C 54.33, H 5.43, N 7.73.

m. p.: decomposes >76.0 °C.

$[\text{Ru}(\text{terpy-C4-Ph})_2][\text{PF}_6]_2$ (M = 1122.03)

terpy-C4-Ph = 5-(4-phenylbutyl)-2,2':6',2''-terpyridine



To a solution of the ligand (66 mg, 0.18 mmol) in EtOH was added $\text{RuCl}_3 \cdot 3\text{H}_2\text{O}$ (37 mg, 0.18 mmol). The mixture was refluxed for 1 h, then after cooling to room temperature the brown precipitate was filtered and washed with EtOH. The brown solid $\text{Ru}(\text{terpy-C4-Ph})\text{Cl}_3$ (48.6 mg, 0.09 mmol) was suspended in ethane-1,2-diol and one equivalent of the ligand (31 mg, 0.09 mmol) was added. The mixture was heated in the microwave (30 sec at 800 W). After cooling to room temperature, an excess of aqueous NH_4PF_6 was added to precipitate the orange-red complex, which was filtered over celite, washed with water and finally washed out with CH_3CN . After evaporation of the solvent, the product was collected as a orange-red solid. Yield: 44.7 mg, 22%.

$^1\text{H-NMR}$ (400 MHz, CD_3CN): δ / ppm 8.66 (2H, t, $J = 7.6$ Hz, T3', T5'), 8.41 (1H, d, $J = 8.8$ Hz, T3''), 8.37 (1H, t, $J = 8.2$ Hz, T4'), 8.31 (1H, d, $J = 7.6$ Hz, T3), 7.86 (1H, td, $J = 7.8, 1.5$ Hz, T4''), 7.67 (1H, dd, $J = 8.4, 1.6$ Hz, T4), 7.28-7.24 (2H, m, P3), 7.21-7.17 (1H, m, T6''), 7.14-7.10 (1H, m, T5''), 7.08 (1H, d, $J = 1.2$ Hz, T6), 7.01 (3H, d, $J = 6.8$ Hz, P2, P4), 2.38 (2H, t, $J = 7.0$ Hz, A4 or A1), 2.33 (2H, t, $J = 6.4$ Hz, A4 or A1), 1.32-1.18 (4H, m, A2, A3).

IR (solid, cm^{-1}): 3332w br, 2926w, 2859w, 1958w, 1601w, 1495w, 1448m, 1381m, 1285w, 1244w, 1024s, 861w, 849w, 781m, 773m, 745m, 695m, 677w, 637w, 622w.

UV/Vis (CH_3CN): λ_{max} , nm (ϵ_{max} , $\text{M}^{-1}\text{cm}^{-1}$): 310 (74500), 477 (14900).

m. p.: decomposes >99.0 °C.

8. Appendix

8.1. Crystal structure data for 1,1'-bis(4-bromobutanoyl)ferrocene (75)

Crystal data

Formula	$C_{18}H_{20}Fe_1Br_2O_2$
Formula weight	484.01
Crystal system	Triclinic
Space group	P-1 (No. 2)
a, b, c [Å]	7.9361(1), 9.6990(1), 13.2486(2)
α, β, γ [°]	100.8341(6), 101.3835(5), 113.2071(6)
V [Å ³]	877.95(2)
Z	2
D (calc) [g·cm ⁻³]	1.831
μ (MoK α) [mm ⁻¹]	5.416
F (000)	480
Crystal size [mm]	0.06 x 0.18 x 0.18

Data collection

Temperature [K]	173
Radiation [Å]	MoK α , 0.71073
θ min (max) [°]	2.391 (27.901)
Total number of reflections	8346
Number of unique reflections	4199
R (int)	0.017
Observed data [$I > 3 \sigma(I)$]	3328

Refinement

Number of reflections	3328
Number of parameters	208
R	0.0255
wR ₂	0.0296
Goodness of fit (GOF)	1.09
Min. and max. residual electron density [eÅ ⁻³]	-0.78, 0.64

Bibliography

- 1 P. A. Brady, R. P. Bonar-Law, S. J. Rowan, C. J. Suckling and J. K. M. Sanders, *Chem. Commun.*, 1996, 319.
- 2 J.-M. Lehn, *Chem. Eur. J.*, 1999, **5**, 2455.
- 3 C. Karan and B. L. Miller, *Drug Discovery Today*, 2000, **5**, 67.
- 4 A. Ganesan, *Angew. Chem. Int. Ed.*, 1998, **37**, 2828.
- 5 S. Otto, R. L. E. Furlan and J. K. M. Sanders, *Drug Discovery Today*, 2002, **7**, 117.
- 6 J. D. Cheeseman, A. D. Corbett, J. L. Gleason and R. J. Kazlauskas, *Chem. Eur. J.*, 2005, **11**, 1708.
- 7 S. Otto, R. L. E. Furlan and J. K. M. Sanders, *Science*, 2002, **297**, 590.
- 8 I. Saur and K. Severin, *Chem. Commun.*, 2005, 1471.
- 9 P. T. Corbett, J. K. M. Sanders and S. Otto, *J. Am. Chem. Soc.*, 2005, **127**, 9390.
- 10 I. Huc and J.-M. Lehn, *Proc. Natl. Acad. Sci. USA*, 1997, **94**, 2106.
- 11 G. R. L. Cousin, S.-A. Poulsen and J. K. M. Sanders, *Chem. Commun.*, 1999, 1575.
- 12 R. L. E. Furlan, G. R. L. Cousins and J. K. M. Sanders, *Chem. Commun.*, 2000, 1761.
- 13 G. R. L. Cousins, R. L. E. Furlan, Y.-F. Ng, J. E. Redman and J. K. M. Sanders, *Angew. Chem.*, 2001, **113**, 437.
- 14 R. L. E. Furlan, Y.-F. Ng, S. Otto and J. K. M. Sanders, *J. Am. Chem. Soc.*, 2001, **123**, 8876.
- 15 S. L. Roberts, R. L. E. Furlan, G. R. L. Cousins and J. K. M. Sanders, *Chem. Commun.*, 2002, 938.
- 16 R. T. S. Lam, A. Belenguer, S. L. Roberts, C. Naumann, T. Jarrosson, S. Otto and J. K. M. Sanders, *Science*, 2005, **308**, 667.
- 17 D. M. Epstein, S. Choudhary, M. R. Churchill, K. M. Keil, A. V. Eliseev and J. R. Morrow, *Inorg. Chem.*, 2001, **40**, 1591.

Bibliography

- 18 M. Hochgürtel, R. Biesinger, H. Kroth, D. Piecha, M. W. Hofmann, S. Krause, O. Schaaf, C. Nicolau and A. V. Eliseev, *J. Med. Chem.*, 2003, **46**, 356.
- 19 O. Ramström, S. Lohmann, T. Bunyapaiboonsri and J.-M. Lehn, *Chem. Eur. J.*, 2004, **10**, 1711.
- 20 P. Wipf, S. Graciela Mahler and K. Okumura, *Org. Lett.*, 2005, **7**, 4483.
- 21 S. Otto, R. L. E. Furlan and J. K. M. Sanders, *J. Am. Chem. Soc.*, 2000, **122**, 12063.
- 22 B. Brisig, J. K. M. Sanders and S. Otto, *Angew. Chem.*, 2003, **115**, 1308.
- 23 J. Leclaire, L. Vial, S. Otto and J. K. M. Sanders, *Chem. Commun.*, 2005, 1959.
- 24 K. R. West, K. D. Bake and S. Otto, *Org. Lett.*, 2005, **7**, 2615.
- 25 A. M. Whitney, S. Ladame and S. Balasubramanian, *Angew. Chem. Int. Ed.*, 2004, **43**, 1143.
- 26 B. R. McNaughton, K. M. Bucholtz, A. Camaaño-Moure and B. L. Miller, *Org. Lett.*, 2005, **7**, 733.
- 27 P. J. Boul, P. Reutenauer and J.-M. Lehn, *Org. Lett.*, 2005, **7**, 15.
- 28 S. Sakai, Y. Shigemasa and T. Sasaki, *Tetrahedron Lett.*, 1997, **38**, 8145.
- 29 I. Huc, M. J. Krische, D. P. Funeriu and J.-M. Lehn, *Eur. J. Inorg. Chem.*, 1999, 1415.
- 30 E. C. Constable, C. E. Housecroft, T. Kulke, C. Lazzarini, E. R. Schofield and Y. Zimmermann, *J. Chem. Soc., Dalton Trans.*, 2001, 2864.
- 31 S. Choudhary and J. R. Morrow, *Angew. Chem. Int. Ed.*, 2002, **41**, 4096.
- 32 J. R. Nitschke and J.-M. Lehn, *Proc. Natl. Acad. Sci.*, 2003, **100**, 11970.
- 33 M. Albrecht, I. Janser, J. Runsink, G. Raabe, P. Weis and R. Fröhlich, *Angew. Chem. Int. Ed.*, 2004, **43**, 6662.
- 34 A. Buryak and K. Severin, *Angew. Chem. Int. Ed.*, 2005, **44**, 7935.
- 35 A. V. Eliseev and M. I. Nelen, *J. Am. Chem. Soc.*, 1997, **119**, 1147.
- 36 E. Stulz, Y.-F. Ng, S. M. Scott and J. K. M. Sanders, *Chem. Commun.*, 2002, 524.
- 37 I. Saur, R. Scopelliti and K. Severin, *Chem. Eur. J.*, 2006, **12**, 1058.
- 38 M. S. Congreve, D. J. Davis, L. Devine, C. Granata, M. O'Reilly, P. G. Wyatt and H. Jhoti, *Angew. Chem. Int. Ed.*, 2003, **42**, 4479.

Bibliography

- 39 V. Goral, M. I. Nelen, A. V. Eliseev and J.-M. Lehn, *Proc. Natl. Acad. Sci.*, 2001, **98**, 1347.
- 40 F. Kröhnke, *Synthesis*, 1976, 1.
- 41 J. Polin, E. Schmolke and V. Balzani, *Synthesis*, 1998, 321.
- 42 M. Heller and U. S. Schubert, *Eur. J. Org. Chem.*, 2003, 947.
- 43 D. L. Jameson and L. E. Guise, *Tetrahedron Lett.*, 1991, **32**, 1999.
- 44 U. S. Schubert and C. Eschbaumer, *Angew. Chem. Int. Ed.*, 2002, **41**, 2892.
- 45 Eds. J. A. McCleverty and T. J. Meyer, *Comprehensive coordination chemistry II, Vol. 1*, Elsevier, Oxford, 2004.
- 46 U. S. Schubert, C. Eschbaumer, O. Hien and P. R. Andres, *Tetrahedron Lett.*, 2001, **42**, 4705.
- 47 P. R. Andres, R. Lunkwitz, G. R. Pabst, K. Böhn, D. Wouters, S. Schmatloch and U. S. Schubert, *Eur. J. Org. Chem.*, 2003, 3769.
- 48 P. R. Andres, H. Hofmeier, B. G. G. Lohmeijer and U. S. Schubert, *Synthesis*, 2003, 2865.
- 49 R.-A. Fallahpour and E. C. Constable, *J. Chem. Soc., Perkin Trans. 1*, 1997, 2263.
- 50 E. Murguly, T. B. Norsten and N. Branda, *J. Chem. Soc., Perkin Trans. 2*, 1999, 2789.
- 51 J. D. Holbrey, G. J. T. Tiddy and D. W. Bruce, *J. Chem. Soc., Dalton Trans.*, 1995, 1769.
- 52 H. Elsbernd and J. K. Beattie, *J. Inorg. Nucl. Chem.*, 1972, **34**, 771.
- 53 H. S. Chow, E. C. Constable, C. E. Housecroft, K. J. Kulicke and Y. Tao, *Dalton Trans.*, 2005, 236.
- 54 C. Kaes, A. Katz and M. W. Hosseini, *Chem. Rev.*, 2000, **100**, 3553.
- 55 E. C. Constable, E. Figgemeier, C. E. Housecroft, J. Olsson and Y. C. Zimmermann, *Dalton Trans.*, 2004, 1918.
- 56 P. D. Beer, J. W. Wheeler and C. P. Moore, *J. Chem. Soc., Dalton Trans.*, 1992, 2667.

Bibliography

- 57 M. G. B. Drew, P. B. Iveson, M. J. Hudson, J. O. Liljenzin, L. Spjuth, P.-Y. Cordier, Å. Enarsson, C. Hill and C. Madic, *J. Chem. Soc., Dalton Trans.*, 2000, 821.
- 58 T. J. Kealy and P. L. Pauson, *Nature*, 1951, **168**, 1039.
- 59 S. A. Miller, J. A. Tebboth and J. F. Tremaine, *J. Chem. Soc.*, 1952, 632.
- 60 E. O. Fischer and W. Pfab, *Z. Naturforsch.*, 1952, **7b**, 377.
- 61 E. Ruch and E. O. Fischer, *Z. Naturforsch.*, 1952, **7b**, 676.
- 62 G. Wilkinson, M. Rosenblum, M. C. Whiting and R. B. Woodward, *J. Am. Chem. Soc.*, 1952, **74**, 2125.
- 63 R. B. Woodward, M. Rosenblum and M. C. Whiting, *J. Am. Chem. Soc.*, 1952, **74**, 3458.
- 64 C. J. Yu, Y. Wan, H. Yowanto, J. Li, C. Tao, M. D. James, C. L. Tan, G. F. Blackburn and T. J. Meade, *J. Am. Chem. Soc.*, 2001, **123**, 11155.
- 65 I. Shevchenko, D. Shakhnin, H. Zhang, M. Lattman and G.-V. Rösenthaller, *Eur. J. Inorg. Chem.*, 2003, 1169.
- 66 E. Lindner, I. Krebs, R. Fawzi, M. Steimann and B. Speiser, *Organometallics*, 1999, **18**, 480.
- 67 T. Mochida, K. Okazawa and R. Horikoshi, *Dalton Trans.*, 2006, 693.
- 68 I. R. Butler, N. Burke, L. J. Hobson and H. Findenegg, *Polyhedron*, 1992, **11**, 2435.
- 69 E. C. Constable, A. J. Edwards, M. D. Marcos, P. R. Raithby, R. Martínez-Máñez, M. J. L. Tendero, *Inorg. Chim. Acta*, 1994, **224**, 11.
- 70 E. C. Constable, A. J. Edwards, R. Martínez-Máñez, P. R. Raithby and A. M. W. Cargill Thompson, *J. Chem. Soc., Dalton Trans.*, 1994, 645.
- 71 I. R. Butler and S. J. McDonald, *Polyhedron*, 1995, **14**, 529.
- 72 M. E. Padilla-Tosta, R. Martínez-Máñez, J. Soto and J. M. Lloris, *Tetrahedron*, 1998, **54**, 12039.
- 73 U. Siemeling, U. Vorfeld, B. Neumann, H.-G. Stammer, M. Fontani and P. Zanello, *J. Organomet. Chem.*, 2001, **637**, 733.
- 74 U. Siemeling, J. Vor der Brüggen, U. Vorfeld, B. Neumann, A. Stammer, H.-G. Stammer, A. Brockhinke, R. Plessow, P. Zanello, F. Laschi, F. Fabrizi de

Bibliography

- Biani, M. Fontani, S. Steenken, M. Stapper and G. Gurzadyan, *Chem. Eur. J.*, 2003, **9**, 2819.
- 75 D. E. Bublitz, *Can. J. Chem.*, 1964, **42**, 2381.
- 76 F. Basolo and R. G. Pearson, *Mechanisms of Inorganic Reactions*, Wiley, New York, 1967.
- 77 I. Bertini and C. Luchinat, *Coord. Chem. Rev.*, 1996, **150**, entire volume and references therein.
- 78 H. Günther, *NMR Spectroscopy: Basic Principles, Concepts and Applications in Chemistry*, Wiley, New York, 1995.
- 79 H. Irving and D. H. Mellor, *J. Chem. Soc.*, 1962, 5222.
- 80 H. A. Schwarz, C. Creutz and N. Sutin, *Inorg. Chem.*, 1985, **24**, 433.
- 81 J. K. Beattie and H. Elsbernd, *Inorg. Chim. Acta*, 1995, **240**, 641.
- 82 R. Ballarini, V. Balzani, M. Clemente-León, A. Credi, M. T. Gandolfi, E. Ishow, J. Perkins, J. Fraser Stoddart, H.-R. Tseng and S. Wenger, *J. Am. Chem. Soc.*, 2002, **124**, 12786.
- 83 H. Bredereck, G. Simchen and R. Wahl, *Chem. Ber.*, 1968, **101**, 4048.
- 84 M. G. Vetelino and J. W. Coe, *Tetrahedron Lett.*, 1994, **35**, 219.
- 85 P. Dupau, T. Renouard and H. Le Bozec, *Tetrahedron Lett.*, 1996, **37**, 7503.
- 86 S. Berger, *200 and More NMR Experiments: A Practical Course*, Wiley, New York, 2004.
- 87 H. Stetter and W. Böckmann, *Chem. Ber.*, 1951, **84**, 834.
- 88 R. J. Geue and G. H. Searle, *Aust. J. Chem.*, 1983, **36**, 927.
- 89 A. Sasse, K. Kiec-Kononowicz, H. Stark, M. Motyl, S. Reidemeister, C. R. Ganellin, X. Ligneau, J.-C. Schwartz and W. Schunack, *J. Med. Chem.*, 1999, **42**, 593.
- 90 E. V. Dehmlow, S. S. Dehmlow, *Phase transfer catalysis*, Verlag Chemie, Weinheim, 1980.
- 91 E. B. Fleischer, A. E. Gebala, A. Levey and P. A. Tasker, *J. Org. Chem.*, 1971, **36**, 3042.
- 92 R. L. Davies and K. W. Dunning, *J. Chem. Soc.*, 1965, 4168.
- 93 G. Anderegg and V. Gramlich, *Helv. Chim. Acta*, 1994, **77**, 685.

Bibliography

- 94 J. Mathieu, P. Gros and Y. Fort, *Chem. Commun.*, 2000, 951.
- 95 E. C. Constable, F. Heitzler, M. Neuburger and M. Zehnder, *J. Am. Chem. Soc.*, 1997, **119**, 5606.
- 96 D. L. Jameson and L. E. Guise, *Tetrahedron Lett.*, 1991, **32**, 1999.
- 97 B. Hasenknopf and J.-M. Lehn, *Helv. Chim. Acta*, 1996, **79**, 1643.
- 98 E. C. Ashby, D. Coleman and M. Gamasa, *J. Org. Chem.*, 1987, **52**, 4079.
- 99 G. Black, E. Depp and B. B. Corson, *J. Org. Chem.*, 1949, **14**, 14.
- 100 E. Borel and H. Deuel, *Helv. Chim. Acta*, 1953, **36**, 51.
- 101 B. F. Bush, V. M. Lynch and J. J. Lagowski, *Organometallics*, 1987, **6**, 1267.
- 102 E. P. Kündig, C. Perret, S. Spichiger and G. Bernardinelli, *J. Organomet. Chem.*, 1985, **286**, 183.
- 103 H. Werner, *Fortschritte der Chemischen Forschung*, 1972, **28**, 141.
- 104 G. Wilkinson, F. G. A. Stone and E. W. Abel, *Comprehensive Organometallic Chemistry*, Pergamon Press, 1982.
- 105 M. A. Bennett and A. K. Smith, *J. Chem. Soc., Dalton Trans.*, 1974, 233.
- 106 R. A. Benkeser, M. L. Burrous, J. J. Hazdra and E. M. Kaiser, *J. Org. Chem.*, 1963, **28**, 1094.
- 107 E. Pretsch, J. Seibl, T. Clerc, W. Simon, *Tables of Spectral Data for Structure Determination of Organic Compounds*, Springer-Verlag, Berlin, 1989.
- 108 K. Mori, *Tetrahedron*, 1974, **30**, 3807.
- 109 J. F. W. Keana and M. D. Ogan, *J. Am. Chem. Soc.*, 1986, **108**, 7951.
- 110 W. A. Herrmann and G. Brauer, *Synthetic Methods of Organometallic and Inorganic Chemistry, Volume 8*, Georg Thieme Verlag, Stuttgart, 1997.
- 111 K. F. Bernady, M. B. Floyd, J. F. Poletto and M. J. Weiss, *J. Org. Chem.*, 1979, **44**, 1438.
- 112 N. Miyashita, A. Yoshikoshi and P. A. Grieco, *J. Org. Chem.*, 1977, **42**, 3772.
- 113 R. K. Crossland and K. L. Servis, *J. Org. Chem.*, 1970, **35**, 3195.
- 114 P. H. Mazzocchi, P. Wilson, F. Khachik, L. Klingler and S. Minamikawa, *J. Org. Chem.*, 1983, **48**, 2981.
- 115 A. Lützen, M. Hapke, H. Staats and J. Bunzen, *Eur. J. Org. Chem.*, 2003, **20**, 3948.

Bibliography

- 116 Y. Hama, Y. Nobuhara, Y. Aso, T. Otsubo and F. Ogura, *Bull. Chem. Soc. Jpn.*, 1988, **61**, 1683.
- 117 P. D. Leeson and J. C. Emmett, *J. Chem. Soc., Perkin Trans. 1*, 1988, 3085.
- 118 E. C. Constable and M. D. Ward, *J. Chem. Soc., Dalton Trans.*, 1990, 1405.
- 119 D. Armspach, E. C. Constable, C. E. Housecroft, M. Neuburger and M. Zehnder, *J. Organomet. Chem.*, 1998, **550**, 193.
- 120 H. S. Chow, E. C. Constable, C. E. Housecroft, K. J. Kulicke and Y. Tao, *Dalton Trans.*, 2005, 236.
- 121 B. Hasenknopf, J.-M. Lehn, B. O. Kneisel, G. Baum and D. Fenske, *Angew. Chem. Int. Ed. Engl.*, 1996, **35**, 1838.
- 122 B. Hasenknopf, J.-M. Lehn, N. Boumediene, A. Dupont-Gervais, A. Van Dorsselaer, B. Kneisel and D. Fenske, *J. Am. Chem. Soc.*, 1997, **119**, 10956.

CURRICULUM VITAE

Barbara Brisig

Personal

Date & place of birth: 21.07.1977, Lugano, Switzerland
Nationality: Swiss
Marital status: Single
E-mail address: bbrisig@yahoo.com

Education

2002-2006: Universität Basel (Switzerland), Department of Chemistry
Ph.D. research "Dynamic combinatorial libraries of complexes with oligopyridine ligands" with Prof. Constable and Prof. Housecroft

2001-2002: University of Cambridge (UK), Department of Chemistry
Diploma work "A catalyst for a Diels-Alder reaction from a dynamic combinatorial library" with Prof. Sanders, Erasmus exchange student

1997-2001: Eidgenössische Technische Hochschule, Zürich (Switzerland),
Department of Chemistry
2002: Diploma work
2001: Schlussdiplom
1999: 2. Vordiplom
1998: 1. Vordiplom

1999-2000: University of Cambridge (UK), Department of Chemistry
Part II, Erasmus exchange student

1993-1997: Liceo Cantonale, Lugano
1997: Matura type C (scientific)

Teaching experience

2002-2006: Universität Basel: Practical class supervisor for first year Pharmacy students, one year as head supervisor

Language skills

Native language: Italian
Foreign languages: French, fluent written and oral
German, fluent written and oral, including teaching experience
English, fluent written and oral

Hobbies

Gymnastics: regional, national and international competitions and exhibitions as individual and in group
Sailing: experience on Laser and cruising sailboat
Music: studied the piano for 4 years
studied the flute for 8 years
study the cello since 2003, played 1 year in the music school orchestra
Olympics: worked as a volunteer at the Olympic and Paralympic Winter Games 2006 in Torino (I), in the function of interpreter for French, German and English

Publication

Selection and amplification of a catalyst from a dynamic combinatorial library.
Barbara Brisig, Jeremy K. M. Sanders and Sijbren Otto, *Angew. Chem.*, 2003, **115**, 1308.